



**Cellular responses to zinc involving the transcription factor**

**ZNF658 and its target genes**

**OGO AGBOR OGO**

Thesis submitted for the degree of Doctor of Philosophy

Institute for Cell and Molecular Biosciences

Faculty of Medical Sciences

Newcastle University

United Kingdom

December 2014

## Abstract

Zinc is an essential trace element that plays a crucial role in catalytic, structural and regulatory functions of many proteins including enzymes and transcription factors; thus maintenance of zinc balance is critical for normal cellular function. Cellular mechanisms that maintain zinc balance include the regulation of genes coding for proteins that play vital roles in zinc homeostasis. These proteins include zinc transporters belonging to the ZIP (SLC39A) and ZnT (SLC30A) families as well as the zinc-binding metallothionein proteins. In contrast to bacterial and yeast systems, a transcription factor responsible for mediating transcriptional repression of a suite of genes in response to elevated zinc levels in mammals has hitherto not been identified. Using Caco-2 cells as a model of human intestinal epithelial cells and detection of protein binding by electrophoretic mobility shift analysis, we show that zinc finger protein ZNF658 binds specifically to the zinc transcriptional regulatory element (ZTRE), previously demonstrated to mediate this response in a panel of three genes: *SLC30A5* (ZnT5 zinc transporter), *SLC30A10* (ZnT10 zinc transporter) and *CBWD* (whose prokaryotic homologs are emerging players in metal biology). We also demonstrate that siRNA-driven reduction of ZNF658 attenuated or abrogated transcriptional repression in response to elevated zinc levels of these same genes by measuring transcript abundance using RT-qPCR and using promoter-reporter gene constructs. In addition, the region of ZNF658 responsible for binding to the ZTRE was identified (the C-terminal zinc finger domain) and the requirement for both sides of the palindromic ZTRE sequence for function was demonstrated. This study therefore identifies the first metazoan transcription factor that plays a pivotal role in the orchestrated cellular response to increased zinc levels to restore cellular zinc balance necessary to achieve a broad spectrum of zinc-dependent functions and begins to probe its molecular action. We also report an important role for the mammalian *CBWD* gene product in protection of cells from either depleted or excess zinc by virtue of the fact that overexpression of recombinant CBWD protein altered cellular tolerance to both elevated and depleted levels of zinc consistent with a homeostatic function. In addition, we present preliminary evidence that changes in the expression of ZNF658 and its target genes, in particular *SLC30A10* (ZnT10), may be related to cell senescence, suggesting that changes in zinc homeostasis are components of this process. Overall, the work presented contributes to understanding zinc regulated gene expression and cellular zinc homeostasis.

## Declaration

I declare that this thesis titled “**Cellular responses to zinc involving the transcription factor ZNF658 and its target genes**” is my own work that has not been submitted for any degree or examination in any university and that all materials used have been acknowledged and referenced.

## **Acknowledgement**

First and foremost I thank Almighty God for His ever-abiding grace throughout the course of this study.

I would like to sincerely thank my meticulous supervisor professor Dianne Ford and co-supervisor Dr Ruth Valentine for their guidance. Your understanding and support throughout made a huge difference to the completion of this programme. I have really learnt a lot from you both.

I am grateful to my family members for upholding me in prayers, and especially Lucy and Amanda for coping with my absence all along. God helping me, I promise to make it up to you all.

I appreciate all my colleagues in the laboratory (both “nuclear” and “extended” members) for their friendship and assistance.

Thank you all my friends at home and abroad for keeping me sane with calls, messages and chats through whatever means.

Finally, I would like to thank the Tertiary Education Trust Fund (TETFund) through the Benue State University (BSU) Makurdi for the sponsorship.

## List of Abbreviations

AD	Alzheimer disease
ADR1	Alcohol dehydrogenase regulator
ANOVA	Analysis of variance
AE	Acrodermatitis enteropathica
ATP	Adenosine triphosphate
APS	Ammonium persulphate
BHK	Baby hamster kidney (cell)
BSA	Bovine Serum Albumin
bp	Base pair
Caco-2	Colorectal adenocarcinoma (cells)
CAT	Chloramphenicol acetyltransferase
CDF	Cation diffusion facilitator
cDNA	Complementary DNA
CHO	Chinese Hamster Ovary
CK2	Protein kinase 2 or casein kinase II
CMV	Cytomegalovirus
CPRG	Chlorophenol-Red $\beta$ -D-galactopyranoside
CoCl <sub>2</sub>	Cobalt chloride
CPD	Cumulative population doubling
CS	Cellular senescence
Ct	Threshold cycle
CuCl <sub>2</sub>	Copper chloride
CVDs	Cardiovascular diseases
ddH <sub>2</sub> O	Double deionised water

DDR	DNA damage response
DMEM	Dulbecco's modified Eagles medium
DNA	Deoxyribose Nucleic Acid
ddNTP	Dideoxynucleotide triphosphate
DEPC	Diethylpyrocarbonate
DMSO	Dimethyl sulphoxide
dNTP	Deoxynucleotide triphosphate
dsDNA	Double stranded DNA
E. coli	Escherichia Coli
EB	Elution buffer
EDTA	Ethylene diamine tetraacetic acid
EAR	Estimated average requirement
EGTA	Ethylene glycol tetraacetic acid
EMBOSS	European molecular biology open software suite
EMSA	Electrophoretic mobility shift assay
EM	Fluorescence emission maximum
ERE	Estrogen response element
EX	Fluorescence excitation maximum
FBS	Foetal bovine serum
FCS	Foetal calf serum
FNB	Food and nutrition board
GAPDH	Glyceraldehyde-3-phosphate dehydrogenase
GIT	Gastrointestinal tract
HCAEC	Human coronary endothelial cell
HEK293	Human embryonic kidney 293 (cell)

HRP	Horseradish peroxidase
HSP	Heat shock protein
hTERT	Human telomerase reverse transcriptase
Kb	Kilobase
KLF	Krüppel-like factor 4
LB	Luria-Bertani (medium)
LNRI	Lower reference nutrient intake
mRNA	Messenger ribonucleic acid
mTOR	Mammalian target of rapamycin
mTORC1	Mammalian target of rapamycin complex 1
NEAA	Non-essential amino acid
NO	Nitric oxide
MDCK	Madin-Darby canine kidney (cell)
MRE	Metal response element
MT	Metallothionein
MTF-1	Metal-Response element-binding transcription factor-1
NiCl <sub>2</sub>	Nickel chloride
OIS	Oncogene-induced senescence
ORF	Open reading frame
PBS	Phosphate buffered saline
PAFR2	Platelet activating factor receptor transcript 2
PCR	Polymerase chain reaction
PD	Population doubling
PNK	Polynucleotide kinase
PVDF	Polyvinylidene difluoride

RISC	RNA-induced silencing complex
RNA	Ribonucleic acid
RNAi	RNA interference
RPM	Revolutions per minute
RT-qPCR	Reverse transcriptase quantitative polymerase chain reaction
SACN	Scientific advisory committee on nutrition
SASP	Senescence associated secretory phenotype
SDS-PAGE	Sodium dodecyl sulphate polyacrylamide gel electrophoresis
SEM	Standard error of the mean
SIPS	Stress-induced premature senescence
SNP	Single nucleotide polymorphism
siRNA	Small Interfering RNA
SOD	Superoxide dismutase
TAE	Tris-acetate EDTA electrophoresis buffer
TBE	Tris-Boric Acid EDTA
TFBS	Transcription factor binding site
TGN	Tran golgi network
TEMED	N,N,N',N'-Tetramethylethylenediamine
TMD	Transmembrane domain
TSS	Transcription start site
UAS1	Upstream activator sequence
UTR	Untranslated region
UV	Ultraviolet
v/v	Volume per volume
w/v	Weight per volume

ZNF658	Zinc finger protein 658
ZTRE	Zinc transcriptional regulatory element
ZIP	Zinc regulated transporter Iron regulate transporter-like protein
ZnCl <sub>2</sub>	Zinc chloride
ZNF658	Zinc finger protein 658
ZnT	Zinc transporter
ZTRE	Zinc transcriptional regulated element

## Table of contents

<b>Abstract.....</b>	<b>ii</b>
<b>Declaration.....</b>	<b>iii</b>
<b>Acknowledgement .....</b>	<b>iv</b>
<b>List of Abbreviations .....</b>	<b>v</b>
<b>Table of contents .....</b>	<b>x</b>
<b>Table of Figures.....</b>	<b>xvii</b>
<b>List of Tables .....</b>	<b>xx</b>
<b>Publications, presentations and abstracts related to this work.....</b>	<b>xxi</b>
<b>Chapter 1 : Introduction .....</b>	<b>1</b>
1.1 The chemistry of zinc.....	1
1.2 Zinc as an essential biological micronutrient.....	1
1.2.1 Zinc absorption and excretion .....	3
1.2.2 Physiological roles of zinc .....	3
1.2.3 Zinc deficiency and toxicity .....	6
1.3 Zinc homeostasis.....	11
1.3.1 Metallothioneins.....	11
1.3.2 Zinc uptake proteins (the ZIP family) .....	15

1.3.3 Zinc efflux proteins (the ZnT family) .....	27
1.4 Transcriptional regulation of zinc homeostatic proteins by zinc .....	39
1.5 Aims and objectives .....	42
<b>Chapter 2 : Materials and Methods .....</b>	<b>43</b>
2.1 Tissue culture techniques .....	43
2.1.1 Growth and maintenance of mammalian cells .....	43
2.1.2 Transient transfection with promoter-reporter/expression plasmids.....	44
2.1.3 Metal treatment .....	45
2.2 Cell viability assay .....	46
2.2. 1 Dye exclusion method (Trypan blue).....	46
2.2.2 The MTT (3-[4, 5-dimethylthiazol-2-yl]-2, 5 diphenyl tetrazolium bromide) assay.	46
2.3 Generation and manipulation of DNA/plasmid constructs .....	48
2.3.1 Design of primers .....	48
2.3.2 Generation of amplicon by PCR .....	48
2.3.3 Generation of DNA insert for cloning .....	49
2.3.4 Agarose gel electrophoresis of DNA .....	49
2.3.5 Purification of DNA products from agarose gels.....	49
2.3.6 Transformation of chemically competent E coli cells.....	50
2.3.7 Screening of transformants (inoculation).....	51
2.3.8 Purification of plasmid from bacterial cultures.....	51
2.3.9 Determination of Nucleic acid (DNA/RNA) concentration.....	51

2.3.10 Digestion of plasmid DNA with restriction endonucleases .....	52
2.3.11 Site-directed mutagenesis (SDM) .....	52
2.3.12 DNA sequencing .....	53
2.4 <i>In vitro</i> methylation.....	53
2.5 Reporter-gene assays .....	53
2.5.1 Preparation of cell lysate .....	53
2.5.2 Measurement of reporter activity ( $\beta$ -Galactosidase specific activity) .....	54
2.6 Determination of protein concentration .....	54
2.7 RNA extraction and RT-PCR .....	55
2.7.1 RNA extraction from cultured mammalian cells .....	55
2.7.2 Treatment of RNA with Dnase I .....	56
2.7.3 Synthesis of cDNA by reverse transcription reaction (RT-PCR) .....	56
2.7.4 Measurement of mRNA expression by RT-qPCR .....	56
2.7.5 Generation of standard curves.....	57
2.8 Statistical analysis .....	57
2.9 Immunoblotting techniques (western blotting).....	58
2.9.1 Preparation of protein sample .....	58
2.9.2 SDS-PAGE electrophoresis .....	58
2.9.3 Protein transfer to PVDF membranes and blocking .....	59
2.9.4 Detection of immunoreactive protein band.....	59
2.10 Immunofluorescence microscopy .....	60

2.11 Electrophoretic mobility shift assay (EMSA).....	61
2.11.1 Preparation of probes .....	61
2.11.2 Preparation of protein extract.....	61
2.11.3 Binding reactions .....	62
2.11.4 Image detection .....	62
<b>Chapter 3 : Investigation of the mechanism of zinc-induced down- regulation of genes; the role of the zinc transcriptional regulatory element (ZTRE).....</b>	<b>63</b>
3.1 Introduction.....	63
3.1.1 Identification of the zinc transcriptional regulatory element (ZTRE).....	63
3.2 Specific objectives .....	64
3.3 Results.....	64
3.3.1 The effect of zinc on transcript levels of SLC30A5 and CBWD genes.....	64
3.3.2 The effect of zinc on promoter activity of SLC30A5 and CBWD genes .....	70
3.3.3 The effect of ZTRE mutation on zinc-induced transcriptional repression of SLC30A5 and CBWD gene promoters .....	74
3.3.4 The effect of deletion of the 5' or 3' components of the SLC30A5 ZTRE on the response to zinc .....	77
3.3.5 Zinc selectivity of the SLC30A5 ZTRE in mediating a transcriptional response.....	80
3.4 Discussion.....	83

## **Chapter 4 : Evidence that the zinc finger protein ZNF658 binds to the Zinc Transcriptional Regulatory Element (ZTRE) to mediate zinc-induced**

### **transcriptional repression .....87**

4.1 Introduction.....	87
4.2 Specific objectives .....	88
4.3 Results.....	88
4.3.1 Identification of the Krüppel associated box (KRAB) domain in ZNF658.....	88
4.3.2 Demonstration that ZNF658 binds to the ZTRE-containing SLC30A5 probe .....	91
4.3.3 Identification of the DNA-binding region of ZNF658 protein and demonstration that ZNF658 binds only a ZTRE with both 5' and 3' components.....	94
4.3.5 Effect of zinc on transcript levels of ZNF658.....	98
4.3.4 siRNA-mediated knockdown of ZNF658 in Caco-2 cells. ....	99
4.3.6 Effect of siRNA-mediated knockdown of ZNF658 on the response to zinc of SLC30A5, SLC30A10 and CBWD genes at the transcript level.....	103
4.3.7 The effect of siRNA-mediated knockdown of ZNF658 on the response of SLC30A5, SLC30A10 and CBWD genes to zinc at the promoter level.....	106
4.3.8 Identification of additional transcription factor binding sites (TFBS) around the ZTRE region.....	109
4.4 Discussion.....	111

**Chapter 5 : Investigation of the role of *CBWD* gene products**

**in metal homeostasis ..... 119**

5.1 Introduction..... 119

5.2 Specific objectives ..... 120

5.3 Results..... 120

5.3.1 Identification of the ZTRE in *CBWD* genes ..... 120

5.3.2 The response of *CBWD* genes to metals other than zinc..... 122

5.3.3 The effect of zinc on *CBWD* protein levels in CHO and Caco-2 cells..... 125

5.3.4 The effect of *CBWD* protein overexpression on intracellular zinc levels ..... 130

5.3.5 Effect of *CBWD* overexpression on cell tolerance to zinc ..... 132

5.3.6 Effect of zinc on *CBWD* protein localization ..... 137

5.3.7 Effect of *CBWD* overexpression on cellular zinc distribution ..... 139

5.3.8 The effect of DNA methylation on *CBWD* promoter activity..... 141

5.4 Discussion..... 144

**Chapter 6 : The effect of endothelial cell senescence on cellular zinc**

**homeostatic processes ..... 149**

6.1 Introduction..... 149

6.2 Specific objectives ..... 154

6.3 Methods..... 154

6.4 Results..... 155

6.4.1 Effect of zinc on HCAEC cell growth ..... 155

6.4.2 Effect of zinc-induced senescence on expression of p16.....	158
6.4.3 Effect of zinc-induced senescence on expression of ZNF658 and its target genes in HCAECs.....	160
6.5 Discussion.....	164
<b>Chapter 7 : Summary and conclusion .....</b>	<b>167</b>
7.1 Summary.....	167
7.2 Conclusion .....	169
7.3 Recommendations for further work.....	170
7.4 References.....	173
7.5 Appendices.....	199
1: pCMV6-Entry vector map .....	199
2: p3XFLAG-CMV vector map.....	200
3: pBlue-TOPO vector map .....	201
4: p3XFLAG-CMV vector map.....	202
5: p3XFLAG-CMV vector sequence .....	203
6: Protein sequences alignment of the human CBWD isoforms using ClusterW2.....	204

## Table of Figures

Figure 1.1: Structure of metallothionein proteins .....	14
Figure 1.2: Schematic representation of predicted general topologies of ZIP and ZnT transporters.....	38
Figure 2.1: Schematic representation of enzymatic reduction of MTT to formazan.....	47
Figure 3.1: Representative real-time PCR amplification plots and standard curves. ....	67
Figure 3.2: Representative melt curves generated from RT-qPCR. ....	68
Figure 3.3: Increased zinc concentration down-regulates transcript levels of <i>SLC30A5</i> and <i>CBWD</i> genes. ....	69
Figure 3.4: Promoter activity of <i>SLC30A5</i> and <i>CBWD</i> genes is repressed by zinc.....	73
Figure 3.5: Mutation of the ZTRE in <i>SLC30A5</i> and <i>CBWD</i> promoter sequences abrogates the response to zinc.....	76
Figure 3.6: Both 5' and 3' ZTRE components are required to mediate transcriptional repression in response to zinc.....	79
Figure 3.7: The <i>SLC30A5</i> ZTRE-mediated response is zinc-specific. ....	82
Figure 4.1: Domain structure representation of the mammalian ZNF658 and the yeast ZAP1 proteins and amino acid sequence alignment highlighting regions of similarity.....	89
Figure 4.2: The KRAB domain sequence of ZNF658 .....	90
Figure 4.3: Sequence of IRD700-labeled <i>SLC30A5</i> probe used in EMSA experiments .....	92
Figure 4.4: ZNF658 binds specifically to the ZTRE in <i>SLC30A5</i> .....	93
Figure 4.5: Schematic diagram showing the inverse PCR technique used to delete zinc fingers 12 – 15 from ZNF658 5 .....	96
Figure 4.6: ZNF658 requires zinc fingers 12 -15 and both 5' and 3' components of the ZTRE to bind. ....	97

Figure 4.7: ZNF658 transcript abundance is unaffected by increased extracellular zinc concentration.....	98
Figure 4.8: The ZNF658 coding region indicating siRNA target sequences.....	100
Figure 4.9: ZNF658 mRNA expression was reduced by approximately 60% with 2 different siRNAs.....	102
Figure 4.10: Knockdown of ZNF658 by siRNA attenuates the response of <i>SLC30A5</i> , <i>SLC30A10</i> and <i>CBWD</i> transcripts to zinc.....	105
Figure 4.11: Knockdown of ZNF658 by siRNA attenuates the response of <i>SLC30A5</i> , <i>SLC30A10</i> and <i>CBWD</i> promoters to zinc .....	108
Figure 4.12: The ZTRE-containing <i>SLC30A5</i> , <i>SLC30A10</i> and <i>CBWD</i> promoters share common transcription factor binding sites for NGRE, NOLF and SP1F proteins .....	110
Figure 5.1: <i>CBWD</i> genes are regulated at the transcript level by metals but not at the promoter level by metals additional to zinc.....	124
Figure 5.2: Restriction digestion confirms <i>CBWD</i> cloning into 3XFLAGPCMV10 vector.	127
Figure 5.3: <i>CBWD</i> protein expression is reduced by increased extracellular zinc concentration .....	129
Figure 5.4: <i>CBWD</i> overexpression alters intracellular zinc status.....	131
Figure 5.5: Increased <i>CBWD</i> protein expression enhances viability of cells exposed to zinc depletion or excess (dye exclusion method). .....	134
Figure 5.6: Increased <i>CBWD</i> protein expression enhances viability of cells exposed to zinc depletion or excess (MTT assay). .....	136
Figure 5.7: Increased zinc concentration did not alter <i>CBWD</i> distribution in Caco-2 cells.	138
Figure 5.8: <i>CBWD</i> proteins appears to redistribute cellular zinc .....	140
Figure 5.9: Methylation of the <i>CBWD</i> promoter reduces its activity.....	143
Figure 6.1: Hallmarks of senescent cells. ....	153

Figure 6.2: Zinc promotes endothelial cell growth arrest ..... 157

Figure 6.3: Zinc-induced endothelial cell growth arrest increased p16 expression..... 159

Figure 6.4: Expression of ZNF658 and its target genes are regulated by cellular senescence  
..... 163

## List of Tables

<i>Table 1.1: Food sources for zinc (taken from <a href="http://ndb.nal.usda.gov/">http://ndb.nal.usda.gov/</a>) .....</i>	2
<i>Table 1.2: Zinc distribution within the body tissues (adapted from Rink &amp; Gabriel, 2000) .....</i>	4
<i>Table 1.3: Examples of zinc-utilizing enzymes (adapted from Rink &amp; Gabriel, 2000) .....</i>	5
<i>Table 1.4: UK Dietary reference values for zinc (mg/kg). LRNI - Lower Reference Nutrient Intake; EAR - Estimated Average Recommended Requirement; RNI - Reference Nutrient Intake. * Indicates no increment. Adapted from the UK National Diet and Nutrition Survey, 2003.....</i>	9
<i>Table 1.5: Tolerable upper intake levels (UL) for zinc. Adapted from the Institute of Medicine Panel report, 2001. ....</i>	10
<i>Table 1.6: Classification of metallothionein isoforms. Adapted from Thirumoorthy et al., 2011 .....</i>	13
<i>Table 3.1: Oligonucleotide sequences and cycle parameters used for RT-qPCR measurements .....</i>	65
<i>Table 3.2: Oligonucleotides used in site-directed mutagenesis of the SLC30A5 ZTRE .....</i>	78
<i>Table 4.1: Oligonucleotide sequences and thermal cycling parameters used in PCR to delete zinc fingers 12 – 15 of ZNF658.....</i>	95
<i>Table 4.2: Sequences of ZNF658 targeted for knockdown and the siRNA sequences used...</i>	101
<i>Table 4.3: Primers and thermal cycling parameters for confirmation of ZNF658 knockdown .....</i>	101
<i>Table 5.1: Multiple copies of CBWD genes contain the ZTRE.....</i>	121
<i>Table 5.2: Primers used for sub-cloning of CBWD3 ORF into the p3XFLAG-CMV10 vector .....</i>	126

## **Publications, presentations and abstracts related to this work**

### **A. Publications**

1. Coneyworth LJ, Jackson KA, Tyson J, Bosomworth HJ, van der Hagen E, Hann GM, **Ogo OA**, Swann DC, Mathers JC, Valentine RA, Ford D (2012).  
Identification of the Human Zinc Transcriptional Regulatory Element (ZTRE): a palindromic protein-binding dna sequence responsible for zinc-induced transcriptional repression. *J Biol Chem.* **287**, 36567-36581
2. **Ogo A Ogo**, John Tyson, Simon J Cockell, Alison Howard Ruth A Valentine Dianne Ford (2014)  
The zinc finger protein ZNF658 regulates the transcription of genes involved in zinc homeostasis and affects ribosome biogenesis through the zinc transcriptional regulatory element (ZTRE) – submitted manuscript
3. Marco Malavolta, Laura Costarelli, Robertina Giacconi, Andrea Basso, Francesco Piacenza, Pierpaoli Elisa, Mauro Provinciali, **Ogo A Ogo**, Dianne Ford  
Accelerated Senescence of Human Coronary Endothelial Cells by a Moderately Excessive Zinc Environment – Manuscript in preparation

### **B. Presentations**

1. Identification of ZNF658 as a factor involved in the transcriptional regulation of zinc homeostasis (Oral)  
9<sup>th</sup> Zinc-UK conference University College London: November 3<sup>rd</sup> 2014
2. Identification of ZNF658 as a factor involved in zinc-induced transcriptional repression of human genes (Poster)  
Gordon Research Conference on Cell Biology of Metals  
Salve Regina University, Rhode Island, USA: August 2013
3. Metal micronutrient homeostasis through a novel gene transcriptional regulatory mechanism  
Human Nutrition Research Centre Research Day & Annual Lecture (Oral)  
Newcastle University: Wednesday 10<sup>th</sup> October, 2012

### **C. Abstracts**

- 1.** Identification of *CBWD* genes as novel players in mammalian zinc homeostasis as  
33<sup>rd</sup> Nigerian Society for Biochemistry and Molecular Biology Conference  
University of Ilorin, Nigeria: Tuesday 11<sup>th</sup> to Friday 14<sup>th</sup> November 2014
- 2.** Identification of ZNF658 as a factor involved in zinc-induced transcriptional  
repression of human genes  
North East Postgraduate Conference  
Newcastle University, UK: 31<sup>ST</sup> October, 2013



## **Chapter 1 : Introduction**

### **1.1 The chemistry of zinc**

Zinc is an important naturally occurring metallic element. It is a member of group 12, period 4, block d and number 30 on the periodic table. It is the 25<sup>th</sup> most abundant element and comprises a reasonable segment of the Earth's crust, where the divalent cation preferentially forms complexes as sulphides, chlorides, carbonates and oxides. Zinc has an atomic number of 30 and 5 stable isotopes: namely <sup>64</sup>Zn, <sup>66</sup>Zn, <sup>67</sup>Zn, <sup>68</sup>Zn and <sup>70</sup>Zn. <sup>64</sup>Zn is the most stable isotope and has a half-life of  $7.0 \times 10^{20}$  years. Other synthetic forms, such as radioactive <sup>65</sup>Zn with a half-life of about 244 days, are often used for research. Although credit for the discovery of pure metallic zinc is often given to Andreas Sigismund Marggraf in 1746, his fellow German alchemist Paracelsus gave the name zinc after the German word Zinke meaning tooth-like, which is reminiscent of its crystal appearance. Zinc compounds are used for industrial and commercial purposes while the divalent ion is of great biological interest owing to its prevalence in many proteins, which is generally attributed to redox stability endowed by the completely filled d-orbital (with 10 outer shell electrons) and to its interaction with ligands in polypeptide chains. These ligands include cysteine, sulphur, histidine, nitrogen and glutamate or aspartate (Berg and Shi, 1996, Maret, 2005) affording a role for zinc in specific protein structural folds such as zinc fingers.

### **1.2 Zinc as an essential biological micronutrient**

Zinc is present in minute quantities in many food sources (Table 1.1). The multiple outcomes of biochemical and/or physiological perturbation of zinc is due to its involvement in a panoply of cellular processes that are essential to life. Zinc is the second most abundant trace element, after iron, in the human body. It is estimated that an average 70-kg adult contains 2.3 g of zinc

(McCall et al., 2000). However, zinc distribution is not easily determined since the element is bound to many macromolecules. In addition, there is no robust, sensitive or specific biomarker of zinc status. The work of Bert Valle (Field et al., 2002) established the presence and importance of zinc in metalloproteins, and it was much later estimated based on the available genome information that up to 10% of the human proteome may require zinc for activity (Andreini et al., 2005). This figure may be an underrepresentation since more recent bioinformatics analysis revealed classes of protein overlooked earlier that may bind zinc (Andreini et al., 2009).

<b>Food</b>	<b>Serving</b>	<b>Zinc (mg)</b>
<b>Oysters</b>	6 medium (cooked)	27-50
<b>Beef</b>	3 ounces (cooked)	3.7 -5.8
<b>Crab, Dungeness</b>	3 ounces (cooked)	4.7
<b>Pork</b>	3 ounces (cooked)	1.9-3.5
<b>Turkey (dark meat)</b>	3 ounces (cooked)	3.0
<b>Baked beans</b>	½ cup	0.9-2.9
<b>Chicken (dark meat)</b>	3 ounces (cooked)	1.6-2.7
<b>Yogurt, fruit, nonfat</b>	1 cup (8 fl. Oz.)	1.8
<b>Cashews</b>	1 ounce	1.6
<b>Chickpeas</b>	½ cup	0.5-1.3
<b>Milk</b>	1 cup (8 fl. Oz.)	1.0
<b>Almonds</b>	1 ounce	0.9
<b>Peanuts</b>	1 ounce	0.9
<b>Cheese, cheddar</b>	1 ounce	0.9

*Table 1.1: Food sources for zinc (taken from <http://ndb.nal.usda.gov/>)*

### ***1.2.1 Zinc absorption and excretion***

Zinc absorption from the diet occurs predominantly in the proximal regions of the human small intestine. The ability of zinc to cross biological membranes by passive diffusion is impaired by the hydrophilicity of the divalent cation, thus specific transport proteins are required for its absorption across the enterocyte brush border membrane and for its translocation from one compartment to another. Zinc absorption could be affected by the chemical form in which it is present in the diet and/or supplementation. The Food and Agriculture Organisation/World Health Organization (FAO/WHO) joint report of 2001 states that zinc in aqueous forms are better absorbed than solid forms, and zinc carbonate is less absorbable compared with zinc sulphate (reviewed by (Krebs, 2000)). Zinc absorption is also affected by age and disease (Rink, 2000). Concurrent consumption of alcohol also inhibits zinc absorption, and has been suggested as a possible cause of zinc deficiency (Mehta et al., 2011), although the type of alcoholic beverage and the strength of the alcohol content are important factors to consider in interpreting such observations. Other factors that may affect zinc absorption include the presence of other divalent metals such as calcium and iron in the gastrointestinal tract (GIT), as well as zinc-binding amino acids such as glycine, cysteine and histidine. Zinc excretion from the body is predominantly via the gut, as intestinal secretions, but also through the skin and kidney.

### ***1.2.2 Physiological roles of zinc***

Zinc is distributed throughout the body tissues (see Table 1.2) consistent with the ubiquitous requirement for zinc at the level of cellular function. Zinc is essential to myriad processes including reproduction (Ebisch et al., 2007), immune response (Salgueiro et al., 2000, Bogden, 2004, Rink and Haase, 2007), cell proliferation (Beyersmann and Haase, 2001), DNA and RNA replication and in response to oxidative stress through its influence on the synthesis and redox

state of the antioxidant glutathione (Kojima-Yuasa et al., 2005). All of the six sub-classes of enzymes include members that are zinc metalloproteins (see Table 1.3).

Tissue	Zinc concentration ( $\mu\text{g/g}$ wet weight)	Percent of total body zinc
Skeletal muscle	51	57
Bone	100	29
Skin	32	6
Liver	58	5
Brain	11	1.5
Kidneys	55	0.7
Heart	23	0.4
Hair	150	~0.1
Blood plasma	1	~0.1

*Table 1.2: Zinc distribution within the body tissues (adapted from Rink & Gabriel, 2000)*

Enzyme	Zinc function	Enzyme class	Reaction involved
Alcohol dehydrogenase (EC 1.1.1.1)	Stability and catalytic	Oxidoreductases	Alcohol metabolism
RNA polymerase (EC 2.7.7.6)	Catalytic	Transferases	DNA synthesis
Alkaline phosphatase (EC 3.1.3.1)	Catalytic	Hydrolases	Dephosphorylation
Carbonic anhydrase (EC 4.2.1.1)	Catalytic	Lyases	Interconversion of CO <sub>2</sub> & H <sub>2</sub> O to HCO <sub>3</sub> <sup>-</sup> & H <sup>+</sup>
Aldolase II (EC 4.1.2.13)	Catalytic	Isomerases	Glycolysis
Aminacyl tRNA synthetase (EC 6.1.1.1)	Catalytic	Ligases/synthetases	Protein synthesis (tyrosine-tRNA ligase)

*Table 1.3: Examples of zinc-utilizing enzymes (adapted from Rink & Gabriel, 2000)*

Newly uncovered roles for zinc include modulation of epithelial cell tight junctions. Wang and colleagues demonstrated that zinc supplementation of Caco-2 cells at 100  $\mu$ M modified tight junction properties (Wang et al., 2013), indicating a potential therapeutic use in managing tight junction leakages caused by many disease conditions. Zinc also plays an important role in facilitating cumulus expansion, which is stimulated by follicle stimulating hormone (FSH) and the release of the egg to the oviduct. This role is exemplified by the observation that ovulation was arrested in mice made zinc-deficient by using the zinc chelator, TPEN, a few days prior to egg release (Tian and Diaz, 2012). It has been shown that zinc is required for the interaction of heparin and fibrinogen necessary for promoting the haemolytic processes (Vu et al., 2009, Fredenburgh et al., 2013). The involvement of zinc in aetiology of many disease conditions such as Alzheimer's disease and age-related macular degeneration (AMD) has been proposed. For instance, the discovery that sub-retinal pigment epithelial deposits accumulate high levels of zinc in AMD patients compared with their control counterparts (Lengyel et al., 2007) suggests a plausible target for managing this condition. A very important role for zinc and a very active area of research through which understanding is increasing rapidly, is its role as a cellular second messenger in signal transduction pathways (Beyersmann and Haase, 2001, Yamasaki et al., 2007), partly orchestrated by activation of protein kinase CK2 through the phosphorylation of the zinc transporter ZIP7 (Taylor et al., 2012). This role of zinc as a signalling molecule has huge implications for intervention in human health and disease thus will sustain the attention of some of the most established researchers in the field of zinc biology over future years.

### ***1.2.3 Zinc deficiency and toxicity***

Zinc deficiency was recognised late in humans (Allen et al., 1981, Prasad, 1996) compared with other organisms such as yeast. About one-fifth of the world's population is affected by

zinc deficiency, and the condition is linked with increasing morbidity and mortality rates particularly among young children. Zinc deficiency is thus a global health problem (Ananda, 2003), with estimated prevalence at greater than 20% (World Health, 2002). The biggest burden of zinc deficiency-induced death is borne by developing African and South-Eastern Asian countries where most staple foods contain high levels of anti-nutritional factors such as phytates (Kambe et al., 2008 ) that limit zinc absorption from diets. Although incidences of severe zinc deficiency occur rarely in humans (except for those associated with acrodermatitis enteropathica; AE), mild to moderate cases (often called marginal zinc deficiency) exist, and can be classified as either primary (acquired from malnutrition) or secondary (arising from genetic alterations that can impair expression of genes coding for zinc homeostatic proteins). Due to the differences in dietary zinc intake as well as the rate of absorption/excretion among individuals, certain subsets of the human population such as children, pregnant/lactating women, strict vegetarians and the elderly are more vulnerable to incidences of zinc deficiency (Prasad, 2012). Additionally, an ageing-related decline in absorptive efficiency as well as epigenetic modifications that may impact on expression of zinc transport proteins (Fairweather-Tait et al., 2008) may further predispose the elderly to zinc deficiency even with adequate zinc intake. A concerted effort to address the inter-individual variations in zinc requirements led the relevant agencies such as the United States Food and Nutrition Board (FNB) and the United Kingdom Scientific Advisory Committee on Nutrition (SACN) to establish dietary requirements for zinc at different life stages. Table 1.4 shows zinc requirement for the UK population, as LRNI (Lower Reference Nutrient Intake), EAR (Estimated Average Requirement) and RNI (Reference Nutrient Intake) values.

An increasing body of evidence associates zinc deficiency with impaired physiological conditions (or diseases). These diseases include altered innate and adaptive immune responses, which were shown to be restored by zinc supplementation, consistent with the essentiality of

zinc as an important player in immune cell function (Ibs and Rink, 2003, Prasad, 2008). Other disease conditions shown to be associated with zinc deficiency include respiratory infections (Aggarwal et al., 2007), pneumonia (Mossad et al., 1996), age-related macular degeneration (AMD) (Evans, 2006), diarrhoea (Saper and Rash, 2009) and attention deficit hyperactivity disorder (ADHD) in children characterised by low plasma zinc concentration (Zamora et al., 2011). A recent meta-analysis of clinical data suggests an association between low zinc levels and depression in humans (Swardfager et al., 2013). In many of the cases, plausible molecular mechanisms underlying these associations are still being elucidated. Zinc supplementation, either as a single component or in concert with other antioxidants such as vitamin A or vitamin C, has been shown to ameliorate these conditions.

On the other hand, excess accumulation of zinc can result in zinc toxicity classified as acute or chronic forms. Acute zinc toxicity is characterised by conditions such as nausea and vomiting. Secondary copper deficiency, characterized by anaemia, decreased levels of erythrocyte SOD as well as increased levels of LDL and decreased HDL levels, is believed to be a consequence of chronic zinc toxicity (Hassan et al., 2000, Willis et al., 2005). The association of excess zinc with these conditions led to the recommendation of an upper limit for zinc intake as shown in Table 1.5. The underlying mechanism of zinc-induced copper deficiency appears to be the spontaneous induction of metallothionein, which in turn sequesters intracellular copper ions thereby impairing systemic copper absorption and circulation. Interestingly, however, zinc-induced copper malabsorption (or vice-versa) does not occur at normal levels of consumption of either of these micronutrients. At the cellular level, excess zinc can produce changes leading to loss of cell membrane integrity, reduced cell proliferation and production of reactive oxygen species that can damage the DNA. The negative impact of zinc deficiency and/or toxicity highlights the need for continued research-driven effort to address these nutritional problems.

Life Stage	Age	LRNI	EAR	RNI
Infants	0-3 months	2.6	3.3	4.0
Infants	4 - 6 months	2.6	3.3	4.0
Infants	7-12 months	3.0	3.8	5.0
Children	1-3 years	3.0	3.8	5.0
Children	4-6 years	4.0	5.0	6.5
Children	7-10 years	4.0	5.4	7.0
<b>Males</b>				
Adolescent	11- 14 years	5.3	7.0	9.0
Adolescent	15- 18 years	5.5	7.3	9.5
Adult/elderly	19- 50+ years	5.5	7.3	9.5
<b>Females</b>				
Adolescent	11- 14 years	5.3	7.0	9.0
Adolescent	15- 18 years	4.0	5.5	7.0
Adult/elderly	19- 50+ years	4.0	5.5	7.0
Preganancy		*	*	*
Lactation	0- 4 months			+6.0
Lactation	4+ months			+2.5

**Table 1.4: UK Dietary reference values for zinc (mg/kg). LRNI - Lower Reference Nutrient Intake; EAR - Estimated Average Recommended Requirement; RNI - Reference Nutrient Intake. \* Indicates no increment. Adapted from the UK National Diet and Nutrition Survey, 2003.**

<b>Age group</b>	<b>Upper limit (UL) in mg/day</b>
Infants 0-6 months	4
Infants 7- 12 months	5
Children 1-3 years	7
Children 4-8 years	12
Children 9-13 years	23
Adolescents 14-18 years	34

*Table 1.5: Tolerable upper intake levels (UL) for zinc. Adapted from the Institute of Medicine Panel report, 2001.*

### **1.3 Zinc homeostasis**

Zinc homeostasis refers to the maintenance of optimal levels of zinc in the face of variations in external supply or release from transient storage. This is achieved in many organisms through a carefully orchestrated mechanism that involves several players. In mammals, zinc homeostasis occurs at three domains: primary, secondary and tertiary. At the primary level, zinc homeostasis is achieved by balancing zinc absorption and endogenous zinc loss within the gastrointestinal tract (GIT), which has the principal role of maintaining whole body zinc homeostasis (Krebs and Hambidge, 2001). The secondary level of zinc homeostasis involves adjustments in urinary zinc concentration and a shift in plasma zinc turnover, which contribute to maintaining the exchangeable zinc pool (EZP) at an appropriate size (Krebs, 2000). The tertiary level involves the activities of zinc homeostatic proteins, which include metallothionein proteins (located mainly within the cytosol) and zinc transporters (localised to the plasma membrane and intracellular compartments). Many of these proteins have been identified across different species and studies on their mechanisms of action as well as their contribution to human disease conditions currently engage many researchers in the field of zinc biology.

#### ***1.3.1 Metallothioneins***

Metallothioneins (MTs) were first discovered by Margoshes & Valee over five decades ago as cadmium-binding proteins in horse kidney (reviewed in (Klaassen et al., 1999)). They are low-molecular weight, cysteine-rich, intracellular metal-binding proteins present in all domains of life. Metallothioneins are attributed roles in heavy metal detoxification (for example cadmium detoxification), maintenance of essential metal homeostasis (such as zinc and copper homeostasis) and antioxidant function (for instance protection against the impact of free radicals). In mammals, four distinct subgroups of MTs encoded by more than 10 different genes (Tai et al., 2003) have been identified and designated MT-1 to MT-4 based on a variety of

features highlighted in Table 1.6. In addition, a recent study using a bottom-up variant of mass spectrometric analysis of enriched acetylated N-terminal tryptic peptides from human cells and tissues identified up to twelve isoforms (Mehus et al., 2014). The mammalian isoforms 1 and 2 are expressed in all organs while MT-3 and MT-4 are found in the central nervous system and stratified tissues respectively (Bell and Vallee, 2009), with other isoforms expressed in different organs including kidney (Andrew Nguyena et al., 2000). Structural studies using X-ray crystallography and nuclear magnetic resonance (NMR) spectroscopy revealed that mammalian MTs contain between 60-68 amino acids with about 20 conserved cysteine residues that form the metal-binding domain. These studies also revealed two distinct globular domains: a more stable alpha domain containing 11-12 cysteine residues and a more reactive beta domain that contains 8-9 cysteine residues (Coyle et al., 2002, Ruttkay-Nedecky et al., 2013) (Figure 1.1). Although MTs bind different numbers of metal ions such as mercury ( $\text{Hg}^{2+}$ ) and lead ( $\text{Pb}^{2+}$ ) with varying degrees of affinity, they predominantly bind zinc, with a stoichiometry of up to 7 ions per molecule (which represents about 20% of the total cellular zinc content under physiological conditions), and copper, also with a stoichiometry of 7 ions per molecule (Andrews, 2001). Studies in several models, including whole animals and cell lines, have shown that expression of the MT proteins is elicited by a number of stimuli including increased abundance of metals such as zinc and copper and bacterial infection as well as other stresses such as hypoxia (Tanji et al., 2003). Metallothionein proteins contribute to zinc homeostasis by sequestering excess zinc when the levels are high, which could be from increased external supply, or by releasing zinc to the various zinc-requiring metalloenzymes under conditions of limited zinc availability (reviewed by (Choi and Bird, 2014)). Effects of changes in zinc levels on MT expression have been documented extensively. For instance, zinc-induced regulation of MT expression in the monocytic cell line (THP-1) (Cao et al., 2001), and zinc-driven changes in MTs at both the transcript and protein levels have been reported in

human tissues as well as cell lines (Wei et al., 2008). Although the involvement of metallothionein proteins in zinc homeostasis is well acknowledged, detailed mechanisms of action are not fully understood. Furthermore, the response to many other stimuli such as free radicals, for example those generated by hydrogen peroxide (H<sub>2</sub>O<sub>2</sub>) (Chung et al., 2005, Ruttkay-Nedecky et al., 2013), coupled with the difficulty of detection by “traditional” methods (owing to their lack of aromatic amino acids that means they evade usual protein detection methods), means that there is much still to be discovered about the functions of these proteins and justifies further research in this field.

Feature	Classification
Metals present	Major: MT-1 & MT-2 Minor: MT-3 & MT-4
Biological system: i. Central nervous system ii. Neurons	MT-1, MT-2 and MT-3 MT-3
Tissue expression: i. Liver and kidney ii. Brain and male reproductive organ iii. Specific to stratified squamous epithelia	MT-1 & MT-2 MT-3 MT-4

**Table 1.6: Classification of metallothionein isoforms. Adapted from Thirumoorthy et al., 2011**

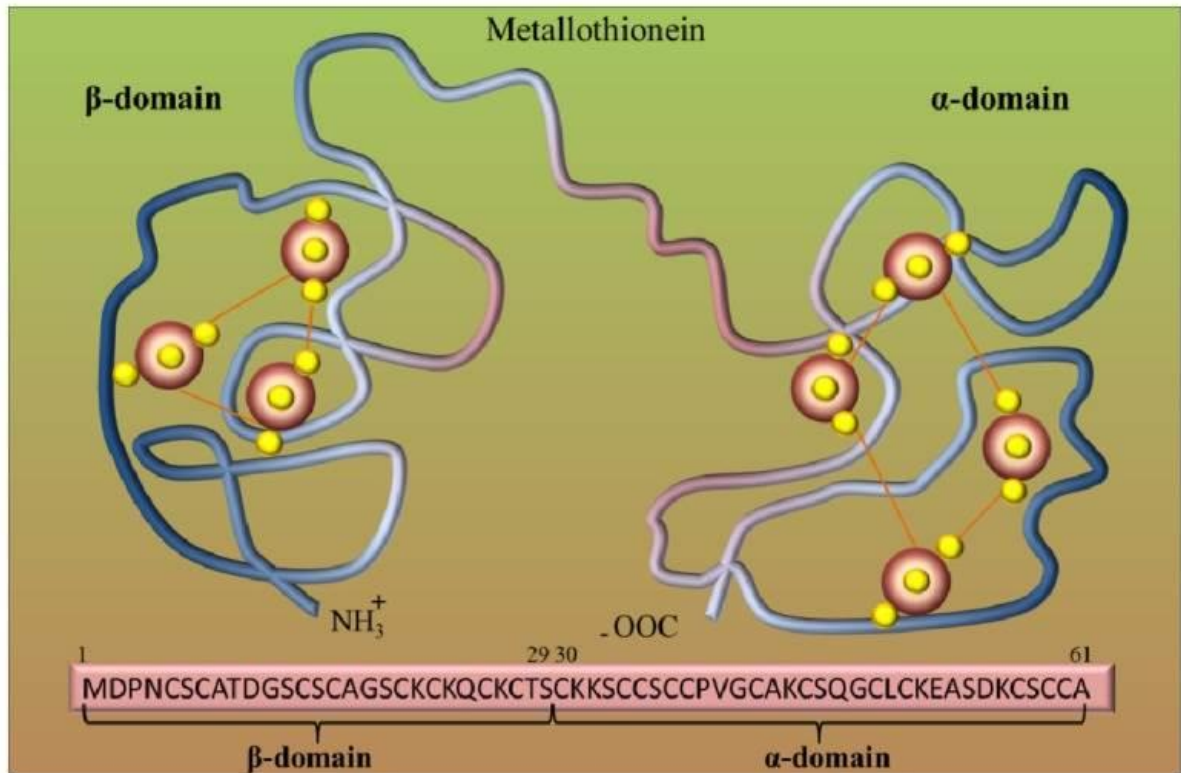


**Figure 1.1: Structure of metallothionein proteins**

A model of metallothionein structure showing two binding sites to 7 zinc atoms (large red beads) through the sulphur ligands (small yellow beads). The two domains as well as amino acid sequence and the conserved cysteine residues within each domain are indicated.

Adapted from Ruttkay-Nedecky, 2013.

### ***1.3.2 Zinc uptake proteins (the ZIP family)***

The zinc-regulated transporters, iron-regulated transporter-like proteins (also called ZRT-IRT-related proteins or ZIPs) are encoded by the SLC39 gene family. Members of this transporter family belong to the larger family of metal ion transporters that are found at all phylogenetic levels, including archaeobacteria, eubacteria and eukaryotes (Gaither and Eide, 2001b). They are named after the first members identified as *Zrt1/Zrt2* and *Irt1*, which transport zinc with low-affinity in *Saccharomyces cerevisiae* and iron with high-affinity in roots of *Arabidopsis thaliana* respectively (Eide, 2004). Across several species, more members of the ZIP family have been identified and characterised over the years. Based on sequence conservation, 14 members belonging to 4 subfamilies (designated I through IV) have been identified in human and mouse (Gaither and Eide, 2001b). Subfamily I comprises the plant and fungal proteins as well as mammalian ZIP9; subfamily II consists of ZIPs 1,2,3; subfamily III or LIV(LZT) contains the mammalian ZIPs 4-8,10 and 12-14; while the fourth subfamily, also called *gufA*, consists of proteins homologous to the *Myxococcus xanthus* proteins (Cousins et al., 2006). The SLC39 proteins are predicted to have eight transmembrane domains (TMDs), with short carboxyl and amino termini both located extracellularly. In addition, they possess a cytoplasmic variable histidine-rich motif on the loop between TMDs III and IV (Figure 1.2). This motif is believed to confer a zinc-binding property, features of which are determined by its length (Guerinot, 2000). Some members of this protein family, specifically ZIPs 11, 12 and 13, do not possess this histidine-rich loop (Kambe et al., 2004). Better conserved between the family members is a motif between TMDs IV and V, which is amphipathic and forms the aqueous channel through which zinc ions pass (Taylor et al., 2007). Members of the ZIP family generally transport zinc from an extracellular compartment (or in some cases from intracellular compartments) to the cytosol, and thus appear to play opposing roles to members of the ZnT

family (see section 1.3.3) in zinc mobilization. Expression patterns and zinc transport activity of the known members are described below.

Human ZIP1 (hZIP1), is encoded by the *SLC39A1* gene located on chromosome 1. Its cDNA clone was isolated from a prostate library using PCR screening and full-length hZIP1 was found to comprise 324 amino acids (Gaither and Eide, 2001b). hZIP1 possesses the predicted membrane topology of the ZIP family and is expressed ubiquitously in human tissues and in a variety of cell types. Zinc uptake activity was inferred as a result of the mRNA being increased in prostate epithelial cells (PC-3 cell line) under the influence of physiological levels of prolactin and testosterone, which also increased zinc uptake (Costello et al., 1999). Overexpression of the hZIP1 coding sequence tagged with the haemagglutinin epitope from a CMV-driven plasmid in human K562 erythroleukemia cells showed its localisation at the plasma membrane and accumulation of radioactive  $^{65}\text{Zn}$  in transfected cells compared with control cells, indicating zinc uptake function (Gaither and Eide, 2001b). Overexpression of hZIP1 in the human prostate cell line, PC-3, demonstrated its  $K_m$  for zinc uptake to be in the nanomolar range (Franklin et al., 2003). Mouse Zip1 was shown to be localised to the basolateral membrane of normal glandular epithelial cells (Dufner-Beattie et al., 2003a), consistent with a role in zinc uptake from interstitial fluids. On the other hand, transient expression of an EGFP/FLAG-tagged hZIP1 construct showed vesicular localisation to endoplasmic reticulum in human cells (Milon et al., 2001), suggesting a role in mobilizing zinc sequestered in intracellular organelles presumably to supplement the cytosolic level during periods of zinc limited supply. These results, in addition to the recent findings showing that overexpression of hZIP1 resulted in enhanced zinc accumulation, whereas siRNA-mediated reduction in its expression caused reduced zinc accumulation in Caco-2 cells (Michalczyk and Ackland, 2013), demonstrate the involvement of ZIP1 in redistribution of cellular zinc, and thus a possible function in cellular zinc homeostasis. A physiological role for ZIP1 in buffering

the effect of zinc deficiency was indicated using knock-out mice. Embryos of pregnant mice that had the *Zip1* gene removed were more susceptible to the effects of zinc restriction revealed as teratogenic defects, when compared with the wild-type mice (Dufner-Beattie et al., 2006). Also, hZIP1 has been shown to be important in prostate cancer. Prostate glands normally express ZIP1 at high levels coupled with accumulation of zinc (Costello et al., 1999). However, in adenocarcinomatous gland expression of the *hZIP1* gene was down-regulated at the mRNA and protein levels with concomitant depletion of zinc levels (Franklin et al., 2005). These findings were corroborated in clear cell renal carcinoma tissues, in which the expression of hZIP1, measured by RT-qPCR, was also down-regulated (Dong et al., 2014). These results were also supported by a report of *hZIP1* expression levels of African American males at risk of prostate cancer compared with their Caucasian counterparts. *hZIP1* expression was down-regulated in the former group compared with the latter (Rishi et al., 2003). These findings led to the proposal that *ZIP1* gene may be a tumor suppressor gene (Desouki et al., 2007), however, further studies are required to support this position.

Human ZIP2 (hZIP2) is encoded by the *SLC39A2* gene located on chromosome 14. The gene encodes a protein of 309 amino acids, which belongs to sub-family II of the ZIP family. hZIP2 was first identified on the basis of sequence homology to ZIP members found in fungi and plants (Gaither and Eide, 2000). ZIP2 shows a more restricted expression profile in human tissues compared to ZIP1, but the mRNA was detected in the prostate, uterus and peripheral blood monocytes by RT-PCR (Cao et al., 2001). The expression profile of hZIP2 appears to differ from that observed in mouse tissues where the mRNA was detected in the liver, ovary and visceral yolk sac also by RT-PCR (Dufner-Beattie et al., 2003a). It was observed in both human embryonic kidney (HEK293) and erythroleukaemia (K562) cells transfected with either a human or mouse overexpression construct for ZIP2 that the protein localised to the plasma membrane and increased uptake of <sup>65</sup>Zn (Gaither and Eide, 2000). ZIP2 zinc uptake activity

was shown to be stimulated by bicarbonate ions ( $\text{HCO}_3^-$ ), suggesting a mechanism of co-transport of zinc along with  $\text{HCO}_3^-$  ions. However, uptake activity, unlike that demonstrated for ZIP1, was dependent on factors including time, temperature and concentration but in an energy-independent manner. In addition, substrate specificity appeared not to be restricted to zinc since other transition metals were shown to inhibit zinc uptake activity by hZIP2 (Gaither and Eide, 2000). Indeed, a role for ZIP2 in iron sequestration was suggested in *Zip2* knock-out mice, in which a reduction in the liver iron store was observed compared with wild-type animals (Peters et al., 2007). A role for ZIP2 in the development of prostate malignancy was also implicated following an observation of its differential expression and a different zinc accumulation pattern in normal prostate gland compared with adenocarcinomatous gland (Desouki et al., 2007). Also, mice made zinc-deficient and in which the *Zip2* gene was deleted showed a greater number of abnormal embryos compared with wild-type (Peters et al., 2007), suggesting a role in adaptation to zinc-limiting conditions including during pregnancy.

The ZIP3 (*SLC39A3*) gene is located on chromosome 19 and encodes a 314-amino acid protein. Human ZIP3 was identified in a manner similar to hZIP2 based on sequence similarity to plant and fungal homologues. hZIP3 expression was first reported in normal prostate gland with localisation to the apical membrane (Desouki et al., 2007). High levels of hZIP3 expression have been reported in bone marrow and spleen, with lower expression levels in small intestine and liver (Liuzzi and Cousins, 2004). Compared to ZIPs 1 and 2, ZIP3 appears to have broader substrate specificity since metals including copper, cadmium, manganese, nickel and cobalt were shown to inhibit uptake of zinc by this protein in mice (Dufner-Beattie et al., 2003a). Experiments using knock-out mice showed that, in comparison with wild-type mice whose embryos were refractory to the effect of zinc deficiency, mice deficient in the *ZIP3* gene exhibited abnormal phenotypic outcomes (Dufner-Beattie et al., 2006). A role in mammary tissue zinc transport was demonstrated following siRNA-mediated reduction in the expression

of ZIP3 mRNA that resulted in decreased zinc uptake and eventual death of HC11 mouse mammary epithelial cells (Kelleher and Lönnnerdal, 2005). Similar to the expression of ZIP1 and ZIP2, ZIP3 expression was down-regulated along with loss of zinc accumulation both at early stages of prostate malignancy and as the tumor progressed (Franklin, 2011), adding ZIP3 to the list of putative tumor suppressor genes.

Human ZIP4 is encoded by the *SLC39A4* gene located on chromosome 8 at q24.3 and encodes a protein of 622 amino acids. The *SLC39A4* gene is now known to be the gene responsible for acrodermatitis enteropathica (AE) in humans (Wang et al., 2002). Acrodermatitis Enteropathica is an autosomal recessive genetic disorder of zinc metabolism resulting from zinc deficiency caused by insufficient absorption of zinc from the intestine, and manifests as symptoms including dermatological lesions and weight loss. Interestingly, these changes due to AE are relieved by zinc supplementation, thus indicating that other transporters in the intestine can contribute to zinc uptake from the diet. High levels of ZIP4 expression were detected in human small intestine and kidney, as well as in the mouse visceral yolk sac (Dufner-Beattie et al., 2004, Wang et al., 2002). Localisation of ZIP4 to the apical membrane of enterocytes revealed by immunohistochemical techniques (Huang et al., 2006) is consistent with a role in dietary zinc absorption. A role in zinc homeostasis was implied by an observed reduction in Zip4 mRNA abundance in response to zinc limitation (Liuzzi et al., 2004). The ability of ZIP4 to mediate zinc uptake was demonstrated in HEK293 cells transfected with mouse Zip4 cDNA (Wang et al., 2004a), by virtue of the transfected cells showing greater uptake of <sup>65</sup>Zn compared with untransfected cells. A role for ZIP4 in mouse embryogenesis was demonstrated using knock-out mice in which a homozygous deletion of the gene resulted in death of embryos at the post-implantation stage (Dufner-Beattie et al., 2007). However, heterozygous Zip4 embryos survived but were more sensitive to zinc deficiency than their wild-

type litter mates (Dufner-Beattie et al., 2007) indicating an important role for ZIP transporters in maintenance of zinc homeostasis during these developmental stages.

Mammalian ZIP5, encoded by the *SLC39A5/Slc39a5* gene is located on chromosome 12 at q13.13 in human and 10 D3 in mouse with amino acid sequence of 540 and 535 for human and mouse respectively. ZIP5 is a member of the LIV-1 subfamily and possesses the conserved peptide motif (HEXPHEXGDFAXLLXXG) in TMD 5, which is characteristic of this subfamily both in human and mouse species (Taylor et al., 2003). ZIP5 mRNA expression has been detected abundantly in tissues including small intestine and pancreas, commensurate with the importance of these tissues in systemic zinc homeostatic control. ZIP5 expression was also detected in breast cells propagated under laboratory conditions but a specific role in this tissue has not been clearly documented (reviewed by (Kelleher et al., 2009)). Unusually, however, its expression is not induced transcriptionally under zinc-limiting conditions (Weaver et al., 2007). Overexpression of ZIP5 in cultured MDCK cells showed its localisation to the basolateral membrane (Wang et al., 2004b, Weaver et al., 2007) suggesting zinc mobilization from the serous membrane into the cytoplasm. Similarly, mouse Zip5 was shown to be localised to the basolateral membrane of murine enterocytes (Huang et al., 2006) and of the visceral yolk sac (Dufner-Beattie et al., 2004), consistent with a role in zinc import from the portal circulation or mammalian circulation respectively. Zip5 zinc uptake activity was demonstrated in HEK293 cells, in which cells transfected with mouse Zip5 cDNA accumulated more zinc compared with untransfected cells (Wang et al., 2004b). Recent studies on the regulation of intestinal zinc metabolism by ZIP5 revealed its ability to modulate zinc excretion in Zip5 knockout mice as well as mobilization into pancreatic acinar cells (Geiser et al., 2013), indicating a central role in zinc homeostasis and in protection against zinc toxicity.

ZIP6 is encoded by the *SLC39A6* gene located on chromosome 18 at q12.2 in human and at 18A2 in mouse. ZIP6 shows sequence similarity with other members of the oestrogen-regulated LIV gene family, thus the gene product is also called LIV-1. hZIP6 comprises of 755 amino acids and possesses many characteristic features of the ZIP family. However, ermelin, a mouse homologue of LIV-1, appears to possess 6, rather than the typical 8 transmembrane domains (Suzuki and Endo, 2002, Taylor and Nicholson, 2003). ZIP6 is expressed at high levels in hormonally modulated tissues such as placenta, kidney, prostate and corpus callosum region of the brain with the highest expression level detected in mammary glands (Taylor et al., 2003). Zip6 expression was detected in mature, elongated spermatids along with Zip1 suggesting a role for ZIP proteins in spermatogenesis and male fertility (Croxford et al., 2011). Overexpression of a V5-tagged ZIP6 construct in Chinese hamster ovary (CHO) cells showed localisation to the plasma membrane, and zinc uptake activity was also demonstrated by virtue of the fact that cells that overexpressed recombinant ZIP6 protein showed increased zinc uptake compared with control cells (Taylor and Nicholson, 2003). Similarly, zinc uptake in SH-SY5Y neuroblastoma cells by ZIP6 has been demonstrated (Chowanadisai et al., 2008). Expression of the *SLC39A6* gene is induced by hormones such as insulin and IGF-1 and has been suggested to be a factor in the etiology of many cancer types including cancer of the breast (Shen et al., 2009), pancreas (Unno et al., 2009) and cervix (Zhao et al., 2007). However, it remains to be fully understood whether changes in ZIP6 expression observed in these malignant tumors is causal or it is an effect of cancer development.

Human ZIP7 protein is encoded by the *SLC39A7* gene located on chromosome 6 at p21.3. This gene was first discovered along with the major histocompatibility complex and later shown to have sequence homology with LIV-1 (Taylor et al., 2004). The protein (469 amino acids in humans) is also called KE4 (a membrane protein that possesses a similar histidine-rich region at TMD 5) (Eide, 2004). Analysis of a panel of human and mouse tissues showed abundant

expression of ZIP7/Zip7 mRNA detected by northern blotting and western blotting also detected the protein in mouse brain and liver tissues (Huang et al., 2005). Immunohistochemistry studies revealed that ZIP7 was localized to the Golgi apparatus, suggesting a role in mobilizing zinc out of this compartment into the cytosol. Zinc transport activity was demonstrated in CHO cells, in which overexpression of a V5-tagged recombinant ZIP7 resulted in increased cytosolic zinc levels in transfected cells compared with untransfected cells (Taylor et al., 2004). Similarly, the role of ZIP7 in facilitating zinc release from the endoplasmic reticulum into the cytosol was demonstrated in mast cells (Yamasaki et al., 2012). Similar to ZIP5 and ZIP6, ZIP7 expression was regulated by iron in addition to zinc (Nam and Knutson, 2012), suggesting a broader substrate specificity. Physiological importance of a zinc transport function for ZIP7 was suggested by the observation that zip7 knock-out in zebrafish have a phenotype that is rescued by zinc supplementation (Yan et al., 2012). A mouse model of alcoholic liver disease showed altered expression of Zip7 mRNA, and alcohol-induced zinc deficiency was proposed to be mediated through oxidative stress affecting Zip7 expression (Sun et al., 2014). Recent studies showed that ZIP7 may play a role in glucose metabolism in skeletal muscle by virtue of the fact that siRNA-driven reduction in ZIP7 expression in C2C12 cells resulted in down-regulation of a suite of genes including the glucose transporter GLUT4 (Myers et al., 2013). Although the mechanism underlying this link has not been elucidated, the finding lend support the role in signalling pathway that may be mediated by the activity of ZIP7.

Human ZIP8 is encoded by the *SLC39A8* gene located on chromosome 4 between 4q22 and 4q24. In comparison to other members of the ZIP family, ZIP8, which is also known as BIGM103 (for BCG-induced integral membrane protein in monocyte clone 103 protein), showed the highest degree of sequence similarity with ZIP14 albeit both proteins possess distinct tissue expression with ZIP8 expressed at higher level in brain tissues compared with

ZIP14 (Taylor et al., 2005). These two proteins differ only in about thirty amino acid residues (460 in ZIP8 compared with 492 in ZIP14) located within the amphipathic region between TMDs IV and V. The amphipathic region is predicted to be the channel through which the zinc ion passes (Eng et al., 1998). Mouse Zip8 protein was detected by immunoblotting in membranes of matured red blood cells (RBC) and mRNA expression was shown to be regulated by zinc deficiency in the same cell type during zinc deprivation (Ryu et al., 2008), implying involvement in zinc mobilization for erythroid differentiation and maturation. ZIP8 zinc uptake ability was demonstrated in CHO cells overexpressing the recombinant protein, and zinc uptake was stimulated by inflammatory cytokines (Begum et al., 2002). The protein has been shown to translocate to the plasma membrane or to mitochondria in response to inflammatory signals (Begum et al., 2002). Although ZIP8 was initially associated with transport of only zinc, its ability to transport iron across the plasma membrane has been demonstrated in human embryonic kidney 293T cells expressing mouse Zip8 (Wang et al., 2012). Other metals that appear to be substrates for ZIP8 include manganese and cadmium (Himeno et al., 2009). ZIP8 has been shown to be a critical protein in zinc-mediated cytoprotection of lung epithelial cells (Besecker et al., 2008), highlighting its importance in cell membrane integrity. ZIP8 also appears to play a role in the response to both cadmium and manganese toxicity (Fujishiro et al., 2012).

ZIP9 is encoded by the *SLC39A9* gene located on human chromosome 14 at q24.1 and contains 307 amino acids. It appears to be a less studied member of the ZIP family partly because of its existence as a single member of the vertebrate subfamily I (Eide, 2004). However, its sub-cellular localization and involvement in zinc removal from the trans-Golgi network was inferred from work in chicken DT40B cells stably expressing a HA-tagged hZIP9 construct, which caused a decrease in the activity of the zinc-dependent Golgi localised enzyme alkaline phosphatase (ALP) (Matsuura et al., 2009). A reduction in alkaline phosphatase activity may

be attributable to removal of zinc from the Golgi apparatus by the overexpressed ZIP9, thus limiting the supply available to the enzyme. In DT40 cells, knockout of the ZIP9 gene suppressed phosphorylation of AKT and ERK, which is necessary to activate the beta cell receptor signalling pathway (Taniguchi et al., 2013).

Mammalian ZIP10 is encoded by the *SLC39A10/Slc39a10* gene located at 2q33.3 and 1C1.1 in human and mouse respectively. hZIP10 was identified through bioinformatics analysis as a protein of 385-amino acids with features characteristic of the ZIP family. ZIP10 expression was detected in kidney, liver, pancreas, brain and intestine (showing the highest expression level) among other human tissues tested (Kaler and Prasad, 2007). Rat Zip10 was first isolated from renal brush border membrane as a 40 kDa protein that showed the highest affinity for zinc in preference to other metals tested (Kumar and Prasad, 1999). The cDNA was later cloned by the same group from renal cortex (Kumar and Prasad, 2000). Overexpression of recombinant ZIP10 in pig kidney epithelial-like cells (LLC-PK1) showed that it was localised to the plasma membrane, and its involvement in zinc uptake was also demonstrated (Kaler and Prasad, 2007). The protein appears to have a role in breast cancer metastasis that is independent of the similar function attributed to ZIP6 (Kagara et al., 2007).

Human ZIP11 (342 amino acids) is encoded by the *SLC39A11* gene located at 17q21.31. It is a unique member of the ZIP family by virtue of being the only known member of the gufA sub-family, which is named after the Gram-negative bacterium *Myxococcus xanthus*, owing to its similarity with the predicted metal transporters designated as channels or porins in this organism (Getsin et al., 2013). Zip11 mRNA was detected in a panel of murine tissues such as pancreas, jejunum, ileum, with the highest expression detected in cecum by RT-PCR (Yu et al., 2013). Mammary cells were also shown to have significant levels of ZIP11 expression consistent with involvement in redistribution of the mammary zinc pool during lactation

(Kelleher et al., 2012b). Immunohistochemistry in cultured mammary cells showed localisation to intracellular compartments, especially the Golgi apparatus and ER, but a specific role has not been identified (Kelleher et al., 2012a). Overexpression of murine Zip11 in human embryonic kidney 293T (HEK293T) cells resulted in increased intracellular zinc accumulation in transfected cells compared with control cells (Yu et al., 2013). In addition, siRNA-mediated reduction in Zip11 expression resulted in a decrease in intracellular zinc levels (Yu et al., 2013) consistent with a zinc uptake function for ZIP11. The plant orthologue of Zip11 has also been recently identified and functionally characterised in maize (zmZIP11) as a potential divalent metal transporter (Li et al., 2013).

The ZIP12 gene (*SLC39A12*) is mapped to 10p12.33 in human and the protein is predicted to have 654 amino acids. ZIP12 expression has been detected in the human eye (Wistow et al., 2002) and brain (Suzuki et al., 2004). In contrast to the apparent localisation of hZIP11 in the intracellular compartment of the mammary gland, hZIP12 protein was associated particularly with the apical cell membrane (Kelleher et al., 2012a), consistent with zinc influx to the cytosol from the extracellular space. ZIP12 has been linked to schizophrenia, a neurological disorder characterised by low brain zinc concentration (reviewed by (Lichten and Cousins, 2009)), but a specific function in this context is not yet defined.

Human ZIP13 (*SLC39A13*) gene, located at 11p11.2, codes for a member of the LIV-1 subfamily with 371 amino acids. The protein topology was first reported by (Bin et al., 2011), who also demonstrated a ZIP13-enhanced increase in metallothionein expression in HEK293T cells and that homodimerization of ZIP13 subunits is necessary for zinc transport. Expression of ZIP13 and zinc-dependent regulation has been shown in many human tissues including testis and pancreas (Yang et al., 2013). Subcellular localization to vesicular compartments under different conditions of zinc availability was demonstrated through immunofluorescence of a

GFP-tagged ZIP13-containing plasmid in both HEK293T and HepG2 cells (Jeong et al., 2012). Similarly, a role in vesicular export of zinc was evident in HEK293T cells transfected with a ZIP13 overexpression construct. Loss-of-function mutation in the *SLC39A13* gene is implicated as a genetic cause of a heritable disorder of connective tissue known as spondylocheiro dysplastic Ehlers-Danlos Syndrome (SCD-EDS) (Beighton et al., 1998, Fukada et al., 2008). A role for ZIP13 in SCD-EDS and in tooth/bone development was identified using knockout mice (reviewed by (Fukada et al., 2011)), but the molecular mechanisms underlying ZIP13-mediated activities are largely unclear.

Human ZIP14 (492 amino acids), which is encoded by the *SLC39A14* gene located at 8p21.3, was identified as a gene product that was induced during adipocyte differentiation (Tominaga et al., 2005). ZIP14 was reported first in 2005 as a member of the LIV-1 subfamily that lacks the characteristic histidine-rich residue in transmembrane domain V (Taylor et al., 2005). Northern blotting analysis of a panel of normal human tissues and tissues from cancer cell lines showed ubiquitous and abundant expression in the liver, pancreas and intestine (Taylor et al., 2005). However, low levels of expression were detected in the brain in comparison with ZIP8, which is the most closely-related family member. ZIP14 was demonstrated to localise to the plasma membrane in K562 cells. Zinc transport activity was demonstrated in spite of the absence of the 'essential' histidine signature motif, thus challenging the widely accepted role of this module in zinc transport. The role of ZIP14 in facilitating uptake of metals additional to zinc, including iron, manganese, nickel and cadmium, was demonstrated in *Xenopus* oocytes injected with the murine Zip14 cDNA (Pinilla-Tenas et al., 2011). ZIP14 mRNA expression and concomitant accumulation of manganese in response to interleukin 6 treatment was shown in neuroblastoma (SH-SY5Y) cells (Fujishiro et al., 2014). Expression of ZIP14 at both mRNA and protein levels was up-regulated by lipopolysaccharides (LPS) treatment in wild-type mice

compared with Zip14 knockout mice (Beker Aydemir et al., 2012), suggesting that ZIP14 could be a marker of immune response disorders.

### ***1.3.3 Zinc efflux proteins (the ZnT family)***

The mammalian ZnT transporters belong to the cation diffusion facilitator (CDF) superfamily of intermembrane divalent metal ion transporters. The CDF transporters have more than 100 members, which are found in all organisms at all phylogenetic levels (Gustin et al., 2011). On the basis of sequence similarity the CDF superfamily members are divided into three classes designated I to III. Class I are mainly prokaryotic members while classes II and III contain both prokaryotic and eukaryotic members in similar proportions (Gaither and Eide, 2001a). The mammalian homologues have representatives spread across classes II and III, and comprise 10 members named ZnT1-10, which are subdivided into 4 subfamilies designated I to IV (Huang and Tepasorndech, 2013). Subfamily I is made up of ZnTs 5 and 7; subfamily II comprises ZnTs 2, 3, 4 and 8; subfamily III is composed of ZnTs 1 and 10, while ZnTs 6 and 9 belong to subfamily IV (Huang and Tepasorndech, 2013). Most members of the ZnT proteins are predicted to have six transmembrane domains with an intracellular histidine/serine-rich loop region between TMDs IV and V (Figure 1.2) and long C-terminal tails. Many features characterise the ZnT family, including zinc efflux from the cytosol to the extracellular compartment or into intracellular vesicles, and homodimerization (for example homooligomerization of ZnT7), which has been shown to be important for zinc transport activity. An emerging phenomenon shown by some members is heterodimerization, in which 2 different members form heteromeric complexes to facilitate zinc transport to targeted cellular compartments. This phenomenon is exemplified by heterodimerisation between Msc2 and Zrg17, which directs zinc to the endoplasmic reticulum in *Saccharomyces cerevisiae* (Ellis et al., 2005), and the dimerization between mammalian ZnT5 and ZnT6 necessary for zinc

transport to the secretory pathway (Suzuki et al., 2005a). In the latter example, ZnT6 is thought to play a structural role owing to the absence of what is described as the transient zinc-binding module; a potential zinc-binding site comprising of 2 aspartate and 2 histidine residues present only in ZnT5 (Ohana et al., 2009, Wu et al., 2011). In spite of many similar features of ZnT transporters, members can be distinguished from one another on the basis of the length as well as the amino acid sequences located upstream of TMD 1, which contains the targeting signal.

ZnT1 is encoded by the *SLC30A1* gene, which is mapped to chromosome 1 in both humans and mice, and it was the first cloned mammalian zinc transporter of the CDF family. ZnT1 (507 amino acids) shows ubiquitous tissue distribution but higher levels of expression were detected in tissues known to be involved in zinc acquisition, recycling and transfer such as the small intestine (Liuzzi et al., 2001, Kambe et al., 2004). Subsequently, localisation to the basolateral membrane in the epithelial cells of the intestine (enterocytes) and kidney was demonstrated, indicating a role in zinc transfer to the portal circulation for systemic distribution and zinc recovery from glomerular filtrate (Cousins et al., 2006). Znt1 has also been shown to localize to the mouse villous yolk sac membrane suggesting involvement in mediating zinc transport from maternal zinc pool to the foetus. Znt1 conferred resistance to high extracellular zinc concentrations in zinc-sensitive baby hamster kidney (BHK) cells, which were transfected with the mouse Znt1 cDNA (Palmiter and Findley, 1995) indicating an efflux function. Immunofluorescence revealed high levels of ZnT1 at the plasma membrane of HepG2 hepatoma cells exposed to zinc and cadmium compared with basal levels, indicating that cadmium, in addition to zinc can induce ZnT1 expression (Urani et al., 2010). The zinc transport activity of ZnT1 has been studied in several cell types including HEK293 cells, leading to the proposal that ZnT1 is a  $Zn^{2+}/H^{+}$  exchanger (Shusterman et al., 2014). A global expression profile of zinc efflux transporters in different subsets of leukocytes in response to changes in zinc concentration identified ZnT1 as the most regulated member of this group

(Overbeck et al., 2008), consistent with a role in mediating zinc homeostasis. Importance of ZnT1 function at the systemic level was reported by Andrews and colleagues in a study showing that homozygous knockout of *Znt1* in the mouse resulted in early embryonic lethality (Andrews et al., 2004).

ZnT2 is encoded by the *SLC30A2* gene, also located on human chromosome 1. The gene produces 2 variants “a” and “b” by alternative splicing with the longer variant encoding a protein of 383 and the shorter one encoding 334 amino acids. Bioinformatics analysis showed that the two isoforms differ only at the N-terminal region (Liuzzi and Cousins, 2004, Lopez and Kelleher, 2009). *Znt2* mRNA has been detected in placenta, kidney, small intestine and mammary gland in the rat (Liuzzi et al., 2003). High levels of *Znt2* were also detected in rat prostate, where it was found to be restricted to zinc-rich regions of the lateral and dorsal lobes (Iguchi et al., 2002). Dietary zinc was shown to modulate expression levels of *Znt2* in rat by inducing increased mRNA expression (Liuzzi et al., 2001). In contrast to ZnT1, which primarily localises to the cell membrane and facilitates zinc efflux into extracellular space, ZnT2 was shown to localise to subcellular organelles (endosome /lysosome vesicles) in BHK cells transfected with rat *Znt2* cDNA (Palmiter et al., 1996a). Immunohistochemical staining of intestine tissues excised from pregnant rats maintained on zinc diet revealed localisation of *Znt2* to the apical region of enterocytes, consistent with involvement of *Znt2* in mobilising zinc from the maternal pool to maintain adequate supply to the foetus (Liuzzi et al., 2003). Overexpression of ZnT2 as an HA-tagged recombinant protein revealed localisation of the two isoforms to different compartments, the longer variant to the secretory compartment and the shorter one to the plasma membrane (Lopez and Kelleher, 2009). Clinical relevance of ZnT2 was identified when it was found that mutation in the *ZnT2* gene resulted in infant zinc deficiency in women with a low milk zinc concentration (Chowanadisai et al., 2006), suggesting a role for ZnT2 in mammary gland zinc homeostasis.

Mammalian ZnT3 was identified through screening a mouse cDNA library using rat Znt2 cDNA (Palmiter et al., 1996b). In mouse, Znt3 is encoded by the *Slc30a3* gene located on chromosome 5. The protein has a predicted topology that is characteristic of the ZnT family members. The human homologue is located on chromosome 2 at p23.3 and encodes a protein of 388 amino acids, which shares greater than 80% identity with both rat and mouse Znt3 proteins (Gaither and Eide, 2001a). Znt3 mRNA was detected in rodent brain and testis and in a human breast epithelial cell line PMC42) (Palmiter et al., 1996b), whereas the protein was detected in mouse spinal cord (Danscher et al., 2003), thus a role in mediating zinc homeostasis between cerebrospinal fluid and the brain was suggested. Although ZnT3 expression was thought to be restricted to brain cells, later studies detected expression in other cell populations including duodenal epithelial cells (Wongdee et al., 2009), human airway cells (Ackland et al., 2007), human adipose cells (Smidt et al., 2007), mouse retina cells (Redenti and Chappell, 2004) and leucocytes (Overbeck et al., 2008). These findings are consistent with a versatile involvement of ZnT3 in cellular zinc homeostasis. In contrast to ZnTs 1 and 2, overexpression of ZnT3 did not affect the response of BHK cells to zinc load, but evidence from knock-out models support the premise that Znt3 may be important in zinc efflux particularly to synaptic vesicles (Cole et al., 1999). Zinc transport activity of ZnT3 is thought to be enhanced by homodimerisation involving tyrosine residues on the protein, a phenomenon that was shown to be induced by oxidative stress, and is required for targeting zinc to synaptic-like micro-vesicles (Salazar et al., 2009). Modulation of ZnT3 expression by factors such as age, hormones and glucose (Patrushev et al., 2012, Beyer et al., 2009), may imply involvement of ZnT3 in multiple disease conditions.

The human ZnT4 gene (*SLC30A4*) located on chromosome 15 encodes a 430 amino acid-long protein, which is similar to ZnT2 and ZnT3 (Huang and Gitschier, 1997). ZnT4 was originally identified unexpectedly by positional cloning while searching for the gene whose mutation was

responsible for the heritable zinc deficiency in the lethal milk (*lm*) mouse, characterised by insufficient zinc in the milk to support the development of suckling pups (Huang and Gitschier, 1997). This mutation (nonsense mutation) was identified as a single nucleotide substitution of C by T at 934 bp within the arginine codon that represents the 297<sup>th</sup> amino acid on the protein (Huang and Gitschier, 1997). *In silico* analysis revealed that the protein contains a leucine zipper motif (Murgia et al., 1999), a unique feature, which is additional to the characteristic features ZnT4 shares with other members of the ZnT family. High levels of expression were detected in rat small intestine, where it was found localised to the apical membrane in suckling pups but predominantly at the basolateral area in older rats (Murgia et al., 1999). Similarly, high levels of mRNA expression were detected in a panel of human samples including testis, brain and small intestine (Liuzzi et al., 2001), as well as mammary gland (Liuzzi et al., 2003) and in adult rat kidney (Ranaldi et al., 2002). Immunohistochemical evidence of stained sections of rat small intestine revealed localisation of Znt4 to endosomes at the basolateral region of enterocytes, consistent with a role in zinc efflux. However, in cultured mouse mammary epithelial cells, Znt4 was found localised to the trans-Golgi network, consistent with a role supplying zinc proteins of the secretory pathway (McCormick and Kelleher, 2012). Zinc efflux function of ZnT4 was demonstrated using a zinc-sensitive yeast strain lacking the *Zrc1* gene ( $\Delta Zrc1$ ), in which expression of mouse *Znt4* cDNA conferred resistance to zinc (Huang and Gitschier, 1997). The zinc transport function of ZnT4 was demonstrated to involve the metal-binding loop located between TMDs IV and V by affinity chromatography using GST-His construct containing the Znt4 putative metal-binding domain (Murgia et al., 1999).

ZnT5 was identified through database searches with sequences homologous to the human ZnT1 and yeast *Zrc1*. ZnT5 exists as splice variants A and B. Variant A (ZnT5A) contains 15 predicted transmembrane domains (TMD) and encodes a protein of 765 amino acids with a predicted molecular weight of 84 kDa (Kambe et al., 2002). Variant B (ZnT5B) has 12

predicted TMD and is a protein of 523 amino acids with a molecular weight of 57 kDa (Cragg et al., 2002). ZnT5 mRNA was detected in human endocrine pancreas, prostate, ovary, kidney and testis (Inoue et al., 2002) and both variants were also detected in a panel of normal human tissues by RT-PCR including kidney, brain, and small intestine (Thornton et al., 2011). Overexpressed ZnT5A was shown to be localised to the Golgi apparatus in HeLa cells (Kambe et al., 2002), and was shown to mediate zinc uptake into this compartment in a concentration-dependent manner. ZnT5B on the other hand, was shown to localise to the apical membrane in enterocytes and zinc uptake into *Xenopus laevis* oocytes expressing the protein was shown to be dependent on the pH (Cragg et al., 2002). Though not proven, differential localization of ZnT5 splice variants was proposed to be dependent on their alternative C-terminal sequences, which thus appears to include the localisation signal (Thornton et al., 2011). The observation that ZnT5B mediated zinc uptake as well as efflux in *Xenopus laevis* oocytes (Valentine et al., 2007) and increased expression of a zinc-induced reporter in Caco-2 cells revealed that the protein is capable of bidirectional zinc transport, thus challenging the paradigm that members of the ZnT family are primarily zinc effluxers. Zinc transport activity of ZnT5 was shown to involve hetero-oligomerisation between ZnT5 and ZnT6 to mediate zinc mobilisation to the secretory pathway (Ellis et al., 2005), a phenomenon that was corroborated by another group as an emerging feature of the CDF zinc transporters (Lichten and Cousins, 2009). The findings above were recently supported by visualisation of ZnT homodimers and heterodimers in live cells using bimolecular fluorescence complementation (BiFC) (Lasry et al., 2014). A role for ZnT5 in normal function at the systemic level was demonstrated by virtue of the fact that deletion of the gene encoding this protein in mice resulted in a plethora of abnormalities including poor growth, cardiac bradyarrhythmia and low bone density (osteopenia) (Inoue et al., 2002). Also, a role for ZnT5 in the cellular stress response was suggested by work in DT40

cells, where a ZnT5/ZnT6 double knock-out meant that cells could not survive tunicamycin-induced stress (Ishihara et al., 2006).

Human ZnT6 is encoded by the *SLC30A6* gene located on chromosome 2 at a position between p21 and p22. The *Slc30a6* gene that codes for the mouse homologue is located on chromosome 17. Znt6 was identified through a search of the EST database using mouse Znt4 amino acid sequence as a protein of 460 amino acids, which possesses a unique serine-rich region in place of the conserved histidine-rich region (Huang et al., 2002). ZnT6 can also be distinguished from other members of the ZnT family by virtue of the fact that it possesses the longest C-terminal sequence made up of 203 amino acids (Huang and Tapaamorndech, 2013). High levels of ZnT6 mRNA expression was detected in tissues such as kidney, liver, brain and small intestine by Northern blotting, however, this mRNA expression did not correlate with protein expression detected using immunoblotting in some tissues especially liver (Huang et al., 2002), suggesting that ZnT6 expression may be subject to some forms of post-transcriptional modification that might influence tissue-specific expression. Indeed, potential sites for phosphorylation or N-glycosylation have been predicted for ZnT6 using bioinformatics tools (Huang et al., 2002). Immunohistochemical analysis of mouse gastrointestinal tract detected Znt6 expression in columnar epithelial cells of the jejunum, colon and cecum and in the gastric chief cells, consistent with a role in intestinal zinc absorption and secretion (Yu et al., 2007). Immunofluorescence studies in normal rat kidney epithelial cells (NRK) using affinity purified antibody against the C-terminal sequence, revealed that ZnT6 was localised to the Golgi network (TGN) but translocates to the cell periphery in response to increased extracellular zinc concentration (Huang et al., 2002), consistent with a role in zinc mobilization from the cytosol into the TGN or zinc export into the extracellular space. ZnT6 expression was shown to be regulated by pro-inflammatory molecules by virtue of the fact that mice treated with lipopolysaccharides (LPS) showed increased ZnT6 mRNA expression compared with

untreated controls (Liuzzi and Cousins, 2004), suggesting that ZnT6 may be involved in the inflammatory response. Zinc transport function of ZnT6 was inferred from studies using wild-type yeast and mutants ( $\Delta Zrt1$ ,  $\Delta Zrt3$  and  $\Delta Msc2$ ) that are deficient in cytoplasmic zinc, in which overexpression of Znt6 resulted in growth inhibition compared with mutants transformed with vector only construct (Huang et al., 2002). Studies in DT40 cells deficient in ZnT5/ZnT6 complex showed that hetero-oligomerisation of these two proteins is required for its zinc transport function (Ishihara et al., 2006). Altered expression of ZnT6 in brain sections of patients with mild cognitive impairment and early stage of Alzheimer's disease (AD) (Smith et al., 2006), as well as in brain tissues of mouse model of AD suggests that ZnT6 may be involved in the etiology of AD (Zhang et al., 2010).

Human ZnT7 is encoded by the *SLC30A7* gene located on chromosome 1 and was identified through a search of EST databases with the amino acid sequence of mouse Znt1. The protein has 376 amino acids and shares up to 95% amino sequence identity with mouse Znt7 (Kirschke and Huang, 2003) documenting the highest sequence similarity by any 2 members of the mammalian ZnT family (Liuzzi and Cousins, 2004). Znt7 mRNA expression was detected in many mouse tissues including liver, spleen, heart, brain, lung and small intestine (Kirschke and Huang, 2003) but the protein showed more restricted expression and was detected only in tissues of small intestine and lung (reviewed by (Lichten and Cousins, 2009). Some levels of Znt7 expression were also detected in mouse retina (Wang et al., 2006), GIT (Yu et al., 2007) and cerebellar cortex (Gao et al., 2009). Overexpression of mouse Znt7 in CHO cells visualised by immunofluorescence microscopy showed localisation to the Golgi apparatus with concomitant accumulation of zinc consistent with a role in zinc efflux from the cytoplasm into the Golgi lumen (Kirschke and Huang, 2003). ZnT7 has been shown to mediate zinc transport to enzymes of the secretory pathway such as alkaline phosphatase (Suzuki et al., 2005a). This role appears less significant compared to that played by the duo of ZnT5 and ZnT6 via hetero-

oligomerisation by virtue of the fact that mutation in the *Znt7* gene in DT40 cells only resulted in a 20% loss in the activity of tissue non-specific alkaline phosphatase (TNAP) (Suzuki et al., 2005b). The reason for this perceived lesser contribution of ZnT7 in activating TNAP may be due to the fact that pull-down assay in DT40 cells transfected with recombinant *Znt7* revealed homo-oligomers (Suzuki et al., 2005b), rather than hetero dimerization between ZnT5 and ZnT6 that was demonstrated in earlier studies to facilitate zinc transport into the secretory pathway. Overexpression of mouse *Znt7* in pancreatic RIN5mf cells was shown to modulate the expression of insulin through MTF-1-dependent mechanism (Huang et al., 2010), thus the protein may be important in glucose metabolism. It was recently reported that overexpression of *Znt7* in MC3T3-E1 cells (mouse osteoblast precursor cell line) resulted in significant protection of these cells from hydrogen peroxide-induced apoptosis (Liang et al., 2013) suggesting an antioxidant role for ZnT7.

Human ZnT8 was identified through a search of EST databases with amino acid sequence of all known human ZnT proteins (Chimienti et al., 2004). The *SLC30A8* gene is mapped to chromosome 8. The protein has 369 amino acids and shows about 42% sequence with ZnT3. Analysis of a panel of 22 mouse tissues by RT-PCR showed that *Znt8* mRNA expression was detected in mouse liver and pancreatic cells with the highest expression detected in mouse islet of Langerhans (Chimienti et al., 2004, Lemaire et al., 2012). Although ZnT8 appears to be expressed predominantly in insulin-secreting beta cells, significant levels of both ZnT8 mRNA and protein expression has been detected in human retinal pigment epithelial (ARPE19) cells (Leung et al., 2008) and in human lymphocytes as well as adipocytes (reviewed by (Davidson et al., 2014). Confocal immunofluorescence analysis of an EGFP (enhance green fluorescent protein) tagged recombinant ZnT8 expressed in insulin-secreting pancreatic cell line (INS-1) showed localisation in the secretory pathway granules, which was observed to overlap with insulin staining pattern (Chimienti et al., 2004) consistent with involvement of ZnT8 in

providing zinc for insulin maturation. Zinc transport function of ZnT8 was demonstrated in HeLa cells stably expressing an EGFP-tagged ZnT8 protein by virtue of the fact that cells transfected with ZnT8-EGFP construct accumulated more zinc compared with cells expressing the vector only construct (Chimienti et al., 2004). Zinc efflux of ZnT8 was observed to be stimulated by glucose thus a role in glucose metabolism in general, and diabetes in particular has been attributed to this protein. Furthermore, a single nucleotide polymorphism (SNP) designated rs13266634, which was found to be more prevalent in subjects of type II diabetes compared to their control counterparts (Sladek et al., 2007) gave evidence in support of the importance of ZnT8 in etiology of diabetes. In addition, aberrant expression of ZnT8 in the retina has been proposed as an underlying factor in the etiology of ischemic retinopathy (DeNiro and Al-Mohanna, 2012). These findings suggest that ZnT8 may be involved in multiple disease conditions.

Human ZnT9 was originally identified on the basis on its similarity to the *HUEL* gene, which was isolated from human embryonic lung cells (MRC-5) (Sim and Chow, 1999). The *HUEL* gene has been mapped to chromosome 4 at p12-p13. The gene encodes a protein of 568 amino acids, which was detected on western blot as a band of ~70 kDa present in both cytosolic and nuclear fractions (Sim et al., 2002). The protein has been found to contain DNA excision repair motif and a nuclear receptor interaction consensus signature LXXLL (where X represents any amino acid (Cousins et al., 2006)). An established role in zinc transport has not been demonstrated for this protein, but evidence based on observed translocation of HUEL from the cytoplasm to the nucleus in human primary hepatocellular carcinoma cell line (PLC/PRF/5) in response to growth arrest inhibitor mimosine, suggests a role in gene regulation rather than in zinc efflux (Sim et al., 2002). Recently, however, ZnT9 was identified among “zinc-transporting network” that may play important role in redistributing zinc within mammary gland and secretion into milk (Kelleher et al., 2012a). Furthermore, RT-PCR analysis of a

cohort of zinc transporters in obese subjects compared to control subjects revealed down-regulation of ZnT9, suggesting that altered expression of this protein may be a possible marker in the aetiology of obesity (Noh et al., 2014).

ZnT10 is encoded by the *SLC30A10* gene located on human chromosome 1 at q41. The protein was identified through an *in silico* analysis of the human genome with known ZnT cDNA and protein sequences (Seve et al., 2004). ZnT10 shows the highest sequence similarity with the ZnT1 compared to other members of ZnT family. ZnT10 expression was thought to be restricted to fetal tissues including liver and brain (Seve et al., 2004), however, evidence from recent studies detected ZnT10 mRNA expression in adult mouse and human brain (Bosomworth et al., 2012) as well as in human liver (Yang et al., 2013). Zinc transport function was demonstrated in neuroblastoma cell line (SH-SH5Y) expressing recombinant ZnT10 protein tagged with a FLAG epitope, which showed translocation to the plasma membrane from the Golgi apparatus in response to zinc (Bosomworth et al., 2012) consistent with zinc efflux role. In addition, ZnT10 has been implicated in manganese homeostasis, evidenced by the observation in SH-SH5Y cells that IL-6-induced reduction in ZnT10 expression affected efficiency of manganese excretion (Fujishiro et al., 2014). Recent observations associating altered ZnT10 expression with Alzheimer's disease (Bosomworth et al., 2013) and a form of brain tumour (glioma) (Lin et al., 2013) suggest that this protein may be involved in etiology of AD.

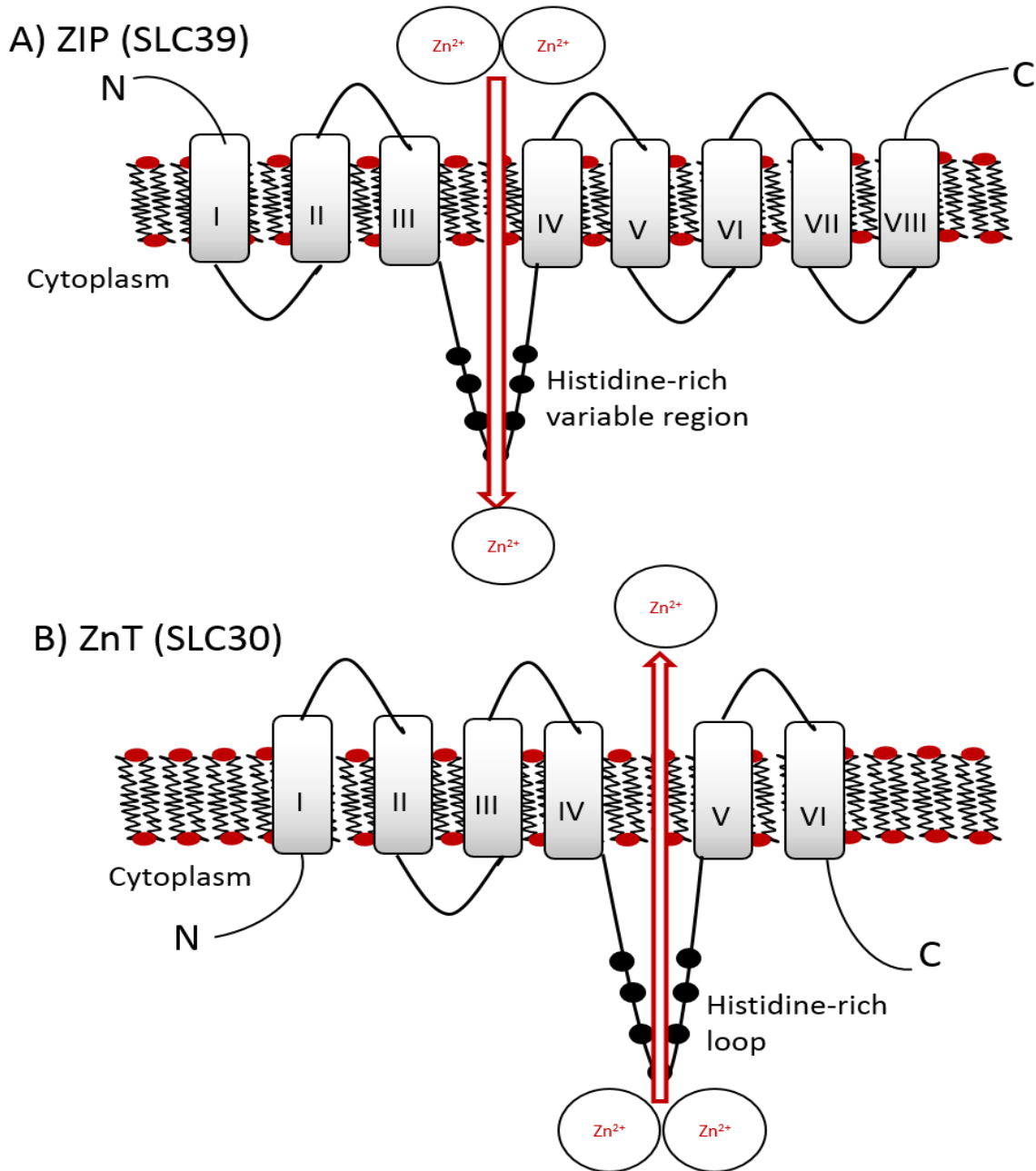


**Figure 1.2: Schematic representation of predicted general topologies of ZIP and ZnT transporters.**

The predicted membrane topologies of SLC39/ ZIP and SLC30/ZnT zinc transporters are shown with the transmembrane domains and conserved histidine-containing regions as well as direction of zinc transport in the cell.

#### 1.4 Transcriptional regulation of zinc homeostatic proteins by zinc

The expression of many genes whose products play important roles in maintaining zinc homeostasis is controlled at the transcriptional level. Transcription factors that have this function are found across all kingdoms of life and include both activators and repressors. A common feature underlying the action of these regulatory proteins in response to altered zinc availability is the recognition of specific sequence elements within promoter regions of their target genes to which they bind and thus effect the transcriptional response. In prokaryotes, the *Escherichia coli* transcriptional regulator ZntR, a homologue of the MerR protein, binds to an inverted repeat sequence comprising 11-11 bp located between -10 and -35 motifs in the *zntA* promoter to mediate *zntA* gene induction in response to increased zinc concentration (Brocklehurst et al., 1999). In contrast to the action of ZntR, the *Bacillus subtilis* metalloregulator Zur effects transcriptional repression of a suite of genes including *yciC* (a homologue of *CobW* gene in *Pseudomonas denitrificans*) under condition of zinc deficiency through binding to a zur box in the promoter of its target genes (Gaballa et al., 2002). Unlike other members of the Fur metalloregulators such as *Bacillus subtilis* peroxide-sensing (*BsPerR*) (Lee and Helmann, 2006) and *Pseudomonas aeruginosa* iron-responsive Fur (*PaFur*) (Pohl et al., 2003), Zur appears to require a more extended binding site comprising the inverted repeat sequence 9-1-9 in the *yciC* promoter for high affinity binding (Gabriel et al., 2008). In comparison with the 7-1-7 repeat element previously demonstrated to be adequate for zinc-dependent transcriptional regulation (Gaballa et al., 2002), this flexibility may be useful in either allowing identification of additional candidate genes that may be regulated by this metalloregulator or in gaining mechanistic insight into its already identified targets in bacterial systems (Gabriel et al., 2008). In eukaryotes, the zinc-responsive transcription factors bzip19 and bzip23 of *Arabidopsis thaliana* belonging to group F of the 10-group basic-region leucine-zipper (bzip) transcription factor family (reviewed by (Jakoby et al., 2002)) have been reported

as factors involved in plant zinc homeostasis. These factors have been shown to play important roles in adaptation to zinc-limiting conditions in *Arabidopsis thaliana* by controlling the expression of zinc uptake proteins such as zips 1, 3, 4, 5, 9 and 12 through binding to one or more copies of a 10 bp palindromic zinc deficiency response element (ZDRE) in the promoter of their gene targets (Assunção et al., 2010). The *Saccharomyces cerevisiae* zinc uptake regulator ZAP1 is a central mediator of yeast zinc homeostasis and it binds to an 11 bp palindromic sequence (zinc response element; ZRE) in the promoters of its target genes including Zrt1 and Zrt2, which have been shown to mediate high zinc affinity and low affinity zinc uptake respectively (Zhao et al., 1998). Although the primary mode of ZAP1-mediated gene regulation in response to zinc limitation is activation of target genes, it also represses certain genes including Zrt2 under zinc-replete condition (Bird et al., 2004). In the fission yeast *Schizosaccharomyces pombe*, a zinc-dependent transcriptional repressor Loz1 (for loss of zinc sensing) has been shown to mediate transcription of the *adh4* gene in response to excess zinc by interacting with a 50 bp *adh4* promoter fragment containing a 7 bp *cis*-acting element thought to be important for this interaction by virtue of the fact that mutation in this element resulted in loss of complex formation between the recombinant Loz1 and the DNA fragment (Corkins et al., 2013). Although a minimal region that conferred zinc responsiveness to Loz1 has been mapped to the C-terminal end of the protein comprising the double zinc fingers (Ehrensberger et al., 2014), a specific zinc-response element is yet to be defined thus the detailed molecular mechanism of zinc-induced, Loz1-mediated transcriptional regulation is not fully established. The presence of multiple binding sites for Loz1 in the *adh4* promoter for other putative transcriptional regulators and the location downstream of the transcription start site of Loz1 DNA response elements appear to contribute to the difficulty in elucidating its mechanisms of zinc-induced transcriptional regulation (Ehrensberger et al., 2014). In higher eukaryotes, regulation of expression of metallothioneins, as well as some members of the ZnT

zinc transporter family in response to changes in zinc levels, is achieved through binding of the metal response element-binding transcription factor (MTF-1) to a consensus metal response element (MRE) in the promoters of these genes (Heuchel et al., 1994, Langmade et al., 2000). In addition to transcriptional activation, MTF-1 also mediates transcriptional repression of a subset of its gene targets, by binding to the same consensus element at positions different from that established for the classical mode of regulation. Both human and murine selenoprotein H genes display this mode of transcriptional regulation, involving the binding of MTF-1 to an MRE located downstream of the transcription start site (Stoytcheva et al., 2010). Mouse (Lichten et al., 2011) and zebrafish Zip10 (Zheng et al., 2008) are also regulated by MTF-1 in this manner. The zinc finger transcription factor Kruppel like factor 4 (KLF-4) has been found to mediate the response of mouse Zip4 to zinc limitation in mouse intestine and in mouse intestinal epithelial cell line MODE-K (Liuzzi et al., 2009). Use of EMSA revealed a binding site for KLF4 within the Zip4 promoter, however the zinc specific response element has not yet been identified.

The regulation of ZnT5 appears complex. The two splice variants have different subcellular localisations but their transcription is driven by a single promoter (Thornton et al., 2011). Down-regulation of *SLC30A5* promoter activity (assessed through measurement of  $\beta$ -galactosidase expression using a gene-reporter construct, in which the expression of  $\beta$ -galactosidase reporter gene was under the control of *SLC30A5* promoter) and ZnT5 mRNA expression was demonstrated in Caco-2 cells in response to elevated extracellular zinc concentrations (Jackson et al., 2007). Efforts to understand the molecular mechanism of this zinc-induced transcriptional repression led to the identification of a sequence element in *SLC30A5* promoter that mediates this response. This sequence element, now called the zinc transcriptional regulatory element (ZTRE), was demonstrated to be independent of an MRE consensus element, which was also found in the *SLC30A5* promoter (Coneyworth et al., 2012).

## **1.5 Aims and objectives**

Following the finding that transcriptional down-regulation of the *SLC30A5* gene in response to elevated extracellular zinc concentration is mediated by the zinc transcriptional regulatory element (ZTRE), a search for the transcriptional factor that acts at this site became a priority. Therefore, the overarching aim of the work described in this thesis was to identify this regulatory factor and investigate its role in mediating zinc homeostasis using the Caco-2 cell line model. A secondary aim that evolved as work progressed was to investigate the effect of zinc on endothelial cell senescence using human coronary endothelial cells. Specific objectives are stated in each chapter.

## Chapter 2 : Materials and Methods

### 2.1 Tissue culture techniques

All tissue culture work described in this thesis was performed in a containment level II laboratory. Mammalian cell cultures were aseptically handled under a class II laminar flow hood. All solutions and reagents as well as plastic consumables were routinely sterilised using high pressure autoclave equipment and were frequently sprayed with 70% ethanol before use in the hood and incubators to avoid cross contamination.

#### *2.1.1 Growth and maintenance of mammalian cells*

Human epithelial colorectal adenocarcinoma (Caco-2) and Chinese Hamster Ovary (CHO) cells were used in this study. Cells were grown routinely in 75 cm<sup>2</sup> flasks (Greiner Bio-one, Gloucestershire, UK) in Dubelco modified Eagle's medium (DMEM, Invitrogen) containing glutamax plus 4.5 g/L glucose and supplemented with 10% v/v fetal bovine serum (FBS, Sigma, Poole, Dorset, UK), 60 µg/ml gentamycin and 1% v/v non-essential amino acid (NEAA)(Life Technologies, UK) (hereafter referred to as medium). Cells were maintained in an incubator with 5% CO<sub>2</sub> at 37°C and regularly visualised using an inverted phase contrast microscope (Olympus CK2). Growth medium was replaced twice weekly and cells were routinely passaged 5- or 7-day intervals post seeding when they had reached >80% confluence. For sub-culturing, growth medium was removed and cells were washed with 10 ml 1 x PBS (phosphate buffered saline containing 137 mM NaCl, 2.7 mM KCl, 4.3 mM NaHPO<sub>4</sub>.7H<sub>2</sub>O, 1.4 mM KH<sub>2</sub>PO<sub>4</sub>, pH 7.4). Cells were detached from the bottom of culture flasks by addition of 2-3 ml solution of 0.05% trypsin plus 0.02% EDTA (Sigma-Aldrich) and incubation for 5 – 10 minutes. Trypsinised cells were diluted in 7-8 ml fresh medium, collected in a 20 ml universal tube and spun at 100 g for 5 minutes. Following centrifugation, the supernatant fluid was discarded and cell pellets were resuspended in 10 ml fresh medium. Fifteen microliters of

this cell suspension was added to an equal volume of 0.4% Trypan blue (Sigma-Aldrich, Dorset, UK) and allowed to incubate for 2 minutes. Cell seeding density was determined by counting cells using Haemocytometer (Neubauer). Cells were reseeded into sterile flasks at 1 million cells per 75 cm<sup>2</sup> flask for continuous culturing or other appropriate cell density depending experimental need (as stated for specific experiments). Cells not required for immediate experiments were frozen in freezing medium containing 90% DMEM and 10% dimethylsulphoxide (DMSO, Sigma) as liquid nitrogen stocks. Cells in freezing medium were dispensed into 1 ml cryovials (Corning, UK), pre-frozen overnight to -80 °C in isopropyl alcohol-containing freezing boxes (Nalgene®), which maintain a gradual reduction in temperature at 1 °C per minute. Frozen cells were transferred to liquid nitrogen for long-term storage (cryopreservation). When required, frozen cells were thawed by placing the cryovials into a water bath at 37 °C. Cells were then mixed with 9 ml pre-warmed fresh medium. The mixture was transferred into 20 ml universal tubes and centrifuged at 100 g for 5 minutes. The supernatant fluid was discarded and 7 ml of fresh DMEM was added to resuspend cell pellets before transferring to a 75 cm<sup>2</sup> flask.

### ***2.1.2 Transient transfection with promoter-reporter/expression plasmids***

Confluent cells were washed with 10 ml PBS, trypsinised and counted as described in section 2.1.1. Cells were typically seeded at  $3.5 \times 10^5$  cells/ml –  $5.0 \times 10^5$  cells/ml in 6- or 12-well plates (Greiner) for transfection experiments. Transfections were carried out when cells had reached about 60-70% confluence, 24 h post-seeding using promoter-reporter plasmids containing promoter sequences of interest or with expression constructs containing protein coding sequence (ORF). Transfection mix was prepared by adding 100 µl DMEM (without supplements) or Opti-MEM® reduced-serum medium (Invitrogen) to 4 µl per well of transfection reagent GeneJammer (Stratagene, Europe, Netherlands) or Lipofectamine® 2000

(Invitrogen) and incubated for 5 minutes at room temperature. Following incubation, 1-2 µg/µl of plasmid was added to the mixture and allowed to incubate for a further 20–30 minutes under the same condition. Culture medium in which cells were grown was replaced with 400 µl or 900 µl fresh medium (for 12 or 6 well plate respectively) prior to addition of 100 µl transfection mix in a drop-wise manner. Cells were then incubated at 37 °C for 3 - 4 h prior to topping up with 500 µl or 1 ml for 12 or 6 well plate with complete DMEM. Transfected cells were incubated for a further 24 h.

For transfection of cells with small interfering RNA (siRNA), two transfection mixes were prepared by adding 5 µl of Lipofectamine® 2000 to 250 µl Opti-MEM® reduced serum medium (mix A) and 10 nM of either target siRNA or control siRNA was added to 250 µl Opti-MEM® (mix B). Each reaction was gently mixed and incubated at room temperature for 5 minutes after which the two reaction mixes were mixed together and incubated for a further 20 minutes at room temperature. Culture medium was replaced with 5% FBS-supplemented DMEM and 500 µl of the transfection mix was added to cells. Cells were incubated in this medium for 24 h prior to metal treatment or total RNA extraction.

### ***2.1.3 Metal treatment***

Cells were incubated in serum-free medium containing ZnCl<sub>2</sub> at 3 µM (used here as control medium for zinc treatment) or 100 µM; CoCl<sub>2</sub> at 100 µM; CuCl<sub>2</sub> at 20 µM and NiCl<sub>2</sub> at 20 µM 24 h post-transfection. For all metal treatments, metal stock solution was prepared to 1000 x in each case by dissolving the appropriate amount of the metal chloride in deionised water. The solution was filtered through a 0.2 µm sterile syringe filter (Corning) and serially diluted when required to achieve the specified concentrations.

## **2.2 Cell viability assay**

A viability assay was conducted to assess cell survival at increasing concentrations of zinc and N, N, N', N'-tetrakis [2-pyridylmethyl] ethylenediamine (TPEN; dissolved in DMSO) in cells transfected with a CBWD overexpression construct. This was carried out using two complementary approaches: the dye exclusion method and MTT assay.

### ***2.2.1 Dye exclusion method (Trypan blue)***

For this procedure, Caco-2 cells were seeded in 6-well plates at  $3 \times 10^5$  cells/ml 24 h prior to transfection with 2  $\mu\text{g}/\mu\text{l}$  of pCMV6-CBWD3-Myc-DDK (Origene, UK) (section 2.4.2). Cells were treated with different concentrations of zinc ranging from 0 to 200  $\mu\text{M}$  or TPEN at concentrations ranging from 0 to 10  $\mu\text{M}$  for 24 h. Cells were prepared for counting as described in section 2.1.1. Relative cell viability (in percentage) was expressed as (number of viable treated cells/number of viable control cells) X 100.

### ***2.2.2 The MTT (3-[4, 5-dimethylthiazol-2-yl]-2, 5 diphenyl tetrazolium bromide) assay***

For measurement of viability by MTT assay, Caco-2 cells were seeded in 96-well format at  $1 \times 10^5$  cells/ml and allowed to grow in complete DMEM (final volume of 100  $\mu\text{l}$ ) for 24 h. After a further 24 h, cells were transfected with the pCMV6-CBWD3-Myc plasmid followed by zinc or TPEN treatment at the specified concentrations. Following treatment, cells were incubated with 20  $\mu\text{l}$  5 mg/ml MTT solution per well at 37°C for 4 h. Formazan (generated from the reduction of tetrazolium salt (Figure 2.1) was then dissolved by the addition of 200  $\mu\text{l}$  DMSO. Absorbance was measured at 570 nm using the FLUORstar Omega plate reader (BMG Labtech). Blank absorbance was measured at 630 nm, which was subtracted from the absorbance of each sample.

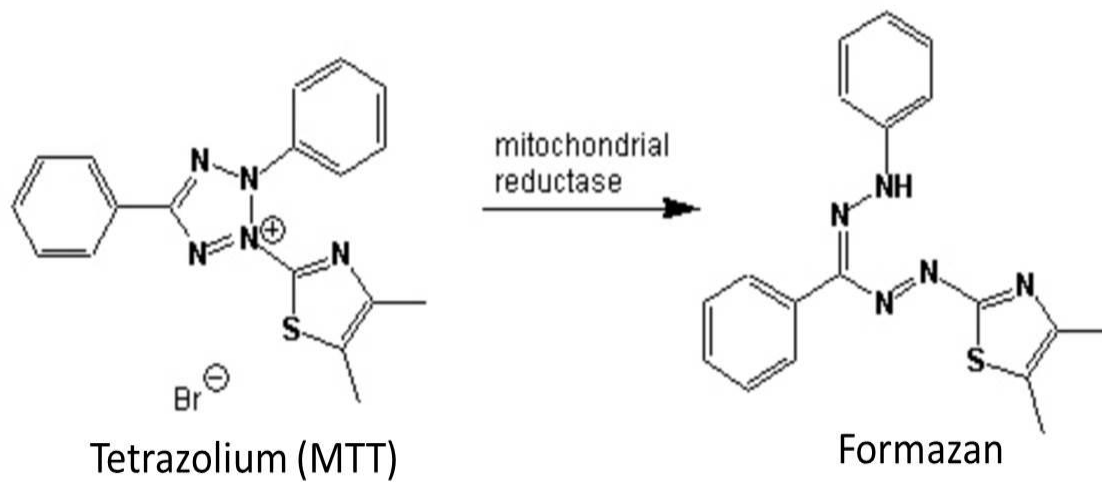


**Figure 2.1: Schematic representation of enzymatic reduction of MTT to formazan**

Mitochondrial reductase catalyses the reduction of tetrazolium salt to formazan crystals.

Picture adapted from <http://en.wikipedia.org/wiki/File:Mttscheme.png>

## **2.3 Generation and manipulation of DNA/plasmid constructs**

### ***2.3.1 Design of primers***

Primers for PCR were designed in line with general guidelines including appropriate length (18 -25) and GC content (50-60%) using software such as primer3 at <http://primer3.ut.ee/> or primerQuest at <https://www.idtdna.com/primerquest/Home/Index>. Primers were checked for self-complementarity, potential for hairpin formation (using the Thermo scientific T<sub>m</sub> calculator at <http://www.thermoscientificbio.com/webtools/tmc/> or Oligo Calc at <http://www.basic.northwestern.edu/biotools/OligoCalc.html>). In some instances, primers included restriction sites as appropriate. Furthermore, primers used in real time PCR were designed to span introns to avoid amplification of genomic DNA. All oligonucleotide primers were synthesised by Eurofins MWG Biotech, UK).

### ***2.3.2 Generation of amplicon by PCR***

Amplicons were generated by PCR were using the TaqPCR master mix kit (Qiagen). Typical reactions (final volume of 50 µl) included the following:

- 25 µl HotStar Taq mix (containing Taq DNA polymerase, 2X buffer, MgCl<sub>2</sub>, dNTPs)
- 1 µl of 10 µM forward primer
- 1 µl of 10 µM reverse primer
- 2 µl of DNA template (concentration was dependent on the template source for example plasmid or genomic DNA)
- Rnase-free water to make up the final reaction volume

In all reactions, a no template reaction containing water in place of DNA was included as negative control. Each reaction was mixed by briefly centrifuging the mixture for 30 – 45

seconds before thermal cycling. Specific reactions were optimised as required by changing the reaction parameters empirically.

### ***2.3.3 Generation of DNA insert for cloning***

DNA fragments used for cloning into pBlue-TOPO vector were amplified from Caco-2 genomic DNA using PCR (see section 2.3) and cloned using appropriate restriction endonucleases. PCR products and vector were mixed in ligation reaction, which typically contained appropriate concentration of vector and insert in 1:3 molar ratio. For preparation of CBWD expression plasmid, the human CBWD3 ORF was excised with *HindIII* and *XbaI* restriction enzymes from pCMV6 vector (Origene,UK) and sub-cloned into p3xFLAG-10 expression vector (Invitrogen).

### ***2.3.4 Agarose gel electrophoresis of DNA***

Agarose gels (typically 1 - 2%) were prepared for analysis of DNA products in 1 X TBE buffer (Tris/Borate/EDTA containing 89 mM Tris-base, 89 mM Boric acid, 2 mM EDTA). Agarose was melted in a microwave and then allowed to cool at room temperature to about 55°C before adding ethidium bromide (2 µg/ml) and pouring. Samples were mixed with 1/5 volume of 5X DNA loading dye (containing 50 mM Tris (pH 8.0), 5 mM EDTA, 50% glycerol (v/v), 50% bromophenol blue (w/v) before loading. Gels were run in 1 X TBE buffer at 100 V for 35 minutes and visualised using UV transillumination (Uvitec BTS-26M, UK).

### ***2.3.5 Purification of DNA products from agarose gels***

Required DNA fragments were excised using sterile scalpel blades under UV light into clean microcentrifuge tubes and were weighed before purification using QIAquick gel extraction kit (Qiagen, Crawley, UK) following the manufacturer's instructions. Briefly, weighed gel slices were dissolved with 5 volumes of solubilisation buffer PBI and heated at 65 °C for about 10

minutes with 2-minute intermittent vortexing until the gel was completely dissolved. The mixture was then transferred to spin columns in 2 ml collection tubes and centrifuged at 13,000 g for 60 s at room temperature. Flow-through was discarded and columns were washed with 0.75 ml wash buffer PE to remove any residual salt and then spun for another 60 s. A further centrifugation step was performed at the same speed and time to dry the columns. Columns were removed and inserted into fresh microcentrifuge tubes. Products were eluted with 30  $\mu$ l elution buffer (EB) added at the spin column centre for 120 s at room temperature before centrifugation for 60 s at 13,000 x g. Products were immediately placed on ice. DNA concentration was measured using a Nanodrop spectrophotometer and products were stored at -20 °C for further use. In some cases, phenol:chloroform was used for DNA purification. This procedure involved making the sample volume up to 200  $\mu$ l with deionised dH<sub>2</sub>O and then adding an equal volume of phenol:chloroform (1:1; pH 8) (Invitrogen) followed by vigorous vortexing for 30 seconds before centrifugation at 13,000 g for 15 minutes at 4 °C. The upper aqueous phase was then transferred to sterile 1.5 ml microcentrifuge tubes while the organic phase containing contaminants was discarded. A 1/10 volume of 3M sodium acetate (pH 5.2) and 2 volumes of ice-cold 100 % ethanol were added and samples were held at -20 °C overnight. The mixture was then centrifuged as described above. The supernatant was discarded and the pellet was resuspended in 20 – 30  $\mu$ l of nuclease-free sterile water and stored at -20 °C.

### ***2.3.6 Transformation of chemically competent *E. coli* cells***

Plasmid or ligation product was used to transform One Shot® chemically competent *E. coli* cells (Invitrogen) for propagation following the manufacturer's protocol. Transformation reaction typically involved the addition of 1-2  $\mu$ l of DNA to one vial (50  $\mu$ l) of competent cells followed by incubation on ice for 30 minutes. Cells were then heat-shocked at 42 °C for 45

seconds and immediately incubated on ice for 2 minutes. Following incubation, 250 µl of LB (Luria Bertani) medium (containing 10 g 2 % tryptone, 5 g 0.5 % yeast extract and 10 g 1 % NaCl per 1000 ml of the medium) pre-warmed (37 °C) was added and transformations were incubated at 37 °C with shaking for 1 hour. One hundred microliters of transformation reaction was spread on antibiotic-treated LB agar plates (containing either 100 µg/ml ampicillin or 50 µg/ml kanamycin). Colonies were grown at 37 °C for 24 h.

### ***2.3.7 Screening of transformants (inoculation)***

Randomly selected colonies were screened by incubating a single colony in 5 ml LB medium containing appropriate antibiotic at 37 °C overnight.

### ***2.3.8 Purification of plasmid from bacterial cultures***

Small scale plasmid preparation was carried out using Quicklyse Miniprep kit (Qiagen) to purify plasmid DNA from bacterial culture grown overnight following the manufacturer's instructions. Briefly, bacterial culture was pelleted by centrifugation at 12,000 g for 60 s, followed by alkaline-based buffer lysis and a series of further centrifugation steps culminating in DNA elution with 20 µl elution buffer QLE into clean microcentrifuge tubes. Large scale plasmid purification involved inoculation of a single colony in a starter culture containing appropriate antibiotics for 7 h at 37°C. Five millilitres of starter culture was used to inoculate 200 ml of LB medium containing 100 µg/ml ampicillin and grown overnight at 37 °C. Cells were pelleted by centrifugation at 6000 g for 15 minutes at 4 °C and DNA was extracted using endotoxin-free maxiprep kit (Qiagen, Crawley, UK).

### ***2.3.9 Determination of Nucleic acid (DNA/RNA) concentration***

DNA or RNA was routinely quantified by spectrophotometric methods using Nanodrop 1000 (Thermo Fisher Scientific Inc. USA). This procedure was carried out by measuring the optical

density (OD) of the samples at two different wavelengths (i.e. 260 nm and 280 nm). The ratio of 260/280 was determined for each sample and the value of 1.8 or 2.0 was acceptable for good quality DNA or RNA respectively. A measure of salt contamination is determined by measuring absorbance ratio at 260/230 and the range of 2.0 - 2.3 was considered acceptable for nucleic acid preparations. The procedure involved taking a blank measurement with 2 µl of water or the buffer in which the samples were dissolved, then 2 µl of each sample was pipetted onto the instrument's pedestal to measure concentrations.

#### ***2.3.10 Digestion of plasmid DNA with restriction endonucleases***

Plasmid DNA was digested with restriction endonucleases in appropriate buffer. Typical restriction reactions contained 10 % (v/v) reaction buffer, 5-10 units of the enzyme in microcentrifuge tubes and the reaction made up to a final volume of 20 µl with sterile water. Reactions were incubated in a water bath at 37°C for 1 – 2 hours. Digested products were then analysed by agarose electrophoresis (section 2.3.4).

#### ***2.3.11 Site-directed mutagenesis (SDM)***

Site-directed mutagenesis (SDM) was carried out to delete either 5' or 3' component of the ZTRE from the pBlueSLC30A5prom construct using PCR. Similarly, specific zinc finger motifs of the transcription factor ZNF658 were deleted from the pCMV6-ZNF658-myc-DDK plasmid. PCR products were treated with *DpnI* (New England Biolabs) to digest the parent (methylated) plasmid, then circularised by T4 DNA ligase in the presence of a phosphate donor (polynucleotide kinase, PNK) (New England Biolabs). Plasmids were gel-purified, quantified and sequenced to ascertain the correct orientation and fidelity of the remaining sequence.

### **2.3.12 DNA sequencing**

All PCR products and/or plasmids were sequenced by Eurofins MWG Operon (MWG Biotech, UK). Plasmid preparations were sent at 100 ng/μl concentrations along with primers at concentrations of 5 – 10 μM in a 15 μl total volume. Sequencing Results were examined manually or by using CLUSTALW2 multi sequence alignment software.

### **2.4 In vitro methylation**

*In vitro* methylation of pBlueCBWD1prom plasmid was carried out using the MSssI/SAM kit (New England Biolabs). The methyl group donor SAM (S-Adenosyl methionine) was diluted with sterile water in 1:8 ratio and the plasmid was diluted to the concentration of 0.2 μg/μl. Methylation reaction contained 0.2 μg/μl pBlueCBWD1prom, 10 x buffer 2, 1600 μM SAM, 4 U/μl enzyme and the volume was made up to 100 μl with water. Mock methylation was prepared with all the components except the methyltransferase enzyme. The reaction was incubated in a water bath at 37 °C for about 120 minutes. More substrate (SAM) and enzyme (MSssI) were added then further incubation for 90 minutes. The efficiency of methylation was confirmed by digesting the product with the isoschizomers *HpaII* (CpG methylation sensitive) and *MspI* (CpG methylation insensitive). DNA was extracted using phenol: chloroform method (see section 2.3.5), resuspended in RNase-free water and the concentration was determined spectrophotometrically (see section 2.3.9).

## **2.5 Reporter-gene assays**

### **2.5.1 Preparation of cell lysate**

Whole cell lysate was prepared for reporter gene (β-Galactosidase) assay from cells harvested 24 h following metal treatment. Cells were washed with 1 ml PBS/well in a 12- or 6-well plate then PBS was replaced with 100 μl or 200 μl lysis buffer (containing 0.25 M Tris pH 7.4,

0.25 % (v/v) NP-40, 2.5 mM EDTA). Cells were frozen in lysis buffer at -20 °C for 30 minutes then thawed at room temperature and collected into 1.5 ml microcentrifuge tubes using sterile cell scrapers (Greiner). Cells were centrifuged at 13,000 g for 5 minutes at 4 °C. Supernatant was transferred to fresh tubes, kept on ice and used the same day for measurement of  $\beta$ -Galactosidase activity.

### ***2.5.2 Measurement of reporter activity ( $\beta$ -Galactosidase specific activity)***

$\beta$ -Galactosidase activity was determined colorimetrically by measuring absorbance of samples at 560 nm following the release of chlorophenol red from the breakdown of the substrate chlorophenol red- $\beta$ -D-galactopyranoside (CPRG, Sigma). Twenty microliters of cell lysate was combined with 130  $\mu$ l 1.2 mg/ml CPRG (prepared in buffer A containing 100 mM NaCl, 25 mM MOPS & 10 mM MgCl<sub>2</sub> pH 7.5) in a 96-well plate. Similarly, 20  $\mu$ l of cell lysate prepared from cells transfected with vector (pBlue TOPO) containing no insert (used as negative control) was combined with the CPRG substrate. The reaction was incubated at 37 °C until a colour change was observed. Reactions were terminated by the addition of 0.5 M Na<sub>2</sub>CO<sub>3</sub> and absorbance was measured using a plate reader (Multiscan Acent). Data were expressed as  $\beta$ -Galactosidase specific activity (U/mg sample protein concentrations determined using the Bradford assay (see section 2.6).

### **2.6 Determination of protein concentration**

Protein concentration was determined using Coomassie Brilliant Blue G-250 dye (Bradford reagent), which when bound to protein under acidic condition undergoes a shift in the wavelength at which absorbance is maximal from 465 nm to 595 nm. In this assay (Bradford assay), a standard solution of 0.1 mg/ml bovine serum albumin (BSA) was diluted to make a concentration range from 0 - 100  $\mu$ g/ml BSA. Fifty microliters (50  $\mu$ l) of each standard solution was pipetted in triplicate into a 96 well plate (SLS Ltd, UK). Cell lysates were diluted 1 in 50

and 50 µl of each sample was pipetted into wells in a 96 well plate. Bradford reagent (Biorad, UK) was diluted 1 in 5 from the stock solution with Milli-Q water and 200 µl was added to each well containing either standard or sample. Absorbance was measured at 595 nm using a plate reader (ThermoLab Systems Multiscan Acent). A standard curve was generated from absorbance readings of the standards and protein concentration of samples was determined from this plot.

## **2.7 RNA extraction and RT-PCR**

### ***2.7.1 RNA extraction from cultured mammalian cells***

RNA was extracted with TRIzol® reagent (Invitrogen, UK). Cells were homogenised with the addition of 1 ml TRIzol per 10 cm<sup>2</sup> surface area (i.e. for each well in a 6-well plate). Cells were incubated at room temperature for 5 minutes, followed by the addition of 200 µl chloroform (Sigma) per ml of TRIzol reagent and the mixture was mixed vigorously by hand for 15 seconds. RNA was extracted using the Purelink® RNA Mini Kit (Life Technologies) following the manufacturer's protocol. Briefly, homogenised cells were incubated at room temperature for 2-3 minutes and centrifuged at 12,000 g for 15 minutes at 4 °C. Four hundred microliters of the aqueous layer was transferred into fresh microcentrifuge tubes and an equal volume of isopropanol was added to precipitate RNA. Seven hundred microliters of the solution was transferred into spin columns in 2 ml collection tubes and centrifuged at 12,000 g for 60 seconds. RNA pellet was then washed with 700 µl of 70% ethanol and centrifuged at 12,000 g for 15 seconds. After an additional wash step, the columns were dried and RNA was eluted into clean microcentrifuge tubes with 30 µl RNase-free water. RNA was quantified and stored at -80 °C for use.

### **2.7.2 Treatment of RNA with Dnase I**

RNA samples were treated with RQ1 RNase-free Dnase I (Promega) enzyme to remove residual genomic DNA. Typically, reactions included, 2 µl of Dnase I buffer, 4.5 units Dnase I, 1 – 2 µg/µl RNA and the volume was made up to 20 µl. Reactions were run in a thermocycler at 37 °C for 30 minutes. Reactions were terminated by addition of 4 µl stop solution (20 mM EGTA (pH 8.0)) and the enzyme was heat-inactivated at 65°C for a further 10 minutes.

### **2.7.3 Synthesis of cDNA by reverse transcription reaction (RT-PCR)**

RNA was reversed-transcribed to generate complementary DNA (cDNA) using Superscript® III reverse transcriptase (Invitrogen). Reactions contained 1 µl 150 ng/ul random primers (Promega, Southampton, UK), 0.4 µl 0.5 mM dNTPs (Bioline, London, UK) and water to the final volume of 20 µl. Reactions were heated to 65°C for 5 minutes on a thermocycler then put on ice prior to the addition of 1 µl 0.1 mM DTT, 4 µl first strand buffer (200 mM Tris-HCl (pH 7.5), 30 mM MgCl<sub>2</sub>, 10 mM spermidine, 50 mM NaCl), 1 µl, 30 U RNasin® (Promega) and 1 µl 200 U reverse transcriptase enzyme. Reverse transcription was carried out at 50 °C for 45 minutes in a single cycle. The enzyme was inactivated at 65 °C for 15 minutes.

### **2.7.4 Measurement of mRNA expression by RT-qPCR**

Transcript levels of *SLC30A5*, *SLC30A10*, *CBWD*, *ZNF658* and *GAPDH* (reference) genes were measured by relative quantification method using the LightCycler® 480 (Roche Applied Sciences, Burgess Hill, UK). Reactions were performed in a LightCycler 96-multiwell using SYBR Green I master mix and composed of 5 µl SYBR Green mix, 1 µl of sense and antisense primers (0.5 µM each), 1 µl of cDNA, and 3 µl water to a final volume of 10 µl. Threshold cycles (CT) at which the fluorescence went above the background threshold were used for calculations. Each sample was run in triplicate in parallel with negative control wells, which

contained water in place of cDNA as no template control (NTC). In addition, melt curve analysis was included in the programme to assess specificity of gene amplification.

### ***2.7.5 Generation of standard curves***

Standard curves were generated for both target and reference genes and were used to confirm linear amplification and to determine efficiency of each amplification. A 1: 4 dilution of cDNA obtained from control samples (untreated cells or cells transfected with control siRNA) was used to generate standard curves. Logarithm of concentration was plotted against CT values to yield amplification curves. Analysis was performed in triplicate and each RT-qPCR analysis was checked to be within the limits of the standard curve. Efficiency values (ranging from 1.8 – 2.0) for either gene of interest or reference gene was calculated using the equation  $E = (10^{-1/\text{slope}})$ . Expression of each gene was calculated by taking the mean value of triplicate CTs relative to those of the reference gene using the modified delta delta CT method (Livak and Schmittgen, 2001). The change in CT value ( $\Delta\text{CT}$ ) between target gene relative to reference gene (s) was calculated for both control and treated samples;  $\Delta\text{CT} = \text{CT target gene} - \text{CT reference gene}$ . Data were normalised to control condition by subtracting  $\Delta\text{CT}$  value for the control group from  $\Delta\text{CT}$  value of the treated group (i.e.  $\Delta\text{CT treated group} - \Delta\text{CT control group}$ ).

### **2.8 Statistical analysis**

Graphs were prepared using GraphPad Prism software version 5. Data used for statistical analysis were either from three replicate measurements in three independent experiments or six replicate measurements in two separate experiments (except otherwise stated in specific figure legends). Data are presented as mean  $\pm$  standard error (SE) of the mean. Significant differences were determined as  $p < 0.05$  by Student's *t* test or one-way ANOVA followed by appropriate post-hoc test (s).

## **2.9 Immunoblotting techniques (western blotting)**

### ***2.9.1 Preparation of protein sample***

Cells were harvested by incubating in 1 ml of cold PBS (prepared by addition of 1 tablet of protease inhibitor to 10 ml PBS) and scraped into microcentrifuge tubes using cell scraper (Fisherbrand® Disposable Cell Lifters, Fisher Scientific). Cells were pelleted by centrifugation at 13,000 g for 5 minutes. Cell pellet was resuspended in 50 µl protein resuspension buffer (containing 5 M NaCl, 1 M Tris-HCl (pH 7.6), 0.5 M EDTA plus 1 tablet of protease inhibitor cocktail) and centrifuged at the same speed for 30 minutes. Supernatant was transferred into fresh microcentrifuge tubes and protein concentration was determined by Bradford assay (see section 2.6).

### ***2.9.2 SDS-PAGE electrophoresis***

Protein sample (5-10 µg) was electrophoresed through 12.5% Sodium Dodecyl Sulphate Polyacrylamide Gels (SDS-PAGE). A 12.5 % resolving gel (40% acrylamide-bis-acrylamide in 37:5:1 ratio, 0.75 M Tris-HCl pH 8.9, 0.1 % SDS, 5.7 mM TEMED, 0.1% ammonium persulfate (APS) and 2 µl TEMED) and 5% stacking gel (40% acrylamide, 0.06 M Tris-HCl pH 6.7, 0.1% SDS, 13.8 mM TEMED, 0.1% APS) were prepared. All gel solutions were purchased from Sigma. Separation solution was poured into pre-set glass plates (BioRad) and overlaid with 1 ml isopropanol and allowed to polymerise for 30 minutes. Stacking gel was added and comb was inserted then allowed to set for a further 20 minutes. Protein samples were prepared for loading by adding each sample to loading buffer (containing 45 mM Tris-HCl pH 6.8, 10% glycerol, 1% SDS, 0.01% bromophenol blue, 50 mM DTT) and heated at 95°C for 5 minutes before loading onto the gel along with ColorBurst Marker MW 8-220 kDa, (Sigma). The gel was immersed in electrophoresis buffer comprising 0.5 M Tris-HCl pH 8.8, 1.9 M glycine and 0.1% SDS and run at 100-120 V for 1 hour.

### ***2.9.3 Protein transfer to PVDF membranes and blocking***

Gels were blotted onto PVDF membrane (Hybond P, Amersham), which was pre-activated by immersing it in 100 % methanol for 30 s and then in transfer buffer (0.04 Tris-HCl pH 8.8, 1.5 M glycine, 0.08% SDS, 20% methanol) for 15 minutes. A gel sandwich was prepared using Whatman 3 mm paper and the gel was transferred onto PVDF membrane at 15 V for 1 h using electroblotting cassette (TE22, GE Life Sciences). PVDF membrane was washed once with PBS containing 0.1 % (v/v) tween 20 in PBS (TPBS) for 5 minutes and membrane was blocked in blocking solution (5% milk powder (w/v), 0.05% Tween-20 (v/v) in PBS) for 1 h. In some cases, membranes were stained using Coomassie staining solution consisting of 10% (v/v) acetic acid, 10% (v/v) Isopropanol and 0.1% (w/v) Coomassie brilliant blue to confirm the presence of protein. In those experiments, gels were incubated in Coomassie stain for 20-30 minutes at room temperature on a rocker. Gels were thereafter destained by immersing in a solution of 25% propanol for 10 minutes and washed with water until blue bands were no longer visible on the gel.

### ***2.9.4 Detection of immunoreactive protein band***

Membranes were probed with primary antibody diluted to 1:1000 in blocking solution for 60 minutes with gentle shaking at room temperature. Following washing with 0.1 % (v/v) TPBS, membranes were incubated with secondary antibody diluted in blocking solution to 1:5000 for 1 hour. After further washing, protein bands were detected by chemiluminescence method using ECL Plus (Amersham). In this method, membranes were incubated in ECL solution at room temperature for 5 minutes, then exposed to X-ray film and visualised with autoradiography. Membranes were stripped using stripping buffer (containing 1.5 % (w/v) glycine, 0.1 % (w/v) SDS and 1 % Tween 20 (v/v) and re-probed with loading control specific antibody (anti-alpha tubulin) diluted 1 in 1000 to confirm equal protein loading.

## 2.10 Immunofluorescence microscopy

Caco-2 cells were seeded at  $5 \times 10^5$  cells/cm<sup>3</sup> onto 13 mm round cover slips (Thermo Scientific) inserted into 6-well plates and maintained in complete DMEM for 24 h. Cells were transfected with protein expression constructs using Lipofectamine 2000™ transfection reagent (Invitrogen). Cells were treated with zinc at 3  $\mu$ M or 100  $\mu$ M concentration 24 h post-transfection. Cells were washed with 1 ml of cold 1x PBS fixed at room temperature with 4% (w/v) paraformaldehyde for 20 minutes. Following fixation, cells were permeabilised in permeabilisation buffer (0.3% (v/v) Triton x-100 + 0.3% (w/v) BSA) for 15 minutes after which 1% SDS was added and incubated at room temperature for 5 minutes to unmask the antigen. Cells were washed in blocking solution (1.6 g BSA, 0.5 g Glycine made up in 200 ml 1x PBS) and probed with primary antibody diluted in blocking solution to 1:250 overnight at 4 °C. Cells were then incubated in fluorophore-conjugated secondary antibody (Alexa Fluor 488; excitation/emission wavelength 495/519 nm) diluted to 1:1000 in blocking solution for 1 h in the dark. After washing, cover slips were mounted in Vectashield mounting medium (containing DAPI for DNA counterstaining; Vector Laboratories Ltd.). Images were visualised using fluorescence microscope (Olympus BX61).

A zinc-specific fluorophore was used to investigate co-localization of CBWD protein with zinc. Transfected Caco-2 cells were pre-loaded with cell-permeable zinc-sensitive fluorochrome (FluoZin-3 AM; (bis-(1, 3-dibutylbarbituric acid; Invitrogen, UK) prepared in phosphate buffered saline to the final concentration of 5  $\mu$ M and incubated at 37°C for 30 minutes. Cells were washed and incubated in PBS for additional 30 minutes at 37°C to allow for cleavage of the AM ester. Cells were then incubated with primary antibody and probed with secondary antibody conjugated to Alexafluor 594 (excitation/ emission wavelength of 560/617 nm) for detection of CBWD protein. Zinc levels were visualized with FluoZin-3-AM

(excitation/emission wavelength 494/516). Images were acquired with confocal microscope (Leica SP2 UV).

## **2.11 Electrophoretic mobility shift assay (EMSA)**

### ***2.11.1 Preparation of probes***

Oligonucleotide primers representing the region of *SLC30A5* containing the ZTRE were synthesised by Integrated DNA Technologies (IDT; Iowa, USA) and labelled at 5' end of the primer with infra-red dye (IRD700). PCR reactions were carried out using *SLC30A5* promoter-reporter construct as template to generate a double stranded labelled probe. For competition experiments, double-stranded competitor oligonucleotide was prepared by annealing two complementary sequences (50 bp) incorporating the ZTRE using annealing buffer (10 mM Tris, 1 mM EDTA, 50 mM NaCl) at 96 °C on a heating block for 10 minutes. The reaction was cooled slowly to room temperature and then stored at -20 °C for use in binding reactions.

### ***2.11.2 Preparation of protein extract***

Protein extracts were prepared from Caco-2 cells transiently transfected with myc-tagged expression constructs (pCMV6ZNF658-myc or pCMV6ZnT8-myc). Cells were washed with 1X PBS and scraped into microcentrifuge tubes, then centrifuged at 1500 g for 5 minutes at 4 °C. Supernatant fluid was removed and cell pellet was resuspended in 1 ml lysis buffer containing 10 mM HEPES (pH 7.9), 1.5 mM MgCl<sub>2</sub>, 10 mM KCl, 0.5 mM DTT, 25% glycerol, 0.1 NP-40 (v/v) and 1 x EDTA-free protease inhibitor cocktail (Roche Applied Bioscience, UK). The mixture was vortexed vigorously and incubated on ice for 15 minutes before centrifuging at 5000 g for 5 minutes. Supernatant containing the cytoplasmic extract was preserved (for ZnT8-transfected cells), while cells transfected with pCMV6ZNF658-Myc construct, the cytoplasmic extract was discarded and the cell pellet resuspended in 100 µl nuclear lysis buffer containing 20 mM HEPES (pH 7.9), 1.5 mM MgCl<sub>2</sub>, 400 mM KCl, 0.5 mM

DTT, 25% glycerol and protease inhibitor. The mixture was incubated on ice for 30 minutes and then centrifuged at 15,000 g for 15 minutes. Supernatant containing the nuclear extract was then collected, quantified and stored at -80 °C for use.

### ***2.11.3 Binding reactions***

Binding reactions were prepared to a final volume of 20 µl using Odyssey EMSA kit (Licor Biosciences, Cambridge, UK). Each reaction contained 1 x binding buffer (10 mM Tris), 50 mM KCl, 1 mM DTT (pH 7.5), 0.25% Tween-20, 1 µg Poly(dI.dC), 50 fmol IRD700-labelled probe and 5 µg protein extract. Binding reactions were incubated at room temperature for 20 minutes in the dark. In competition experiments, 200-fold molar excess over the probe of double stranded competitor oligonucleotide was included in the binding reaction. Supershift experiments included in the binding reactions 1 µg anti-Myc/FLAG antibody added to the binding reaction after an initial 20 minutes pre-incubation. After a further 20 minutes, 2 µl of 10x orange loading dye was added to each reaction tube and the mixture was loaded onto 7.5 % precast gels (Bio-Rad Laboratory, Hemel Hemstead, UK), which were pre-run in 0.5 x TBE (44.5 mM Tris-Base, 44.5 mM Boric acid, 1 mM EDTA) at 100 V for 45 minutes to remove excess SDS. Gels were run at 100 V for 75 minutes at 4 °C in the dark.

### ***2.11.4 Image detection***

Images were detected using the Odyssey infrared imager (Licor Biosciences, Cambridge, UK) with resolution set at 169 µm and focus offset at 1.5 mm (which equals the thickness of the plate plus half of the thickness of the gel). Scans were performed at different intensities to optimise image quality. Data were collected using the 700 nm channel, as optimum to detect the IRD700 dye.

# Chapter 3 : Investigation of the mechanism of zinc-induced down-regulation of genes; the role of the zinc transcriptional regulatory element (ZTRE)

## 3.1 Introduction

### 3.1.1 Identification of the zinc transcriptional regulatory element (ZTRE)

In preceding work, a zinc-induced transcriptional repression of the promoter of the zinc transporter gene *SLC30A5* was observed in Caco-2 cells exposed to elevated levels of extracellular zinc (100  $\mu$ M or 150  $\mu$ M) compared to 3  $\mu$ M zinc. The possibility that this zinc-induced repression may be mediated by a metal response element (MRE) consensus motif present within the *SLC30A5* promoter (at position -404 to -410) was excluded by showing the response was retained when it was deleted (Jackson et al., 2008). The zinc-responsive region in this promoter was mapped to within the region -154 to +50 relative to the transcription start site. Use of a series of overlapping double-stranded oligonucleotides spanning this region as competitors in electrophoretic mobility shift analysis (EMSA) identified a palindromic sequence (CACTCCC(CC)GGGAGTG) at the -91 to -76 bp site of the predicted transcription start site (TSS) as the binding site of a protein or protein complex presumed to mediate the response to zinc. The element, now called the Zinc Transcriptional Regulatory Element (ZTRE), was shown by mutation in a promoter-reporter construct to be responsible for the zinc-induced repression of *SLC30A5* (Coneyworth et al., 2012). The ZTRE had also been identified in the region upstream of the transcription start in the genes *SLC30A10* (coding for number 10 member of the efflux zinc transporter family) and *CBWD* (coding for a COBW domain-containing protein) (Coneyworth et al., 2012).

### 3.2 Specific objectives

The specific objectives of the work presented in this chapter were to investigate if:

- the transcript levels of the *CBWD* gene is reduced by increased zinc;
- *SLC30A5* and *CBWD* promoter activities were down-regulated by elevated zinc;
- the zinc transcriptional regulatory element was responsible for zinc-induced transcriptional repression of *SLC30A5* and *CBWD* genes.

### 3.3 Results

#### 3.3.1 The effect of zinc on transcript levels of *SLC30A5* and *CBWD* genes

Zinc regulation of *SLC30A5* and *SLC30A10* at transcript levels was previously reported as an observation that increasing extracellular zinc concentration reduced mRNA abundance for both genes in both Caco-2 and SH-SY5Y cell lines (Jackson et al., 2007, Bosomworth et al., 2012). To examine if *CBWD* genes are regulated in a similar manner by zinc, endogenous transcript levels of *CBWD* genes, along with those of *SLC30A5* as a positive control, were measured by RT-qPCR in Caco-2 cells exposed to zinc at control and elevated levels. Caco-2 cells were incubated in a medium containing zinc at concentrations of 3  $\mu\text{M}$  and 100  $\mu\text{M}$  for 24 hours, after which total RNA was extracted using Trizol reagent and reversed transcribed to complementary DNA (cDNA). Measurements were carried out using the LightCycler 480 (Roche) with SYBR Green master mix I in a 96-well plate format. Primers and cycle parameters are as listed in Table 3.1. Amplification plots and standard curves (Figure 3.1) for *SLC30A5*, *CBWD* and *GAPDH* (control) were generated from 1:2 or 1:10 serial dilutions of cDNA from control cells. Efficiency for each target amplification was calculated from standard curves using the formula  $E = 10^{(-1/\text{slope})}$ . Melt curve analysis was also included in the programme as a post amplification analysis to confirm specificity of the amplified product (Figure 3.2). Messenger RNA (mRNA) levels of target genes were expressed relative to transcript levels of

*GAPDH* and normalised to the 3  $\mu\text{M}$  zinc control condition. The results indicated significant reduction in transcript levels of both genes in response to an extracellular zinc concentration of 100  $\mu\text{M}$  compared with the control condition (Figure 3.3), confirming previous results for *SLC30A5* and demonstrating the regulation of *CBWD* genes by zinc.

Gene/ Genbank accession number	Primer sequences	Amplicon length (bp)	Cycling parameters (for 45 cycles)
<i>SLC30A5</i> NM_0022902	2051 GGTGGAGGCATGAATGCT <sub>2068</sub> 181 CAGAGTGGGTCAGCGATGAAC <sub>2161</sub>	116	95 °C – 10 s 95 °C – 5 s 60 °C – 10 s 72 °C – 10 s
<i>SLC30A10</i> (NM_018713.2)	844 CGTAGCAGGTGATTCTTCAAC <sub>865</sub> 956 CATCTCCCATCACATGCAAAA <sub>935</sub>	113	95 °C – 10 s 95 °C – 5 s 60 °C – 10 s 72 °C – 10 s
<i>CBWD1</i> (NM_018491)	891 CCAGGAACACAACCTCACCT <sub>915</sub> 1151 CCTCCAGCTCACTGGAGTC <sub>1132</sub>	256	95 °C – 10 s 95 °C – 5 s 60 °C – 10 s 72 °C – 10 s
<i>GAPDH</i> (NM_002046.4)	185 TGAAGGTCGGAGTCAACGGATTTG <sub>209</sub> 312 CATGTAAACCATGTAGTTGAGGTC <sub>289</sub>	117	95 °C – 10 s 95 °C – 5 s 60 °C – 10 s 72 °C – 10 s

**Table 3.1: Oligonucleotide sequences and cycle parameters used for RT-qPCR measurements**

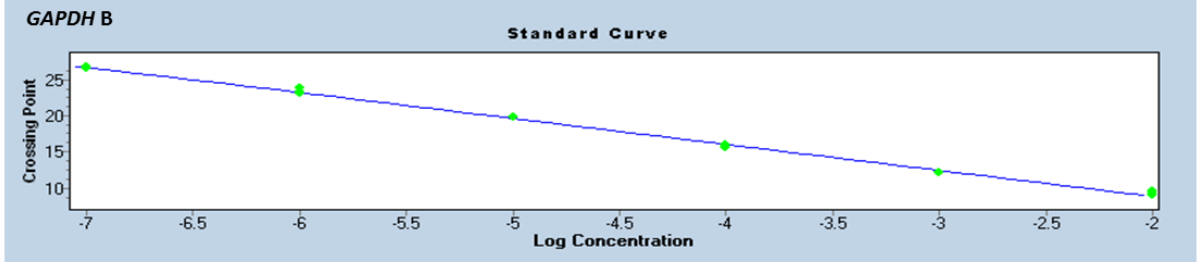
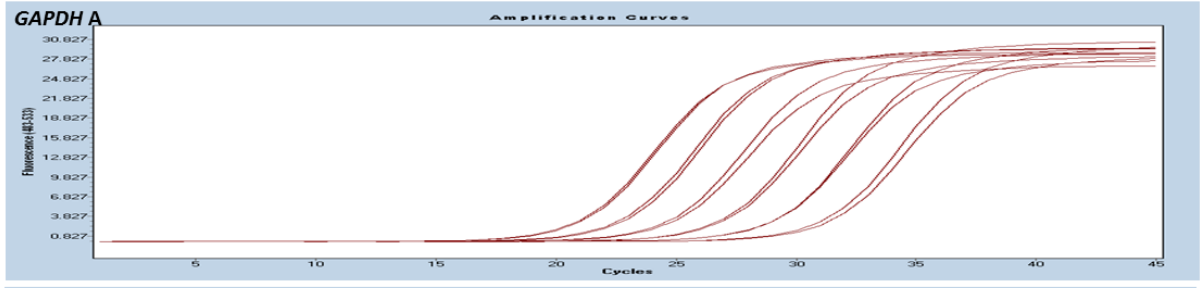
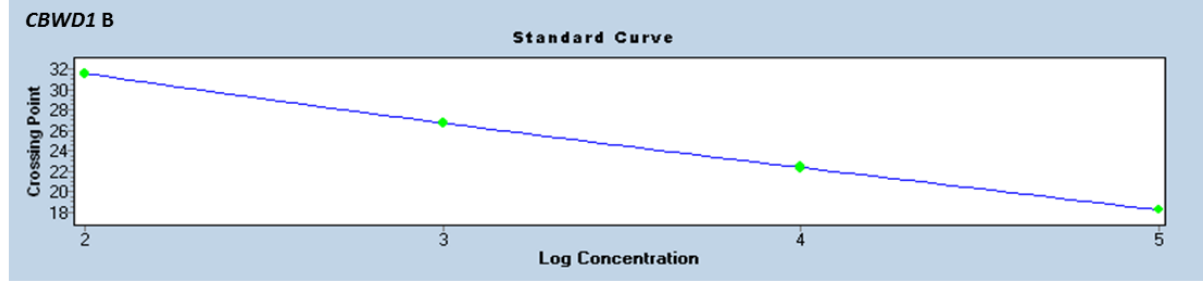
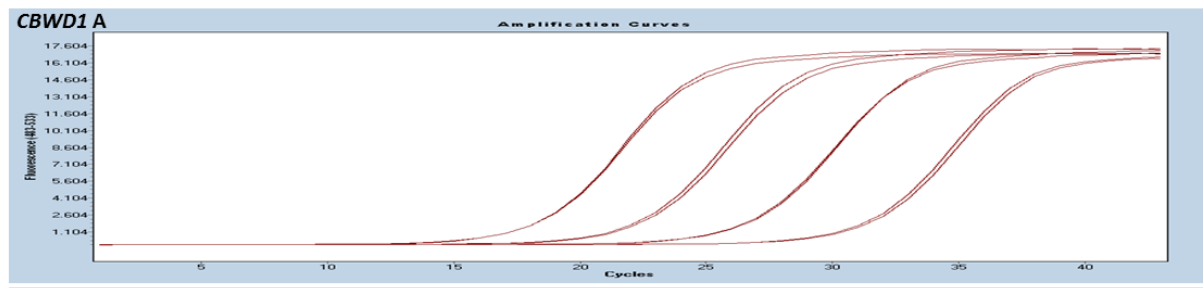
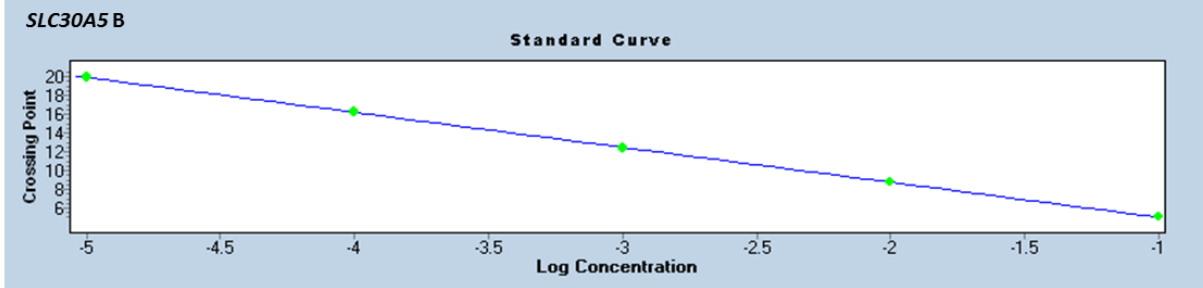
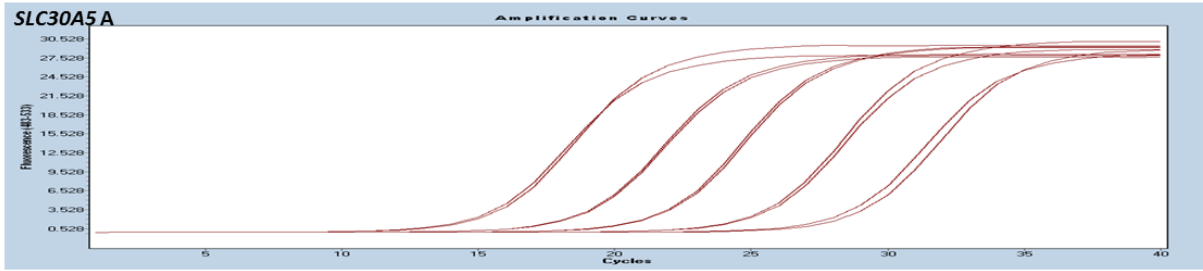


**Figure 3.1: Representative real-time PCR amplification plots and standard curves.**

For each gene, panel A shows the amplification plots generated using primers listed in Table 3.1 for *SLC30A5*, *CBWD* and *GAPDH* genes using cDNA from untreated cells diluted serially two fold (for the *GAPDH* gene) or tenfold (for *SLC30A5* and *CBWD* genes). Panel B shows each corresponding standard curve.

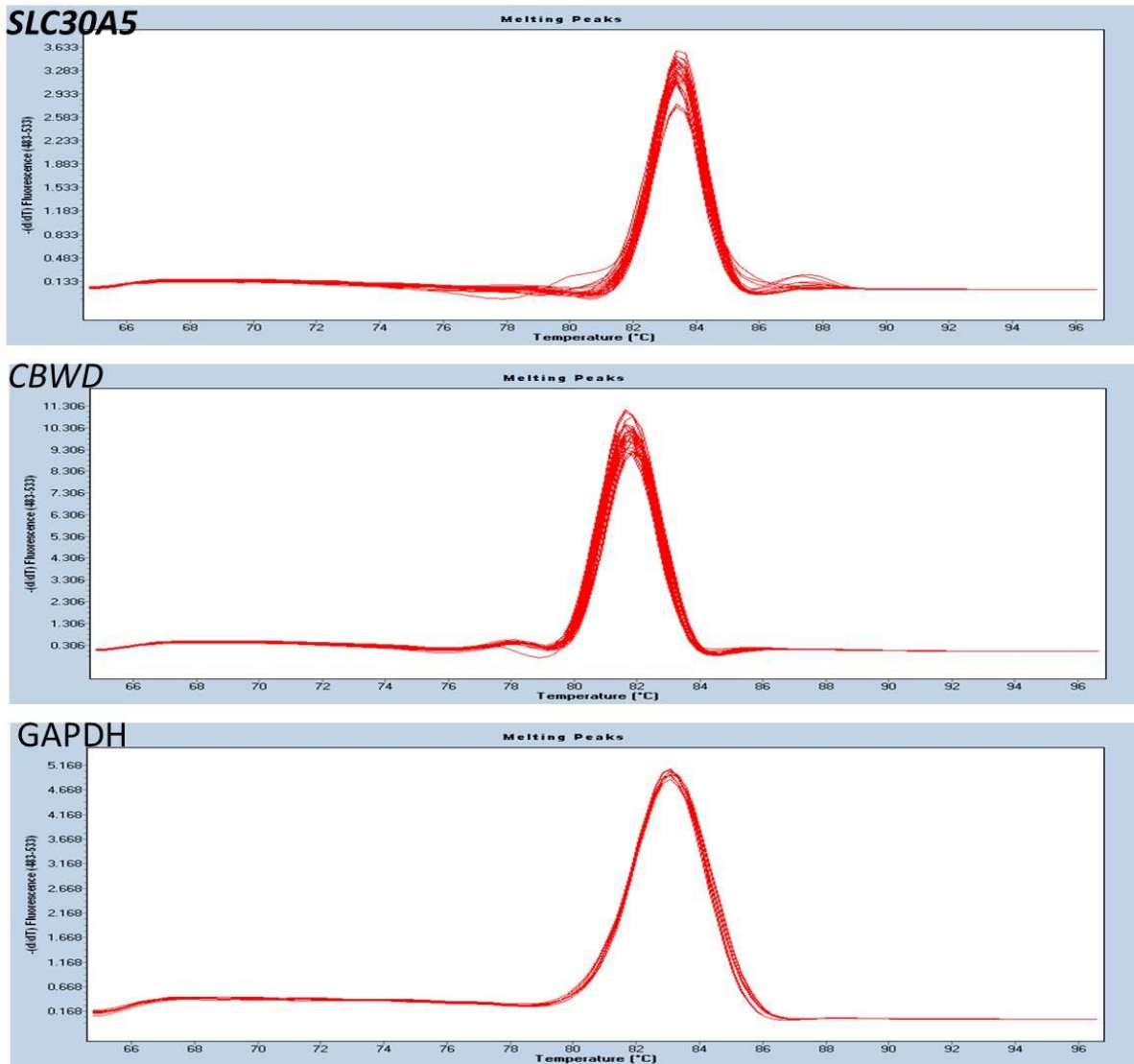


**Figure 3.2: Representative melt curves generated from RT-qPCR.**

Melt curves were generated as a post amplification process included in the RT-qPCR programme to test for primer specificity in amplifying individual genes. DNA was incubated at 65 °C for 60 s then dissociated by increasing the temperature up to 95 °C at 1 °C per every 15 s interval.

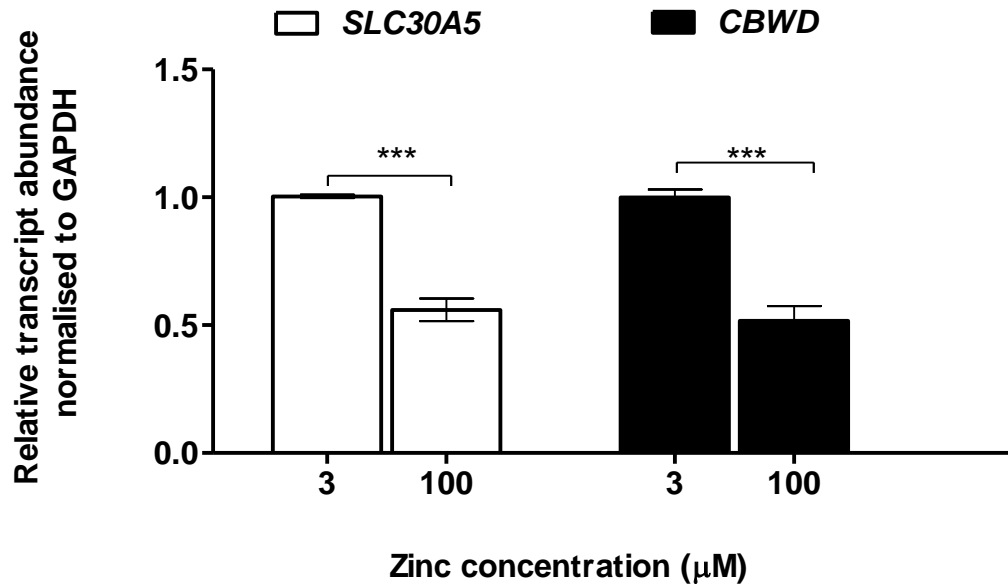


**Figure 3.3: Increased zinc concentration down-regulates transcript levels of *SLC30A5* and *CBWD* genes.**

Caco-2 cells were seeded at  $5 \times 10^5$  cells/well in 6-well plates and grown in DMEM for 24 h. Twenty four hours post seeding, cells were maintained in serum-free DMEM containing zinc chloride added at 3 μM (control medium) or 100 μM. After a further 24 h, total RNA was extracted from cells using Trizol reagent and reverse-transcribed to cDNA. Transcript levels of *SLC30A5* and *CBWD* genes were measured by RT-qPCR relative to transcript levels of GAPDH (reference gene) and are expressed normalised to the control condition. Data are expressed as mean  $\pm$  SEM for  $n = 9$ . \*\*\* $P < 0.001$  determined by Student's unpaired t-test.

### 3.3.2 *The effect of zinc on promoter activity of SLC30A5 and CBWD genes*

To investigate the molecular mechanism underlying the reduction in endogenous transcript levels of *SLC30A5* and *CBWD* genes in response to increased zinc concentration, the region upstream of the start of transcription for each gene was used to generate promoter-reporter constructs. The *SLC30A5* plasmid contained the promoter region spanning the bases -950 to +50 relative to the transcription start site (TSS), and including the ZTRE (here called pBlue*SLC30A5*prom) while the *CBWD* promoter-reporter construct included the promoter sequence corresponding to the bases -680 to +262 relative to the TSS, which includes the ZTRE (here referred to as pBlue*CBWD1*prom). The respective promoter sequences were generated using genomic DNA extracted from Caco-2 cells in a standard polymerase chain reaction (PCR). The PCR products were purified then subcloned into the vector pBLUE TOPO (Invitrogen) upstream of the bacterial  $\beta$ -galactosidase gene (*lacZ*). Plasmid purified from positive clones of *E. coli* was sequenced to confirm the correct sequence of the insert and its orientation. Production of endotoxin-free plasmid was then carried out using purification kits as described in section 2.3.8. Caco-2 cells were transfected with each plasmid construct, treated with zinc 24 h post-transfection and cell lysates were prepared for measurement of reporter gene activity ( $\beta$ -galactosidase activity) after a further 24 h. A negative control (pBlue TOPO vector with no insert) was included and the  $\beta$ -gal specific activity values were subtracted from all data. Results showed reduction in the levels of  $\beta$ -galactosidase activity in cells treated with 100  $\mu$ M zinc compared with 3  $\mu$ M zinc (Figure 3.4; panel A), suggesting a ZTRE-dependent transcriptional repression in response to elevated zinc level. As a positive control, the promoter activity of a zinc-responsive human metallothionein 2a (MT2A) promoter spanning bases -358 to +40 relative to the TSS in the same pBlue-TOPO vector (pBlueMT2Aprom) was measured. As expected,  $\beta$ -galactosidase specific activity in cell lysates transfected with the MT2A

plasmid construct showed a zinc-induced transcriptional up-regulation upon addition of 100  $\mu\text{M}$  compared with 3  $\mu\text{M}$  zinc (panel B), confirming that cells responded to zinc as had been observed previously (Jackson et al., 2008).

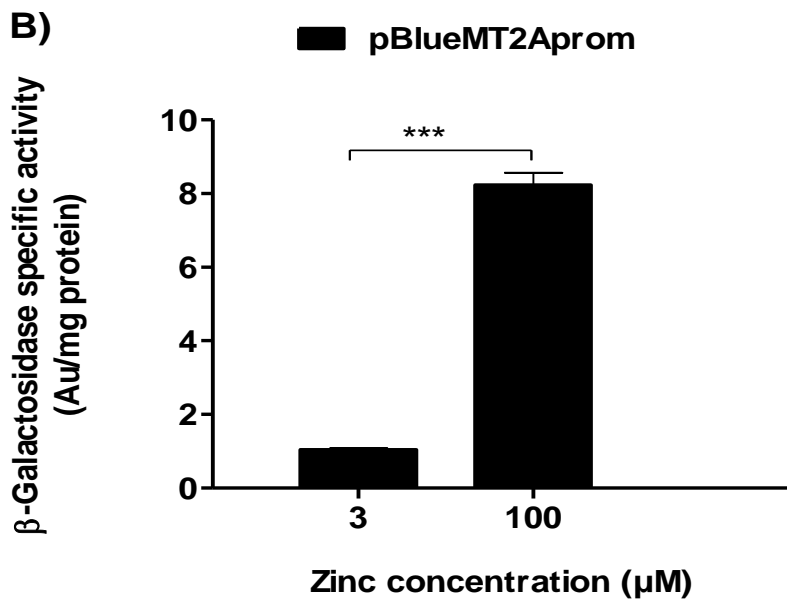
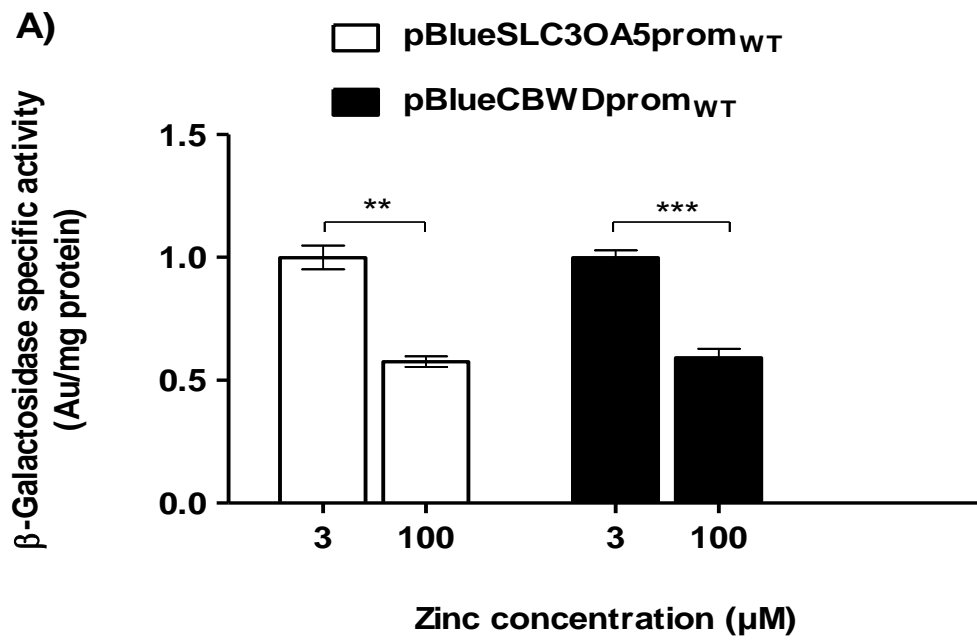


**Figure 3.4: Promoter activity of *SLC30A5* and *CBWD* genes is repressed by zinc.**

Caco-2 cells were seeded at  $3 \times 10^5$  cells/well in 12-well plates and grown in DMEM for 24 h. Twenty four hours post seeding, cells were transiently transfected with pBlue*SLC30A5*prom<sub>WT</sub>, pBlue*CBWD1*prom<sub>WT</sub> or pBlueMT2Aprom (positive control) plasmids. Twenty four hours after transfection, cells were maintained in serum-free DMEM containing zinc chloride added at 3  $\mu$ M (control medium) and 100  $\mu$ M for another 24 h. After a further 24 h, cell lysates were prepared for measurement of promoter activity as  $\beta$ -galactosidase specific activity. Panel A shows results for pBlue*SLC30A5*prom and pBlue*CBWD1*prom while panel B shows the response of the pBlueMT2Aprom positive control. Data plotted as mean  $\pm$  SEM normalised to the control condition for  $n \geq 6$ . \*\*\*P < 0.001, \*\*P < 0.01, determined by Student's unpaired t-test.

### ***3.3.3 The effect of ZTRE mutation on zinc-induced transcriptional repression of SLC30A5 and CBWD gene promoters***

To determine if the ZTRE rather than other sequences within *SLC30A5* and *CBWD* promoter constructs mediates transcriptional repression in response to zinc, the sequence in the promoter-reporter constructs was mutated to a random sequence. This was achieved using a PCR-based strategy that substituted the ZTRE sequence in pBlue*SLC30A5*prom<sub>WT</sub> - CACTCCC (CC) GGGAGTG - with the sequence GGTAGCC (CC) GGGAGTG. The mutated construct is referred to as pBlue*SLC30A5*prom<sub>MUT</sub>. The same mutation was introduced into the pBlue*CBWD*prom<sub>WT</sub> construct in place of the ZTRE sequence CACTCCC (CC) GGGAGTG to generate the mutant *CBWD* promoter-reporter construct pBlue*CBWD1*prom<sub>MUT</sub>. Caco-2 cells were transfected with these mutant constructs, treated with zinc and cell lysates were prepared for the measurement of beta-galactosidase specific activity as described previously. Background activity was measured in cell lysates transfected with vector (pBlue TOPO) containing no insert and the values were subtracted from all other data. Consistent with the predicted role of the ZTRE in zinc-induced transcriptional repression, both plasmid constructs carrying the substituted version of the ZTRE showed no transcriptional repression in response to elevated zinc levels (Figure 3.5). Beta-galactosidase specific activity measured in cell lysates prepared from cells transfected with the MT2A promoter reporter plasmid gave results consistent with its zinc-induced transcription, providing a positive control.

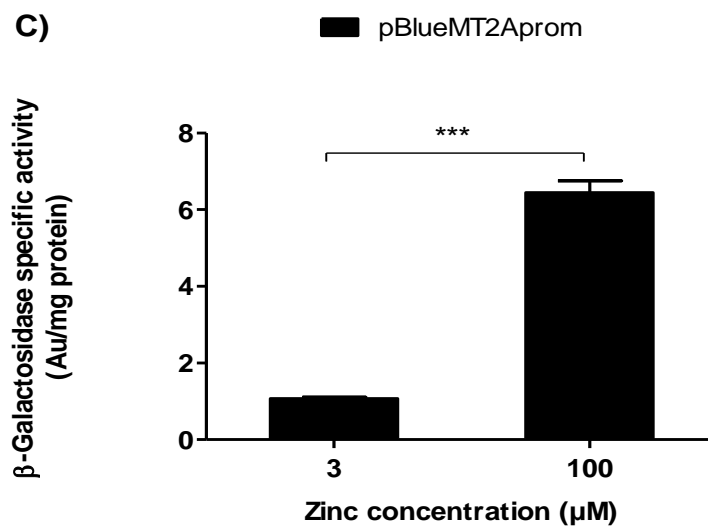
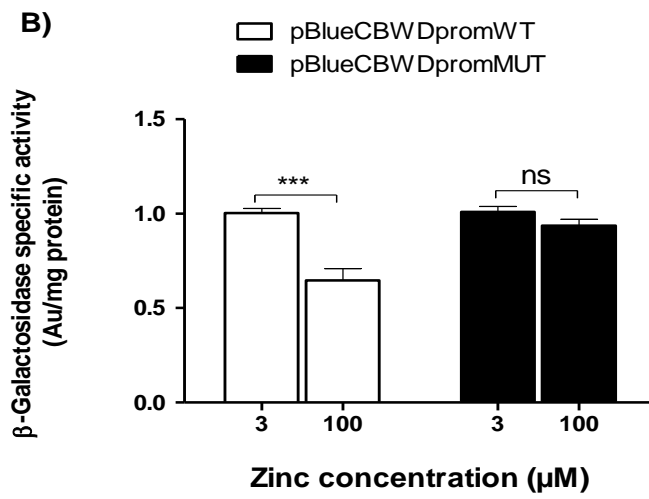
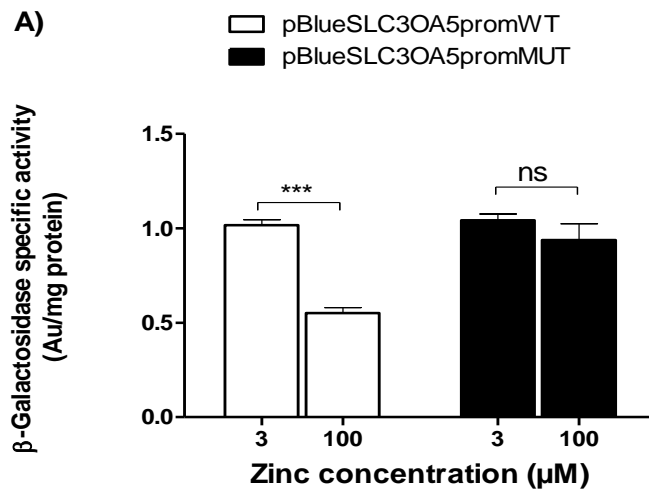


**Figure 3.5: Mutation of the ZTRE in *SLC30A5* and *CBWD* promoter sequences abrogates the response to zinc.**

Caco-2 cells were seeded at  $3 \times 10^5$  cells/well in 12-well plates and grown in DMEM for 24 h. Twenty four hours post seeding, cells were transfected with pBlue*SLC30A5*prom<sub>WT</sub>, pBlue*SLC30A5*prom<sub>MUT</sub>, pBlue*CBWD1*prom<sub>WT</sub> or pBlue*CBWD1*prom<sub>MUT</sub> plasmids. After a further 24 h, cells were maintained in serum-free DMEM containing zinc chloride added at 3  $\mu$ M (control medium) or 100  $\mu$ M for another 24 h. After a further 24 h, cell lysates were prepared for measurement of promoter activity as  $\beta$ -galactosidase specific activity. Panels A and B show response to zinc by *SLC30A5* and *CBWD1* while the response to zinc by *MT2A* (used as a positive control) is shown in panel C. Data are plotted as mean  $\pm$  SEM normalised to the control condition for  $n \geq 6$ . \*\*\*\*P < 0.001, \*\*P < 0.01, ns is non-significant determined by Student's unpaired t-test.

### ***3.3.4 The effect of deletion of the 5' or 3' components of the SLC30A5 ZTRE on the response to zinc***

To determine if both 5' and 3' components of the ZTRE are required to mediate transcriptional repression in response to elevated extracellular zinc, site-directed mutagenesis was carried out to delete one or other of the two sides of the palindromic sequence. Mutagenic oligonucleotides incorporating the desired mutation (listed in Table 3.2) were used to amplify the promoter sequence containing the ZTRE in pBlueSLC30A5prom<sub>WT</sub> in a PCR reaction. Products were then digested with *DpnI* endonuclease (target sequence: 5'-Gm<sub>6</sub>ATC-3', Promega), which discriminates between the parental methylated DNA template and the newly synthesised (non-methylated) mutation-containing plasmid. The plasmid was then transformed into Top10 competent cells (Invitrogen) followed by screening of positive colonies by small scale plasmid preparation, then sequencing (MWG Eurofins) to confirm the deletion and fidelity of the rest of the sequence in the plasmid construct. Caco-2 cells were transfected with endotoxin-free preparations of the mutagenised pBlueSLC30A5\_5'ZTREprom or pBlueSLC30A5\_3'ZTREprom plasmids using Lipofectamine 2000 (Invitrogen) followed by zinc treatment and measurement of promoter activity as described previously. As shown in Figure 3.6 (A and B), the removal of either the 5' or 3' component of the palindromic sequence resulted in the loss of transcriptional repression in response to elevated zinc concentration. These results demonstrate that a functional ZTRE requires both sides of the linker region.

Name	Forward	Reverse
3' <i>SLC30A5</i> ZTRE	GCGCAGACGCAAGGCTGGGC <u>GGGAGTGAGGGTTGCTGGG</u>	CCCAGCAACCCTCACTCCCGCCC AGCCTTGCGTCTGCGC
5' <i>SLC30A5</i> ZTRE	CGCAAGGCTGGGC <u>ACTCCCC</u> AGGGTTGCGGGCCTGATGAC	GTCATCAGGCCCGCAACCCTGGG GAGTGCCCAGCCTTGCG

**Table 3.2: Oligonucleotides used in site-directed mutagenesis of the *SLC30A5* ZTRE**

In each primer set, the underlined sequence in the forward primer represents the end of the palindromic sequence that remained in the *SLC30A5* promoter-reporter construct after deletion.

Primer sequences are given in the 5' to 3' direction.

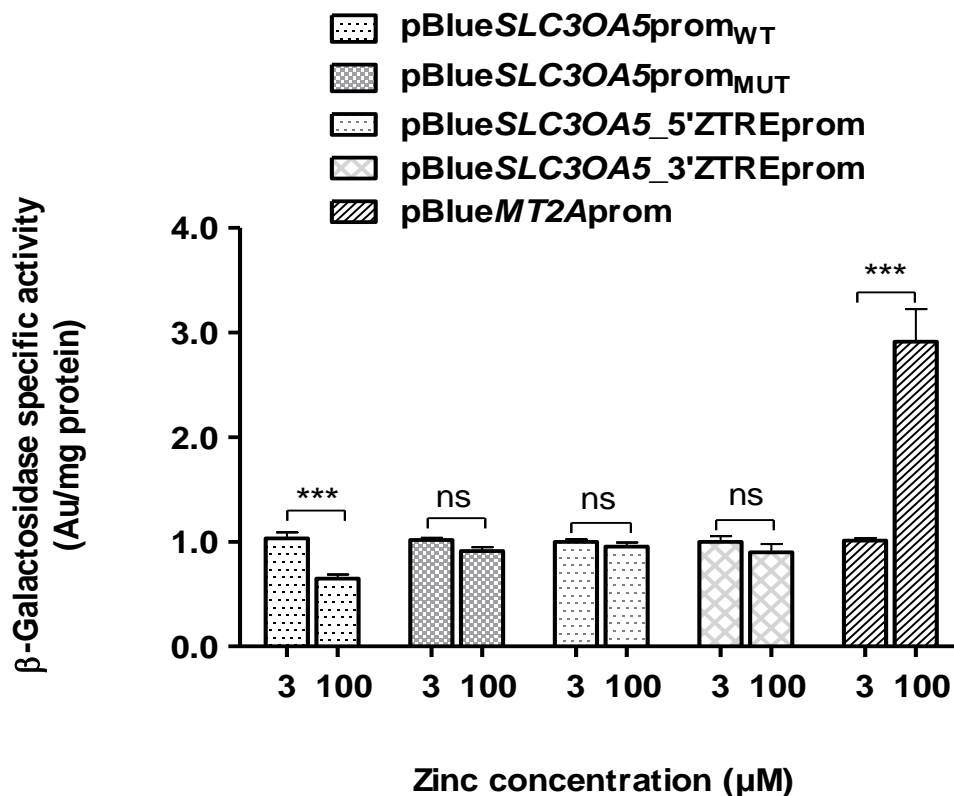


**Figure 3.6: Both 5' and 3' ZTRE components are required to mediate transcriptional repression in response to zinc.**

Caco-2 cells were seeded at  $3 \times 10^5$  cells/well in 12-well plate and grown in DMEM for 24 h. Twenty four hours post seeding, cells were transiently transfected with pBlueSLC30A5prom<sub>WT</sub>, pBlueSLC30A5prom<sub>MUT</sub>, pBlueSLC30A5\_5'ZTREprom, pBlueSLC30A5\_3'ZTREprom or pBlueMT2Aprom (positive control) plasmids. After a further 24 h, cells were maintained in serum-free DMEM containing zinc chloride added at 3 µM (control medium) and 100 µM for another 24 h. After a further 24 h, cell lysates were prepared for measurement of promoter activity as β-galactosidase specific activity. Data plotted are mean ± SEM from repeated experiments and normalised to control condition for n = 6 -12. \*\*\*P<0.001, \*\*P<0.01, ns is non-significant determined by Student's unpaired t-test.

### ***3.3.5 Zinc selectivity of the SLC30A5 ZTRE in mediating a transcriptional response***

Previous experiments revealed that only zinc and none of a panel of other metals tested including cobalt, copper, nickel and magnesium could induce the binding of a regulatory factor to the ZTRE-containing *SLC30A5* probe in EMSA. Similarly, only zinc could restore binding of the putative protein factor following inhibition by depleting zinc levels with a zinc chelator (Coneyworth et al., 2012), thus metals other than zinc were not promising candidates for ZTRE-dependent transcriptional regulation. Here, the effect of metals other than zinc on the promoter activity of the *SLC30A5* gene was tested by treating Caco-2 cells transfected with the pBlue*SLC30A5* promoter reporter plasmid with copper (Cu, 20  $\mu$ M), nickel (Ni, 20  $\mu$ M), cobalt (Co, 100  $\mu$ M) in addition to zinc at 3  $\mu$ M and 100  $\mu$ M following the standard protocol as described previously. The concentrations of metals other than zinc were chosen based on previous observations that change in gene expression was observed at these levels. The response to these metals of the *SLC30A5* promoter was assessed by measurement of  $\beta$ -galactosidase specific activity in cell lysates. Results showed that the activity of the *SLC30A5* promoter was unaffected by all the metals tested as there was no difference in  $\beta$ -gal specific activity between cells incubated with control medium and cells treated with the metals at concentrations indicated (Figure 3.7, panel A), consistent with the previous EMSA results that the ZTRE-mediated response of *SLC30A5* promoter is zinc-specific. The zinc-responsive metallothionein promoter reporter construct (pBlueMT2Aprom) showed the expected response to zinc (panel B), and was included as a positive control.

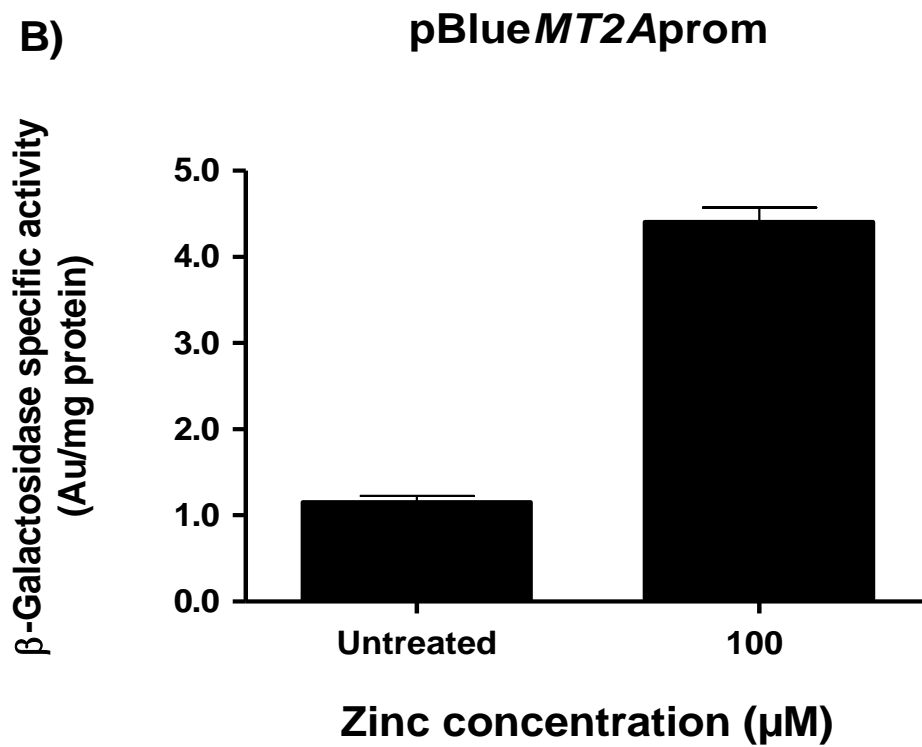
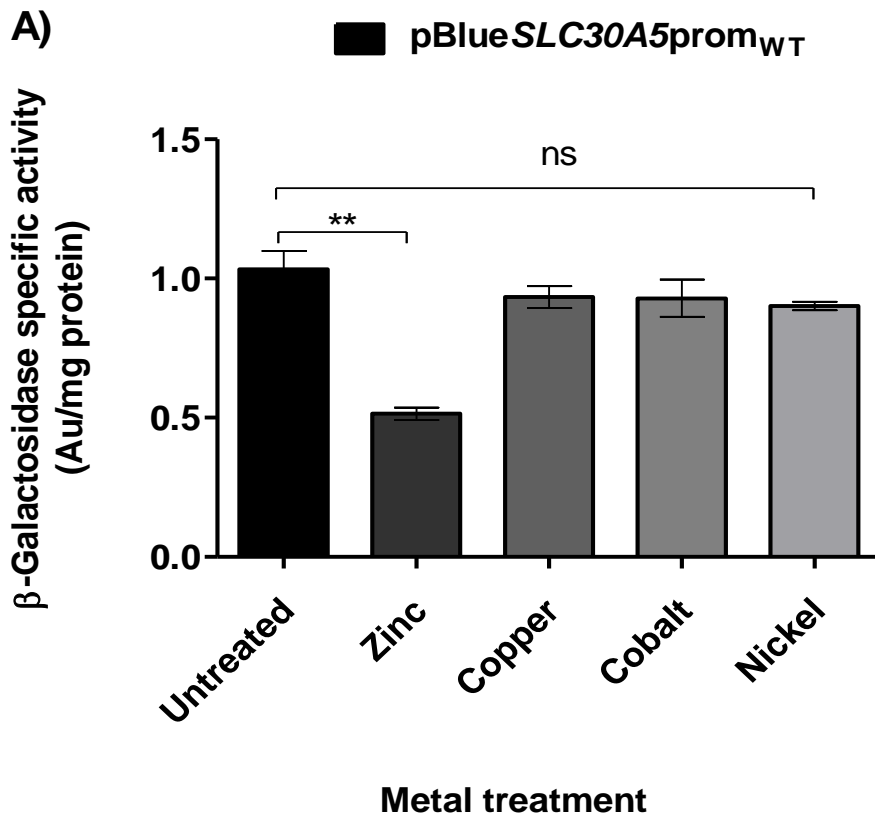


**Figure 3.7: The *SLC30A5* ZTRE-mediated response is zinc-specific.**

Caco-2 cells were seeded at  $5 \times 10^5$  cells/well in 12-well plates and grown in DMEM for 24 h. Twenty four hours post seeding, cells were transiently transfected with pBlue*SLC30A5*prom or pBlueMT2Aprom (positive control) plasmids. Twenty four hours after transfection, cells were maintained in serum-free DMEM containing ZnCl<sub>2</sub> added at 3 μM (control), 100 μM; CuCl<sub>2</sub> at 20 μM; CoCl<sub>2</sub> at 100 μM; or NiCl<sub>2</sub> at 20 μM for another 24 h. After a further 24 h, cell lysates were then prepared for measurement of promoter activity as β-galactosidase specific activity. Data plotted are mean ± SEM normalised to the control condition for n = 6 for 3 independent experiments. \*\*P <0.01, \*\*\*P <0.001, ns is non-significant as determined using one-way ANOVA followed by Bonferroni post-hoc test.

### 3.4 Discussion

Regulation of gene expression at the transcriptional level in response to environmental cues is mediated by the recognition and binding of regulatory proteins to specific DNA elements at promoters of target genes. Metal-induced transcriptional regulation of gene expression is a well-documented example of sequence-mediated transcriptional regulation that contributes towards restoring metal balance across many species. The bacterial transcriptional repressor Zur, for example, regulates the activity of zinc uptake proteins under zinc-limiting conditions by recognising and binding to a 7-1-7 consensus sequence (Shin et al., 2007). The yeast ZAP1 mediates transcriptional regulation in response to perturbations in cellular zinc levels by binding to an 11 bp zinc responsive element (ZRE) within the promoter of its target genes including its own promoter (Zhao et al., 1998). The mammalian metal response element-binding transcription factor (MTF-1) activates its target genes including *SLC30A1* and metallothionein, by binding to a 7 bp MRE consensus sequence at these promoters. Binding of MTF-1 to MREs at other promoters such as those of human and mouse selenoprotein H genes (Stoytcheva et al., 2010), as well as in the gene coding for Zip10 in mouse and zebrafish (Lichten et al., 2011, Zheng et al., 2008), can result in transcriptional repression, demonstrating the existence of a bimodal activity in response to changes in cellular zinc status that depends on MRE context.

The work presented in this chapter was conducted to investigate the regulation of *SLC30A5* and *CBWD* genes by zinc at both transcript and promoter levels, and to investigate the importance of the ZTRE in mediating this response. The observed response to zinc of *SLC30A5* mRNA levels confirms previous reports using the same cell line model (Jackson et al., 2007). Similar observations of down-regulation at the mRNA level at higher zinc levels have also been reported for the mouse *Slc39a4* gene (Dufner-Beattie et al., 2003b), the human *SLC30A1*

gene (measured in a cohort of human subjects on zinc supplementation) (Cragg et al., 2005) and the Krüppel-like factor 4 (*KLF4*) gene in HT-29 cells (Kindermann et al., 2005). In Caco-2 cells, mRNA levels of MTF-1 and its homologue MTF-2 were reduced in response to increased extracellular zinc concentration (Jackson et al., 2009). The transcript levels of *SLC30A10* (ZnT10 zinc efflux protein) were also reduced in both Caco-2 and human neuronal SH-SY5Y cells (Bosomworth et al., 2012) at higher extracellular zinc concentration. Repression of the mammalian *CBWD* gene transcripts by zinc, a gene for which no known role has been previously reported, and which is shown for the first time by work presented in this chapter, may be a component of the mechanism to restore balance in response to variation in external supply.

The reduction in activity of a promoter-reporter construct containing the ZTRE upstream of the TSS in the *CBWD1* gene promoter reveals that *CBWD* genes are repressed by zinc in a manner similar to regulation of *SLC30A5*. Replacement of the *CBWD1* ZTRE with a random sequence (the same random sequence as used in an inactivated *SLC30A5* promoter-reporter construct) resulted in abolishment of the transcriptional response to zinc, revealing functionality of the ZTRE as opposed to any other region of the promoter in this response.

There are many examples of transcriptional regulation mediated by palindromic DNA sequences. However, there seems to be paucity of evidence concerning whether or not only one side of such a palindromic sequence can be functional. We thus deleted one or other component of the ZTRE in an *SLC30A5* promoter-reporter construct and examined the effect on the response to zinc revealing that only when both elements were present was a response to zinc observed. It remains to be determined if retaining a sequence that is not palindromic yet has two components that each separately matches the ZTRE consensus sequence (CACTCCC (CC) GGGAGTG; (Coneyworth et al., 2012)) is still functional. Moreover, the length of the

inter-palindromic linker required is yet to be defined. Deletion mutations have also been employed in other work to study the activity or binding to DNA sequences of regulatory proteins such as the transcriptional repressor, Zur, in which deletion of the 3' component of the Zur box palindromic sequence of the *ZnuD* gene, abrogated Zur binding (Pawlik et al., 2012). Also, transcriptional activity of yeast transcription factor HAP1 was curtailed when the 3' side of the triplet CGG was substituted with CGC in the palindromic upstream activating sequence (UAS) of its target gene *CYC1* (which encodes an isoform of cytochrome c (Ha et al., 1996)) and transcriptional enhancer activity of the hr5 (an *Autographa californica* multiple nucleopolyhedrovirus gene expression enhancer) was reduced when half site of its 28-bp palindromic sequence was replaced by site-directed mutagenesis (Rodems and Friesen, 1995). The observation that the promoter activity of *SLC30A5* was non-responsive to metals tested other than zinc suggests that these metals cannot substitute for zinc in ZTRE-mediated transcriptional repression of the *SLC30A5* promoter. It is reported that zinc homeostatic genes/proteins can show a response to zinc at different concentrations in what is described as a bell-shape curve. For example, the zinc transporter ZnT1 mRNA levels increased with increasing zinc concentrations and peaked at 150  $\mu$ M but were reduced at 200  $\mu$ M in Caco-2 cells (Shen et al., 2008). Similarly, regulation of ZnT5 followed this pattern (Cragg et al., 2005). However, it is yet to be determined if this response across a full range is dependent on the ZTRE, and would be an interesting area for further pursuit.

Also, ZnT5 has been shown to localise as a dimer with ZnT6 to the Golgi apparatus, where it appears to supply zinc to enzymes of the secretory pathway (Fukunaka et al., 2009). Its repression by zinc may represent a mode of regulation consistent with its role in cellular zinc uptake (Valentine, 2007) rather than this alternative function.

In summary, the evidence presented reveals that *CBWD* genes in addition to *SLC30A5* are regulated by zinc and demonstrates the involvement of the *ZTRE* in mediating this response, which appears to be zinc-specific.

## **Chapter 4 : Evidence that the zinc finger protein ZNF658 binds to the Zinc Transcriptional Regulatory Element (ZTRE) to mediate zinc-induced transcriptional repression**

### **4.1 Introduction**

ZNF658 was studied as a candidate regulatory protein that mediates transcriptional repression of genes that contain the ZTRE in response to elevated extracellular zinc concentration. It was discovered by MALDI-TOF mass spectrometry in the tryptic digest of a band seen using EMSA with an *SLC30A5* probe containing the ZTRE sequence (unpublished work by John Tyson and Dianne Ford). Bioinformatics analysis shows that ZNF658 is a member of the ubiquitous C2H2 zinc finger-containing protein group and belongs to the Krüppel-like proteins, which were discovered on the basis of homology to the *Drosophilla melanogaster* Krüppel protein (Dang et al., 2000). This protein family has diverse cellular functions and represents up to 1% of human zinc-requiring proteins (Hoovers et al., 1992). However, only a few members of this group have been studied and none has been reported to mediate transcriptional down-regulation of multiple genes in response to zinc. ZNF658 protein has five predicted isoforms designated X1 through X5 (according to NCBI Reference Sequence). Variants X1, X2 and X3 have 1059 amino acids while X4 and X5 have 1053 and 751 amino acids respectively. Alignment of the amino acid sequence of isoform X1 with the *Saccharomyces cerevisiae* genome database at <http://www.yeastgenome.org/> using BLASTP programme showed similarity with ZAP1 (Figure 4.1), the yeast transcription factor that plays a central role in zinc homeostasis. Inspection of the amino acid sequence of ZNF658 for the motif C-X<sub>2</sub>-C- X<sub>12</sub>-H- X<sub>3</sub>-H revealed 21 zinc fingers, of which zinc fingers 12 -17 share of similarity with the ZAP1 zinc fingers 3 -7, corresponding to the ZAP1 DNA binding domain (Figure 4.1).

## 4.2 Specific objectives

The objectives of the work presented in this chapter were to investigate if:

- ZNF658 binds directly to the ZTRE;
- ZNF658 mediates zinc-induced transcriptional repression of genes that include the ZTRE;

## 4.3 Results

### 4.3.1 Identification of the Krüppel associated box (KRAB) domain in ZNF658

Zinc finger-containing transcription factors can possess an effector motif called the Krüppel Associated Box (KRAB) domain, typically located at the N-terminal region (Bellefroid et al., 1991, Lupo et al., 2013). The domain is evolutionarily conserved among many species and has been demonstrated to confer transcriptional repressor activity on the proteins that contain the domain (Margolin et al., 1994a, Lorenz et al., 2001). The KRAB-containing zinc finger proteins (KRAB-ZFPs) represent the single largest family of regulatory proteins in mammals (Urrutia, 2003), and they function by recruiting corepressors such as KRAB associated protein 1 (KAP1) (also called transcriptional intermediary factor 1 (TIF1)) (Looman et al., 2004). The KRAB domain in ZNF658 was identified through an *in silico* search for conserved protein domains using NCBI conserved domain search at <http://www.ncbi.nlm.nih.gov/Structure/cdd/wrpsb.cgi>. The KRAB domain is represented with a hatched box in Figure 4.1 and its sequence alignment with the KRAB domain of some randomly selected members of the KRAB-ZFP family is shown in Figure 4.2.

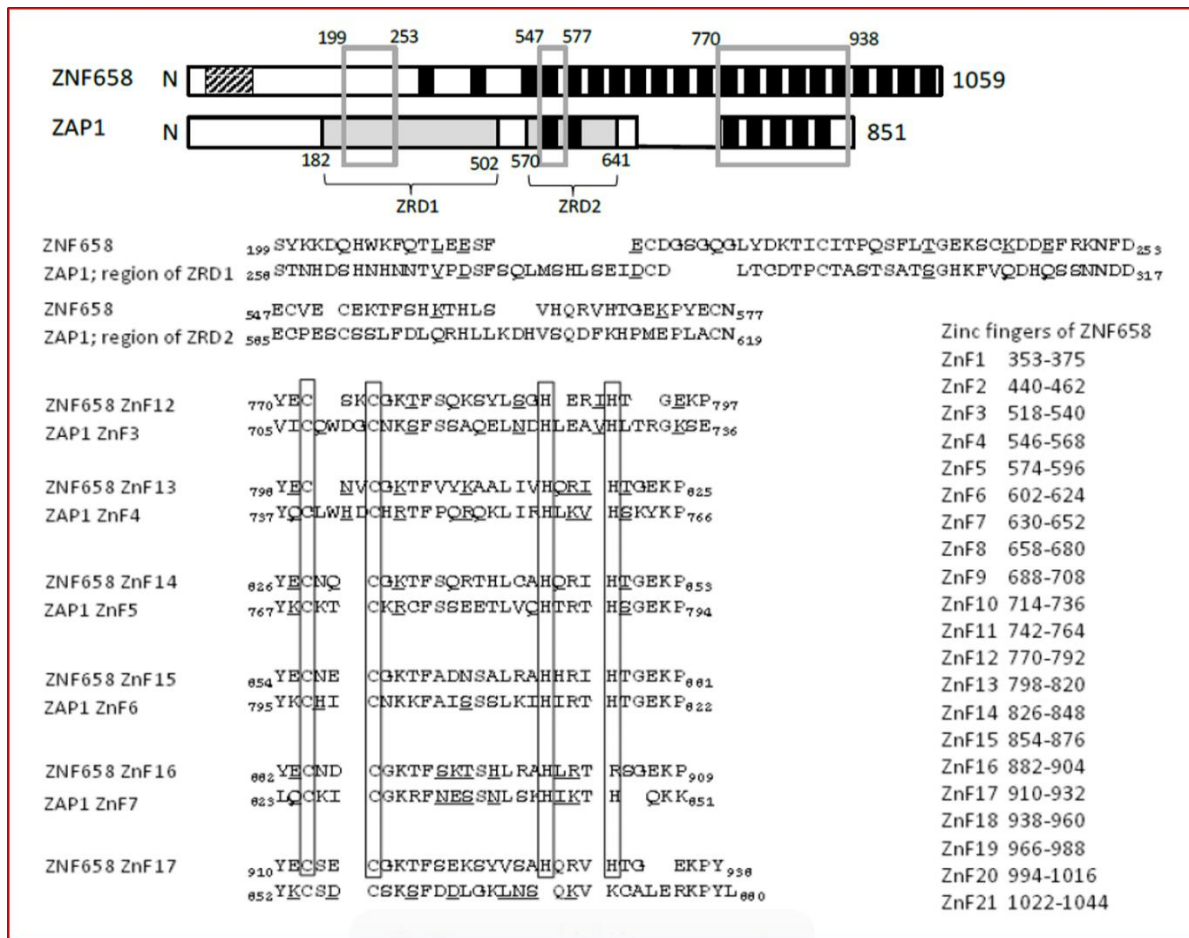


**Figure 4.1: Domain structure representation of the mammalian ZNF658 and the yeast ZAP1 proteins and amino acid sequence alignment highlighting regions of similarity**

The amino acid sequence of ZNF658 was aligned with the yeast genome database at (<http://www.yeastgenome.org/>). The alignment with the lowest E-value ( $3.7e^{-30}$ ) was with the ZAP1 protein. The 21 and 7 zinc fingers of both ZNF658 and ZAP1 proteins are indicated by vertical black boxes while open grey boxes show regions of similarity. The zinc-responsive domains (ZRDs) of ZAP1 are indicated as ZRD1 and ZRD2 with amino acid numbers indicated. Regions of ZNF658 zinc fingers 12 -16 that match exactly with ZAP1 zinc fingers 3 -7 are shown. The amino acids representing the zinc finger motifs are indicated while conservative amino acids are underlined. Positions of the 21 ZNF658 zinc fingers are also indicated to the right of the figure. The hatched box at the N-terminus of ZNF658 represents a KRAB box domain.

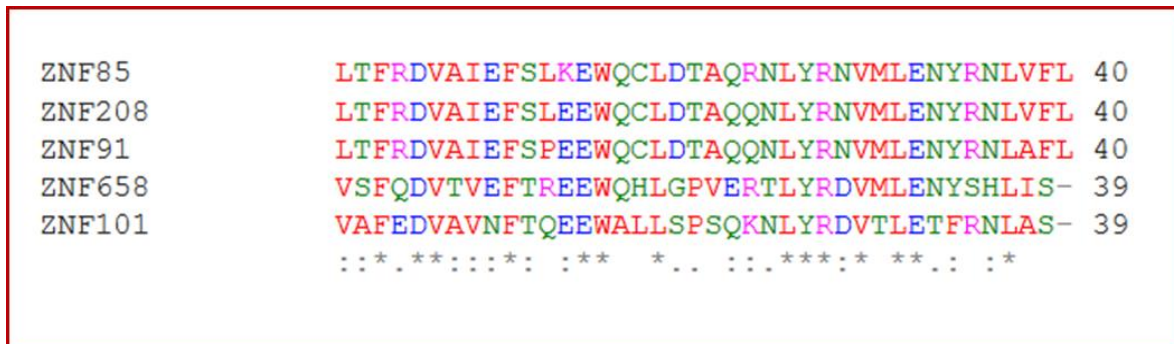


**Figure 4.2: The KRAB domain sequence of ZNF658**

The KRAB domain (and KRAB A) was identified through a search for conserved domains at <http://www.ncbi.nlm.nih.gov/Structure/cdd/wrpsb.cgi>, using the amino acid sequence of human ZNF658 and 5 other randomly selected KRAB-ZFPs. Alignment by ClustalW2 of these sequences is shown. Amino acids highlighted in red, green, magenta and blue indicate hydrophobic, hydrophilic, basic and acidic, respectively. Asterisks (\*) indicate fully conserved amino acids; the symbol : indicates amino acids with strongly similar properties; the symbol . indicates amino acids with weakly similar properties; a dash (-) indicates missing amino acids.

### ***4.3.2 Demonstration that ZNF658 binds to the ZTRE-containing SLC30A5 probe***

Electrophoretic mobility shift analysis (EMSA) was used to determine if ZNF658 binds to the ZTRE. Protein extract prepared from Caco-2 cells transiently expressing recombinant ZNF658 with a C-terminal myc tag was incubated with a 204 bp *SLC30A5* labelled probe (corresponding to bases -154 to +51 relative to the TSS (Figure 4.3; panel A), which was previously defined as the minimum length required that conferred zinc-responsive transcriptional repression to *SLC30A5* (Jackson et al., 2007). This probe contains the ZTRE at position -91 to -76 relative to the TSS. In some binding reactions excess (200-fold) competitor oligonucleotide sequence that included the ZTRE (Figure 4.3; panel B) was included. As shown in Figure 4.4, incubation of protein extract from cells transfected with recombinant ZNF658 resulted in a band that was retarded (lane 2) compared with the free probe (lane 1). Addition of the excess unlabelled double-stranded competitor oligonucleotide reduced the complex formed between the protein extract and the probe, demonstrating specificity of the band observed (lane 3). When anti-myc antibody was included in the binding reaction, a further shift in the complex (supershift) was observed, indicated by the arrow to the right of the figure (lane 4), demonstrating that the complex formed represented the labelled probe with ZNF658 bound to the ZTRE. These results demonstrate that ZNF658 binds directly to the ZTRE.

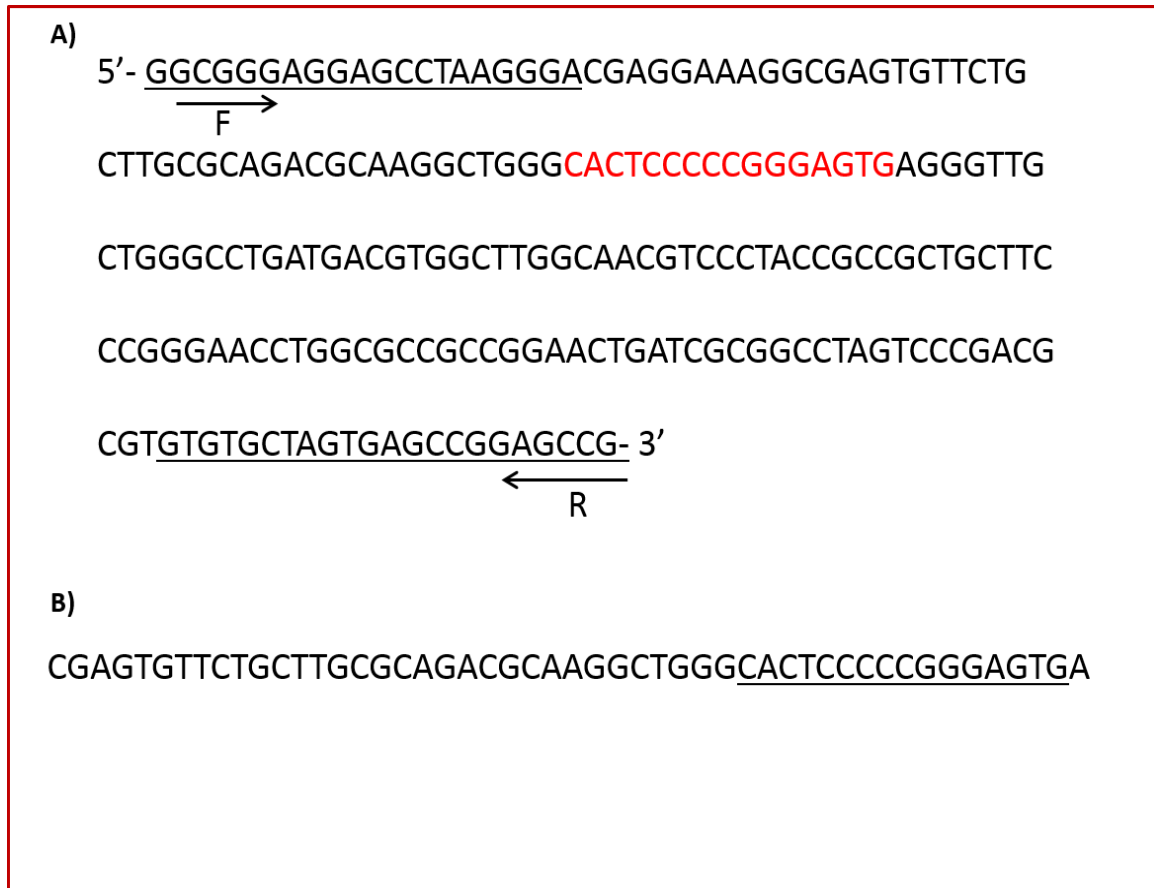


**Figure 4.3: Sequence of IRD700-labeled *SLC30A5* probe used in EMSA experiments**

The 204 bp *SLC30A5* promoter probe sequence (panel A) spanning the region -154 to +50 relative to the transcription start site and including the zinc transcriptional regulatory element (highlighted in red) was amplified by PCR from the pBlue*SLC30A5*prom template to make a double stranded probe using IRD700-labelled (IDT) primers (underlined). Panel B shows the 50 bp sequence of the double stranded competitor oligonucleotide used in competition EMSA with the ZTRE underlined.

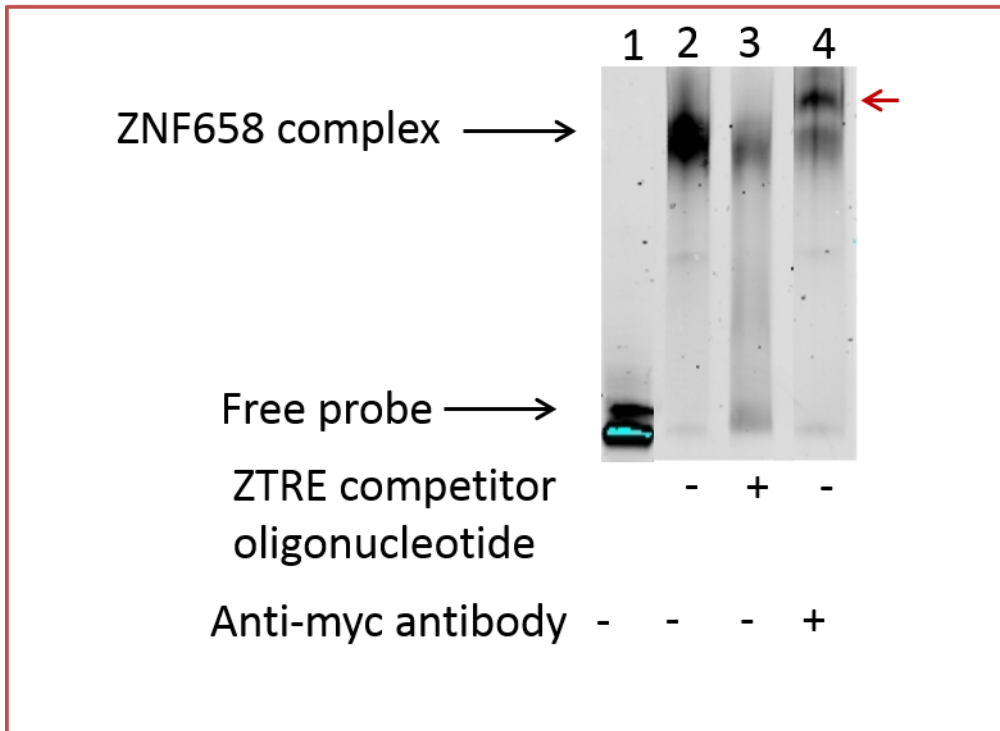


**Figure 4.4: ZNF658 binds specifically to the ZTRE in *SLC30A5***

Caco-2 cells were grown in 6-well plate for 24 h. Cells were transiently transfected with pCMV6-ZNF658-myc-DDK (Origene) construct. After a further 24 h, nuclear extract from cells expressing ZNF658 were prepared. Five microgramme (5 µg) protein was incubated with 50 fmol IRD700-labelled probe for 20 minutes at room temperature after which the mixture was electrophoresed through a non-denaturing 7.5 % polyacrylamide precast gel (Biorad) for 70 minutes at 100 V. Competition EMSA included in the binding reaction a 200-fold excess over the probe (2.5 picomoles). Supershift EMSA included anti-myc antibody at 1µg in the binding reaction 20 minutes after binding reaction was incubated and a further 10 minutes before electrophoresis. Representative images of repeated experiments are shown. The arrow to the right of the figure indicates the supershifted band.

### ***4.3.3 Identification of the DNA-binding region of ZNF658 protein and demonstration that ZNF658 binds only a ZTRE with both 5' and 3' components.***

To gain some mechanistic insight on the binding properties of the ZNF658 zinc finger modules, zinc fingers 12-15, which spans the region 770 – 905 in the amino acid sequence and is the region of ZNF658 homologous to the DNA binding domain of ZAP1 (Figure 4.1), were deleted. The deletion was created in the plasmid pCMV6, which contains the full ZNF658 sequence fused to a myc-DDK epitope, using oligonucleotide primers listed in Table 4.1 to amplify the entire plasmid but excluding the region to be deleted (Figure 4.5). The mutant construct is designated ZNF658<sup>Δ770-904</sup>-myc-DDK. Protein extract was then prepared from cells expressing wild type recombinant ZNF658 and from cells expressing the mutant ZNF658. Protein extracts were incubated with either the *SLC30A5* probe containing full ZTRE or where the 3' component was excluded. No band was formed when cells were incubated the labelled probe with protein extracts from cells expressing the mutant protein. (Figure 4.6, lane 5), indicating that the ability of ZNF658 to bind the ZTRE is dependent on the presence of zinc fingers 12 -15. Likewise, no complex formed when the probe lacked the 3' component of the ZTRE and ZNF658 (lane 6), demonstrating that ZNF658 requires both 5' and 3' components of the ZTRE to bind.

<b>Primer name</b>	<b>Sequences (5'-3')</b>	<b>Cycling parameters</b>
ZNFDEL_Fwd	<sup>2878</sup> TCA GGG GAG AAG CCC TAT GAA TGC AGT G <sup>2905</sup> (28)	98 °C (3 min) then 35 cycles of 98 °C (30 s), 72 °C (30 s), 72 °C (4 min),
ZNFDEL_Rev	<sup>2459</sup> GGG TTT CTC CCC TGT GTG AAT TCT CCG ATG <sup>2430</sup> (30)	98 °C (3 min) then 35 cycles of 98 °C (30 s), 72 °C (30 s), 72 °C (4 min),

**Table 4.1: Oligonucleotide sequences and thermal cycling parameters used in PCR to delete zinc fingers 12 – 15 of ZNF658**

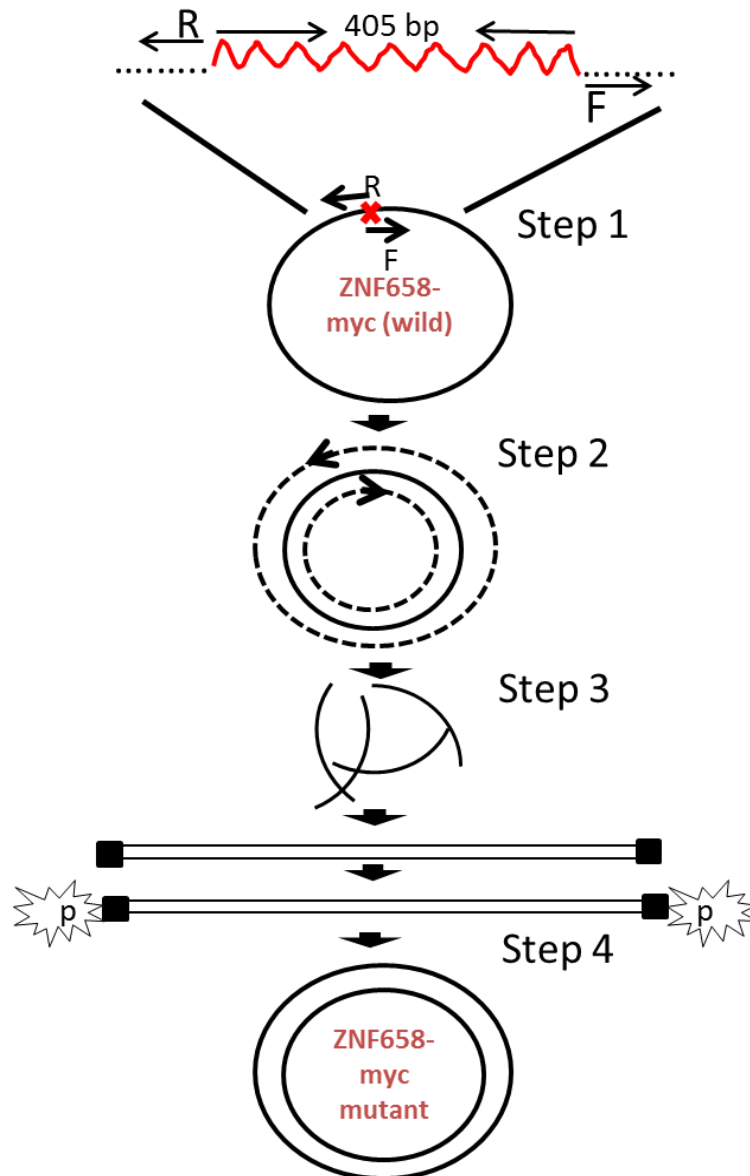


**Figure 4.5: Schematic diagram showing the inverse PCR technique used to delete zinc fingers 12 – 15 from ZNF658**

Primers ('R' and 'F') were designed to delete the 405 bp region, corresponding to zinc fingers 12-15 (x, step 1) and represented in red as a wavy line in the expanded view through an inverse PCR procedure (step 2) using the wild type plasmid construct as template. The PCR product was then treated with *DpnI* to digest the parent template (step 3) and annealed to give a linear product, which was then phosphorylated and circularized by addition of T4 DNA ligase-containing polynucleotide kinase (PNK) with ATP as the phosphate donor (step 4) to generate the mutant construct.

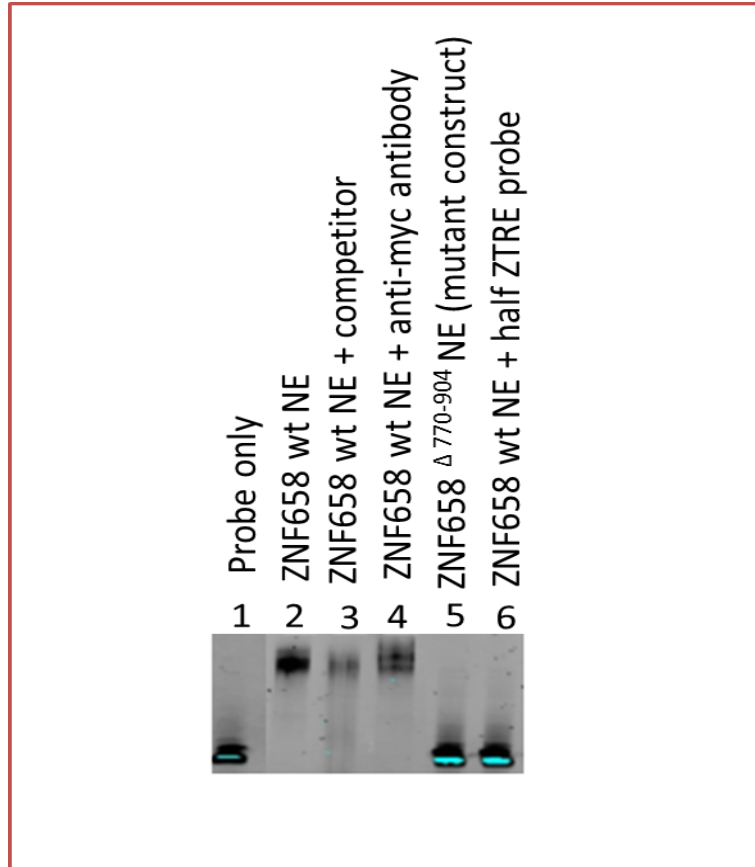


**Figure 4.6: ZNF658 requires zinc fingers 12 -15 and both 5' and 3' components of the ZTRE to bind.**

Caco-2 cells were seeded at  $5 \times 10^5$  cells /well in 6-well plates and grown in DMEM for 24 h. Cells were transiently transfected with pCMV6-ZNF658-myc-DDK (wild type; lanes 2 - 4) or pCMV6-ZNF658 $\Delta^{770-904}$ -myc-DDK (mutant; lane 5) constructs 24 h later. After a further 24 h, nuclear extracts were prepared and 5  $\mu$ g protein in each case was incubated with 50 fmol IRD700-labelled SLC30A5 probe containing an intact ZTRE (lanes 2 -5) or labelled probe containing only 5' end of the ZTRE (lane 6) for 60 minutes at room temperature after which the mixture was electrophoresed through a non-denaturing 7.5 % polyacrylamide precast gel (Biorad) for 70 minutes at 100 V. For competition and supershift EMSA, excess unlabelled probe (lane 3), and anti myc antibody were included in the binding reactions. A representative image of 3 repeated experiments is shown. NE indicates nuclear extract, wt indicates wild type.

#### 4.3.4 Effect of zinc on transcript levels of ZNF658

To examine if ZNF658 transcript levels were altered in response to increased extracellular zinc, ZNF658 mRNA levels were measured by RT-qPCR and expressed relative to GAPDH mRNA levels under control conditions (3  $\mu\text{M}$  zinc) and at an elevated zinc concentration (100  $\mu\text{M}$ ). As indicated in Figure 4.7, there was no significant difference between ZNF658 mRNA levels under the two conditions, suggesting that ZNF658 transcript levels are unaffected by extracellular zinc concentration.

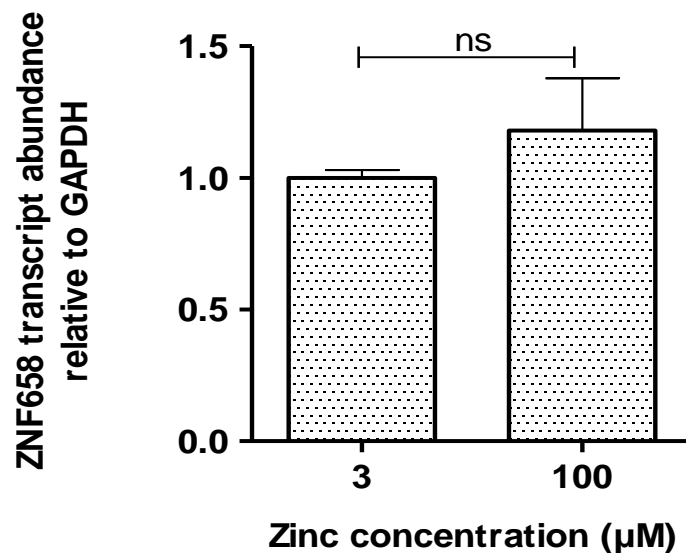


**Figure 4.7: ZNF658 transcript abundance is unaffected by increased extracellular zinc concentration**

Caco-2 cells were seeded at  $5 \times 10^5$  cells/well in 6-well plates and maintained in DMEM for 24 h. Twenty four hours post seeding, cells were incubated in serum-free DMEM containing zinc chloride added at 3  $\mu\text{M}$  (control medium) or 100  $\mu\text{M}$  for another 24 h. Total RNA was extracted using Trizol reagent and reverse-transcribed to cDNA. ZNF658 transcript levels relative to GAPDH mRNA levels were measured by RT-qPCR and normalised to control condition. Data are expressed as mean  $\pm$  SEM for  $n \geq 6$ . NS indicates non-significant by Student's unpaired t-test.

#### ***4.3.5 siRNA-mediated knockdown of ZNF658 in Caco-2 cells***

To determine if ZNF658 was responsible for the response to zinc of genes repressed by a mechanism dependent on the ZTRE, the effect of knockdown on these gene responses was determined. Two siRNAs targeted at different regions of the ZNF658 coding sequence (Figure 4.8) were designed to reduce expression. Sequences including those of the siRNA and the target sequences on the gene are listed in Table 4.2. Oligonucleotides used to confirm knockdown including cycling parameters are shown in Table 4.3. Cells were transfected with the siRNAs and RNA was prepared for quantitative measurement of ZNF658 expression relative to transcript levels of *GAPDH*. When normalised to control siRNAs, the ZNF658-targeted siRNAs reduced expression of the gene by approximately 60 % (Figure 4.9), confirming the efficacy of siRNA to reduce gene expression.

```

5'CTTTAGGTCTGCGCGGGAGCCGAGGCTGCGCACCTGGGCTGAACCTCCACAGTCCTCTACACTTCCAG
GAGCAGCAGAAAATGAACATGTCAGGCATCAGTGTTCATCCAGGACGTGACTGTGGAATCACCCGGG
AGGAGTGGCAGCACCTGGGCCCTGTCGAGAGGACGCTGTACAGAGATGTGATGCTGGAGAACTACAGCCA
CCTCATCTCAGTGGGATATTGCATTACTAAACCTAAGGTGATCTCCAAGTTGGAGAAAGGAGAAGAGCCA
TGGTCTTTAGAAGATGAATTCCTGAACCAGAGGTACCCAGGGTATTTTAAAGTTGATCACATCAAAGGGA
TCCGGGAAAAACAAGAAAAACCTCTGTGGCAAGAAATATTCATCAGTGTGCTGACAAAACATTGAGTAA
AGAAGGACAGAAAGTTTTAGAAAAACCATTTAATCTGGAAATAGCTCCAGAGCTTTCAGAAAAAATATCC
TGTAATGTGACTCACACAGAATGAATTTGCCAGTTGCTTCTCAATTAATTATAAGTGAAGAAAAATATT
CAAGAAAGAAGACTGAATACATGAATGTGTGTGAGAACTGCAGCTTGATATTAAGCATGAGAAAGCTCA
TGCTGAAGAGAAATCTTATGAACATGGTGAAAATGCTAAAGCTTTCAGTTATAAGAAAGATCAGCATTGG
AAATTTCAAACCTTTGGAGGAATCTTTGAATGTGATGGATCTGGACAAGGTTTATATGATAAGACAATTT
GTATTACACCTCAGAGTTTTCTAACAGGAGAAAAAGTCTGTAAGGATGATGAATTTAGAAAAAACTTTGA
TAAATCACTTTATTTAACACATGAGAACTGACACAAGGGGAAATGCTCTGATCTTAATGAATATGGG
ACATCTGTGACAAAACCACCGCTGTTGAATACAATAAAGTTCACATGGCTATGACACACTATGAGTGTA
ATGAAAGGGGGATTAATTTAGTAGGAAGTACCCCTCACTCAATCTCAGAGAACTATTACAGGATGGAG
TGCTTTTAAAAGCAATAAATGTGAAGAAAATTTAGCCAGAGCTCAGCCATATAGTACATCAGAAAAACA
CAAGCTGGAGATAAATTTGGTGAACATAATGAATGTACAGATGCCCTCTACCAGAAATTAGACTTTACAG
CACATCAGAGAATTCACACAGAAGATAAATTCTACCTTTCTGATGAACATGGGAAATGCAGAAAATCCTT
TTACCGGAAAGCACACCTCATTACAGCATCAGAGGCCCACTCAGGAGAGAAAACCTACCAATATGAGGAA
TGTGCAAAATCCTTTTGTCAAGTTCACATCCTATTTCAGCATCCTGGAACCTATGTGGGATTCAAACCTT
ATGAATGTAATGAATGTGGGAAAGCTTTCTGTGAGAATTCAAACCTCAGTAAACATCTGAGAATTCACAC
AAAAGAGAAACCTTGTGATAACAATGGCTGTGGGAGATCTACAAGTCACCCCTCATAGGACACCAGAAA
ACAGATGCAGAGATGGAACCTGTGGTGGCAGTGAATATGGGAAGACATCACATCTCAAAGGACATCAGA
GAATTCATGGGGGAGAAACCCCTATGAATGATTTGAATGTGGGAAAACCTTCTCCAAGACATCACATCT
CAGAGCACATCAGAGAATTCACACAGGTGAAAAACCCCTATGAATGTGTTGAATGTGAGAAAAACTTCTCT
CACAAGACACACCTCAGTGTACATCAGAGAGTTCACACAGGGGAGAAACCCCTATGAATGTAATGACTGTG
GGAAATCTTTTACCTATAACTCAGCCCTGAGAGCACATCAAAGAATTCACACAGGTGAGAAGCCCTATGA
ATGCAGTGACTGTGAGAAAACCTTTGCCATAATTCAGCCCTCAGAGCACATCATAGAATTCACACGGGG
GAGAAACCTTATGAATGTAATGAATGTGGAAGTCTTTTGCCATATTTCTGTTCTCAAGGCACATCAA
GAATTCACACAGGGGAGAAACCCCTATGAATGTAATGAATGTGGGAGATCTTTCACCTACAATTACAGCCT
GAGAGCACATCAGAGAATTCACACAGGTAGAAAACCCCTATGAATGTAGTACTGTGAGAAAACCTTTGCC3'

```

**Figure 4.8: The ZNF658 coding region indicating siRNA target sequences**

The portions of the sequence highlighted in red (from 5' to 3') were targets for siRNA-mediated silencing with siRNA 1(3/4 exon junction) and siRNA 2 (exon 5) respectively.

ZNF658 (NM_033160.5) sequence identity	siRNA sequences (5'-3')
Target sequence for siRNA1	<sub>289</sub> CAGUGGGGAUUAUUGCAUUACUA <sub>309</sub> TT
siRNA1(Ambion)	Sense strand GUGGGGAUUAUUGCAUUACUATT Antisense strand UAGUAAUGCAAUAUCCCACTG
Target sequence for siRNA 2	<sub>2143</sub> GGAGATCTTTACCTACAATT <sub>2163</sub> TT
siRNA2 (Qiagen)	Sense strand GGACCAGGAUUGCAGCCUatt Antisense strand UAGGCUGCAAUCCUGGUCCct

**Table 4.2: Sequences of ZNF658 targeted for knockdown and the siRNA sequences used**

Primer name	Sequence (5'-3')	Cycling parameters for 45 cycles
ZNF658_Fwd	GCT GCG CAC CTG GGC TGA AC	95 °C (5 s), 60 °C (10 s), 72 °C (10 s)
ZNF658_Rev	CCC GGG TGA ATT CCA CAG TCA CG	95 °C (5 s), 60 °C (10 s), 72 °C (10 s)

**Table 4.3: Primers and thermal cycling parameters for confirmation of ZNF658 knockdown**

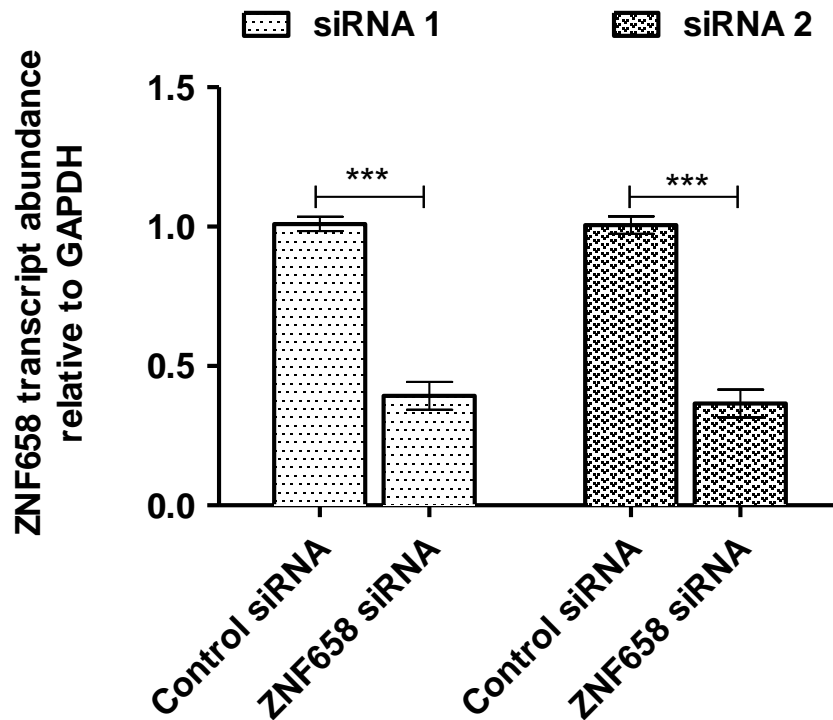
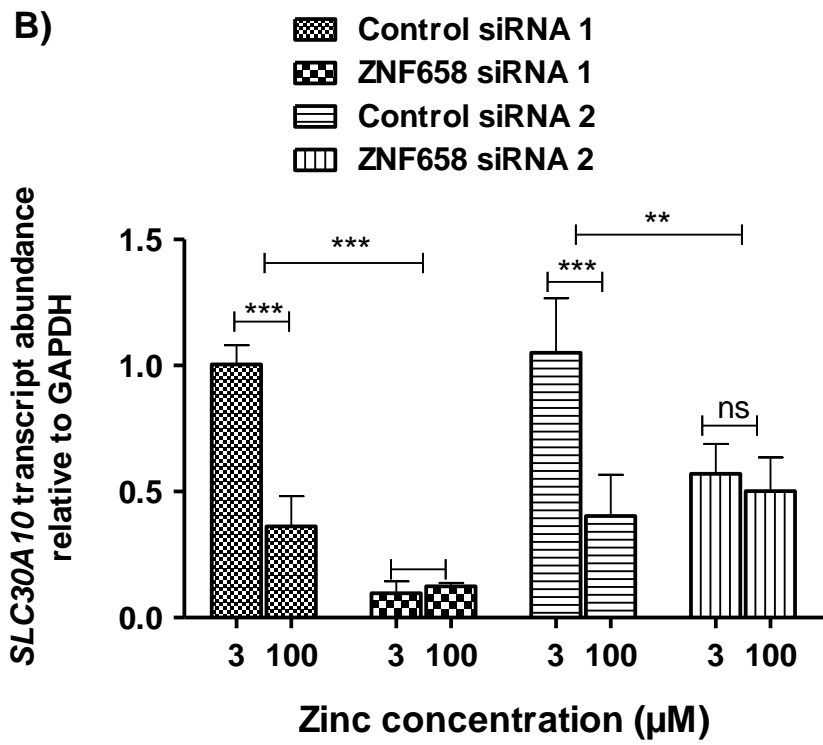
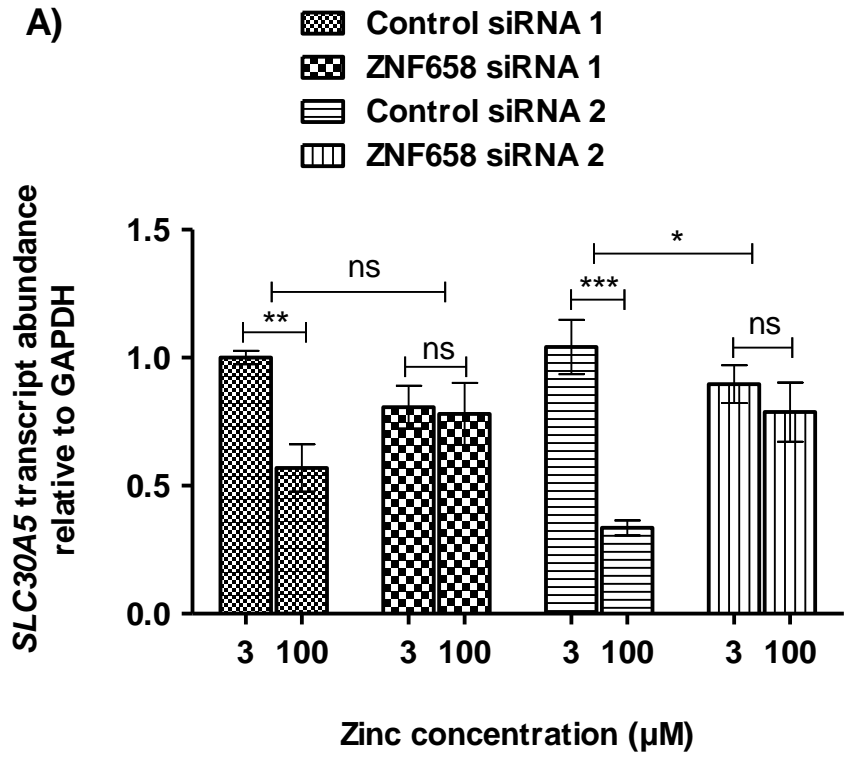


**Figure 4.9: ZNF658 mRNA expression was reduced by approximately 60% with 2 different siRNAs**

Caco-2 cells were seeded in 6-well plates and maintained in DMEM for 24 h. Twenty four hours later cells were treated with 10 nM ZNF658-specific or control siRNAs 1 or 2. After a further 24 h, total RNA was extracted using Trizol reagent and reversed transcribed to cDNA using SuperScript® III reverse transcriptase (Life Technologies). ZNF658 mRNA levels normalised to control siRNA were expressed relative to transcript levels of GAPDH measured by RT-qPCR. Data presented are mean  $\pm$  SEM for 3 independent experiments (siRNA1) and 2 independent experiments (siRNA2) with each performed in triplicate. \*\*\* represents  $p < 0.001$  relative to control siRNA by Student's unpaired two-tailed t-test.

#### ***4.3.6 Effect of siRNA-mediated knockdown of ZNF658 on the response to zinc of SLC30A5, SLC30A10 and CBWD genes at the transcript level***

To determine if knockdown of ZNF658 affect the response to zinc of genes known to be regulated via the ZTRE-mediated mechanism, the transcript levels of these genes were measured by RT-qPCR in cells with reduced expression of ZNF658. As shown in Figure 4.10, mRNA levels of *SLC30A5*, *SLC30A10* and *CBWD* genes were reduced in response to treatment with zinc at 100  $\mu$ M compared with 3  $\mu$ M zinc when cells were transfected with the control siRNA. However, the effect of zinc on the transcript levels of these genes was abrogated as a consequence of transfection with ZNF658-specific siRNAs. siRNA1 treatment resulted in the reduction of *SLC30A10* endogenous transcripts (panel B), while siRNA2 affected endogenous transcript levels of all the 3 genes (panels A, B, C). However, the response to zinc in each case was abolished. These results suggest that ZNF658 is involved in mediating the response of *SLC30A5*, *SLC30A10* and *CBWD* genes to zinc.



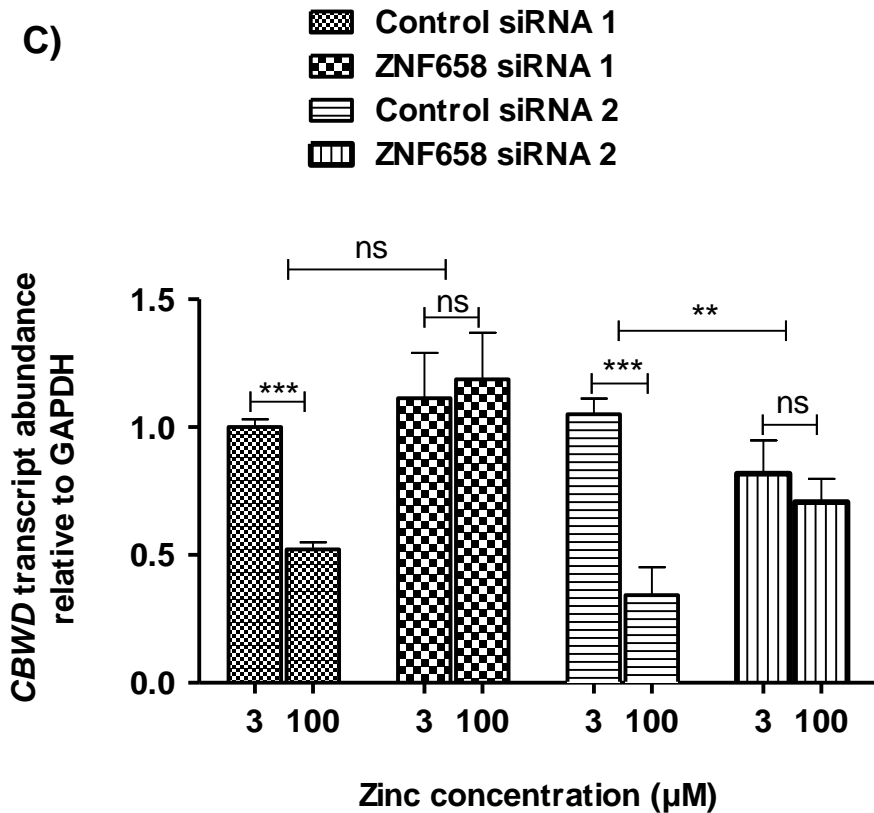


**Figure 4.10: Knockdown of ZNF658 by siRNA attenuates the response of *SLC30A5*, *SLC30A10* and *CBWD* transcripts to zinc**

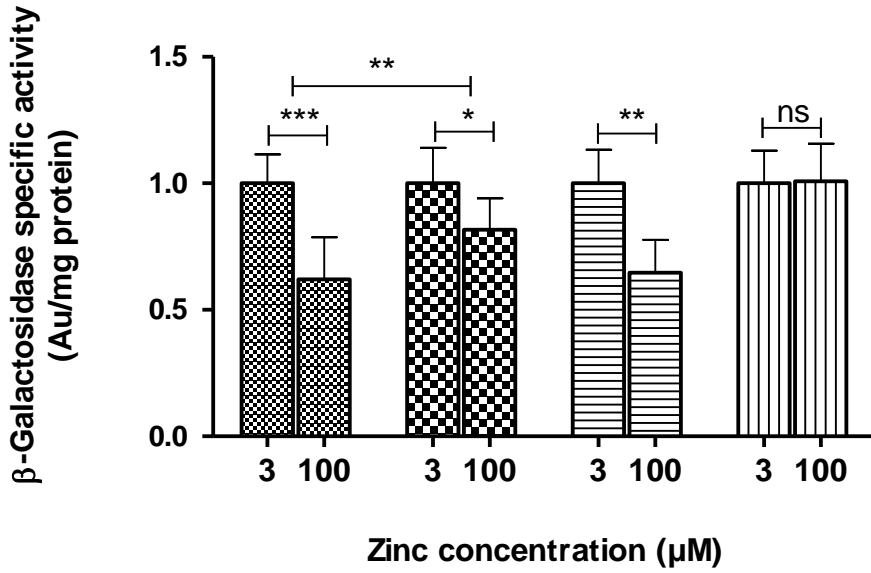
Caco-2 cells were seeded at  $5 \times 10^5$  cells/well in 6-well plates and grown in DMEM for 24 h. Twenty four hours post seeding, cells were transfected with 10 nM of either siRNA 1 or siRNA 2 or negative control siRNA in each case, in 5 % serum-supplemented DMEM for 24 h. Cells were maintained in serum-free DMEM containing zinc chloride added at 3  $\mu$ M (control medium) and 100  $\mu$ M for another 24 h. After a further 24 h, total RNA was extracted using Trizol reagent and reverse-transcribed to cDNA. Transcript levels of *SLC30A5*, *SLC30A10* and *CBWD* genes were measured by RT-qPCR relative to transcript levels of GAPDH reference. Data are expressed as mean  $\pm$  SEM for  $n \geq 6$  normalised to 3  $\mu$ M zinc condition. \* $P < 0.05$ , \*\* $P < 0.01$ \*\*\* $P < 0.001$  by Student's unpaired t-test. For multiple comparisons between different siRNAs, one-way ANOVA followed by Tukey's post-test was used.

#### ***4.3.7 The effect of siRNA-mediated knockdown of ZNF658 on the response of SLC30A5, SLC30A10 and CBWD genes to zinc at the promoter level***

To test further if ZNF658 is pivotal in the ZTRE-mediated response of *SLC30A5*, *SLC30A10* and *CBWD* genes to zinc, promoter activity of each of these genes was measured in response to zinc under condition of ZNF658 knockdown using promoter-reporter gene assay. The rationale behind this experiment was that if ZNF658 plays a role in mediating zinc-induced ZTRE-dependent transcriptional repression, then reducing its expression with siRNA would affect the response to zinc of promoters that contain the ZTRE. As shown in Figure 4.11, treatment with 100  $\mu$ M zinc resulted in repression of expression of a reporter gene driven by *SLC30A5*, *SLC30A10* and *CBWD* ZTRE-containing promoters in cells co-transfected with pBlue*SLC30A5*prom<sub>WT</sub>, pBlue*SLC30A10*prom<sub>WT</sub> or pBlue*CBWD1*prom constructs with control siRNA. However, this response to zinc was abolished under ZNF658 knockdown condition, in which cells were co-transfected with pBlue*SLC30A10*prom<sub>WT</sub> or pBlue*CBWD1*prom constructs (panels B, C), whereas the response was attenuated in cells transfected with pBlue*SLC30A5*prom<sub>WT</sub> plasmid (panel A). These results show that ZNF658 is required for the response to zinc of the *SLC30A5*, *SLC30A10* and *CBWD1* promoters and thus add to the evidence that ZNF658 plays an important role in orchestrating transcriptional repression of these genes in response to elevated extracellular zinc concentration.

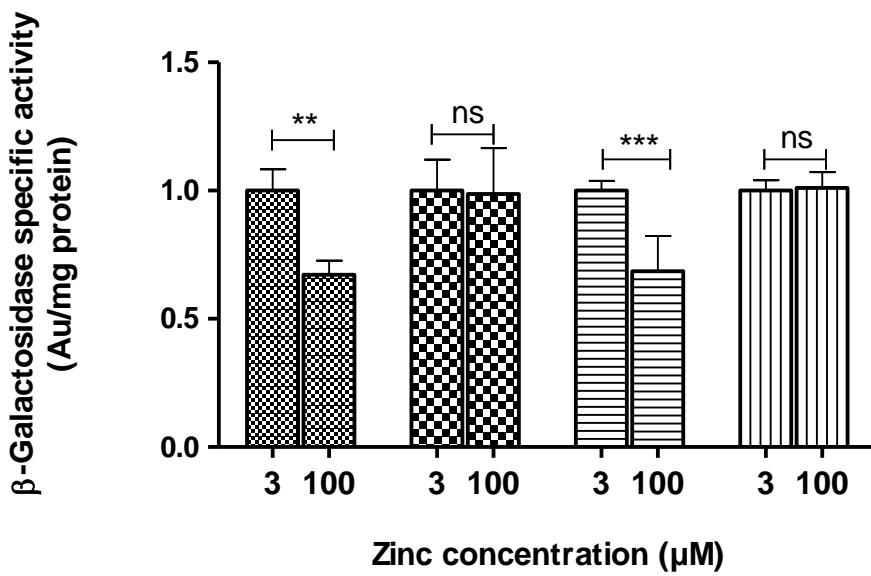
**A) *SLC30A5***

- Control siRNA 1
- ZNF658 siRNA 1
- Control siRNA 2
- ZNF658 siRNA 2



**B) *SLC30A10***

- Control siRNA 1
- ZNF658 siRNA 1
- Control siRNA 2
- ZNF658 siRNA 2



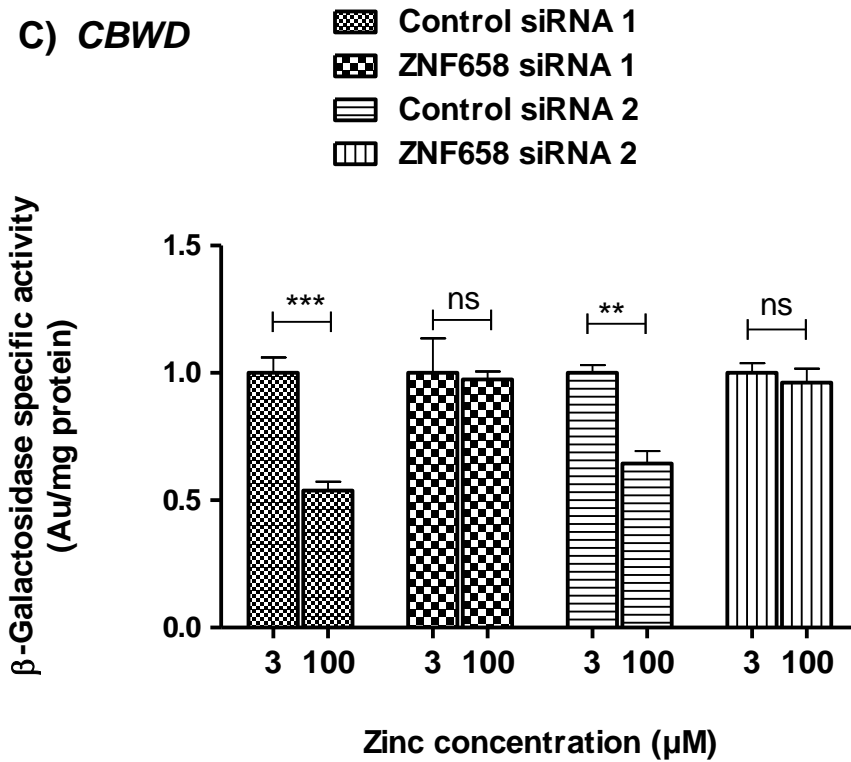


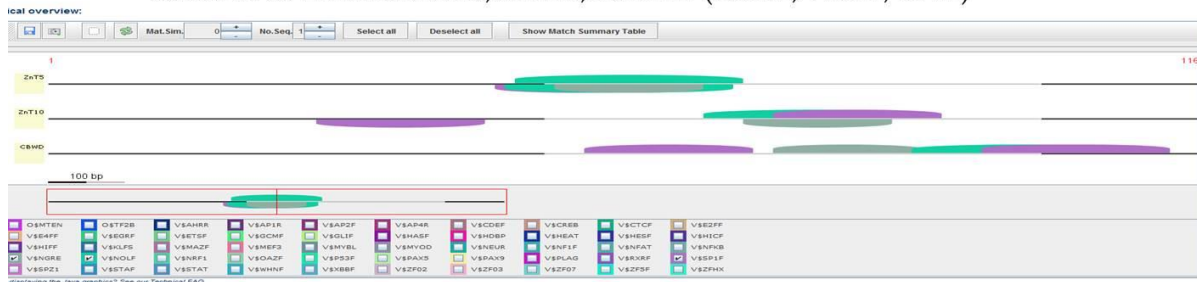
**Figure 4.11: Knockdown of ZNF658 by siRNA attenuates the response of *SLC30A5*, *SLC30A10* and *CBWD* promoters to zinc**

Caco-2 cells were seeded at  $5 \times 10^5$  cells/well in 6-well plates and grown in DMEM for 24 h. Twenty four hours post seeding, cells were co-transfected with 10 nM of either siRNA 1 or siRNA 2 or negative control siRNAs with *SLC30A5*, *SLC30A10* and *CBWD* promoter-reporter constructs for 24 h. Cells were maintained in serum-free DMEM containing zinc chloride added at 3  $\mu\text{M}$  (control medium) and 100  $\mu\text{M}$  for another 24 h. After a further 24 h, cell lysates were prepared for measurement of reporter activity as specific  $\beta$ -galactosidase activity in arbitrary units. Data represented are expressed as mean  $\pm$  SEM for  $n = 6 - 12$  for 3 separate experiments (siRNA1) and 2 independent experiments (siRNA2). \* $P < 0.05$ , \*\* $P < 0.01$ \*\*\* $P < 0.001$  by Student's unpaired t-test and one-way ANOVA analysis was used for multiple comparisons.

#### ***4.3.8 Identification of additional transcription factor binding sites (TFBS) around the ZTRE region***

Identification of additional transcription factor (TF) binding sites close to known sites of binding and action of TFs known to regulate the expression of specific genes can indicate which other TFs may work in synergy to regulate gene expression in response to specific cues. To determine if the promoter regions of *SLC30A5*, *SLC30A10* and *CBWD1* genes contain the same or similar binding sites for additional transcription factors, thus indicating common interacting partners for the transcription factor that binds directly to the ZTRE, an *in silico* search for transcription factor binding sites (TFBSs) using Genomatix software MatInspector at [www.genomatix.de](http://www.genomatix.de) was carried out. The promoter sequence spanning -50 to + 50 bp relative to the position of the ZTRE was searched for transcription factor binding sites in each of the gene promoters. Putative TFBSs were identified by modifying the matrix threshold defined by the programme with a significant probability set at  $p = 0.05$ . The TFBSs for NGRE, NOLF and SP1F transcription regulators were identified in all the three genes (Figure 4.12).

Genomatix analysis - transcription factor binding sites -50 to +50 relative to ZTRE in ZNT5, ZnT10, CBDW1 (NGRE, NOLF, SP1F)



**ZnT5** (NGRE 52-66 (-) caCTCCcgggggagt; NOLF 47-69 (-) cctcacTCCCgggggagtgccca; 48-70 (+) gggcacTCCCcggggagtggagg; SP1F 46-62 (-) cccgGGGgagtgccag)  
 TAAGGGACGAGGAAAGGCGAGTGTCTGCTTGCGCAGACGCAAGGCTGGGCACTCCCC  
CGGGAGTGAGGGTTGCTGGGCCTGATGACGTGGCTTGGCAACGTCCCTACCGCCGCTG

**ZnT10** (NGRE 71-85 (-) gcCGCCcaggggagc; NOLF 67-89 (+) ctgctcTCCCctgggagcgcgcg; SP1F 28-44 (-) gtggggGGCGcggcgcg 74-90 (+) cccctGGGcggcgccgg)  
 GGAGGCGGGTACCGGGCTCACGGATCCGCGCCGCGCCCCACCTGTGGCTGCGCGCG  
GGGTGGGCTGCGCTCCCCTGGGCGGCGCCGGGCGCCCGGGGCTGGTGGCGAGATGGG

**CBDW1** (NGRE 91-105 (+) acCTCCcgggggggt; NOLF 88-110 (+) cccacTCCCcggggggtgtggc; SP1F 55-71 (+) cccaGGGcgtgtccag 97-113 (+) cccgGGGgtgtggctaa)  
 TGGTTAGTGCGCCCTAAGGACTCTCCGCAGCGTCGCTCAGGTTACAGAACACGCCCAGG  
GGCGTGTCCAGCTGTCGTCGGGAGAGCCCACTCCCCGGGGGTGTGGCTAAGG

**Figure 4.12: The ZTRE-containing *SLC30A5*, *SLC30A10* and *CBWD* promoters share common transcription factor binding sites for NGRE, NOLF and SP1F proteins**

The promoter sequence corresponding to -50 to +50 bp relative to the position of the ZTRE as used in the *SLC30A5*, *SLC30A10* and *CBWD* promoter-reporter constructs were used to search for possible common TFBSs using Genomatix software. TFBS for NGRE, NOLF and SP1F were identified based on defined significant p-value of 0.05. The position of the ZTRE is underlined in each panel.

#### 4.4 Discussion

The involvement of zinc in many processes requires that its levels are carefully controlled to prevent adverse physiological effects that may result from inadequacy or excess. Pivotal to this regulation are transcriptional regulatory proteins, which exert their effects through binding to DNA elements within promoter regions of target genes. Several of these important transcription factors that play roles in controlling zinc homeostasis have been identified in both prokaryotic and eukaryotic organisms. For instance, the bacterial transcription factors belonging to SmtB/ArsR families are repressors in non-metal bound form, however, on binding metal, dissociate from DNA to derepress expression of genes coding for proteins that confer cellular resistance to increased metal levels (including zinc) (reviewed by (Busenlehner et al., 2003, Ma et al., 2009)). The zinc-responsive regulator of bacterial ABC transporters Zur, belonging to the iron uptake regulator (Fur) family, in the presence of two or three zinc ions forms a protein-zinc complex that interacts with DNA resulting in transcriptional repression of genes belonging to the “zinc-response operon” (reviewed by (Hantke, 2001, Choudhury and Srivastava, 2001, Waldron and Robinson, 2009)). In higher organisms, only a few transcription factors with roles in metal-induced transcriptional regulation have been reported. The *Saccharomyces cerevisiae* transcriptional regulator ZAP1 mediates up-regulation of many genes including those coding for the high affinity ZRT1 and low affinity ZRT2 under zinc limiting conditions by binding to zinc responsive element within these gene promoters (Zhao et al., 1998, Eide, 2009). In addition to the primary mode of regulation by ZAP1, it also mediates transcriptional repression of a subset of its target genes such as *ADH1*, *ADH3* and *ZRT2* under conditions of increased zinc concentration (Bird et al., 2006, Bird et al., 2004). Among metazoan zinc-responsive transcription factors is metal response element-binding transcription factor (MTF1), which appears to have been given most attention. The MTF1 protein has a DNA binding domain comprising 6 zinc finger motifs at the N-terminus (Jiang et

al., 2003). Binding of up to 7 atoms of zinc by zinc fingers 1, 5, and 6, which are located at the N-terminal DNA binding domain (Günther et al., 2012), induces a conformational change in the protein, which appears to both drive translocation to the nucleus and induction of binding to the metal response element (MRE). Binding of MTF1 to MREs found in mammalian genes including those coding for the membrane zinc effluxer ZnT1 and metallothionein proteins generally (although not exclusively) result in transcriptional activation, resulting in detoxification of heavy metals or maintenance of essential homeostasis. In addition, MTF1 also mediates transcriptional repression of some genes such as those coding for Zip10 in both zebrafish (Zheng et al., 2008) and mouse (Lichten et al., 2011). Similarly, the zinc finger transcription factor Krüppel-like factor 4 (KLF4) has been attributed a role in mediating adaptive regulation of the zinc transporter ZIP4 by binding to the KLF4 response element within the *Zip4* gene promoter (Liuzzi et al., 2009). A eukaryotic repressive transcription factor, loss of zinc sensing 1 (*Loz1*), which represses expression of genes such as *zrt1* under zinc replete conditions has been identified in the fission yeast (Corkins et al., 2013). However, the identity of a transcription factor that mediates transcriptional repression of multiple genes to coordinate homeostatic control under conditions of increased zinc availability has not been reported in metazoans.

The results presented in this chapter document evidence in support of ZNF658 being a mediator of zinc-induced negative regulation of genes that play significant roles in mammalian zinc homeostasis. Although amino sequence alignment shows that ZNF658 is most similar to the yeast ZAP1, which is described as the central player in yeast zinc homeostasis, their mode of gene regulation is in contrast to each other. The mode of regulation in which ZAP1 promotes up-regulation of transcription, as opposed to down-regulation by ZNF658, may be explained by the observation that certain regions of the proteins are not similar and these disparate regions could serve as sites of interaction for other regulatory/accessory proteins that may be required

to synergically orchestrate transcription. This scenario appears to be prevalent among transcription factors. For instance, studies using chromatin immunoprecipitation and coimmunoprecipitation assays revealed the requirement for MTF-1 to work in concert with many proteins such as the histone acetyl transferase p300/CBP and with SP1 for induction of the mouse metallothionein 1 (MT-1) transcription in response to zinc (Li et al., 2008), and with hypoxia-inducible transcription factor-1 alpha (HIF-1 alpha) to mediate transcription of the *MT-1* gene in response to stress posed by low oxygen condition (Murphy et al., 2008). Similarly, the mammalian transcriptional repressor delta EF1, a member of the Krüppel-type C<sub>2</sub>H<sub>2</sub> family, has been shown to bind to the E2-box (CACCTG) with its 2 zinc fingers at promoters of its target genes, including the *ER-α* promoter, but acts to repress transcription through a transrepression mechanism by forming complexes with corepressors including C-terminal-binding proteins 1 and 2 (CtBP1 and CtBP2) (Furusawa et al., 1999). Also, the five-zinc finger-containing Krüppel-like transcription factor Gli-similar 2 (Glis2) orchestrates transcriptional repression (but can also be an activator) through interaction with CtBP1, as identified by two-hybrid analysis (Kim et al., 2005).

The presence of numerous zinc fingers (in which a zinc ion is centrally coordinated by 2 cysteine residues in β-sheet conformation and 2 histidine residues within α-helix conformation) on a single regulatory protein is characteristic of the ubiquitous C<sub>2</sub>H<sub>2</sub> sub-family of transcription factors seen in many species. Examples include the 29 C<sub>2</sub>H<sub>2</sub>-carrying Rat O/E-1-associated zinc finger protein (Roaz), involved in olfactory neuronal cell differentiation (Tsai and Reed, 1997), and the human zinc finger protein 268, which contains 24 zinc finger motifs and is implicated in early human liver development (Sun et al., 2004). Although C<sub>2</sub>H<sub>2</sub> is a common motif in this protein family, differential DNA recognition and binding is conferred by the non-conserved amino acid residues that make up the zinc finger loop as well as the intervening amino acids between the zinc fingers (linker region), which differ widely (reviewed

by (Iuchi, 2001). In addition, the observed substitution of histidine (H) with arginine (R) in the 16<sup>th</sup> zinc finger motif of ZNF658 may be important in influencing gene repression by acting as a receptor site for interaction with coregulators other than Krüppel-associated protein 1 (KAP1) as has been shown for the zinc finger protein Nizp1, which also contains this C2HR substitution (Nielsen et al., 2004). The multiple zinc fingers of ZNF658 may be a feature of the protein that allows binding to a diverse range of gene targets through motifs other than the ZTRE to mediate cellular function(s). Indeed, the KRAB-containing zinc finger proteins have been thought to be involved in a plethora of biological functions such as cell proliferation and cell cycle regulation, which may be facilitated by these multiple zinc fingers (reviewed by (Lupo et al., 2013). Inspection of the amino acid sequence of ZNF658 identified a 61-amino acid region located between 8 and 68 amino acids known as a Krüppel-like associated box domain (KRAB domain). Although the KRAB domain is a conserved region of about 75 amino acids, it has been established that a minimum of 45 amino acid residues is sufficient for transcriptional repression (Margolin et al., 1994b), thus it is not unreasonable to expect the 61 amino acids found in the ZNF658 KRAB to be functional. A subset of the amino acid string corresponding to amino acids 47 – 68 at the N-terminal end of the putative KRAB domain is identical to a sequence known to bind corepressor/accessory proteins including KAP-1 (Ryan et al., 1999). Thus, the large number of zinc fingers of ZNF658 and the presence of KRAB binding modules are likely to be involved in specific interactions with accessory proteins that play a role in zinc-induced transcriptional repression.

A previously observed increase in intensity of the band on EMSA seen when nuclear extracts from Caco-2 cells treated with zinc at 150  $\mu$ M were incubated with the labelled zinc-responsive *SLC30A5* promoter sequence (Jackson et al., 2007) (Coneyworth et al., 2012) seems to indicate increase abundance of the binding protein, now known to be ZNF658, in the extract. However,

the current data show that an increase in zinc concentration does not affect ZNF658 transcript abundance. A possible explanation for this apparent discrepancy may be the difference in the concentration of zinc used (150  $\mu$ M in the previous experiment but 100  $\mu$ M in the present study). A more likely explanation is that the band represents a complex of proteins that include ZNF658 and that other proteins in the complex are expressed at greater abundance when zinc concentration is increased.

Electrophoretic mobility shift analysis showed that binding of protein extracts from cells transfected with the recombinant ZNF658 protein to the ZTRE-containing *SLC30A5* probe was specific, by virtue of competition with addition of excess unlabelled probe. The binding protein was confirmed as ZNF658 when antibody against the myc epitope attached to the recombinant protein was included in the binding reaction, leading to a major proportion of the original band being supershifted. A residual band of the original mobility remained in the presence of anti-myc antibody in the binding reaction, and may be due to a complex of proteins rather than ZNF658 alone binding to the ZTRE-containing probe. This scenario is analogous to the zinc-dependent transcriptional regulation of *Mt1* promoter, mediated by the MTF1, in which the transcription factor forms a complex with the histone acetyltransferase p300/CBP and with the transcription factor Sp1 (Li et al., 2008).

The deletion of five zinc fingers located in the putative DNA-binding domain (DBD) resulted in loss of binding of ZNF658 to the ZTRE-containing probe, indicating that the ability of ZNF658 to bind to the ZTRE to mediate transcriptional repression may be resident in this region of the protein. Large deletions of over 600 amino acids have been used to map transcription factor DNA binding domains including that for ZAP1, which is located at the carboxyl-terminal region corresponding to amino acid residues 705-880 comprising the zinc fingers 3 -7 (Bird et al., 2000, Frey et al., 2011). The mapping of the binding function of

ZNF658 to this region suggests that the region, which is analogous to the ZAP1 DNA binding domain, may perform the same function. Future investigations should aim to identify specific amino acid residues that are central to its binding ability. Specific deletions have been employed to identify serine 98 (Ser98) as a necessary amino acid residue for the yeast ADR1 transcription factor DNA binding ability in both *in vitro* and *in vivo* studies (Kacherovsky et al., 2008).

Although siRNA-driven knockdown of ZNF658 could not be confirmed at the protein level owing to non-availability of commercial antibody, the use of 2 independent siRNAs to achieve knockdown lends confidence to the data. A similar strategy was used to confirm the function of the transcription factor KLF4 to reduce *SLC39A4* gene expression (Liuzzi et al., 2009). We observed that knockdown of ZNF658 also resulted in reduction of the endogenous transcript levels of the target genes, indicating that the transcription factor may be required for basal transcription of these genes in addition to mediating transcriptional repression in response to zinc. A dual role for zinc finger-containing transcription factors appear to be prevalent. This assertion is supported by the discovery that a genome-wide chromatin immunoprecipitation followed by sequencing (ChIP-seq) in K562 cells revealed an appreciable number of gene targets that were found to be positively regulated by the KRAB-containing ZNF263 (Fietze et al., 2010). An alternative interpretation is that ZNF658 possibly mediates transcriptional repression with less zinc bound than is the case when it is required at the promoter region for gene transcription. Effects on endogenous transcript abundance of *SLC30A5*, *SLC30A10* and *CBWD* genes were different between genes and between the two siRNAs. While siRNA1 reduced the endogenous transcript levels of only ZnT10 (*SLC30A10*), siRNA2 resulted in the reduction of the endogenous transcripts of all 3 genes. A likely explanation for this apparent difference may be due to the fact that the two siRNAs target different combinations of variants of the ZNF658 gene. This explanation may be supported by the fact that the two siRNAs

targeted different regions of ZNF658 coding sequence, in which siRNA1 sequence targets exon5 but siRNA2 sequence targets the exon 3/4 boundary. Additionally, the position of the ZTRE relative to the TSS in each of the genes (that is upstream of TSS in *SLC30A5* and *CBWD1* but downstream of TSS in *SLC30A10*) (Coneyworth et al., 2012), may be responsible for the differential effects of siRNA1 on the endogenous transcript levels of these genes. Such differential location of a response element was noted to result in non-classical repression of the mouse *Slc39a10* gene (Lichten et al., 2011). The most significant effect of ZNF658 knockdown, however, is the loss of the zinc-induced transcriptional repression of these target genes, confirming involvement of this transcription factor in mediating this response.

Genomatix matInspector using position weight matrix (PWM) (Kel et al., 2003) identified a huge list of possible transcription factor binding sites close to the ZTRE in *SLC30A5*, *SLC30A10* and *CBWD1* genes. Increased stringency and thus reliability was achieved by applying a statistical limit, which in this case was p-value adjusted to 0.05. Putative binding sites for NGRE, NOLF and SP1F factors were identified within 50 bp of the ZTRE in all three ZNF658 target genes, suggesting that these factors may interact with ZNF658 as possible coregulators to mediate zinc-induced transcriptional regulation. Although NOLF response elements have been recognised within the GABA<sub>A</sub> receptor subunit gene promoters (Steiger and Russek, 2004), evidence for specific involvement in gene regulation is scarce. On the other hand, NGRE binding sites are DNA sequences necessary for glucocorticoid-induced repression of gene transcription. This transcription factor has been shown to mediate repression of the bovine prolactin gene (PRL3) (Subramaniam et al., 1999) through a mechanism that includes (but not exclusively) competition with another transcription factor (AP-1) for binding to a site that overlaps its own recognition sequence (Necela and Cidlowski, 2004). Similarly, the SP1F transcription factor family consists of a GC-Box enriched factor found within promoter sequences of some heat shock-responsive genes including those coding for HSP70

and HSP90. Its binding sequence is also a potential binding site for KLF5/ SP1 transcription factors as well as specificity protein 1, and it is implicated in chromatin silencing (Augustin et al., 2011). Identification of these potential coregulator sites within promoters of ZNF658 target genes gives reason to determine through future work if these transcription factors act alongside ZNF658 in the zinc-responsive control of gene expression.

In conclusion, the evidence presented in this chapter supports the hypothesis that ZNF658 plays important roles in orchestrating the transcriptional response of multiple genes whose products are involved in maintaining zinc homeostasis, thus providing the first report of a metazoan transcription factor with potential to coordinate gene expression in response to zinc through transcriptional repression. Compared with prokaryotic species, only a few metal-sensing transcriptional regulators have been documented in eukaryotes, thus identification of ZNF658 fills a significant gap and advances our understanding of the molecular players that are involved in the complex eukaryotic metal-induced regulation of gene expression.

## Chapter 5 : Investigation of the role of *CBWD* gene products in metal homeostasis

### 5.1 Introduction

The human *CBWD* genes (coding for COBW domain-containing proteins) were initially identified through an *in silico* search for the presence of the ZTRE within promoters of human genes. The occurrence of the ZTRE in multiple isoforms of genes in the *CBWD* gene family, for which no known role in mammalian metal homeostasis has been established, was intriguing and motivated investigation into a likely involvement of *CBWD* gene products in cellular zinc homeostasis and also homeostasis of other metals. Recent analyses from comparative genomics and phylogenetic studies suggest that bacterial homologs of CBWD protein belonging to the metal homeostasis-associated COG0523 sub-family of P-loop GTPases may be important in prokaryotic metal biology (Haas et al., 2009, Sydor et al., 2013). The *CBWD* ZTRE has been demonstrated to mediate gene repression in response to increased extracellular zinc concentration in Caco-2 cells (see chapter three). The work presented in this chapter was carried out with the aim to gain some insight into a possible role for *CBWD* gene products in mammalian metal homeostasis by investigating regulation by metals other than zinc, regulation by zinc at the protein level, as well as the effect of increased expression of CBWD proteins on cell viability at different zinc concentrations and on cellular zinc distribution. The effect of *in vitro* methylation on *CBWD* promoter activity was also investigated, following publication of a data set identifying genes in mouse intestine that underwent a change in DNA methylation with ageing, in which *CBWD* was among the most affected genes (Maegawa et al., 2010).

## 5.2 Specific objectives

Specific objectives addressed through the work in this chapter were to investigate:

- the regulation of *CBWD* genes by metals other than zinc;
- the effect of zinc on *CBWD* expression at the protein level
- the effect of overexpression *CBWD* protein on zinc distribution and on cell tolerance to variations in cellular zinc content;
- the effect of *in vitro* DNA methylation on *CBWD* promoter activity

## 5.3 Results

### 5.3.1 Identification of the ZTRE in *CBWD* genes

Following identification of the *SLC30A5* ZTRE, an *in silico* search of the human genome using the programme Fuzznuc (EMBOSS) was conducted to determine if other genes include the ZTRE sequence in their promoters (Lisa Coneyworth, PhD thesis, 2009). The *SLC30A5* ZTRE sequence (CACTCCC; representing the 5' component of the palindromic sequence) was used for the search allowing only one mismatch in the 2 halves of the palindrome. Many candidate genes harbouring sequences similar to the *SLC30A5* ZTRE sequence were identified. Of particular interest was the presence of the ZTRE in multiple isoforms of *CBWD* genes (boxed in Table 5.1) with a linker region comprising of 2 nucleotides similar to that present in the *SLC30A5* ZTRE.

Chromosome	Gene	Position of gene on chromosome	Position of ZTRE on chromosome	ZTRE sequence	Distance upstream of predicted TSS (bp)
5	SLC30A5	68425674-68436323	68425662 - 68425547	CACTCCC[CC]GGGAGGTG	27
20	MATN4	43355962-43370381	43370425 - 43370445	CCCTCCC[ACTGGCA]GGGAGGG	49
12	EMG1	6950254-6955399	6950203 - 6950217	CCCTCCC[A]GGGAGGG	50
12	PHB2	6944778-6950152	6950203 - 6950217	CCCTCCC[A]GGGAGGG	50
16	CCDC102A	56103591-56127978	56128030 - 56128046	CCCTCCC[GG]GGGAGGG	52
12	GLT8D3	40763356-40824948	40824987 - 40825006	CCCTCCC[CCGGGC]GGGAGGG	58
1	LPHN1	14119549-14177997	14178094 - 14178108	CCCTCCC[G]GGGAGGG	97
9	CBWD3	69671823-69729991	69730112 - 69730127	CACGCC[AG]GGGCGTG	136
9	CBWD1	111041-169032	169193 - 169208	CACGCCACGGGCGTG	170
12	ELK3	95112338-95185737	95112149 - 95112166	CCCTCCCCTGGGGAGGG	189
5	SIL1	138310309-138561964	138562109 - 138562128	CCCTCCCCTGGGGAGGG	200
2	KIDINS220	8786511-8895181	8895237 - 8895253	CACGCCCTGGGCGTG	200
9	CBWD5	70046705-70052593	70046529 - 70046544	CACGCCCTGGGCGTG	200
9	CBWD3	68494405-68552350	68552531 - 68552546	CACGCCACGGGCGTG	250
11	TSGA10IP	65469691-65484010	65469322 - 65469340	CACTCCCAGCCTGGGAGTG	300
8	SGK3	67850016-67936811	67850315 - 67850328	CACACCCGGGCGTG	300
2	HSPD1	198059553-198072885	198073249 - 198073267	CCCTCCCCTGGGGAGGG	365
2	HSPD1	198059553-198072885	198073253 - 198073267	CCCTCCCCTGGGGAGGG	368
17	HDA5	39509647 - 39556540	39556925 - 39556945	CCCTCCCGCGGTCCGGGAGGG	385
5	HSPA9	137918923-137939014	137939485 - 137939501	CACACCCCGGGGTGTG	400
17	TEX14	53989038-54124415	54124964 - 54124945	CACGCCCAAGCGAGGGCGTG	500
17	RAD51	54124962-54166691	54124945 - 54124964	CACGCCCAAGCGAGGGCGTG	500
7	BRI3	97748923-97758775	97748445 - 97748458	CACACCCGGGTGTG	500
18	DLGAP1	3488837-3870135	3869406 - 3869423	CACGCCCGAGGGG	729
16	CFDP1	73885109-74024888	73884266 - 73884282	CACACCCGACGGGTGTG	843
9	ZNF483	113327260-113346533	113326066 - 113326085	CACTCCCTTTGAGAGGAGTG	1100
19	ZNF260	41693434-41711010	41712161 - 41712181	CCCTCCCATGGCGGGGAGGG	1151
10	SYCE1	135217395-135232866	135234126 - 135234147	CCCTCCCCTGGCCCTGGAGGG	1240
10	SPRN	135084069-135088066	135089331 - 135089352	CCCTCCCTGGCCCTGGGAGGG	1265
11	PAX6	31767034-31789455	31791203 - 31791223	CCCTCCCTGTTTCCCTGGGAGGG	1748
7	NOS3	150319080-150342609	150317302 - 150317317	CCCTCCCAGGGAGG	1778
2	CBWD1/2	113911853-113918064	113911677 - 113911692	CACGCCACGGGCGTG	2000
X	NRK	104953192-105089258	104951072 - 104951093	CCCTCCCACCTGGGAGGG	2000
1	NFIA	61320883-61694624	61318275 - 61318295	CCCTCCCACCGGGAGGGAGGG	2588
X	TMEM28	68641803-68669076	68639082 - 68639100	CCCTCCCTCTATGGGAGGG	2721
1	GRIK3	37039201-37272431	37275247 - 37275267	CCCTCCCGGTCTAGGGAGGG	2836
9	ARID3C	34611455-34618011	34620971 - 34620991	CCCTCCCTGATGCTGGGAGGG	2960
X	SLC9A6	134895252-134957094	134892025 - 134892043	CACTCCCTGGATGGGAGTG	3000
19	ZNF526	47416332-47424193	47413170 - 47413185	CCCTCCCACGGGAGGG	3000
11	BCL9L	118272061-118286823	118289468 - 118289486	CCCTCCCACAGGGGAGGG	3000
22	IGLL1	22245313-22252495	22255529 - 22255514	CACGCCCCGGGTGTG	3019
2	RNPEPL1	241156777-241166816	241153200 - 241153218	CACTCCTAAAATAGGAGTG	3500
20	LPIN3	39402974-39422636	39426285 - 39426306	CCCTCCCTGTGGCCAGGGAGGG	3649
7	SP8	20788426-20793030	20784526 - 20784540	CCCTCCCAGGGAGGG	3900
11	ZSIG13	86189139-86341478	86185922 - 86185940	CCCTCCCACCTGGGGAGGG	4000
11	PRSS23	86189139-86199921	86185922 - 86185940	CCCTCCCACCTGGGGAGGG	4000
20	EMILIN3	39422020-39428912	39426285 - 39426306	CCCTCCCTGTGGCCAGGGAGGG	4000
1	SLC26A9	204148800-204179211	204183836 - 204183851	CACTCCTTAGGAGTG	4625
1	PROX1	212227909-212238226	212222633 - 212222654	CCCTCCCAGGGACCGGGAGGG	5255

**Table 5.1: Multiple copies of *CBWD* genes contain the ZTRE**

*In silico* search of the human genome was conducted for matches to the *SLC30A5* ZTRE using Fuzznuc software (EMBOSS). Candidate genes identified are shown in the table and include multiple copies of *CBWD* genes (indicated in red boxes). The ZTRE sequences, location on the chromosome and distance of the ZTRE from predicted transcription start site of each gene are also stated.

### ***5.3.2 The response of CBWD genes to metals other than zinc***

The ZTRE has been shown previously to be indispensable for zinc-regulation of *SLC30A5* and *CBWD* promoter activity through expression of promoter-reporter constructs in Caco-2 cells (sections 3.3.2 and 3.3.3). In addition, zinc-induced reduction of mRNA levels of *SLC30A5*, *SLC30A10* (which also include a ZTRE) and *CBWD* genes had been demonstrated (Coneyworth et al., 2012) but response to other metals has only been carried out for *SLC30A5* (section 3.3.5) and *SLC30A10* (Bosomworth et al., 2012). Here, the effect of other metals on expression of *CBWD* genes both at transcript and promoter levels was explored by treating Caco-2 cells with three different metals at the concentrations tested in experiments reported in section 3.3.5, which tested if they affect *SLC30A5* activity. Similar to the results obtained for *SLC30A5*, the *CBWD1* promoter showed no response to any metal tested other than zinc (Figure 5.1 panel A). The metallothionein promoter response to increased zinc concentration was included as a positive control (panel B). Intriguingly, however, there was significant response to all the metals tested of *CBWD* genes evidenced by reduction of the mRNA levels (measured by RT-qPCR using primers unable to distinguish between the different isoforms) compared with the control condition (panel C), suggesting that *CBWD* genes may be involved in handling metals other than zinc in mammalian cells.

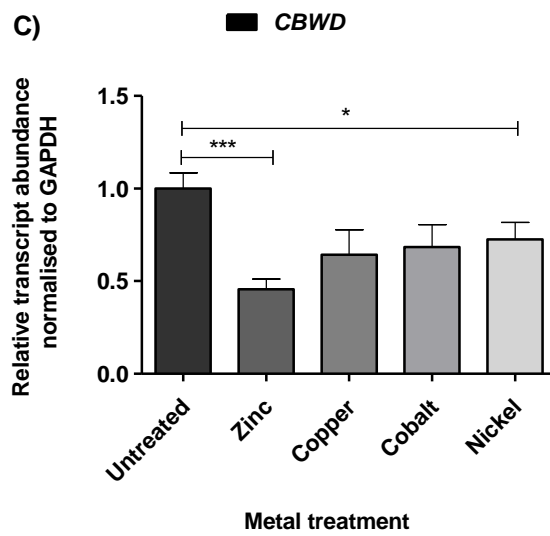
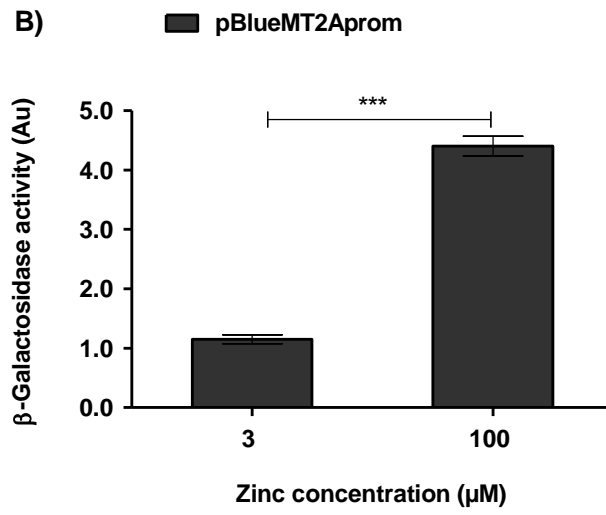
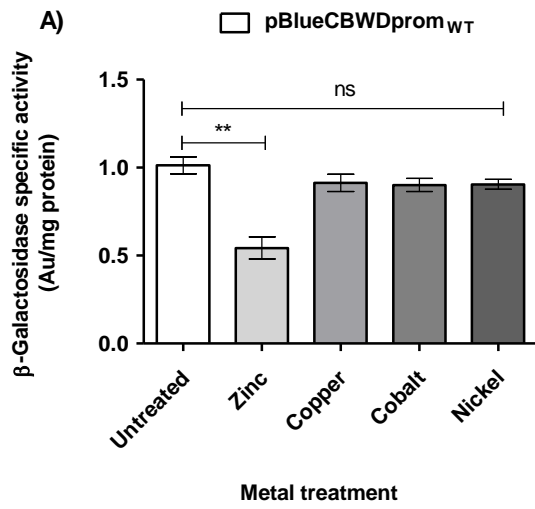


**Figure 5.1: *CBWD* genes are regulated at the transcript level by metals but not at the promoter level by metals additional to zinc.**

Caco-2 cells were seeded at  $5 \times 10^5$  cells/well in 6-well plate and grown in DMEM for 24 h. Twenty four hours post seeding, cells were transiently transfected with pBlue*CBWD*prom and pBlueMT2Aprom (control for reporter assay) plasmids. Twenty four hours after transfection, cells were maintained in serum-free DMEM containing ZnCl<sub>2</sub> added at 3  $\mu$ M (control), 100  $\mu$ M; CuCl<sub>2</sub> at 20  $\mu$ M; CoCl<sub>2</sub> at 100  $\mu$ M; and NiCl<sub>2</sub> at 20  $\mu$ M for another 24 h. After a further 24 h, cell lysates were prepared for measurement of promoter activity as  $\beta$ -galactosidase specific activity expressed relative to protein concentration (panels A and B). For RT-qPCR measurements (panel C), total RNA was extracted 24 h following metal treatment at concentrations indicated in the figure. Data plotted are mean  $\pm$  SEM normalised to the control condition for n = 6 for 3 independent experiments (gene-reporter assay); n= 6 for 2 independent repeats (RT-qPCR). \*P <0.05, \*\*P <0.01, \*\*\*P <0.001, ns indicates non-significant as determined using Student's unpaired t-test (for MT2a data) and one-way ANOVA then Bonferonni post-hoc test for multiple comparisons.

### ***5.3.3 The effect of zinc on CBWD protein levels in CHO and Caco-2 cells***

The effect of zinc on *CBWD* gene transcripts and on the promoter was explored in experiments documented in sections 3.3.1 and 3.3.2 respectively. A direct method to determine if zinc affects *CBWD* expression at the protein level was not possible owing to non-availability of *CBWD* antibody. Consequently, the effect of zinc on *CBWD* protein expression was examined by overexpressing recombinant *CBWD* protein with a FLAG/MYC epitope tag from a CMV promoter using the p3XFLAG-CMV10 vector (Sigma Aldrich) in Caco-2 cells. The recombinant *CBWD* protein with myc-DDK epitope tag had previously been expressed from the pCMV6 vector (OriGene) in CHO (Chinese Hamster Ovary) cells (Dianne Ford, personal communication) but expression was not achieved using the pCMV6 vector, hence the choice of a different vector (p3XFLAG-CMV10) to achieve expression in Caco-2 cells. In this experiment, the *CBWD3* ORF was amplified from the pCMV6-myc-DDK entry vector using primers that included *HindIII* and *XbaI* restriction sites as listed in Table 5.2 and sub-cloned as an N-terminal FLAG epitope tag into the p3XFLAG-CMV10 expression vector. Competent Top 10 cells were transformed with the ligation reaction, then plasmid was prepared and digested with the same restriction endonucleases and analysed by agarose gel electrophoresis to confirm the presence and size of insert (Figure 5.2). Plasmid preparations were also sequenced to ensure fidelity of the *CBWD* coding sequence. The construct containing the *CBWD* ORF is hereafter referred to as p3XFLAG-CMV10-*CBWD3*. Endotoxin-free preparations of pCMV6-*CBWD3*-myc-DDK and p3XFLAG-CMV10-*CBWD3* were used to transfect CHO and Caco-2 cells respectively. Cells were treated with 3  $\mu$ M (control) and 100  $\mu$ M concentrations of zinc and total protein was extracted for analysis by western blotting (see section 2.9). As indicated in Figure 5.3, *CBWD* protein expression detected by antibody against the FLAG/MYC epitope was significantly reduced by zinc at 100  $\mu$ M in both Caco-2 and CHO

cells compared with 3  $\mu$ M (panel A), indicating an effect consistent with the observed down-regulatory effect of zinc at the transcriptional level. Densitometric quantification of band intensities of the recombinant CBWD protein expressed in Caco-2 cells is represented in the graph (panel B).

Name	Sequence
CBWD3- <i>HindIII</i> (forward)	<u>CGCG</u> aag ctt ATG TTA CCG GCT GTT GGA TCT
CBWD3- <i>XbaI</i> (reverse)	<u>GCGC</u> tct aga TTA TGT ACA AAC TTG ATC TTC TTT G

**Table 5.2: Primers used for sub-cloning of CBWD3 ORF into the p3XFLAG-CMV10 vector**

Sequences of oligonucleotides including spacer (underlined) and restriction sites (lower case) are shown.

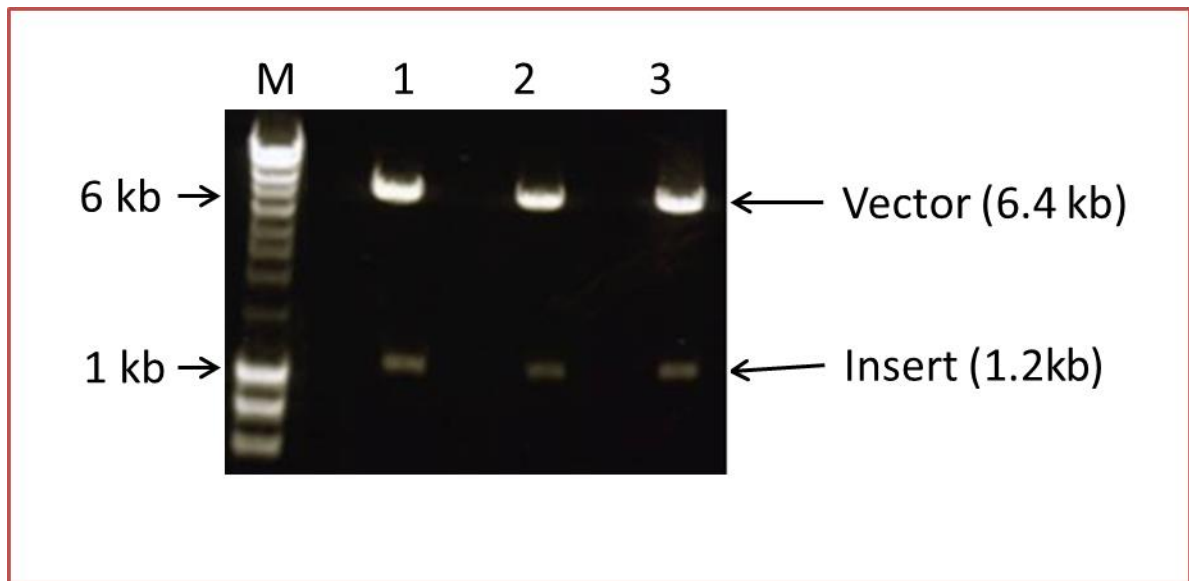


**Figure 5.2: Restriction digestion confirms CBWD cloning into 3XFLAGPCMV10 vector**

The CBWD3 ORF was amplified from the pCMV6-entry vector (Origene) with *Hind*III and *Xba*I restriction sites on the 5' and 3' ends respectively by PCR and was run on gel electrophoresis. The insert cut with *Hind*III and *Xba*I was ligated with T4 DNA ligase into 3XFLAGPCMV10 vector cut with the same restriction enzymes. Successful subcloning was confirmed by restriction digestion using *Hind*III and *Xba*I of 3 randomly selected transformed *E coli* clones. M indicates DNA molecular weight marker; 1, 2 and 3 represent different clones selected for digestion.

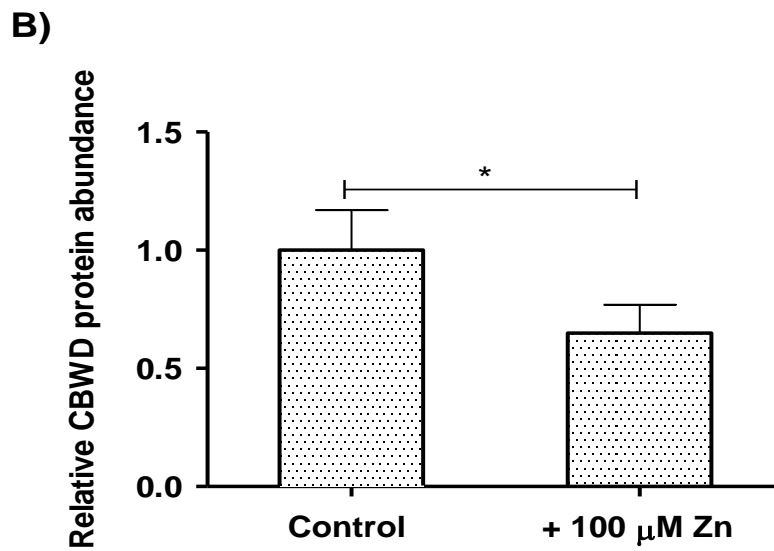
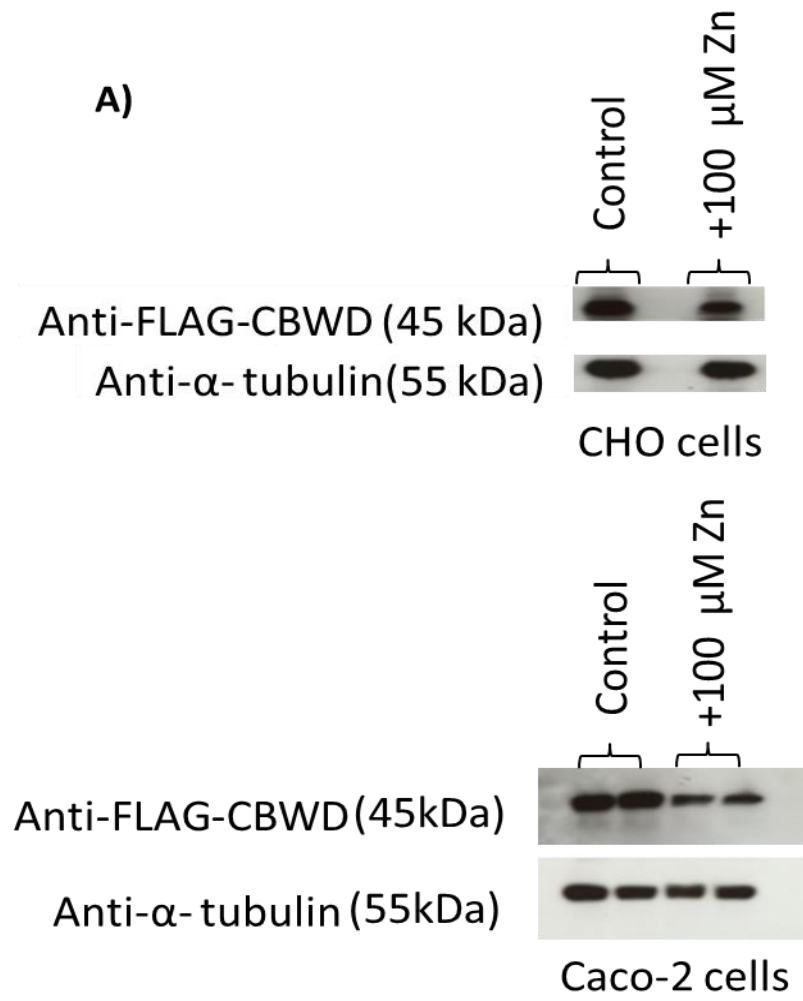


**Figure 5.3: CBWD protein expression is reduced by increased extracellular zinc concentration**

Caco-2 and CHO cells were seeded at  $5 \times 10^5$  cells/cm<sup>2</sup> in 6-well plates and grown in DMEM for 24 h. Twenty four post seeding, cells were transiently transfected with 3xFLAGCBWD3(Caco-2) and pCMV6-CBWD3(CHO) expression plasmids. Twenty four hours after transfection, cells were treated with zinc sulphate at 3  $\mu$ M (control) and 100  $\mu$ M. After a further 24 h, total protein was extracted for western blot analysis using  $\alpha$ -tubulin as the loading control. Representative images are shown in panel A and densitometric analysis of CBWD band intensities (expressed in Caco-2 cells) as a ratio of  $\alpha$ -tubulin expression is presented in panel B. Data are representative of 3 independent experiments. \*P < 0.05 by Student's unpaired t-test.

#### ***5.3.4 The effect of CBWD protein overexpression on intracellular zinc levels***

To determine the effect of increased CBWD expression on intracellular zinc levels, the changes in promoter activity of a zinc-responsive human metallothionein gene (*MT2A*) was measured in Caco-2 cells at extracellular zinc concentrations of 3  $\mu$ M to 100  $\mu$ M. The rationale was that promoter activity would be increased (possibly at both zinc concentrations) if CBWD increased intracellular zinc, and would be reduced if CBWD reduced intracellular zinc. CBWD protein expressed from the 3XFLAGpCMV10 vector (3xFLAGpCMV10-CBWD3 construct) was co-expressed with a *MT2A* promoter-reporter construct (pBlue-*MT2A*). This method was employed previously to investigate the functional role of ZnT5 variant B (ZnT5B) in zinc uptake in the same cell line model (Valentine, 2007). Activity of the *MT2A* promoter was measured in cell lysates prepared from Caco-2 cells transfected with the plasmids and treated with zinc. As shown in Figure 5.4, overexpression of CBWD significantly reduced the activity of the *MT2A* promoter at both concentrations of zinc in cells transfected with pBlue*MT2A* plus 3xFLAGpCMV10CBWD3 compared to cells transfected with the *MT2A* promoter reporter construct plus vector only (no CBWD insert), suggesting that CBWD plays a role in manipulating intracellular levels of zinc available to activate the *MT2A* promoter.

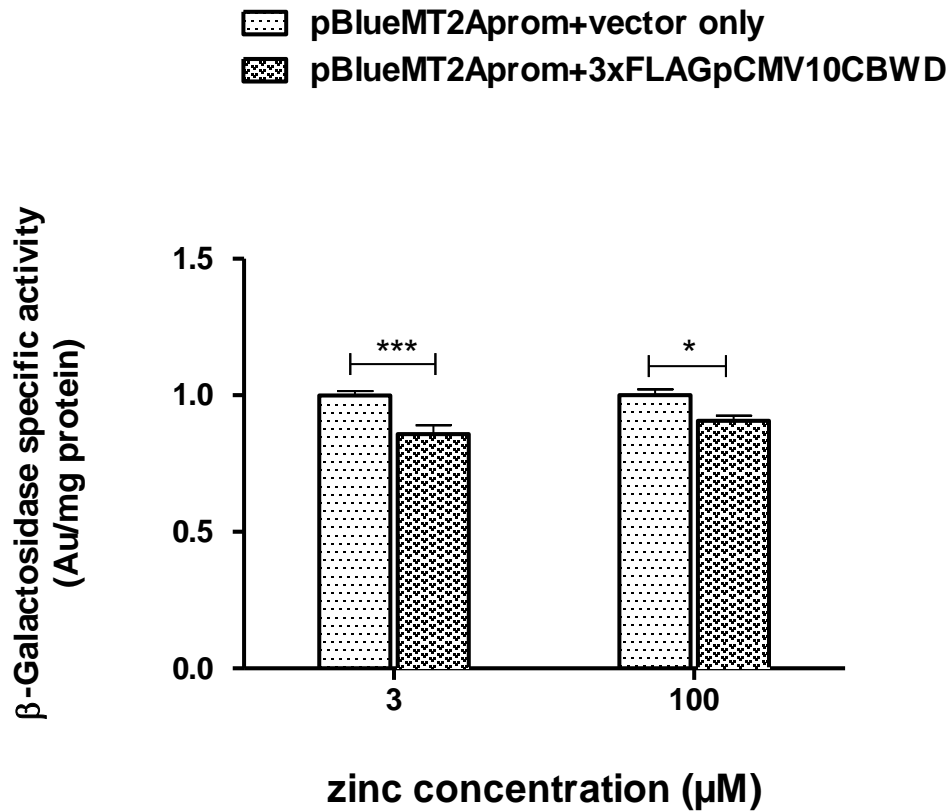


**Figure 5.4: CBWD overexpression alters intracellular zinc status.**

Caco-2 cells were seeded at  $5 \times 10^5$  cells/well in 12-well plates and grown in DMEM for 24 h. Twenty four hours post seeding, cells were transiently co-transfected with pBlueMT2A, plus either 3xFLAGpCMV10-CBWD3 or vector only (3xFLAGpCMV10). After a further 24 h, cells were maintained in serum-free DMEM containing zinc chloride added at 3 µM (control medium) and 100 µM for another 24 h. Cell lysates were then prepared for measurement of promoter activity as β-galactosidase specific activity. Data plotted are mean ± SEM for n = 6 for 3 separate experiments; ns indicates non-significant determined by Student's unpaired t-test.

### ***5.3.5 Effect of CBWD overexpression on cell tolerance to zinc***

It is well documented that cell viability is compromised at extreme levels of zinc availability. To gain some insight into the possibility that CBWD proteins may affect tolerance to extreme variations in zinc supply, reflective of a role in zinc homeostasis, the effect of increased expression of CBWD protein on the survival of Caco-2 cells exposed to zinc at increased and depleted levels was investigated. Cell viability was measured using dye exclusion (trypan blue) and MTT methods. Caco-2 cells were seeded at  $5 \times 10^5$ /well in 6-well plate for dye exclusion or  $10^5$  cells /well 96-well plate for MTT assays respectively. Cells were then treated with 150  $\mu$ M zinc or 10  $\mu$ M TPEN (chosen because of an observed decrease in cell survival under these conditions), then cell survival was measured using exclusion of trypan blue. A range of concentrations of zinc (0, 50, 100, 150, 200  $\mu$ M) and TPEN (0, 0.5, 1, 2, 5, 10  $\mu$ M) were used for more detailed investigation using the MTT assay. For the dye exclusion assay, cells were prepared by centrifugation and cell pellets were resuspended in serum-free medium. Aliquots of cells were mixed with an equal volume of trypan blue dye (Invitrogen) for cell counting using a haemocytometer. Cell images were captured with an AMG EVOS XL digital inverted microscope (Bothel, WA, USA). For the MTT assay, cells were incubated with MTT solution following treatment with zinc and TPEN. Formazan crystals were dissolved in 10% DMSO and absorbance was measured at 570 nm with blank measurement at 630 nm. Absorbance measurement at 630 nm (blank) for each well was subtracted from the corresponding measurement at 570 nm. The absorbance of non-treated cells (control) was set as the reference (100 % viability) and the viability of treated cells in the two groups (with or without CBWD protein) was expressed relative to this value. After treatment with TPEN, cells without CBWD overexpressed protein and stained with Trypan blue were at lower density on visual inspection compared with cells that overexpressed CBWD, suggesting that CBWD increased tolerance to

zinc depletion (Figure 5.5, panel A), whereas there was no apparent difference in cell density in zinc-treated cells with or without CBWD overexpression (Figure 5.5, panel B). However, the results of the MTT assay, which is a quantitative measure of cell viability, revealed that cells that overexpressed CBWD protein showed more tolerance to both zinc depletion by TPEN and to increased zinc concentration compared with control cells (without CBWD overexpression) (Figure 5.6, panels A and B). These results indicate that the presence of CBWD protein extends the cells range of tolerance to altered zinc levels, suggesting a role in buffering/sequestering intracellular zinc and/or regulating zinc influx/efflux.

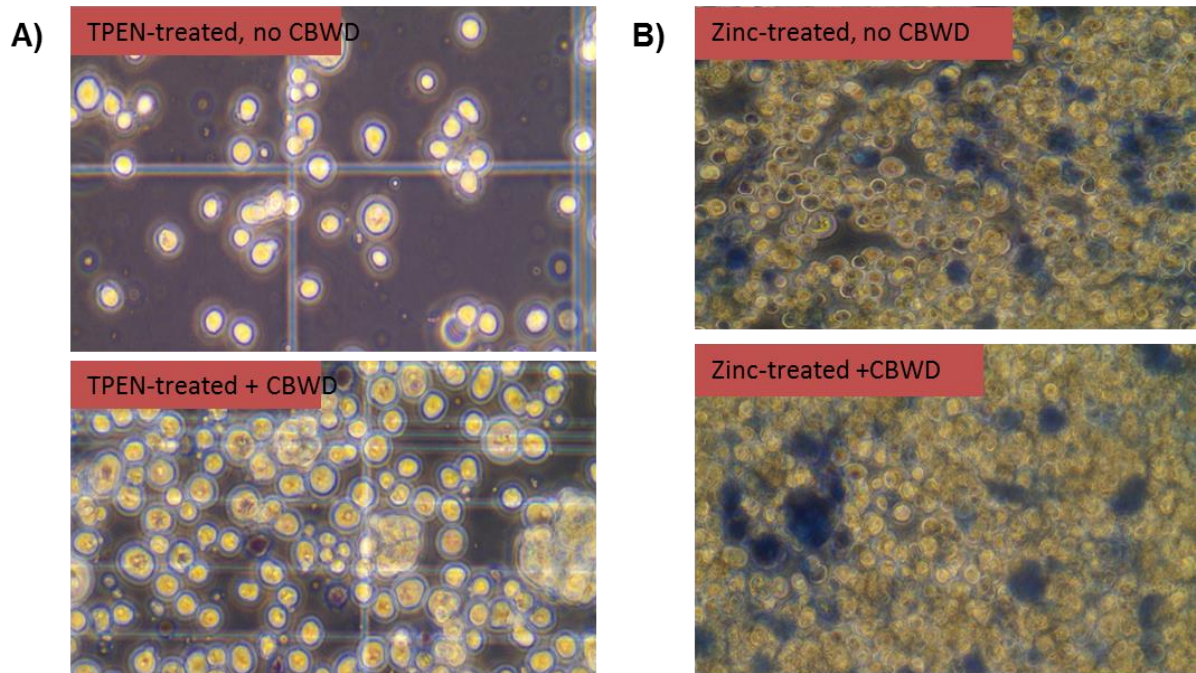
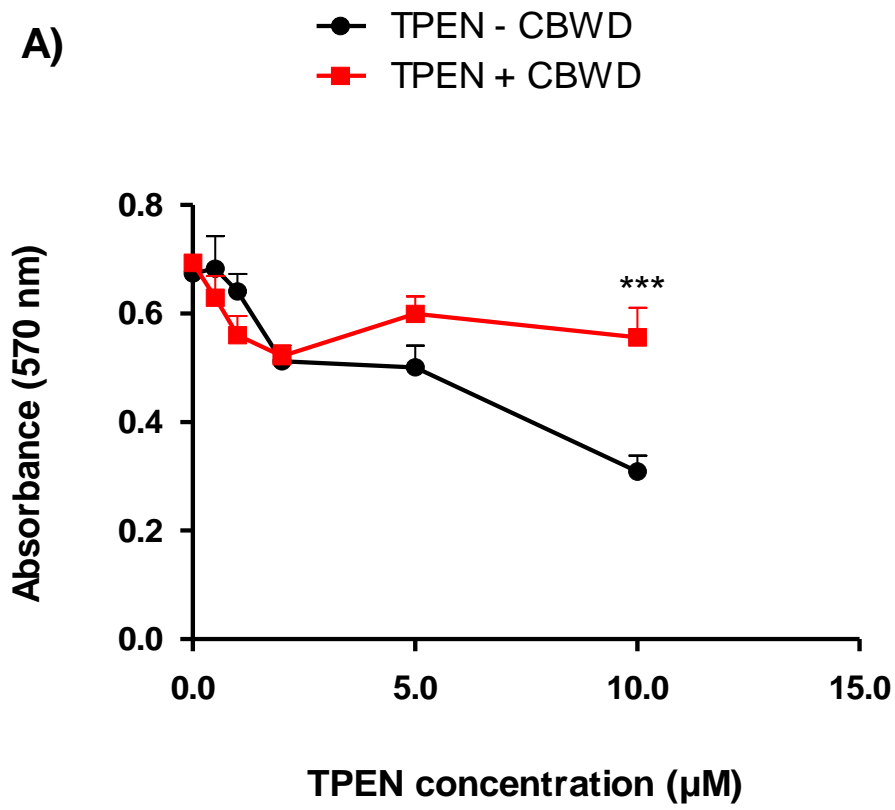


**Figure 5.5: Increased CBWD protein expression enhances viability of cells exposed to zinc depletion or excess (dye exclusion method).**

Caco-2 cells were seeded at  $5 \times 10^5$  cells /well in 6-well plates and grown in DMEM for 24 h. Twenty four hours post seeding, cells were transiently transfected with the 3xFLAGpCMV10-CBWD3 expression construct. After a further 24 h, cells were maintained in serum-free DMEM containing zinc chloride at  $150 \mu\text{M}$  or  $10 \mu\text{M}$  for TPEN for another 24 h. Cells were prepared by centrifugation and cell pellets were resuspended in fresh medium. Equal volumes of cell suspension and Trypan blue were mixed and spotted onto a Haemocytometer (Neubauer) for counting using a light microscope (Olympus CK2) (result not shown). Cell images shown were taken using an EVOS XL digital inverted microscope.

A)



B)

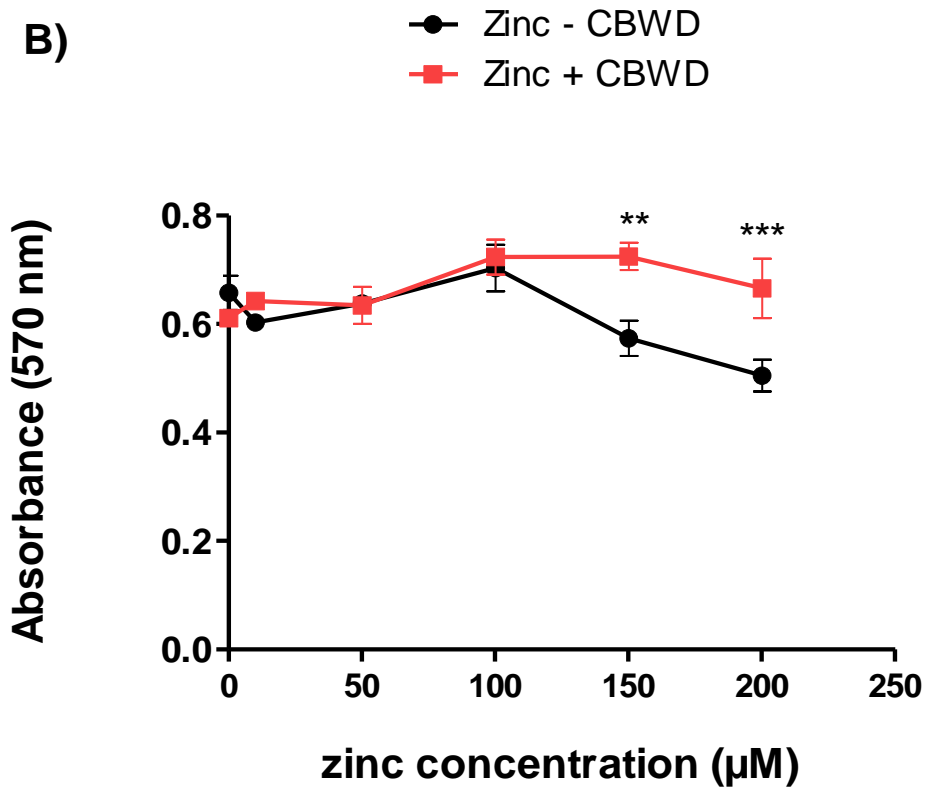
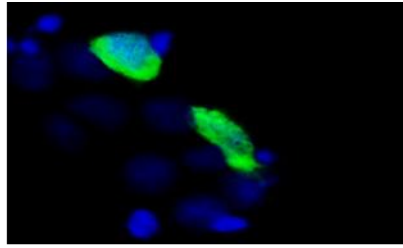


**Figure 5.6: Increased CBWD protein expression enhances viability of cells exposed to zinc depletion or excess (MTT assay).**

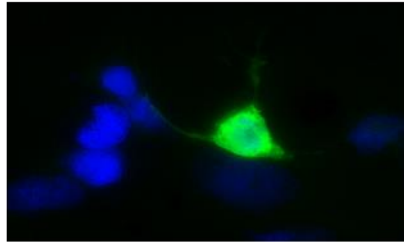
Caco-2 cells were seeded at 10,000 cells /well in 96-well plates and grown in DMEM for 24 h. Twenty four hours post seeding, cells were transiently transfected with the 3xFLAGpCMV10-CBWD3 expression plasmid. After a further 24 h, cells were maintained in serum-free DMEM containing zinc chloride/TPEN at concentrations indicated on the x axes. Twenty four hours post treatment, cells were incubated with 5 mg/ml MTT, using 20  $\mu$ l per well at 37°C for 4 h after which formazan crystals were dissolved by addition of 200  $\mu$ l 10% DMSO. Absorbance was measured at 570 nm using a FLUORstar Omega plate reader (BMG Labtech) with background measurement at 630 nm. Data are presented as mean  $\pm$  SEM for n = 6 for 4 separate experiments. \*P < 0.05; \*\*P < 0.01 by one-way ANOVA.

### ***5.3.6 Effect of zinc on CBWD protein localization***

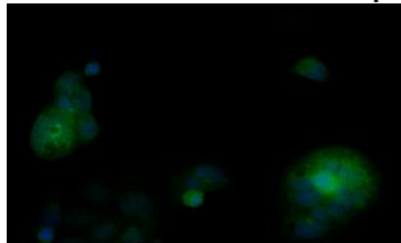
To determine if localisation of CBWD protein was affected by zinc, Caco-2 cells were transiently transfected with the 3xFLAGpCMV10-CBWD3 construct or 3xFLAG-BAP control plasmid containing no CBWD insert (used as negative control) 24 h after seeding cells on 13 mm cover slips in a 6-well plate. Twenty four hours following transfection, cells were treated with zinc at 100  $\mu$ M or 3  $\mu$ M. After a further 24 h, cells were fixed in 4 % paraformaldehyde (PFA) at room temperature for 20 minutes and thereafter permeabilised with 0.3 % Triton-100 in PBS for 15 minutes, followed by incubation in 1 % SDS to unmask the antigen for 10 minutes. Mouse anti-FLAG antibody (M2, Sigma) was prepared at a 1:250 dilution and cells were incubated in this overnight. Cells were then washed in PBS before incubating for 1 h with rabbit anti-mouse secondary antibody conjugated with Alexafluor 488 (ex/em = 496/519) at a 1:1000 dilution. After three washes, cells were mounted on a microscope slide with DAPI-containing Vectashield mounting medium and visualized using an Olympus BX61 fluorescence microscope. As shown in Figure 5.7, the pattern of CBWD protein localisation appeared to be diffuse throughout the cells including the nucleus. There was no difference in the localisation of CBWD protein between cells at 3  $\mu$ M zinc compared with cells treated with 100  $\mu$ M zinc, suggesting that changes in extracellular zinc concentration did not affect CBWD localisation.



FLAG-CBWD + 3  $\mu$ M zinc



FLAG-CBWD +100  $\mu$ M Zinc



FLAG-BAP (negative control)

**Figure 5.7: Increased zinc concentration did not alter CBWD distribution in Caco-2 cells.**

Caco-2 cells were grown on cover slips in 6-well plates for 24 h. Twenty four hours later, cells were transfected with 3xFLAGpCMV10-CBWD3 or FLAG-BAP (as negative control) followed by zinc treatment after a further 24 h. Cells were then fixed with 4 % paraformaldehyde and permeabilised with 0.3 % triton x-100. Cells were thereafter probed with mouse anti-FLAG antibody (1:250) overnight. After washing, cells were incubated with goat anti mouse Alexafluor488 for 1 h. Following washing, cells were mounted on a slide with Vectashield containing DAPI for nuclear staining and images were acquired by fluorescent microscopy.

### ***5.3.7 Effect of CBWD overexpression on cellular zinc distribution***

As reported in section 5.3.5, cells that expressed CBWD protein at higher levels showed increased tolerance to zinc depletion and excess. We examined if this action of CBWD proteins is achieved through cellular redistribution of zinc. To achieve this, the zinc-sensitive fluorescent probe FluoZin-3 was used to visualise cellular location of zinc in cells that expressed the recombinant CBWD protein at increased levels compared with control cells. As shown in Figure 5.8, zinc appeared to be present in a punctate distribution in the cytoplasm of cells at endogenous levels of CBWD protein expression (panel A), whereas in cells with overexpressed recombinant CBWD protein this distribution of zinc appeared similar but somewhat less diffuse (panel B).

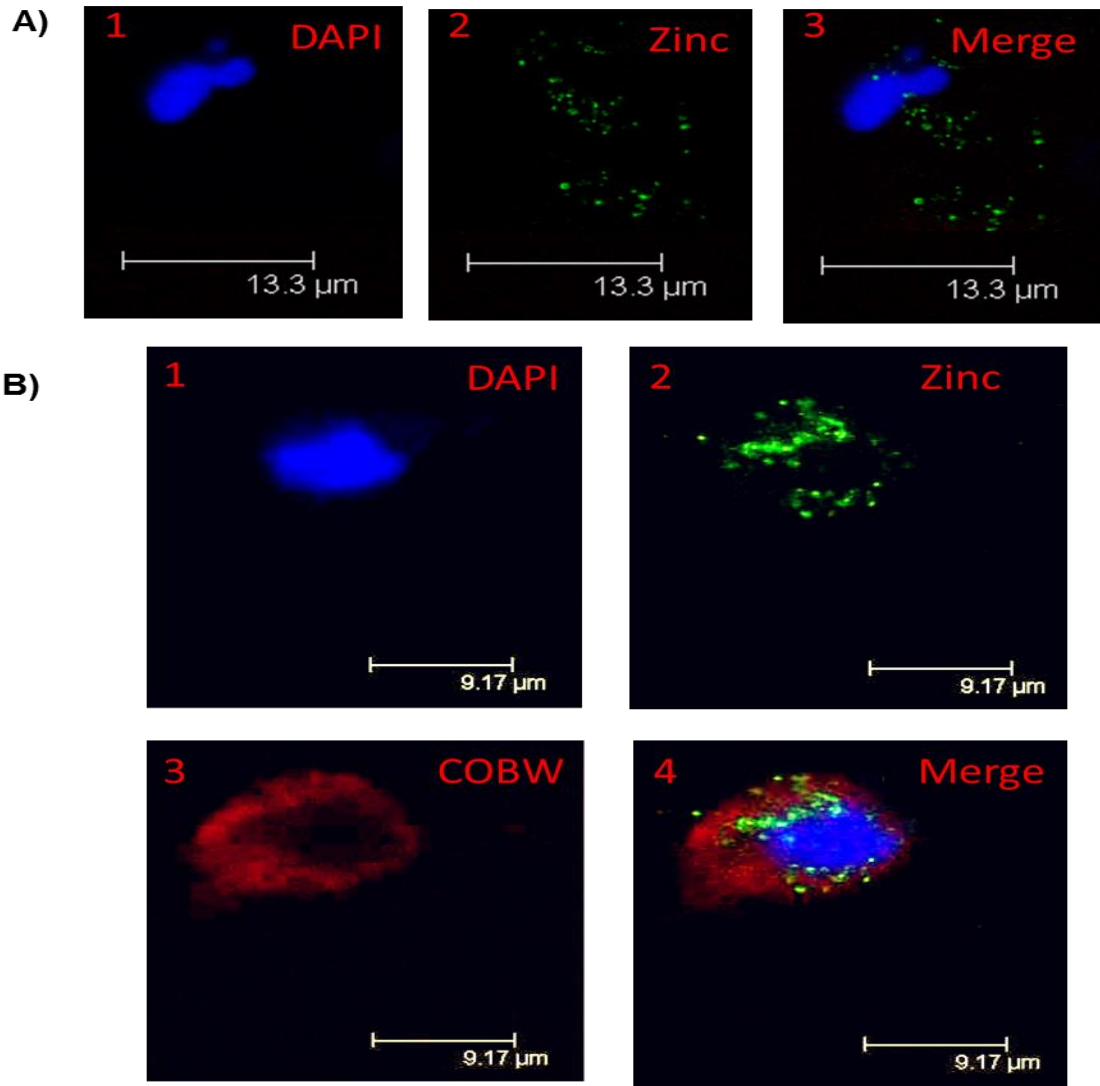


**Figure 5.8: CBWD proteins appears to redistribute cellular zinc**

Caco-2 cells were grown on cover slips in 6-well plates for 24 h. Twenty four hours later, cells were preloaded with FluoZin-3 for 30 min before zinc treatment (panel A). In panel B, cells were transfected with 3xFLAG pCMV10-CBWD 24 h after seeding followed by preloading with FluoZin-3 and then zinc treatment after a further 24 h. Cells transfected with CBWD recombinant construct were treated with mouse anti-FLAG antibody and probed with goat anti mouse Alexafluor 594. Cells were then fixed, permeabilised and imaged using a confocal microscope (Leica SP2 UV).

### 5.3.8 *The effect of DNA methylation on CBWD promoter activity*

The *CBWD* ZTRE includes proximal CpG sites within the promoter sequence included in the promoter-reporter construct that may be sensitive to DNA methylation. It is known that DNA methylation patterns are altered by factors such as age and environmental exposures, including nutrients. Identifying zinc-responsive genes that are sensitive to methylation, which could affect responses to changes in zinc levels, may give a better understanding of how zinc homeostasis is affected by factors such as ageing and different environmental exposures. It was found previously that methylation of the CpG dinucleotides in the ZTRE in *SLC30A5* and those adjacent to it inhibited the ability of the competitor oligonucleotide to outcompete the binding of the protein factor (subsequently identified as ZNF658) in nuclear extracts prepared from Caco-2 cells to the *SLC30A5* probe in EMSA (Coneyworth et al., 2012). This experiment indicated that methylation of the ZTRE affects binding of ZNF658. Moreover, a report of changes in DNA methylation in ageing mouse intestine found *CBWD* to be among the genes most affected (Maegawa et al., 2010). To investigate the effect of DNA methylation on promoter activity, *in vitro* methylation of the *CBWD* promoter sequence (containing 4 CpG sites around the ZTRE) in the pBlue*CBWD*prom construct was undertaken using CpG methyltransferase enzyme (MSssI). Successful methylation was confirmed by agarose gel electrophoresis using methylation sensitive and methylation insensitive restriction endonucleases (*Hpa*II and *Msp*I respectively), after which the plasmid was purified and made transfection-ready by endotoxin-free plasmid preparations. Caco-2 cells were transiently transfected with the methylated and unmethylated constructs. A mouse Sushi repeat-containing protein, X-linked 2 (*SRPX2*) promoter-reporter construct, both methylated and unmethylated, was used as a negative control (to demonstrate that any effect of DNA methylation on  $\beta$ -galactosidase specific activity driven by the *CBWD* promoter was not due to a direct effect on  $\beta$ -galactosidase ORF). Promoter activity was measured in cell lysates by measuring  $\beta$ -

galactosidase activity. Cells that were transfected with the methylated plasmid showed decreased promoter activity, evident by a reduction in the  $\beta$ -galactosidase specific activity compared with the activity in cells transfected with unmethylated plasmid (Figure 5.9), indicating that DNA methylation represses the activity of the *CBWD* promoter. As expected, there was no difference in promoter activity between the methylated and unmethylated *SRPX2* promoter-reporter construct.

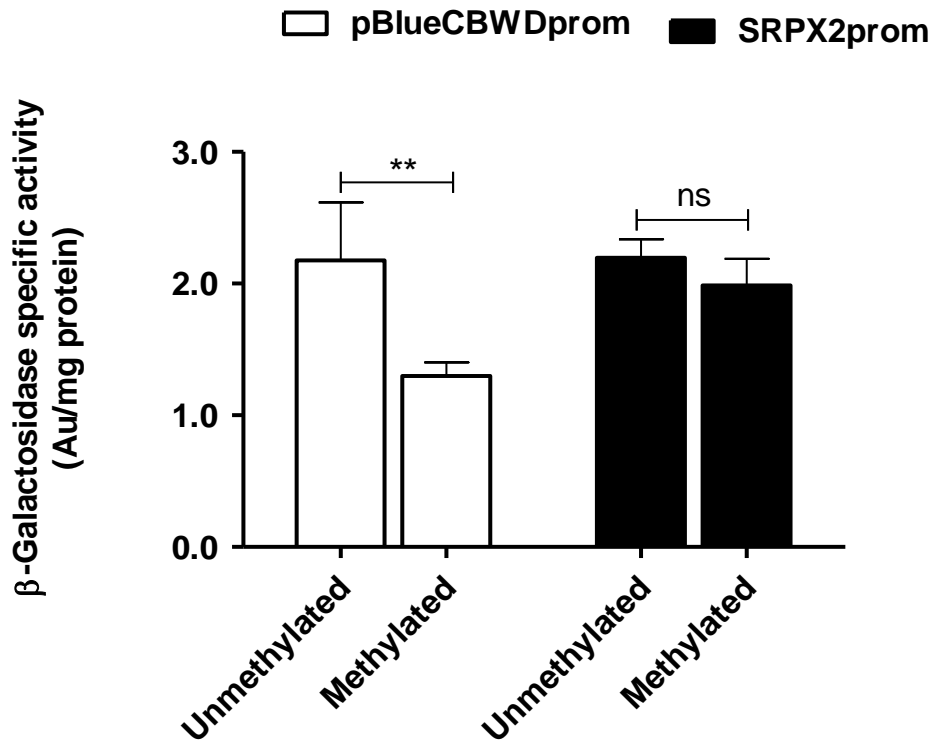


**Figure 5.9: Methylation of the CBWD promoter reduces its activity.**

Caco-2 cells were seeded at  $3 \times 10^5$  cells/cm<sup>2</sup> in 12-well plates and grown in DMEM for 24 h. Twenty four post seeding, cells were transiently transfected with methylated and unmethylated pBlueCBWD1prom or mouse SRPX2 promoter-reporter plasmids (negative control). Twenty four hours after transfection, cell lysates were prepared for measurement of promoter activity as β-galactosidase specific activity expressed relative to protein concentration. Data are plotted as mean ± SEM for n = 9 from 3 separate experiments. \*\*P < 0.01 determined by Student's unpaired t-test.

## 5.4 Discussion

The *CBWD* gene family, whose names reflect the presence of a domain similar to the cobalamin synthesis protein cobW C-terminal domain in *Pseudomonas denitrificans* (Wong et al., 2004), have wide representation across the bacterial phylum. The *CBWD* genes were originally identified through genome screening of the human chromosome 2-fusion site, which revealed additional genes within the region that arose from segmental duplication events. Specifically, duplication of nine genes at 2qFus, 9pter, 9p11.2 and 9q13 sites uncovered four members of *CBWD* and *FOXD4*-like gene families with evidence of transcriptional activity (Fan et al., 2002). The human *CBWD* gene family consists of six isoforms numbered from 1 to 6 and having different cytogenetic locations; *CBWD1* is located in the sub-telomeric region of the p-arm at 9p24.3, *CBWD3*, *CBWD5* and *CBWD6* are all located in the pericentromeric region of the q-arm of chromosome 9 at 9q13 and 9q21.11 respectively with *CBWD4* (also at the same position) designated as a pseudogene. *CBWD2* on the other hand is located within the pericentromeric region on the q-arm of chromosome 2 at a position equivalent to 2q13. Despite the different chromosomal location, the *CBWD* genes exhibit a remarkable nucleotide and amino acid sequence conservation as revealed by sequence alignment using ClusterW2 software (see appendix F). Although no known function has been established for eukaryotic *CBWD* gene products, prokaryotic homologs have been proposed to have a role in the cobalamin biosynthetic pathway owing to their association with an operon of genes coding for known components of the pathway (Crouzet et al., 1991). Members of this operon encode proteins with characteristics similar to the G3E P-loop-containing GTPases subfamily of the COG0523 protein family, including a conserved putative metal binding CXXC motif at the N-terminal domain and histidine-rich residues at the carboxy terminal domain, seen also in the *Pseudomonas denitrificans* CobW protein. The presence of a histidine-rich region in the C-terminal domain of *CBWD* proteins suggests a metal-binding function. *CBWD* homologues

have also been identified within the zinc-dependent Zur regulon in *Anabaena* (blue-green algae) (Napolitano et al., 2012) supporting the assertion that these genes have roles in zinc homeostasis or the response to fluctuation in the zinc supply. Homologues of *CBWD* in *Bacillus subtilis* appear to have roles in cell survival under conditions of zinc limitation evidenced by the fact that mutants defective in a protein belonging to the COG0523 family showed growth defects in zinc-deficient medium (Gaballa and Helmann, 1998), which was rescued following zinc repletion (Gaballa et al., 2002). Also, a metallochaperone function for members of the bacterial COG0523 family has been inferred (Haas et al., 2009). Metallochaperones with known roles in metal homeostasis such as the antioxidant protein 1 (Atx1) for copper (Shin et al., 2012), and the mitochondrial iron-binding protein, frataxin for iron (Bulteau et al., 2004) have been identified. The copper chaperone for superoxide dismutase (CCS), which guides and also inserts copper into the apoprotein of SOD1 (Ba et al., 2009), as well as fraxatin (iron-binding protein), which escorts iron to the point of entry into the metallocenter of ferrochelatase, the terminal enzyme in heme biosynthesis have also been identified. Given that a zinc metallochaperone has not yet been identified, determining if *CBWD* proteins perform this role would be an important contribution to metal biology.

The effect of zinc availability on expression of *CBWD* gene transcripts in Caco-2 cells measured by RT-qPCR demonstrates zinc regulation of these genes at the transcriptional level, an observation that was replicated at the post-transcriptional level when recombinant *CBWD* protein was overexpressed as C-terminal and N-terminal MYC/FLAG-tagged forms in two mammalian cell lines. *CBWD* protein expression in this model was driven by the CMV promoter, but the possibility that zinc-induced down-regulation of *CBWD* protein may be a result of regulation of CMV promoter activity by zinc was ruled out based on previous reports demonstrating an increased (rather than reduced)  $\beta$ -galactosidase activity driven by the CMV promoter in response to increased extracellular zinc concentration (Coneyworth et al., 2012).

Had zinc had an effect on transcription of the transgene it would thus have been in the opposite direction to the change in protein levels observed in the present study. The findings thus indicate that either CBWD protein translation is reduced and/or degradation is increased at higher levels of zinc in mammalian cells.

The effect of increased CBWD protein expression on intracellular zinc status was assessed by using a zinc-responsive *MT2A* promoter reporter construct. A reduction in  $\beta$ -galactosidase specific activity driven by the *MT2A* promoter was observed in cells that co-expressed CBWD along with the *MT2A* promoter. This effect was observed at extracellular zinc concentrations of both 3  $\mu$ M and 100  $\mu$ M. These results indicate actions consistent with the involvement of CBWD in zinc trafficking or buffering that resulted in decreased activation of the zinc-responsive *MT2A* promoter.

The effect of increased expression of CBWD protein on the range of cell tolerance to zinc was investigated by testing survival of Caco-2 cells exposed to depleted and excess levels of zinc. The observed decreased cell viability at low and high zinc concentrations in this study is commensurate with other published findings (for example (Shen et al., 2008)). Cells that overexpressed CBWD protein showed increased tolerance to the effect of zinc depletion or excess, suggesting that the presence of CBWD proteins may offer protection against deleterious effects of zinc. Functional studies of many proteins in protecting cells against metal-induced toxicity have been achieved through overexpression approaches. The contribution of the zinc efflux protein ZnT1 to increased resistance to zinc was demonstrated through overexpression of rat ZnT1 in baby hamster kidney (BHK) cells (Palmiter and Findley, 1995) and increased tolerance to cadmium-induced toxicity in human trophoblastic cells (McAleer and Tuan, 2001). ZnT2- mediated increased tolerance to zinc (Palmiter et al., 1996a) using this approach has been reported through this method while overexpression of a ZnT10 myc-tagged construct in

HEK293 cells resulted in improved cell viability as well as enhanced tolerance to zinc challenge (Patrushev et al., 2012). It has also been reported that the expression of rat HSP27 cDNA in mouse embryonic stem (ES) cells conferred increased resistance to toxicity induced by metals including cadmium and mercury (Wu and Welsh, 1996). Enhanced expression of TRPV6, a calcium channel that has been implicated in the transport of cadmium and zinc, was similarly demonstrated to delay toxicity to cadmium and zinc in TRPV6-expressed HEK293 cells (Kovacs et al., 2013).

The discovery that CBWD increased the window of tolerance to zinc prompted investigation into whether this indicated role is effected by redistribution of zinc within the cell. The result showed that overexpression of CBWD protein appeared to modify the distribution of the intracellular zinc pool. In cells overexpressing CBWD there appeared to be a less punctate distribution of zinc compared to control cells. Punctate staining with zinc probes has been observed with RhodZin-3 in the mitochondria (Sensi et al., 2003) but of direct relevance to the pattern of staining observed in this experiment is the punctate staining of worms cultured with zinc added at 100  $\mu$ M with FluoZin3 in the lysosome (Roh et al., 2012). Thus it is possible, though not yet demonstrated with any clarity, that CBWD may influence the uptake or efflux of zinc from lysosomes. The current data remain preliminary and there is a need to apply a more rigorous approach to studying the effect of CBWD expression on intracellular zinc distribution for example through parallel use of markers of specific sub-cellular compartments such as LysoTracker.

Methylation of CpG dinucleotides within a promoter sequence can block binding of regulatory proteins to recognition sites. Electrophoretic mobility shift analysis of the effect of methylating residues within the binding site for the growth factor independence (Gfi-1) protein at its target promoter sequences interfered with binding (Zweidler-Mckay et al., 1996). Similarly, binding

of the transcription factors cAMP response element-binding protein (CREB) and specificity protein 1 (SP1) in nuclear extracts prepared from neuroblastoma cells to the mammalian type 1 neurofibromatosis (NF1) regulatory region was impeded as a result of methylation of CpG dinucleotides at this site (Mancini et al., 1999). The binding of a regulatory protein (now identified to be ZNF658) in cellular extracts prepared from zinc-treated Caco-2 cells to the ZTRE was inhibited as a result of the methylation of the CpG sites within and around this motif in the *SLC30A5* promoter (Coneyworth et al., 2012). We show here that *in vitro* methylation of the *CBWD* promoter repressed expression of the  $\beta$ -galactosidase reporter gene in a promoter-reporter construct demonstrating that methylation of sites within this region affects transcription, presumably through influences on the binding of transcription factors. Given that the ZTRE in *CBWD* includes 4 CpG pairs that could potentially be methylated and that, as shown in chapter 5, ZNF658 knockdown can affect endogenous levels of *CBWD* expression, methylation of the ZTRE specifically may contribute to this suppressed transcription. Further work, for example using EMSA to determine directly if there is an influence of methylation on ZNF658 binding, is however required to determine if this is the case.

The findings presented in this chapter give preliminary but plausible evidence in support of the involvement of *CBWD* gene products in cellular zinc homeostasis; however, future investigation is required to fully explore this proposition.

## **Chapter 6 : The effect of endothelial cell senescence on cellular zinc homeostatic processes**

### **6.1 Introduction**

Zinc plays a regulatory role in nitric oxide (NO) signalling, a process necessary for maintaining membrane integrity of endothelial cells (Meerarani et al., 2000). Endothelial cells form the thin monolayer that lines the interior surface of the entire cardiovascular system (comprising the blood and lymphatic vessels). They form an interface between the circulating blood and the vessel wall and fulfil a selective barrier function. Zinc deficiency or excess can induce pro-inflammatory events in endothelial cells likely to have negative consequences for vascular health. Also endothelial cell senescence has been implicated in ageing-related vascular degeneration (Kovacic et al., 2011, Shan et al., 2014); thus, understanding the link between endothelial cell function in health and disease and zinc homeostasis may be valuable in targeting approaches to mitigate the effects of vascular disease.

Cellular senescence (CS), first described by Hayflick in 1965, is a phenomenon involving a permanent state of cell cycle arrest that is characterised by loss of proliferative capacity, which is a hallmark of ageing. Cellular senescence is induced by factors including telomere shortening, as a result of which cells gradually reach their Hayflick limit after many rounds of cell divisions triggering the DNA damage response (DDR). This form of senescence due to erosion of the proliferative telomere barrier is often referred to as replicative senescence. Telomere shortening was shown to be critical for replicative senescence in experiments where the catalytic component of the human telomerase holoenzyme hTERT (human telomerase reverse transcriptase) was overexpressed from a CMV-driven pCI-neo-hTERT-HA construct in human fibroblasts (Counter et al., 1998), which resulted in abolishment of the end of replication block thereby allowing continuous replication. Other factors such as stress or

mitogenic signals (aberrant expression of oncoproteins) can induce senescence independent of telomere shortening and it is termed premature senescence. Stress-induced premature senescence (SIPS) may result from the presence at critical concentrations of nutrients or growth factors or exposure to sub-cytotoxic stressors such as hydrogen peroxide. Stress-induced cell cycle arrest was shown to be a telomere-independent mechanism of cellular senescence in human fibroblasts, in which changing culture conditions to represent physiological conditions resulted in immortalised cells showing no decline in telomerase activity or telomere length (Ramirez et al., 2001). Also, in mouse embryonic fibroblasts (MEFs), non-telomere-driven senescence was demonstrated through inactivation of p53 and could be achieved despite ablation of the retinoblastoma protein (pRb) family of genes, which are important in replicative senescence (Dannenberg et al., 2000). On the other hand, oncogene-induced senescence (OIS), which was first observed to cause cell cycle arrest following expression of human RAS (HRAS) in normal human fibroblasts (Serrano et al., 1997), was shown to induce cellular senescence in concert with p53 (Ferbeyre et al., 2002, Campisi and di Fagagna, 2007). Under these conditions, overexpression of hTERT failed to abrogate induction of senescence, indicating that OIS is independent of the pathway mediated by telomere shortening (reviewed by (Kuilman et al., 2010). Irrespective of the triggers or mechanisms, progression to cellular senescence appears to be through a common pathway involving p53 and p16INK4a/Rb (Larsson, 2011, Mirzayans et al., 2010). Common traits of senescence include growth arrest, activation of senescence-associated  $\beta$ -galactosidase and secretion of cytokines, chemokines, growth factors and proteases. Collectively these features comprise the senescence-associated secretory phenotype (SASP) (Figure 6.1) (Rodier and Campisi, 2011). These features, along with activation of the mammalian target of rapamycin complex1 (mTORC1), which is emerging as an additional marker (Hasty et al., 2013), distinguish senescent cells from their quiescent counterparts.

A general view, supported by an accumulating body of evidence, is that cellular senescence is a mechanism that prevents neoplastic transformation (Dimri et al., 2000). However, this proposed tumor-suppressive effect of cellular senescence is still controversial, and it appears that cellular senescence can promote some forms of cancer growth, depending on the physiological context (reviewed in (Campisi, 2013). Cellular senescence is also thought to accelerate the ageing phenotype through alteration of tissue microenvironments, which also promotes age-related diseases (reviewed by (Malavolta et al., 2014)). In particular, endothelial cell senescence is associated with cellular dysfunction, which may result in the onset of age-related cardiovascular diseases. Cardiovascular diseases (CVDs), are the leading cause of mortality globally (Alwan, 2011) and are predicted to remain the single leading cause of death worldwide (Mathers and Loncar, 2006). Although a specific contribution of cellular senescence to the pathogenesis of CVD is unresolved, the presence of senescent cells in human aorta at sites of atherosclerosis has been shown (Vasile et al., 2001). Improved understanding of the molecular mechanisms that underlie these associations might offer useful opportunities for developing therapeutic strategies against age-related diseases in general and cardiovascular diseases in particular. Recently, a role for micronutrients such as zinc in ameliorating incidences of age-related disorders due to its effects on the health of endothelial cells has been reported in some studies, but the molecular details are still poorly understood. Zinc safeguards endothelial cell integrity by providing protection against apoptosis (Meerarani et al., 2000). Variations in zinc supply may modulate the activity of senescence-inducing factors. Consequently, maintenance of zinc homeostasis is central to the health and function of the vasculature and may contribute to reducing the progression of senescence-driven age-related pathologies such as atherosclerosis. Emerging evidence suggests that cellular senescence, which is a component of the mammalian ageing may be affected by alterations in cellular zinc homeostasis (Patrushev et al., 2012). In the preceding chapters, we explored the mechanism of

zinc-induced transcriptional repression of genes with roles in zinc homeostasis and identified the regulatory factor that mediates this component of zinc homeostasis. Given that dysregulation of zinc homeostasis is a feature of many ageing-related diseases, understanding the molecular mechanism that underlie this association would be important in the effort to develop intervention strategies to ameliorate effects arising from perturbations in zinc balance on the ageing phenotype.

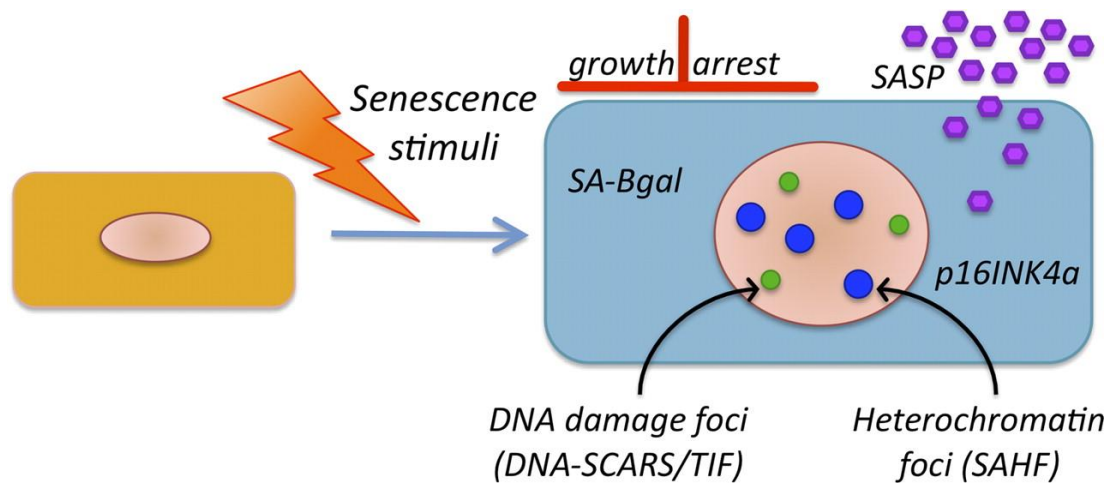


**Figure 6.1: Hallmarks of senescent cells.**

Senescent cells differ from other nondividing (quiescent, terminally differentiated) cells in several ways; although no single feature of the senescent phenotype is exclusively specific. Hallmarks of senescent cells include an essentially irreversible growth arrest; expression of SA-Bgal and p16INK4a; robust secretion of numerous growth factors, cytokines, proteases, and other proteins (SASP); and nuclear foci containing DDR proteins (DNA-SCARS/TIF) or heterochromatin (SAHF). The pink circles in the nonsenescent cell (left) and senescent cell (right) represent the nucleus (adopted from (Rodier and Campisi, 2011)).

## 6.2 Specific objectives

The specific objectives of the work reported in this chapter were to investigate using an endothelial cell model:

- the effect of zinc on endothelial cell growth and progression to the senescent state;
- changes in expression of the transcription factor ZNF658 and its target genes.

## 6.3 Methods

Cell culture and RNA extraction were performed at Dr Marco Malavolta's laboratory at the National Institute of Health & Science on Ageing, Ancona, Italy. Human Coronary Artery Endothelial Cells (HCAECs) were purchased from Clonetics Corporation (Lonza) and cultured in endothelial basal medium (EBM) supplemented with EGM-2 or EGM-2/MV SingleQuots containing 0.1% rh-EGF (human recombinant epidermal growth factor), 0.04% hydrocortisone, 0.1% VEGF (vascular endothelial growth factor), 0.4% rh-FGF-B (human recombinant fibroblast growth factor), 0.1% rh-IGF-1 (insulin-like growth factor) 0.1% ascorbic acid, 0.1% heparin, 0.1% GA-1000 (gentamicin sulfate plus amphotericin B) and 5 % fetal calf serum. For experiments, cells were plated at a seeding density of 2,500 cells/cm<sup>2</sup> in T25 flasks and incubated at 37 °C and 5% CO<sub>2</sub> with normal medium or normal medium supplemented with 50 μM ZnSO<sub>4</sub>. The medium was changed every 48 hours. Cell cultures reached confluence after 6-7 days, as assessed by light microscopic examination, and they were passaged at weekly intervals. After trypsinization and before replating, harvested cells were counted using a haemocytometer and the number of population doublings (PDs) were calculated using the following formula: population doubling = 3.32\*(log<sub>10</sub>F – log<sub>10</sub>I) (where F indicates the number of cells at the end of the passage and I the number of cells when seeded), according to the original method (Maciag et al., 1981). Endothelial cell aging was studied by subjecting endothelial cells to subsequent passages until two consecutive population doublings

equal or below 0 associated with senescence morphological changes revealed by microscopy examination. Cumulative population doubling (CPD) was calculated as the sum of all the changes in PD. At the end of each passage, each cell aliquot was frozen. Total RNA was extracted from HCAECs using the RNeasy Mini Kit (Qiagen, Hilden, Germany), according to the manufacturer's instructions. RNA concentration was determined by Nanodrop and samples were kept at -80 °C for measurement of gene expression using RT-qPCR.

## **6.4 Results**

### ***6.4.1 Effect of zinc on HCAEC cell growth***

To determine whether the presence of zinc affected the growth of HCAECs, cells were subjected to serial passage and growth was monitored as cumulative population doubling. As indicated in Figure 6.2, cells in both untreated and zinc-treated groups appeared to undergo growth arrest after passage nine; however, zinc-treated cells underwent earlier growth arrest compared with control cells, suggesting that zinc stimulated transition to senescence in endothelial cells. These results were confirmed by observation of changes in cell morphology. Cells grown at higher zinc concentration were larger in size, had increased expression of the senescence marker p16 and had increased senescence-associated  $\beta$ -galactosidase staining compared with control cells. These experiments were conducted by Dr Marco Malavolta.

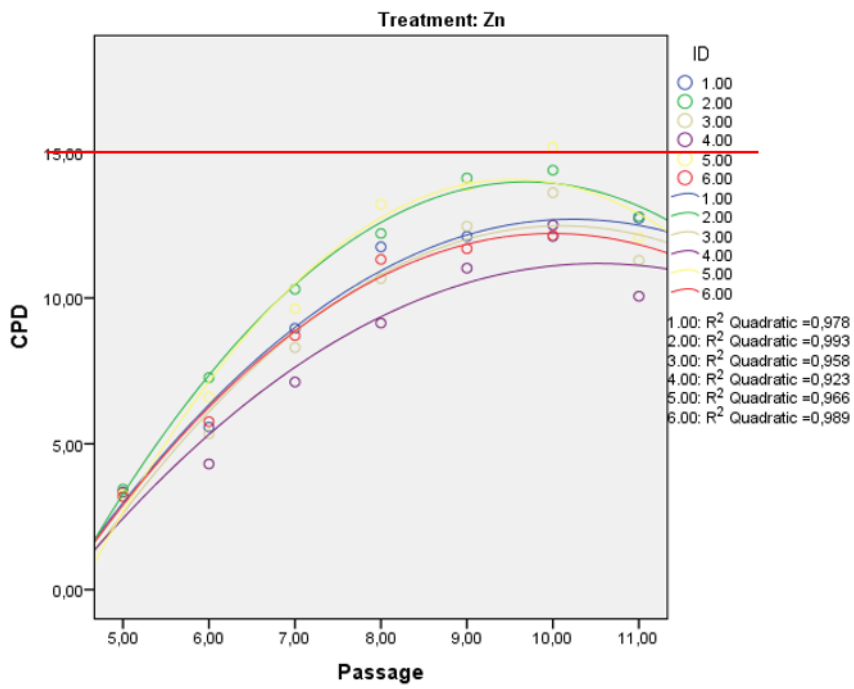
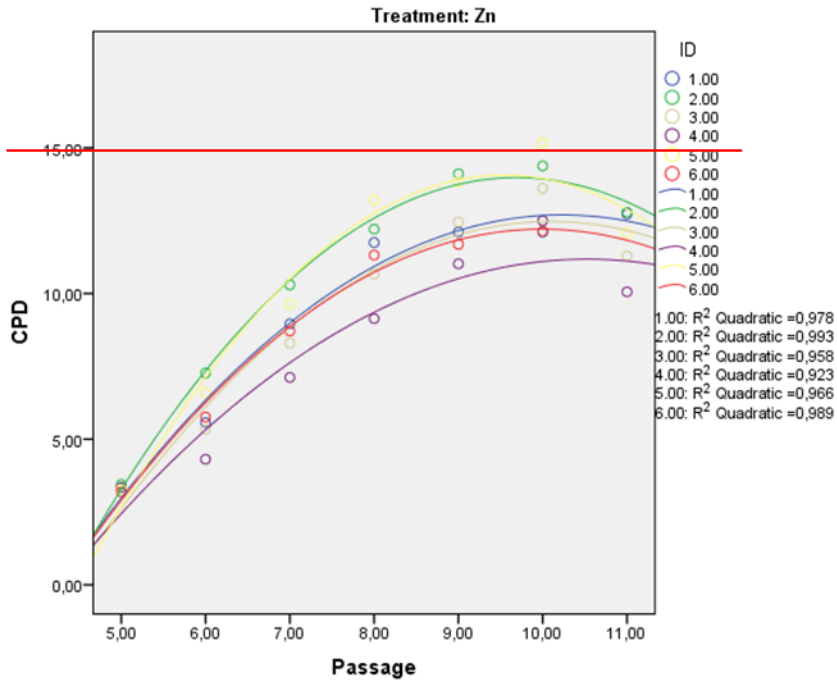


**Figure 6.2: Zinc promotes endothelial cell growth arrest**

Human Coronary Artery Endothelial Cells (HCAECs) cultured in endothelial basal medium (EBM) supplemented with growth factors were treated with zinc at 50  $\mu$ M or grown under control conditions and allowed to grow until 6-7 days. Cells were passaged serially and harvested cells counted. Cumulative population doubling (CPD) were calculated using the formular  $3.32 * (\log_{10}F - \log_{10}I)$  over consecutive population doublings where F is the number of cells at the end of the passage and I is the number of cells when first seeded. The red line is in arbitrary threshold shown to emphasize the difference in the growth curves. Each different coloured line shows an independent population of cells (n = 6 for each condition).

### 6.4.2 Effect of zinc-induced endothelial cell senescence on expression of p16

To examine if HCAEC cells underwent replicative senescence induced by zinc, mRNA levels of p16, a cell cycle inhibitor known to regulate senescence pathway were measured by RT-qPCR. As shown in

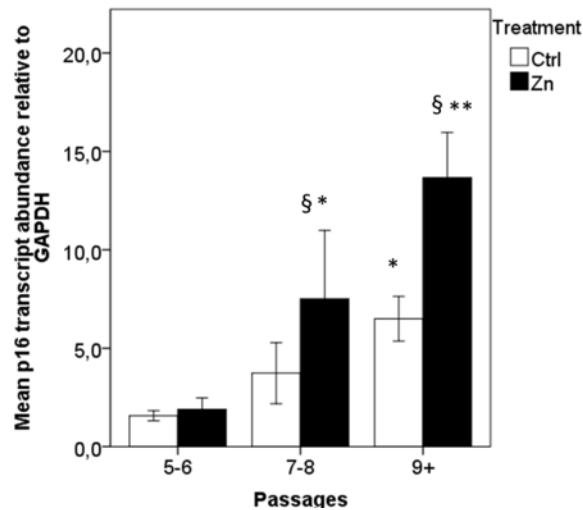
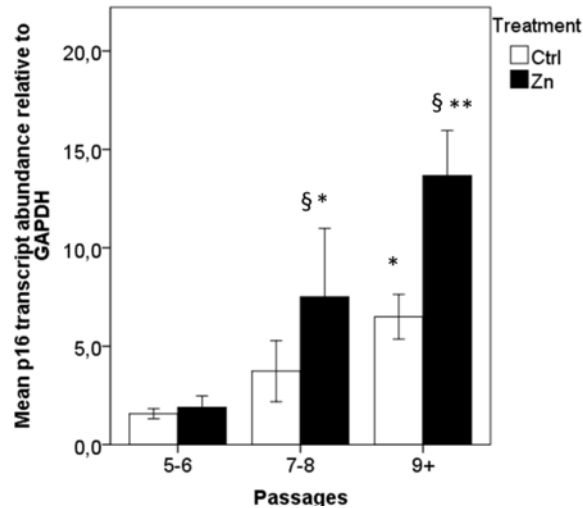


Figure 6.3, mean expression of p16 relative to mean expression of  $\beta$ -actin was consistently increased with increasing passage number in zinc-treated cells compared with untreated cells, suggesting that zinc promotes progression of endothelial cells from quiescent to senescent state. Measurement of p16 mRNA was carried out by Dr Marco Malavolta.

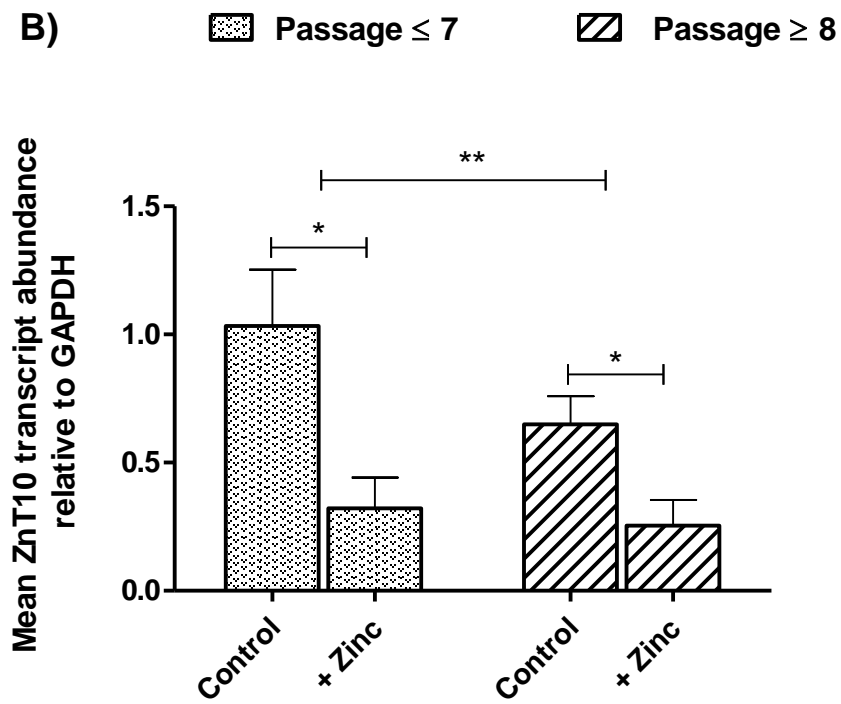
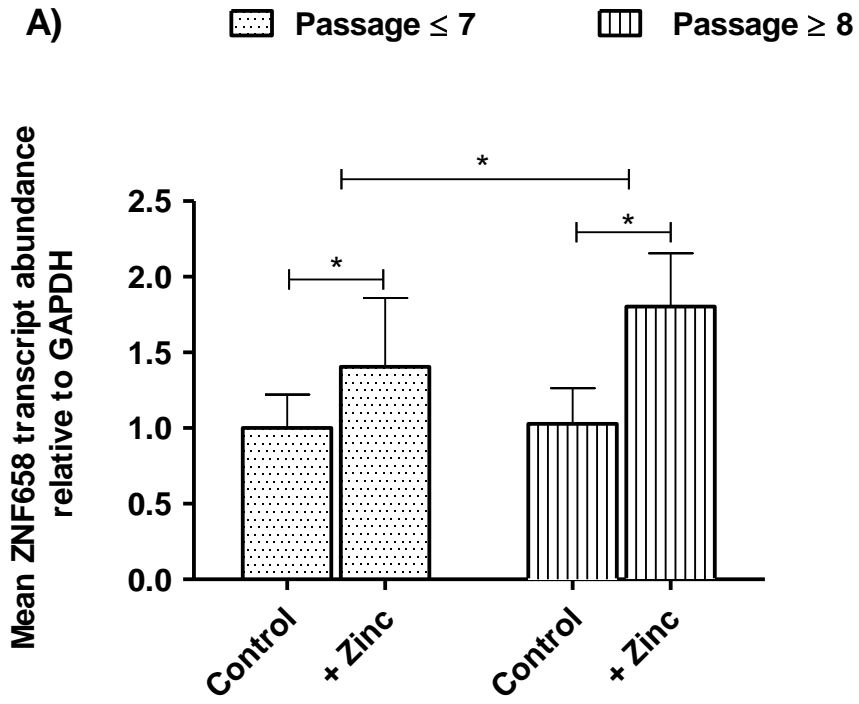


### Figure 6.3: Zinc-induced endothelial cell growth arrest increased p16 expression

Human Coronary Artery Endothelial Cells (HCAECs) cultured in endothelial basal medium (EBM) supplemented with growth factors were treated with zinc at 50  $\mu$ M and allowed to grow until 6-7 days. Upon confluence, cells were subjected to serial passages until the end of two consecutive population doublings. Cells were then frozen and RNA was subsequently prepared using the SV total RNA isolation system (Promega, Madison, USA). Transcript levels of p16 were measured by RT-qPCR expressed relative to transcript levels of  $\beta$ -actin. Data are expressed as mean  $\pm$  SEM for n = 3 and compared between the control condition and zinc treatment. \*P < 0.05 (for passage number comparison), §P < 0.01 (for treatment comparison) by Student's unpaired t-test.

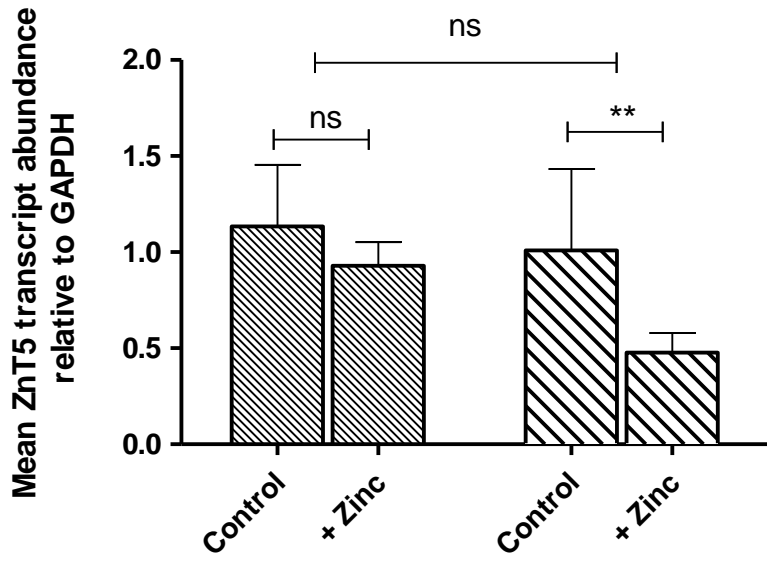
### ***6.4.3 Effect of zinc-induced senescence on expression of ZNF658 and its target genes in HCAECs***

To examine the effect of zinc-induced endothelial cell senescence on the expression of ZNF658 and its target genes, mRNA was prepared from cells at each passage under both control and supplemented conditions and levels of specific mRNAs were measured by RT-qPCR. Expression of each gene was assessed relative to *GAPDH* as a mean over early ( $\leq 7$ ) and late ( $\geq 8$ ) passage numbers. As shown in Figure 6.4, ZNF658 mRNA expression was up-regulated as cells progressed towards the senescent state (panel A). In contrast, transcript levels of the ZNF658 target genes (ZnT10, ZnT5 and CBWD) were down-regulated (panels B, C and D), consistent with the known repressive effect of ZNF658 on these targets.



C)

▨ Passage ≤ 7      ▩ Passage ≥ 8



D)

▤ Passage ≤ 7      ▥ Passage ≥ 8

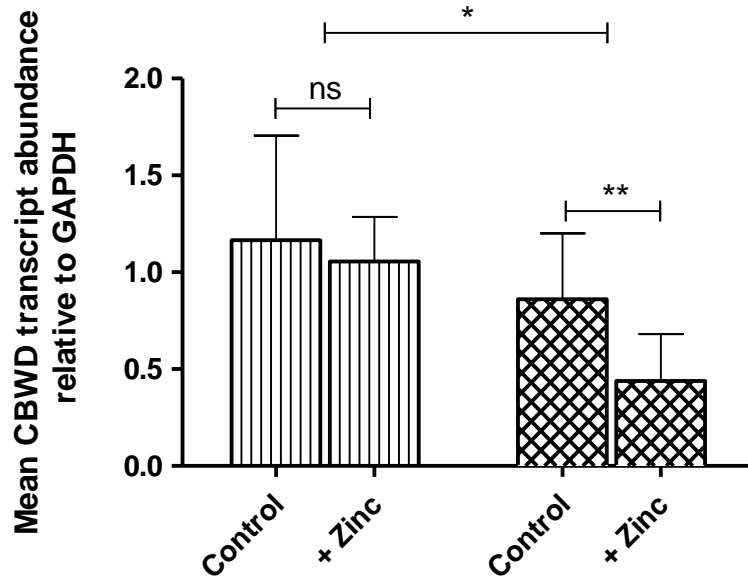


**Figure 6.4: Expression of ZNF658 and its target genes are regulated by cellular senescence**

Human Coronary Artery Endothelial Cells (HCAECs) cultured in endothelial basal medium (EBM) supplemented with growth factors were treated with zinc at 50  $\mu$ M and allowed to grow until 6-7 days. Upon confluence, cells were subjected to serial passages until the end of two consecutive population doublings. Cells were then frozen and RNA was subsequently prepared using the RNeasy Mini Kit (Qiagen). Transcript levels of ZNF658, ZnT10, ZnT5 and CBWD were measured by RT-qPCR expressed relative to transcript levels of *GAPDH*. Data are expressed as mean  $\pm$  SEM for n = 3 and compared between the control condition and zinc treatment between earlier  $\leq$  7 and later  $\geq$  8 passages. \*P < 0.05, \*\*P < 0.01 by Student's unpaired t-test.

## 6.5 Discussion

We established in an epithelial cell line (Caco-2) that the ZNF658 transcription factor represses the expression of genes coding for members of the CDF zinc transporter family and *CBWD* gene family in response to elevated zinc levels, suggesting an important role for this factor in zinc homeostasis. Here, we present preliminary evidence that up-regulation of ZNF658 and down-regulation of its known target genes (*SLC30A5*, *SLC30A10* and *CBWD*) are associated with a senescent phenotype in human coronary artery endothelial cells. This gene expression profile appears more robust as the cells transit from early to late passages, entering growth arrest after passage nine (9). Senescent cells are defined by specific gene expression signatures, which include secretion of pro-inflammatory factors such as interleukins 6 and 8 (IL-6, IL-8), vascular endothelial growth factor and matrix metalloproteases (Coppé et al., 2010), together characterising what is generally termed the senescence-associated secretory phenotype. Accumulation of senescent cells over time is known to alter the tissue microenvironment and predisposes cells to age-related decline in adaptive immunity (immunosenescence) (McElhaney and Effros, 2009) and other age-associated pathologies. A marker of cellular senescence used over the years has been senescence-associated  $\beta$ -galactosidase (SA- $\beta$ -gal), which is a histochemical marker that distinguishes senescent cells from quiescent ones in many cell models including human vascular endothelial cells of the aorta (Vasile et al., 2001) and arteries (Minamino et al., 2002). Examination of cell morphology and the SA- $\beta$ -gal staining pattern of cultured HCAECs at different passage numbers revealed increased cell size, with positive SA- $\beta$ -gal staining, at late passages ( $\geq 8$ ) compared with early passages ( $\leq 7$ ) (Dr Marco Malavolta, unpublished data). These results are consistent with other findings that indicate growth arrest and progression to senescence for aortic endothelial cells at late passages (8 -10) (Wang et al., 2008).

The observation that expression of cyclin-dependent kinase inhibitor 2a (p16) was increased in late passages ( $\geq 8$ ) compared with lower passage ( $\leq 7$ ) appears consistent with the expression pattern of this marker in our model. This protein (p16) regulates the cell cycle by inactivating cyclin-dependent kinases that phosphorylate pRB, which is necessary for cell progression from G1 to S-phase, has been a useful marker of cellular senescence. These results are in agreement with elevated levels of p16 mRNA and protein levels in human fibroblasts undergoing senescence (Alcorta et al., 1996) (Beauséjour et al., 2003). Similarly, up-regulation of p16 expression has been shown to correlate with replicative senescence in human fibroblast (Mirzayans et al., 2010) and in human airway epithelial cells (Fischer et al., 2013) at later passages compared with early passages. Our data also indicate that the presence of a higher concentration of zinc (50  $\mu$ M) in the medium expedited the transition of cells into the senescent state, and corresponding augmented responses of ZNF658 and its target genes were observed. It thus appears that zinc promotes senescence in endothelial cells. The mechanism underlying this transition is unknown. The mTOR pathway is an attractive candidate mechanism given that its activity has been shown to be modulated by zinc (Lynch et al., 2001). Statistical analysis (Dr Marco Malavolta, personal communication) revealed that p16 expression correlated positively with repression of *SLC30A10* (ZnT10) and *CBWD* genes, and with the ratio of ZNF658 to ZnT10 but not with *SLC30A5* (ZnT5). The correlation with p16 expression was particularly marked for the ratio of ZNF658 to ZnT10, thus this ratio may be a good potential marker of senescence to explore in future work. For example it would be of interest to determine if the ratio correlates with clinical features of vascular disease and/or ageing.

Given that cellular senescence contributes to suppression of tumorigenesis *in vivo* (Ogrunc and d'Adda di Fagagna, 2011), and that zinc appears to drive this process, an avenue for pharmacological intervention against cancer development may be possible when further

evidence to support these findings becomes available. Also, given the fact that cellular senescence is cell-type specific (Bianchi-Smiraglia, 2012), identification of markers in senescent phenotypes may also be diverse. Thus, the ZNF658/ZnT10 ratio may represent a plausible marker of cellular senescence specific for endothelial cells.

## Chapter 7 : Summary and conclusion

### 7.1 Summary

Zinc has attracted much interest in the last decade owing to its pleiotropic involvement in cellular processes relevant to life. Coordinated regulation of multiple genes in response to changes in zinc supply is a central tenet of cellular zinc homeostasis that is essential for the survival of every organism. Many aspects of zinc homeostatic control are not fully understood in spite of the increasing body of research output documenting identification and characterisation of zinc transport proteins. In mammals these transporters comprise two families each with multiple members. The overall aim of this study was to investigate the mechanism of zinc-induced transcriptional repression of genes with likely roles in zinc homeostasis by identifying the regulatory protein that mediate this response through the previously discovered zinc transcriptional regulatory element (ZTRE).

In **chapter three**, we refer to a search of the genome for occurrences of the ZTRE discovered initially within the zinc-responsive *SLC30A5* gene promoter, which codes for the zinc transporter ZnT5. The search revealed that the ZTRE appears in many genes within the human genome out of which a functional copy has been found in *SLC30A10* (coding for the zinc transporter ZnT10) (Bosomworth et al., 2012). Of particular interest in this study is the discovery that *CBWD* genes (coding for COBW domain-containing proteins) also harbour this zinc-responsive element; and has been shown through the current work that the ZTRE in *CBWD1* is functional in the context of it mediating transcriptional repression in response to increased extracellular concentrations of zinc. The ZTRE was shown here to be functional only with both sides of the palindromic motif intact by virtue of the fact that promoter-reporter constructs lacking either side did not respond to zinc.

**Chapter four** reports the identity of the transcription factor that binds to the ZTRE – zinc finger protein 658 (ZNF658). Work presented in this chapter shows that ZNF658 mediates transcriptional repression of *SLC30A5*, *SLC30A10* and *CBWD* genes at elevated extracellular zinc concentrations. ZNF658 was initially identified through mass spectrometry analysis of a DNA-protein complex detected by electrophoretic mobility shift analysis (EMSA) using nuclear extracts prepared from Caco-2 cells and was shown to be similar to the yeast ZAP1 protein, which mediates the transcriptional response to a low zinc supply. The fact that the primary mode of zinc-response gene regulation mediated by ZAP1 and ZNF658 are different could be due to non-similar regions of the two proteins, which may recruit different co-regulators and/or other accessory proteins. We show here using nuclear extracts prepared from Caco-2 cells overexpressing recombinant ZNF658 protein with a myc epitope tag that ZNF658 binds specifically to the ZTRE by demonstrating a supershift of the corresponding band on EMSA using an anti-myc antibody. We also show by deletion of part of the protein that the DNA binding domain is at the C-terminus (consistent with the presence of this domain in other members of the KRAB-containing zinc finger transcription factors. This region incorporates at least some of zinc fingers 12 to 15, which is consistent with the alignment with the known DNA binding domain of yeast ZAP1. We demonstrate that reduced expression of ZNF658, achieved using siRNA, attenuated or abrogated the response of *SLC30A5*, *SLC30A10* and *CBWD* genes to zinc load, thus confirming the role of this factor in this process. Work presented in chapter four thus reveals the identity of the first known mammalian transcription factor that is responsible for coordinating repression of multiple genes in response to increased extracellular zinc supply, indicating a central role in mammalian zinc homeostasis. An unexpected observation was that knockdown of ZNF658 using one of the two siRNAs (and both siRNAs in the case of *SLC30A10*) reduced endogenous transcript levels of *SLC30A5* and *CBWD* genes studied, which may indicate a role for the ZNF658 in stabilizing the mRNA levels

of its target genes in addition to mediating the transcriptional response to zinc, or may reflect that ZNF658 is required for basal transcription of its target genes as shown for some transcription factors.

**In chapter five**, we consider the likely role of the human *CBWD* gene products in metal homeostasis. As well as responding to zinc, *CBWD* genes also responded to other metals including copper, nickel and cobalt, suggesting a more general role in metal homeostasis. A role for *CBWD* protein in buffering zinc is suggested based on the observation that cells overexpressing the recombinant protein could better tolerate zinc restriction and excess compared with control cells. *CBWD* proteins appear to affect the cellular distribution of zinc, as shown by a less diffuse and more punctate pattern distribution of zinc fluorophore FluoZin-3 in cells that expressed the recombinant protein. These findings are consistent with *CBWD* having a function in zinc homeostasis, which remains to be understood.

Preliminary evidence suggesting the role of zinc in promoting cellular senescence is documented in **chapter six**. In addition, it is reported that the senescent phenotype features an increase in ZNF658 expression and a reduction in the expression of (some of) its target genes. In particular the ZNF658/ZnT10 mRNA ratio showed a tight correlation with expression of the senescence marker p16, and thus is a possible additional biomarker of cellular senescence worthy of further investigation.

## **7.2 Conclusion**

In conclusion, results from this research have made significant contributions towards advancing the understanding of molecular mechanisms that underlie cellular homeostatic control in response to fluctuation in zinc availability through identification of a novel transcriptional regulatory protein, ZNF658. Although a transcription factor with the primary role of gene repression under excess zinc has been identified in the fission yeast

*Schizosaccharomyces pombe*, this study reports the first primarily repressive zinc-responsive transcription factor in the mammalian cell. Preliminary observations suggest that ZNF658 and its expression relative to its gene targets, in particular *SLC30A10*, may be a biomarker of cellular senescence.

### **7.3 Recommendations for further work**

- The presence of the ZTRE in many candidate genes, some of which include heat shock proteins, may reflect wider roles for ZTRE-dependent gene regulation in mammals and thus merits further investigation for example by work based on measurement of the responses to zinc of specific transcript levels or using promoter-reporter constructs under conditions when ZNF658 expression is manipulated, analogous to the work on *SLC30A5*, *SLC30A10* and *CBWD* presented in this thesis.
- Further work is needed to identify the specific sub-cellular location for CBWD proteins for example by immunofluorescence using trackers that are targeted at specific cellular compartments. This method would give insight into the specific location within the cell in which CBWD may influence zinc uptake/efflux/sequestration.
- The findings that *CBWD* transcript levels were altered by metals other than zinc, suggest that ZNF658 acting at the ZTRE may play important roles in a homeostatic response to metals additional to zinc, which should be investigated. Approaches could include determining if CBWD overexpression affect cell tolerance to extreme concentrations of these additional metals and investigate how CBWD overexpression affects the intracellular distribution.
- To gain more insight into the function of CBWD proteins, future work should identify CBWD binding partners through approaches including co-immunoprecipitation

coupled with mass spectrometry. In addition, EMSA could be employed to study the effect of methylation of the CpG sites around *CBWD ZTRE* on the binding of ZNF658.

- Our results using site-directed mutagenesis and EMSA mapped the ZNF658 DNA binding domain to the carboxyl-terminal 135 amino acids, which comprises the zinc fingers 12 -15. Further research should identify which of the finger (s) is/are most important in zinc sensing and/or binding by sequential individual knockout.
- To gain insight into the metalloregulatory function of ZNF658, biophysical techniques such as isothermal titration calorimetry (ITC) could be employed to measure the strength of zinc binding using purified recombinant zinc finger peptides comprising for example, zinc finger pairs from the putative ZNF658 DNA-binding domain. The affinity of ZNF658 to metals other than zinc to ZNF658, could be tested by using ITC also and/or NMR spectroscopy.
- The mechanism behind the putative dual roles of ZNF658 in mediating transcriptional repression in response to zinc and stabilising transcripts of its target genes and/or being a requirement for basal transcription of its gene targets should be explored. Approaches could include measurement of mRNA turnover/degradation (mRNA steady-state-expression) by RT-PCR after blocking transcription using actinomycin D in cells expressing wild type ZNF658 compared with cells in which the expression ZNF658 has been manipulated.
- Better understanding of the global role of ZNF658 in gene regulation may be obtained if the full complement of the genes regulated by this transcription factor is identified, for example through chromatin immunoprecipitation followed by sequencing (ChIP-seq). Alternatively, more precise and effective approaches for gene knockdown, such as the CRISPR/CAS9 system, could be employed to manipulate the expression of

ZNF658 for downstream functional studies on the response to zinc of ZNF658 gene targets.

## 7.4 References

- ACKLAND, M. L., ZOU, L., FREESTONE, D., VAN DE WAASENBURG, S. & MICHALCZYK, A. A. 2007. Diesel exhaust particulate matter induces multinucleate cells and zinc transporter-dependent apoptosis in human airway cells. *Immunology and cell biology*, 85, 617-622.
- AGGARWAL, R., SENTZ, J. & MILLER, M. A. 2007. Role of zinc administration in prevention of childhood diarrhea and respiratory illnesses: a meta-analysis. *Pediatrics*, 119, 1120-1130.
- ALCORTA, D. A., XIONG, Y., PHELPS, D., HANNON, G., BEACH, D. & BARRETT, J. C. 1996. Involvement of the cyclin-dependent kinase inhibitor p16 (INK4a) in replicative senescence of normal human fibroblasts. *Proceedings of the National Academy of Sciences*, 93, 13742-13747.
- ALLEN, J. I., KAY, N. E. & MCCLAIN, C. J. 1981. Severe zinc deficiency in humans: association with a reversible T-lymphocyte dysfunction. *Annals of internal medicine*, 95, 154-157.
- ALWAN, A. 2011. *Global status report on noncommunicable diseases 2010*, World Health Organization.
- ANANDA, S. P. 2003. Zinc deficiency. *BMJ*, 326, 409-410.
- ANDREINI, C., BANCI, L., BERTINI, I. & ROSATO, A. 2005. Counting the Zinc-Proteins Encoded in the Human Genome. *Journal of Proteome Research*, 5, 196-201.
- ANDREINI, C., BERTINI, I. & ROSATO, A. 2009. Metalloproteomes: A Bioinformatic Approach. *Accounts of Chemical Research*, 42, 1471-1479.
- ANDREW NGUYENA, ZHANG JINGB, PAUL S MAHONEYA, RODNEY DAVIS, SURESH C SIKKAA, KRISHNA C AGRAWALC & ABDEL-MAGEEDA, A. B. 2000. In vivo gene expression profile analysis of metallothionein in renal cell carcinoma. *Cancer Letters*, 160, 133-140.
- ANDREWS, G. K. 2001. Cellular zinc sensors: MTF-1 regulation of gene expression. *BioMetals* 14, 223-237.
- ANDREWS, G. K., WANG, H., DEY, S. K. & PALMITER, R. D. 2004. Mouse zinc transporter 1 gene provides an essential function during early embryonic development. *genesis*, 40, 74-81.
- ASSUNÇÃO, A. G. L., HERRERO, E., LIN, Y.-F., HUETTEL, B., TALUKDAR, S., SMACZNIAK, C., IMMINK, R. G. H., VAN ELDIK, M., FIERS, M., SCHAT, H. & AARTS, M. G. M. 2010. Arabidopsis thaliana transcription factors bZIP19 and bZIP23 regulate the adaptation to zinc deficiency. *Proceedings of the National Academy of Sciences*, 107, 10296-10301.

- AUGUSTIN, R., LICHTENTHALER, S. F., GREEFF, M., HANSEN, J., WURST, W. & TRÜMBACH, D. 2011. Bioinformatics Identification of Modules of Transcription Factor Binding Sites in Alzheimer's Disease-Related Genes by In Silico Promoter Analysis and Microarrays. *International Journal of Alzheimer's Disease*, 2011, 13.
- BA, L. A., DOERING, M., BURKHOLZ, T. & JACOB, C. 2009. Metal trafficking: from maintaining the metal homeostasis to future drug design. *Metallomics*, 1, 292-311.
- BEAUSÉJOUR, C. M., KRTOLICA, A., GALIMI, F., NARITA, M., LOWE, S. W., YASWEN, P. & CAMPISI, J. 2003. Reversal of human cellular senescence: roles of the p53 and p16 pathways. *The EMBO journal*, 22, 4212-4222.
- BEGUM, N. A., KOBAYASHI, M., MORIWAKI, Y., MATSUMOTO, M., TOYOSHIMA, K. & SEYA, T. 2002. Mycobacterium bovis BCG Cell Wall and Lipopolysaccharide Induce a Novel Gene, BIGM103, Encoding a 7-TM Protein: Identification of a New Protein Family Having Zn-Transporter and Zn-Metalloprotease Signatures. *Genomics*, 80, 630-645.
- BEIGHTON, P., PAEPE, A. D., STEINMANN, B., TSIPOURAS, P. & WENSTRUP, R. J. 1998. Ehlers-Danlos syndromes: revised nosology, Villefranche, 1997. *American journal of medical genetics*, 77, 31-37.
- BEKER AYDEMIR, T., CHANG, S.-M., GUTHRIE, G. J., MAKI, A. B., RYU, M.-S., KARABIYIK, A. & COUSINS, R. J. 2012. Zinc Transporter ZIP14 Functions in Hepatic Zinc, Iron and Glucose Homeostasis during the Innate Immune Response (Endotoxemia). *PLoS ONE*, 7, e48679.
- BELL, S. G. & VALLEE, B. L. 2009. The metallothionein/thionein system: an oxidoreductive metabolic zinc link. *ChemBioChem*, 10, 55-62.
- BELLEFROID, E. J., PONCELET, D. A., LECOCQ, P. J., REVELANT, O. & MARTIAL, J. A. 1991. The evolutionarily conserved Kruppel-associated box domain defines a subfamily of eukaryotic multifingered proteins. *Proc Natl Acad Sci USA*, 88, 3608 - 3612.
- BERG, J. M. & SHI, Y. 1996. The Galvanization of Biology: A Growing Appreciation for the Roles of Zinc. *Science*, 271, 1081-1085.
- BESECKER, B., BAO, S., BOHACOVA, B., PAPP, A., SADEE, W. & KNOELL, D. L. 2008. The human zinc transporter SLC39A8 (Zip8) is critical in zinc-mediated cytoprotection in lung epithelia. *American Journal of Physiology-Lung Cellular and Molecular Physiology*, 294, L1127-L1136.
- BEYER, N., COULSON, D., HEGGARTY, S., RAVID, R., IRVINE, G., HELLEMANS, J. & JOHNSTON, J. 2009. ZnT3 mRNA levels are reduced in Alzheimer's disease post-mortem brain. *Molecular Neurodegeneration*, 4, 1-10.
- BEYERSMANN, D. & HAASE, H. 2001. Functions of zinc in signaling, proliferation and differentiation of mammalian cells. *BioMetals*, 14, 331-341.

- BIANCHI-SMIRAGLIA, A. 2012. Controversial aspects of oncogene-induced senescence. *Cell Cycle*, 11, 4147-4151.
- BIN, B.-H., FUKADA, T., HOSAKA, T., YAMASAKI, S., OHASHI, W., HOJYO, S., MIYAI, T., NISHIDA, K., YOKOYAMA, S. & HIRANO, T. 2011. Biochemical Characterization of Human ZIP13 Protein A HOMO-DIMERIZED ZINC TRANSPORTER INVOLVED IN THE SPONDYLOCHEIRO DYSPLASTIC EHLERS-DANLOS SYNDROME. *Journal of Biological Chemistry*, 286, 40255-40265.
- BIRD, A., EVANS-GALEA, M. V., BLANKMAN, E., ZHAO, H., LUO, H., WINGE, D. R. & EIDE, D. J. 2000. Mapping the DNA binding domain of the Zap1 zinc-responsive transcriptional activator. *Journal of Biological Chemistry*, 275, 16160-16166.
- BIRD, A. J., BLANKMAN, E., STILLMAN, D. J., EIDE, D. J. & WINGE, D. R. 2004. The Zap1 transcriptional activator also acts as a repressor by binding downstream of the TATA box in ZRT2. *The EMBO journal*, 23, 1123-1132.
- BIRD, A. J., GORDON, M., EIDE, D. J. & WINGE, D. R. 2006. Repression of ADH1 and ADH3 during zinc deficiency by Zap1-induced intergenic RNA transcripts. *The EMBO journal*, 25, 5726-5734.
- BOGDEN, J. D. 2004. Influence of zinc on immunity in the elderly. *The journal of nutrition, health & aging*, 8, 48-54.
- BOSOMWORTH, H. J., ADLARD, P. A., FORD, D. & VALENTINE, R. A. 2013. Altered Expression of ZnT10 in Alzheimer's Disease Brain. *PloS one*, 8, e65475.
- BOSOMWORTH, H. J., THORNTON, J. K., CONEY WORTH, L. J., FORD, D. & VALENTINE, R. A. 2012. Efflux function, tissue-specific expression and intracellular trafficking of the Zn transporter ZnT10 indicate roles in adult Zn homeostasis. *Metallomics*, 4, 771-779.
- BROCKLEHURST, K. R., HOBMAN, J. L., LAWLEY, B., BLANK, L., MARSHALL, S. J., BROWN, N. L. & MORBY, A. P. 1999. ZntR is a Zn(II)-responsive MerR-like transcriptional regulator of zntA in Escherichia coli. *Molecular Microbiology*, 31, 893-902.
- BULTEAU, A.-L., O'NEILL, H. A., KENNEDY, M. C., IKEDA-SAITO, M., ISAYA, G. & SZWEDA, L. I. 2004. Frataxin acts as an iron chaperone protein to modulate mitochondrial aconitase activity. *Science*, 305, 242-245.
- BUSENLEHNER, L. S., PENNELLA, M. A. & GIEDROC, D. P. 2003. The SmtB/ArsR family of metalloregulatory transcriptional repressors: structural insights into prokaryotic metal resistance. *FEMS microbiology reviews*, 27, 131-143.
- CAMPISI, J. 2013. Aging, cellular senescence, and cancer. *Annual review of physiology*, 75, 685-705.
- CAMPISI, J. & DI FAGAGNA, F. D. A. 2007. Cellular senescence: when bad things happen to good cells. *Nature reviews Molecular cell biology*, 8, 729-740.

- CAO, J., BOBO, J. A., LIUZZI, J. P. & COUSINS, R. J. 2001. Effects of intracellular zinc depletion on metallothionein and ZIP2 transporter expression and apoptosis. *Journal of leukocyte biology*, 70, 559-566.
- CHIMIANTI, F., DEVERGNAS, S., FAVIER, A. & SEVE, M. 2004. Identification and cloning of a  $\beta$ -cell-specific zinc transporter, ZnT-8, localized into insulin secretory granules. *Diabetes*, 53, 2330-2337.
- CHOI, S. & BIRD, A. J. 2014. Zinc'ing sensibly: controlling zinc homeostasis at the transcriptional level. *Metallomics*.
- CHOUHDURY, R. & SRIVASTAVA, S. 2001. Zinc resistance mechanisms in bacteria. *Current Science*, 81, 768-775.
- CHOWANADISAI, W., LÖNNERDAL, B. & KELLEHER, S. L. 2006. Identification of a mutation in SLC30A2 (ZnT-2) in women with low milk zinc concentration that results in transient neonatal zinc deficiency. *Journal of Biological Chemistry*, 281, 39699-39707.
- CHOWANADISAI, W., LÖNNERDAL, B. & KELLEHER, S. L. 2008. Zip6 (LIV-1) regulates zinc uptake in neuroblastoma cells under resting but not depolarizing conditions. *Brain research*, 1199, 10-19.
- CHUNG, M. J., WALKER, P. A., BROWN, R. W. & HOGSTRAND, C. 2005. ZINC-mediated gene expression offers protection against H<sub>2</sub>O<sub>2</sub>-induced cytotoxicity. *Toxicology and Applied Pharmacology*, 205, 225-236.
- COLE, T. B., WENZEL, H. J., KAUFER, K. E., SCHWARTZKROIN, P. A. & PALMITER, R. D. 1999. Elimination of zinc from synaptic vesicles in the intact mouse brain by disruption of the ZnT3 gene. *Proceedings of the National Academy of Sciences*, 96, 1716-1721.
- CONEYWORTH, L. J., JACKSON, K. A., TYSON, J., BOSOMWORTH, H. J., VAN DER HAGEN, E., HANN, G. M., OGO, O. A., SWANN, D. C., MATHERS, J. C., VALENTINE, R. A. & FORD, D. 2012. Identification of the Human Zinc Transcriptional Regulatory Element (ZTRE). *Journal of Biological Chemistry*, 287, 36567-36581.
- COPPÉ, J.-P., DESPREZ, P.-Y., KRTOLICA, A. & CAMPISI, J. 2010. The senescence-associated secretory phenotype: the dark side of tumor suppression. *Annual Review of Pathological Mechanical Disease*, 5, 99-118.
- CORKINS, M. E., MAY, M., EHRENSBERGER, K. M., HU, Y.-M., LIU, Y.-H., BLOOR, S. D., JENKINS, B., RUNGE, K. W. & BIRD, A. J. 2013. Zinc finger protein Loz1 is required for zinc-responsive regulation of gene expression in fission yeast. *Proceedings of the National Academy of Sciences*, 110, 15371-15376.
- COSTELLO, L. C., LIU, Y., ZOU, J. & FRANKLIN, R. B. 1999. Evidence for a zinc uptake transporter in human prostate cancer cells which is regulated by prolactin and testosterone. *Journal of Biological Chemistry*, 274, 17499-17504.

- COUNTER, C. M., MEYERSON, M., EATON, E. N., ELLISEN, L. W., CADDLE, S. D., HABER, D. A. & WEINBERG, R. A. 1998. Telomerase activity is restored in human cells by ectopic expression of hTERT (hEST2), the catalytic subunit of telomerase. *Oncogene*, 16, 1217-1222.
- COUSINS, R. J., LIUZZI, J. P. & LICHTEN, L. A. 2006. Mammalian Zinc Transport, Trafficking, and Signals. *Journal of Biological Chemistry*, 281, 24085-24089.
- COYLE, P., PHILCOX, J. C., CAREY, L. C. & ROFE, A. M. 2002. Metallothionein: the multipurpose protein. *Cellular and Molecular Life Sciences CMLS*, 59, 627-647.
- CRAGG, R. A., CHRISTIE, G. R., PHILLIPS, S. R., RUSSI, R. M., KÜRY, S., MATHERS, J. C., TAYLOR, P. M. & FORD, D. 2002. A Novel Zinc-regulated Human Zinc Transporter, hZTL1, Is Localized to the Enterocyte Apical Membrane. *Journal of Biological Chemistry*, 277, 22789-22797.
- CRAGG, R. A., PHILLIPS, S. R., PIPER, J. M., VARMA, J. S., CAMPBELL, F. C., MATHERS, J. C. & FORD, D. 2005. Homeostatic regulation of zinc transporters in the human small intestine by dietary zinc supplementation. *Gut*, 54, 469-478.
- CROUZET, J., LEVY-SCHIL, S., CAMERON, B., CAUCHOIS, L., RIGAULT, S., ROUYEZ, M. C., BLANCHE, F., DEBUSSCHE, L. & THIBAUT, D. 1991. Nucleotide sequence and genetic analysis of a 13.1-kilobase-pair *Pseudomonas denitrificans* DNA fragment containing five cob genes and identification of structural genes encoding Cob(D)alamin adenosyltransferase, cobyrinic acid synthase, and bifunctional cobinamide kinase-cobinamide phosphate guanylyltransferase. *Journal of Bacteriology*, 173, 6074-6087.
- CROXFORD, T. P., MCCORMICK, N. H. & KELLEHER, S. L. 2011. Moderate zinc deficiency reduces testicular Zip6 and Zip10 abundance and impairs spermatogenesis in mice. *The Journal of nutrition*, 141, 359-365.
- DANG, D. T., PEVSNER, J. & YANG, V. W. 2000. The biology of the mammalian Krüppel-like family of transcription factors. *The international journal of biochemistry & cell biology*, 32, 1103-1121.
- DANNENBERG, J.-H., VAN ROSSUM, A., SCHUIJFF, L. & TE RIELE, H. 2000. Ablation of the retinoblastoma gene family deregulates G1 control causing immortalization and increased cell turnover under growth-restricting conditions. *Genes & development*, 14, 3051-3064.
- DANSCHER, G., WANG, Z., KIM, Y. K., KIM, S. J., SUN, Y. & JO, S. M. 2003. Immunocytochemical localization of zinc transporter 3 in the ependyma of the mouse spinal cord. *Neuroscience letters*, 342, 81-84.
- DAVIDSON, H. W., WENZLAU, J. M. & O'BRIEN, R. M. 2014. Zinc transporter 8 (ZnT8) and  $\beta$  cell function. *Trends in Endocrinology & Metabolism*, 25, 415-424.

- DENIRO, M. & AL-MOHANNA, F. A. 2012. Zinc transporter 8 (ZnT8) expression is reduced by ischemic insults: a potential therapeutic target to prevent ischemic retinopathy. *PloS one*, 7, e50360.
- DESOUKI, M. M., GERADTS, J., MILON, B., FRANKLIN, R. B. & COSTELLO, L. C. 2007. hZip2 and hZip3 zinc transporters are down regulated in human prostate adenocarcinomatous glands. *Molecular cancer*, 6, 37.
- DIMRI, G. P., ITAHANA, K., ACOSTA, M. & CAMPISI, J. 2000. Regulation of a senescence checkpoint response by the E2F1 transcription factor and p14ARF tumor suppressor. *Molecular and cellular biology*, 20, 273-285.
- DONG, X., KONG, C., ZHANG, Z., LIU, X., ZHAN, B., CHEN, Z. & SHI, D. hZIP1 that is down-regulated in clear cell renal cell carcinoma is negatively associated with the malignant potential of the tumor. *Urologic Oncology: Seminars and Original Investigations*, 2014. Elsevier.
- DUFNER-BEATTIE, J., HUANG, Z. L., GEISER, J., XU, W. & ANDREWS, G. K. 2006. Mouse ZIP1 and ZIP3 genes together are essential for adaptation to dietary zinc deficiency during pregnancy. *genesis*, 44, 239-251.
- DUFNER-BEATTIE, J., KUO, Y.-M., GITSCHIER, J. & ANDREWS, G. K. 2004. The Adaptive Response to Dietary Zinc in Mice Involves the Differential Cellular Localization and Zinc Regulation of the Zinc Transporters ZIP4 and ZIP5. *Journal of Biological Chemistry*, 279, 49082-49090.
- DUFNER-BEATTIE, J., LANGMADE, S. J., WANG, F., EIDE, D. & ANDREWS, G. K. 2003a. Structure, function, and regulation of a subfamily of mouse zinc transporter genes. *Journal of Biological Chemistry*, 278, 50142-50150.
- DUFNER-BEATTIE, J., WANG, F., KUO, Y.-M., GITSCHIER, J., EIDE, D. & ANDREWS, G. K. 2003b. The Acrodermatitis Enteropathica Gene ZIP4 Encodes a Tissue-specific, Zinc-regulated Zinc Transporter in Mice. *Journal of Biological Chemistry*, 278, 33474-33481.
- DUFNER-BEATTIE, J., WEAVER, B. P., GEISER, J., BILGEN, M., LARSON, M., XU, W. & ANDREWS, G. K. 2007. The mouse acrodermatitis enteropathica gene Slc39a4 (Zip4) is essential for early development and heterozygosity causes hypersensitivity to zinc deficiency. *Human molecular genetics*, 16, 1391-1399.
- EBISCH, I. M. W., THOMAS, C. M. G., PETERS, W. H. M., BRAAT, D. D. M. & STEEGERS-THEUNISSEN, R. P. M. 2007. The importance of folate, zinc and antioxidants in the pathogenesis and prevention of subfertility. *Human Reproduction Update*, 13, 163-174.
- EHRENSBERGER, K. M., CORKINS, M. E., CHOI, S. & BIRD, A. J. 2014. The Double Zinc Finger Domain and Adjacent Accessory Domain from the Transcription Factor Loss of Zinc Sensing 1 (Loz1) are Necessary for DNA Binding and Zinc Sensing. *Journal of Biological Chemistry*.

- EIDE, D. J. 2004. The SLC39 family of metal ion transporters. *Pflügers Archiv*, 447, 796-800.
- EIDE, D. J. 2009. Homeostatic and Adaptive Responses to Zinc Deficiency in *Saccharomyces cerevisiae*. *Journal of Biological Chemistry*, 284, 18565-18569.
- ELLIS, C. D., MACDIARMID, C. W. & EIDE, D. J. 2005. Heteromeric Protein Complexes Mediate Zinc Transport into the Secretory Pathway of Eukaryotic Cells. *Journal of Biological Chemistry*, 280, 28811-28818.
- ENG, B. H., GUERINOT, M. L., EIDE, D. & SAIER JR, M. H. 1998. Sequence analyses and phylogenetic characterization of the ZIP family of metal ion transport proteins. *The Journal of membrane biology*, 166, 1-7.
- EVANS, J. R. 2006. Antioxidant vitamin and mineral supplements for slowing the progression of age-related macular degeneration. *Cochrane Database Syst Rev*, 2.
- FAIRWEATHER-TAIT, S. J., HARVEY, L. J. & FORD, D. 2008. Does ageing affect zinc homeostasis and dietary requirements? *Experimental Gerontology*, 43, 382-388.
- FAN, Y., NEWMAN, T., LINARDOPOULOU, E. & TRASK, B. J. 2002. Gene content and function of the ancestral chromosome fusion site in human chromosome 2q13–2q14. 1 and paralogous regions. *Genome Research*, 12, 1663-1672.
- FERBEYRE, G., DE STANCHINA, E., LIN, A. W., QUERIDO, E., MCCURRACH, M. E., HANNON, G. J. & LOWE, S. W. 2002. Oncogenic ras and p53 cooperate to induce cellular senescence. *Molecular and cellular biology*, 22, 3497-3508.
- FIELD, L. S., LUK, E. & CULOTTA, V. C. 2002. Copper Chaperones: Personal Escorts for Metal Ions. *Journal of Bioenergetics and Biomembranes*, 34, 373-379.
- FISCHER, B. M., WONG, J. K., DEGAN, S., KUMMARAPURUGU, A. B., ZHENG, S., HARIDASS, P. & VOYNOW, J. A. 2013. Increased expression of senescence markers in cystic fibrosis airways. *American Journal of Physiology-Lung Cellular and Molecular Physiology*, 304, L394-L400.
- FRANKLIN, R., FENG, P., MILON, B., DESOUKI, M., SINGH, K., KAJDACSZY-BALLA, A., BAGASRA, O. & COSTELLO, L. 2005. hZIP1 zinc uptake transporter down regulation and zinc depletion in prostate cancer. *Molecular Cancer*, 4, 32.
- FRANKLIN, R. B. 2011. Decreased zinc and downregulation of ZIP3 zinc uptake transporter in the development of pancreatic adenocarcinoma. *Cancer biology & therapy*, 12, 297-303.
- FRANKLIN, R. B., MA, J., ZOU, J., GUAN, Z., KUKOYI, B. I., FENG, P. & COSTELLO, L. C. 2003. Human ZIP1 is a major zinc uptake transporter for the accumulation of zinc in prostate cells. *Journal of Inorganic Biochemistry*, 96, 435-442.
- FREDENBURGH, J. C., LESLIE, B. A., STAFFORD, A. R., LIM, T., CHAN, H. H. & WEITZ, J. I. 2013. Zn<sup>2+</sup> Mediates High Affinity Binding of Heparin to the  $\alpha$ C Domain of Fibrinogen. *Journal of Biological Chemistry*, 288, 29394-29402.

- FREY, A. G., BIRD, A. J., EVANS-GALEA, M. V., BLANKMAN, E., WINGE, D. R. & EIDE, D. J. 2011. Zinc-Regulated DNA Binding of the Yeast Zap1 Zinc-Responsive Activator. *PLoS ONE*, 6, e22535.
- FRIETZE, S., LAN, X., JIN, V. X. & FARNHAM, P. J. 2010. Genomic Targets of the KRAB and SCAN Domain-containing Zinc Finger Protein 263. *Journal of Biological Chemistry*, 285, 1393-1403.
- FUJISHIRO, H., YANO, Y., TAKADA, Y., TANIHARA, M. & HIMENO, S. 2012. Roles of ZIP8, ZIP14, and DMT1 in transport of cadmium and manganese in mouse kidney proximal tubule cells. *Metallomics*, 4, 700-708.
- FUJISHIRO, H., YOSHIDA, M., NAKANO, Y. & HIMENO, S. 2014. Interleukin-6 enhances manganese accumulation in SH-SY5Y cells: implications of the up-regulation of ZIP14 and the down-regulation of ZnT10. *Metallomics*, 6, 944-949.
- FUKADA, T., ASADA, Y., MISHIMA, K., SHIMODA, S. & SAITO, I. 2011. Slc39a13/Zip13: A Crucial Zinc Transporter Involved in Tooth Development and Inherited Disorders. *Journal of Oral Biosciences*, 53, 1-12.
- FUKADA, T., CIVIC, N., FURUICHI, T., SHIMODA, S., MISHIMA, K., HIGASHIYAMA, H., IDAIRA, Y., ASADA, Y., KITAMURA, H. & YAMASAKI, S. 2008. The zinc transporter SLC39A13/ZIP13 is required for connective tissue development; its involvement in BMP/TGF- $\beta$  signaling pathways. *PLoS One*, 3, e3642.
- FUKUNAKA, A., SUZUKI, T., KUROKAWA, Y., YAMAZAKI, T., FUJIWARA, N., ISHIHARA, K., MIGAKI, H., OKUMURA, K., MASUDA, S., YAMAGUCHI-IWAI, Y., NAGAO, M. & KAMBE, T. 2009. Demonstration and Characterization of the Heterodimerization of ZnT5 and ZnT6 in the Early Secretory Pathway. *Journal of Biological Chemistry*, 284, 30798-30806.
- FURUSAWA, T., MORIBE, H., KONDOH, H. & HIGASHI, Y. 1999. Identification of CtBP1 and CtBP2 as corepressors of zinc finger-homeodomain factor  $\delta$ EF1. *Molecular and cellular biology*, 19, 8581-8590.
- GABALLA, A. & HELMANN, J. D. 1998. Identification of a Zinc-Specific Metalloregulatory Protein, Zur, Controlling Zinc Transport Operons in *Bacillus subtilis*. *Journal of bacteriology*, 180, 5815-5821.
- GABALLA, A., WANG, T., YE, R. W. & HELMANN, J. D. 2002. Functional Analysis of the *Bacillus subtilis* Zur Regulon. *Journal of Bacteriology*, 184, 6508-6514.
- GABRIEL, S. E., MIYAGI, F., GABALLA, A. & HELMANN, J. D. 2008. Regulation of the *Bacillus subtilis* yciC Gene and Insights into the DNA-Binding Specificity of the Zinc-Sensing Metalloregulator Zur. *Journal of Bacteriology*, 190, 3482-3488.
- GAITHER, L. A. & EIDE, D. J. 2000. Functional Expression of the Human hZIP2 Zinc Transporter. *Journal of Biological Chemistry*, 275, 5560-5564.
- GAITHER, L. A. & EIDE, D. J. 2001a. Eukaryotic zinc transporters and their regulation. *BioMetals*, 14, 251-270.

- GAITHER, L. A. & EIDE, D. J. 2001b. The Human ZIP1 Transporter Mediates Zinc Uptake in Human K562 Erythroleukemia Cells. *Journal of Biological Chemistry*, 276, 22258-22264.
- GAO, H.-L., FENG, W.-Y., LI, X.-L., XU, H., HUANG, L. & WANG, Z.-Y. 2009. Golgi apparatus localization of ZNT7 in the mouse cerebellum.
- GEISER, J., DE LISLE, R. C. & ANDREWS, G. K. 2013. The Zinc Transporter Zip5 (Slc39a5) Regulates Intestinal Zinc Excretion and Protects the Pancreas against Zinc Toxicity. *PloS one*, 8, e82149.
- GETSIN, I., NALBANDIAN, G., YEE, D., VASTERMARK, A., PAPANODITIS, P., REDDY, V. & SAIER, M. 2013. Comparative genomics of transport proteins in developmental bacteria: *Myxococcus xanthus* and *Streptomyces coelicolor*. *BMC Microbiology*, 13, 279.
- GUERINOT, M. L. 2000. The ZIP family of metal transporters. *Biochimica et Biophysica Acta (BBA) - Biomembranes*, 1465, 190-198.
- GÜNTHER, V., LINDERT, U. & SCHAFFNER, W. 2012. The taste of heavy metals: Gene regulation by MTF-1. *Biochimica et Biophysica Acta (BBA) - Molecular Cell Research*, 1823, 1416-1425.
- GUSTIN, J., ZANIS, M. & SALT, D. 2011. Structure and evolution of the plant cation diffusion facilitator family of ion transporters. *BMC Evolutionary Biology*, 11, 76.
- HA, N., HELLAUER, K. & TURCOTTE, B. 1996. Mutations in Target DNA Elements of Yeast HAP1 Modulate Its Transcriptional Activity without Affecting DNA Binding. *Nucleic Acids Research*, 24, 1453-1459.
- HAAS, C., RODIONOV, D., KROPAT, J., MALASARN, D., MERCHANT, S. & DE CRECY-LAGARD, V. 2009. A subset of the diverse COG0523 family of putative metal chaperones is linked to zinc homeostasis in all kingdoms of life. *BMC Genomics*, 10, 470.
- HANTKE, K. 2001. Bacterial zinc transporters and regulators. *BioMetals*, 14, 239-249.
- HASSAN, H. A., NETCHVOLODOFF, C. & RAUFMAN, J.-P. 2000. Zinc-induced copper deficiency in a coin swallower. *The American Journal of Gastroenterology*, 95, 2975-2977.
- HASTY, P., SHARP, Z. D., CURIEL, T. J. & CAMPISI, J. 2013. mTORC1 and p53. *Cell Cycle*, 12, 20-25.
- HEUCHEL, R., RADTKE, F., GEORGIEV, O., STARK, G., AGUET, M. & SCHAFFNER, W. 1994. The transcription factor MTF-1 is essential for basal and heavy metal-induced metallothionein gene expression. *The EMBO journal*, 13, 2870.
- HIMENO, S., YANAGIYA, T. & FUJISHIRO, H. 2009. The role of zinc transporters in cadmium and manganese transport in mammalian cells. *Biochimie*, 91, 1218-1222.

- HOOVERS, J. M. N., MANNENS, M., JOHN, R., BLIEK, J., VAN HEYNINGEN, V., PORTEOUS, D., LESCHOT, N. J., WESTERVELD, A. & LITTLE, P. F. R. 1992. High-resolution localization of 69 potential human zinc finger protein genes: a number are clustered. *Genomics*, 12, 254-263.
- HUANG, L. & GITSCHIER, J. 1997. A novel gene involved in zinc transport is deficient in the lethal milk mouse. *Nature genetics*, 17, 292-297.
- HUANG, L., KIRSCHKE, C. P. & GITSCHIER, J. 2002. Functional Characterization of a Novel Mammalian Zinc Transporter, ZnT6. *Journal of Biological Chemistry*, 277, 26389-26395.
- HUANG, L., KIRSCHKE, C. P., ZHANG, Y. & YU, Y. Y. 2005. The ZIP7 Gene (Slc39a7) Encodes a Zinc Transporter Involved in Zinc Homeostasis of the Golgi Apparatus. *Journal of Biological Chemistry*, 280, 15456-15463.
- HUANG, L. & TEPAAMORNDECH, S. 2013. The SLC30 family of zinc transporters—A review of current understanding of their biological and pathophysiological roles. *Molecular aspects of medicine*, 34, 548-560.
- HUANG, L., YAN, M. & KIRSCHKE, C. P. 2010. Over-expression of ZnT7 increases insulin synthesis and secretion in pancreatic  $\beta$ -cells by promoting insulin gene transcription. *Experimental Cell Research*, 316, 2630-2643.
- HUANG, Z. L., DUFNER-BEATTIE, J. & ANDREWS, G. K. 2006. Expression and regulation of SLC39A family zinc transporters in the developing mouse intestine. *Developmental Biology*, 295, 571-579.
- IBS, K.-H. & RINK, L. 2003. Zinc-Altered Immune Function. *The Journal of Nutrition*, 133, 1452S-1456S.
- IGUCHI, K., USUI, S., INOUE, T., SUGIMURA, Y., TATEMATSU, M. & HIRANO, K. 2002. High-Level Expression of Zinc Transporter-2 in the Rat Lateral and Dorsal Prostate. *Journal of andrology*, 23, 819-824.
- INOUE, K., MATSUDA, K., ITOH, M., KAWAGUCHI, H., TOMOIKE, H., AOYAGI, T., NAGAI, R., HORI, M., NAKAMURA, Y. & TANAKA, T. 2002. Osteopenia and male-specific sudden cardiac death in mice lacking a zinc transporter gene, Znt5. *Human molecular genetics*, 11, 1775-1784.
- ISHIHARA, K., YAMAZAKI, T., ISHIDA, Y., SUZUKI, T., ODA, K., NAGAO, M., YAMAGUCHI-IWAI, Y. & KAMBE, T. 2006. Zinc transport complexes contribute to the homeostatic maintenance of secretory pathway function in vertebrate cells. *Journal of Biological Chemistry*, 281, 17743-17750.
- IUCHI, S. 2001. Three classes of C2H2 zinc finger proteins. *Cellular and Molecular Life Sciences CMLS*, 58, 625-635.
- JACKSON, K. A., HELSTON, R. M., MCKAY, J. A., O'NEILL, E. D., MATHERS, J. C. & FORD, D. 2007. Splice variants of the human zinc transporter ZnT5 (SLC30A5) are

- differentially localized and regulated by zinc through transcription and mRNA stability. *Journal of Biological Chemistry*, 282, 10423-10431.
- JACKSON, K. A., VALENTINE, R. A., CONEYWORTH, L. J., MATHERS, J. C. & FORD, D. 2008. Mechanisms of mammalian zinc-regulated gene expression. *Biochemical Society Transactions*, 36, 1262–1266.
- JACKSON, K. A., VALENTINE, R. A., MCKAY, J. A., SWAN, D. C., MATHERS, J. C. & FORD, D. 2009. Analysis of differential gene-regulatory responses to zinc in human intestinal and placental cell lines. *British journal of nutrition*, 101, 1474-1483.
- JAKOBY, M., WEISSHAAR, B., DRÖGE-LASER, W., VICENTE-CARBAJOSA, J., TIEDEMANN, J., KROJ, T. & PARCY, F. 2002. bZIP transcription factors in Arabidopsis. *Trends in Plant Science*, 7, 106-111.
- JEONG, J., WALKER, J. M., WANG, F., PARK, J. G., PALMER, A. E., GIUNTA, C., ROHRBACH, M., STEINMANN, B. & EIDE, D. J. 2012. Promotion of vesicular zinc efflux by ZIP13 and its implications for spondylocheiro dysplastic Ehlers–Danlos syndrome. *Proceedings of the National Academy of Sciences*, 109, E3530-E3538.
- JIANG, H., DANIELS, P. J. & ANDREWS, G. K. 2003. Putative zinc-sensing zinc fingers of metal-response element-binding transcription factor-1 stabilize a metal-dependent chromatin complex on the endogenous metallothionein-I promoter. *Journal of Biological Chemistry*, 278, 30394-30402.
- KACHEROVSKY, N., TACHIBANA, C., AMOS, E., FOX III, D. & YOUNG, E. T. 2008. Promoter binding by the Adr1 transcriptional activator may be regulated by phosphorylation in the DNA-binding region. *PLoS One*, 3, e3213.
- KAGARA, N., TANAKA, N., NOGUCHI, S. & HIRANO, T. 2007. Zinc and its transporter ZIP10 are involved in invasive behavior of breast cancer cells. *Cancer science*, 98, 692-697.
- KALER, P. & PRASAD, R. 2007. Molecular cloning and functional characterization of novel zinc transporter rZip10 (Slc39a10) involved in zinc uptake across rat renal brush-border membrane. *American Journal of Physiology-Renal Physiology*, 61, F217.
- KAMBE, T., NARITA, H., YAMAGUCHI-IWAI, Y., HIROSE, J., AMANO, T., SUGIURA, N., SASAKI, R., MORI, K., IWANAGA, T. & NAGAO, M. 2002. Cloning and characterization of a novel mammalian zinc transporter, zinc transporter 5, abundantly expressed in pancreatic  $\beta$  cells. *Journal of Biological Chemistry*, 277, 19049-19055.
- KAMBE, T., WEAVER, B. P. & ANDREWS, G. K. 2008 The Genetics of Essential Metal Homeostasis During Development. *Genesis*, 46, 214–228.
- KAMBE, T., YAMAGUCHI-IWAI, Y., SASAKI, R. & NAGAO, M. 2004. Overview of mammalian zinc transporters. *Cellular and Molecular Life Sciences CMLS*, 61, 49-68.

- KEL, A. E., GÖBLING, E., REUTER, I., CHEREMUSHKIN, E., KEL-MARGOULIS, O. V. & WINGENDER, E. 2003. MATCHM: a tool for searching transcription factor binding sites in DNA sequences. *Nucleic Acids Research*, 31, 3576-3579.
- KELLEHER, S. L. & LÖNNERDAL, B. 2005. Zip3 plays a major role in zinc uptake into mammary epithelial cells and is regulated by prolactin. *American Journal of Physiology-Cell Physiology*, 288, C1042-C1047.
- KELLEHER, S. L., SEO, Y. A. & LOPEZ, V. 2009. Mammary gland zinc metabolism: regulation and dysregulation. *Genes & nutrition*, 4, 83-94.
- KELLEHER, S. L., VELASQUEZ, V., CROXFORD, T. P., MCCORMICK, N. H., LOPEZ, V. & MACDAVID, J. 2012a. Mapping the zinc-transporting system in mammary cells: Molecular analysis reveals a phenotype-dependent zinc-transporting network during lactation. *Journal of Cellular Physiology*, 227, 1761-1770.
- KELLEHER, S. L., VELASQUEZ, V., CROXFORD, T. P., MCCORMICK, N. H., LOPEZ, V. & MACDAVID, J. 2012b. Mapping the zinc-transporting system in mammary cells: Molecular analysis reveals a phenotype-dependent zinc-transporting network during lactation. *Journal of cellular physiology*, 227, 1761-1770.
- KIM, S.-C., KIM, Y.-S. & JETTEN, A. M. 2005. Krüppel-like zinc finger protein Gli-similar 2 (Glis2) represses transcription through interaction with C-terminal binding protein 1 (CtBP1). *Nucleic acids research*, 33, 6805-6815.
- KINDERMANN, B., DÖRING, F., FUCHS, D., PFAFFL, M. & DANIEL, H. 2005. Effects of increased cellular zinc levels on gene and protein expression in HT-29 cells. *Biometals*, 18, 243-253.
- KIRSCHKE, C. P. & HUANG, L. 2003. ZnT7, a novel mammalian zinc transporter, accumulates zinc in the Golgi apparatus. *Journal of Biological Chemistry*, 278, 4096-4102.
- KLAASSEN, C. D., LIU, J. & CHOUDHURI, S. 1999. Metallothionein: an intracellular protein to protect against cadmium toxicity. *Annual review of pharmacology and toxicology*, 39, 267-294.
- KOJIMA-YUASA, A., UMEDA, K., OHKITA, T., OPARE KENNEDY, D., NISHIGUCHI, S. & MATSUI-YUASA, I. 2005. Role of reactive oxygen species in zinc deficiency-induced hepatic stellate cell activation. *Free Radical Biology and Medicine*, 39, 631-640.
- KOVACIC, J. C., MORENO, P., NABEL, E. G., HACHINSKI, V. & FUSTER, V. 2011. Cellular Senescence, Vascular Disease, and Aging: Part 2 of a 2-Part Review: Clinical Vascular Disease in the Elderly. *Circulation*, 123, 1900-1910.
- KOVACS, G., MONTALBETTI, N., FRANZ, M.-C., GRAETER, S., SIMONIN, A. & HEDIGER, M. A. 2013. Human TRPV5 and TRPV6: Key players in cadmium and zinc toxicity. *Cell Calcium*, 54, 276-286.

- KREBS, N. F. 2000. Overview of zinc absorption and excretion in the human gastrointestinal tract. *The Journal of nutrition*, 130, 1374S-1377S.
- KREBS, N. F. & HAMBIDGE, K. M. 2001. Zinc metabolism and homeostasis: the application of tracer techniques to human zinc physiology. *BioMetals*, 14, 397-412.
- KUILMAN, T., MICHALOGLOU, C., MOOI, W. J. & PEEPER, D. S. 2010. The essence of senescence. *Genes & Development*, 24, 2463-2479.
- KUMAR, R. & PRASAD, R. 1999. Purification and characterization of a major zinc binding protein from renal brush border membrane of rat. *Biochimica et Biophysica Acta (BBA) - Biomembranes*, 1419, 23-32.
- KUMAR, R. & PRASAD, R. 2000. Functional characterization of purified zinc transporter from renal brush border membrane of rat. *Biochimica et Biophysica Acta (BBA) - Biomembranes*, 1509, 429-439.
- LANGMADE, S. J., RAVINDRA, R., DANIELS, P. J. & ANDREWS, G. K. 2000. The Transcription Factor MTF-1 Mediates Metal Regulation of the Mouse ZnT1 Gene. *Journal of Biological Chemistry*, 275, 34803-34809.
- LARSSON, L.-G. Oncogene-and tumor suppressor gene-mediated suppression of cellular senescence. *Seminars in cancer biology*, 2011. Elsevier, 367-376.
- LASRY, I., GOLAN, Y., BERMAN, B., AMRAM, N., GLASER, F. & ASSARAF, Y. G. 2014. In Situ Dimerization of Multiple Wild Type and Mutant Zinc Transporters in Live Cells Using Bimolecular Fluorescence Complementation. *Journal of Biological Chemistry*, 289, 7275-7292.
- LEE, J.-W. & HELMANN, J. D. 2006. Biochemical characterization of the structural Zn<sup>2+</sup> site in the Bacillus subtilis peroxide sensor PerR. *Journal of Biological Chemistry*, 281, 23567-23578.
- LEMAIRE, K., CHIMIANTI, F. & SCHUIT, F. 2012. Zinc transporters and their role in the pancreatic  $\beta$ -cell. *Journal of Diabetes Investigation*, 3, 202-211.
- LENGYEL, I., FLINN, J. M., PETŐ, T., LINKOUS, D. H., CANO, K., BIRD, A. C., LANZIROTTI, A., FREDERICKSON, C. J. & VAN KUIJK, F. J. G. M. 2007. High concentration of zinc in sub-retinal pigment epithelial deposits. *Experimental eye research*, 84, 772-780.
- LEUNG, K. W., LIU, M., XU, X., SEILER, M. J., BARNSTABLE, C. J. & TOMBRANTINK, J. 2008. Expression of ZnT and ZIP zinc transporters in the human RPE and their regulation by neurotrophic factors. *Investigative ophthalmology & visual science*, 49, 1221-1231.
- LI, S., ZHOU, X., HUANG, Y., ZHU, L., ZHANG, S., ZHAO, Y., GUO, J., CHEN, J. & CHEN, R. 2013. Identification and characterization of the zinc-regulated transporters, iron-regulated transporter-like protein (ZIP) gene family in maize. *BMC Plant Biology*, 13, 114.

- LI, Y., KIMURA, T., HUYCK, R. W., LAITY, J. H. & ANDREWS, G. K. 2008. Zinc-induced formation of a coactivator complex containing the zinc-sensing transcription factor MTF-1, p300/CBP, and Sp1. *Molecular and cellular biology*, 28, 4275-4284.
- LIANG, D., XIANG, L., YANG, M., ZHANG, X., GUO, B., CHEN, Y., YANG, L. & CAO, J. 2013. ZnT7 can protect MC3T3-E1 cells from oxidative stress-induced apoptosis via PI3K/Akt and MAPK/ERK signaling pathways. *Cellular Signalling*, 25, 1126-1135.
- LICHTEN, L. A. & COUSINS, R. J. 2009. Mammalian Zinc Transporters: Nutritional and Physiologic Regulation. *Annual Review of Nutrition*, 29, 153-176.
- LICHTEN, L. A., RYU, M.-S., GUO, L., EMBURY, J. & COUSINS, R. J. 2011. MTF-1-Mediated Repression of the Zinc Transporter *Zip10* Is Alleviated by Zinc Restriction. *PLoS ONE*, 6, e21526.
- LIN, Y., CHEN, Y., WANG, Y., YANG, J., ZHU, V. F., LIU, Y., CUI, X., CHEN, L., YAN, W., JIANG, T., HERGENROEDER, G. W., FLETCHER, S. A., LEVINE, J. M., KIM, D. H., TANDON, N., ZHU, J.-J. & LI, M. 2013. ZIP4 is a novel molecular marker for glioma. *Neuro-Oncology*, 15, 1008-1016.
- LIUZZI, J. P., BLANCHARD, R. K. & COUSINS, R. J. 2001. Differential regulation of zinc transporter 1, 2, and 4 mRNA expression by dietary zinc in rats. *The Journal of Nutrition*, 131, 46-52.
- LIUZZI, J. P., BOBO, J. A., CUI, L., MCMAHON, R. J. & COUSINS, R. J. 2003. Zinc transporters 1, 2 and 4 are differentially expressed and localized in rats during pregnancy and lactation. *The Journal of Nutrition*, 133, 342-351.
- LIUZZI, J. P., BOBO, J. A., LICHTEN, L. A., SAMUELSON, D. A. & COUSINS, R. J. 2004. Responsive transporter genes within the murine intestinal-pancreatic axis form a basis of zinc homeostasis. *Proceedings of the National Academy of Sciences of the United States of America*, 101, 14355-14360.
- LIUZZI, J. P. & COUSINS, R. J. 2004. Mammalian zinc transporters. *Annu. Rev. Nutr.*, 24, 151-172.
- LIUZZI, J. P., GUO, L., CHANG, S.-M. & COUSINS, R. J. 2009. Krüppel-like factor 4 regulates adaptive expression of the zinc transporter *Zip4* in mouse small intestine. *American Journal of Physiology-Gastrointestinal and Liver Physiology*, 296, G517-G523.
- LIVAK, K. J. & SCHMITTGEN, T. D. 2001. Analysis of Relative Gene Expression Data Using Real-Time Quantitative PCR and the  $2^{-\Delta\Delta CT}$  Method. *Methods*, 25, 402-408.
- LOOMAN, C., HELLMAN, L. & ÅBRINK, M. 2004. A novel Krüppel-associated box identified in a panel of mammalian zinc finger proteins. *Mammalian genome*, 15, 35-40.
- LOPEZ, V. & KELLEHER, S. 2009. Zinc transporter-2 (ZnT2) variants are localized to distinct subcellular compartments and functionally transport zinc. *Biochem. J*, 422, 43-52.

- LORENZ, P., KOCZAN, D. & THIESEN, H.-J. 2001. Transcriptional repression mediated by the KRAB domain of the human C2H2 zinc finger protein Kox1/ZNF10 does not require histone deacetylation. *Biological chemistry*, 382, 637-644.
- LUPO, A., CESARO, E., MONTANO, G., ZURLO, D., IZZO, P. & COSTANZO, P. 2013. KRAB-zinc finger proteins: a repressor family displaying multiple biological functions. *Current genomics*, 14, 268.
- LYNCH, C. J., PATSON, B. J., GOODMAN, S. A., TRAPOLSI, D. & KIMBALL, S. R. 2001. Zinc stimulates the activity of the insulin-and nutrient-regulated protein kinase mTOR. *American Journal of Physiology-Endocrinology And Metabolism*, 281, E25-E34.
- MA, Z., JACOBSEN, F. E. & GIEDROC, D. P. 2009. Coordination chemistry of bacterial metal transport and sensing. *Chemical reviews*, 109, 4644-4681.
- MACIAG, T., HOOVER, G. A., STEMERMAN, M. B. & WEINSTEIN, R. 1981. Serial propagation of human endothelial cells in vitro. *The Journal of cell biology*, 91, 420-426.
- MAEGAWA, S., HINKAL, G., KIM, H. S., SHEN, L., ZHANG, L., ZHANG, J., ZHANG, N., LIANG, S., DONEHOWER, L. A. & ISSA, J.-P. J. 2010. Widespread and tissue specific age-related DNA methylation changes in mice. *Genome Research*, 20, 332-340.
- MALAVOLTA, M., COSTARELLI, L., GIACCONI, R., PIACENZA, F., BASSO, A., PIERPAOLI, E., MARCHEGANI, F., CARDELLI, M., PROVINCIALI, M. & MOCCHEGIANI, E. 2014. Modulators of cellular senescence: mechanisms, promises, and challenges from in vitro studies with dietary bioactive compounds. *Nutrition Research*.
- MANCINI, D. N., SINGH, S. M., ARCHER, T. K. & RODENHISER, D. I. 1999. Site-specific DNA methylation in the neurofibromatosis (NF1) promoter interferes with binding of CREB and SP1 transcription factors. *Oncogene*, 18.
- MARET, W. 2005. Zinc coordination environments in proteins determine zinc functions. *Journal of Trace Elements in Medicine and Biology*, 19, 7-12.
- MARGOLIN, J. F., FRIEDMAN, J. R., MEYER, W. K., VISSING, H., THIESEN, H.-J. & RAUSCHER, F. J. 1994a. Krüppel-associated boxes are potent transcriptional repression domains. *Proceedings of the National Academy of Sciences*, 91, 4509-4513.
- MARGOLIN, J. F., FRIEDMAN, J. R., MEYER, W. K., VISSING, H., THIESEN, H. J. & RAUSCHER, F. J. 1994b. Krüppel-associated boxes are potent transcriptional repression domains. *Proceedings of the National Academy of Sciences*, 91, 4509-4513.
- MATHERS, C. D. & LONCAR, D. 2006. Projections of global mortality and burden of disease from 2002 to 2030. *PLoS medicine*, 3, e442.
- MATSUURA, W., YAMAZAKI, T., YAMAGUCHI-IWAI, Y., MASUDA, S., NAGAO, M., ANDREWS, G. K. & KAMBE, T. 2009. SLC39A9 (ZIP9) regulates zinc homeostasis

in the secretory pathway: characterization of the ZIP subfamily I protein in vertebrate cells. *Bioscience, biotechnology, and biochemistry*, 73, 1142-1148.

MCALEER, M. F. & TUAN, R. S. 2001. Metallothionein overexpression in human trophoblastic cells protects against cadmium-induced apoptosis. *In Vitro & Molecular Toxicology: A Journal of Basic and Applied Research*, 14, 25-42.

MCCALL, K. A., HUANG, C.-C. & FIERKE, C. A. 2000. Function and Mechanism of Zinc Metalloenzymes. *The Journal of Nutrition*, 130, 1437S-1446S.

MCCORMICK, N. H. & KELLEHER, S. L. 2012. ZnT4 provides zinc to zinc-dependent proteins in the trans-Golgi network critical for cell function and Zn export in mammary epithelial cells. *American Journal of Physiology-Cell Physiology*, 303, C291-C297.

MCELHANEY, J. E. & EFFROS, R. B. 2009. Immunosenescence: what does it mean to health outcomes in older adults? *Current opinion in immunology*, 21, 418-424.

MEERARANI, P., RAMADASS, P., TOBOREK, M., BAUER, H.-C., BAUER, H. & HENNIG, B. 2000. Zinc protects against apoptosis of endothelial cells induced by linoleic acid and tumor necrosis factor  $\alpha$ . *The American journal of clinical nutrition*, 71, 81-87.

MEHTA, A. J., JOSHI, P. C., FAN, X., BROWN, L. A. S., RITZENTHALER, J. D., ROMAN, J. & GUIDOT, D. M. 2011. Zinc Supplementation Restores PU.1 and Nrf2 Nuclear Binding in Alveolar Macrophages and Improves Redox Balance and Bacterial Clearance in the Lungs of Alcohol-Fed Rats. *Alcoholism: Clinical and Experimental Research*, 35, 1519-1528.

MEHUS, A. A., MUHONEN, W. W., GARRETT, S. H., SOMJI, S., SENS, D. A. & SHABB, J. B. 2014. Quantitation of Human Metallothionein Isoforms: A Family of Small, Highly Conserved, Cysteine-rich Proteins. *Molecular & Cellular Proteomics*.

MICHALCZYK, A. & ACKLAND, M. L. 2013. hZip1 (hSLC39A1) regulates zinc homeostasis in gut epithelial cells. *Genes & Nutrition*, 8, 475-486.

MILON, B., DHERMY, D., POUNTNEY, D., BOURGEOIS, M. & BEAUMONT, C. 2001. Differential subcellular localization of hZip1 in adherent and non-adherent cells. *FEBS Letters*, 507, 241-246.

MINAMINO, T., MIYAUCHI, H., YOSHIDA, T., ISHIDA, Y., YOSHIDA, H. & KOMURO, I. 2002. Endothelial Cell Senescence in Human Atherosclerosis: Role of Telomere in Endothelial Dysfunction. *Circulation*, 105, 1541-1544.

MIRZAYANS, R., ANDRAIS, B., SCOTT, A., PATERSON, M. C. & MURRAY, D. 2010. Single-cell analysis of p16INK4a and p21WAF1 expression suggests distinct mechanisms of senescence in normal human and Li-Fraumeni Syndrome fibroblasts. *Journal of Cellular Physiology*, 223, 57-67.

MOSSAD, S. B., MACKNIN, M. L., MENDENDORP, S. V. & MASON, P. 1996. Zinc Gluconate Lozenges for Treating the Common Cold: A Randomized, Double-Blind, Placebo-Controlled Study. *Annals of Internal Medicine*, 125, 81-88.

- MURGIA, C., VESPIGNANI, I., CERASE, J., NOBILI, F. & PEROZZI, G. 1999. Cloning, expression, and vesicular localization of zinc transporter Dri 27/ZnT4 in intestinal tissue and cells. *American Journal of Physiology-Gastrointestinal and Liver Physiology*, 277, G1231-G1239.
- MURPHY, B. J., KIMURA, T., SATO, B. G., SHI, Y. & ANDREWS, G. K. 2008. Metallothionein induction by hypoxia involves cooperative interactions between metal-responsive transcription factor-1 and hypoxia-inducible transcription factor-1 $\alpha$ . *Molecular Cancer Research*, 6, 483-490.
- MYERS, S. A., NIELD, A., CHEW, G.-S. & MYERS, M. A. 2013. The zinc transporter, slc39a7 (zip7) is implicated in glycaemic control in skeletal muscle cells. *PLoS one*, 8, e79316.
- NAM, H. & KNUTSON, M. D. 2012. Effect of dietary iron deficiency and overload on the expression of ZIP metal-ion transporters in rat liver. *Biometals*, 25, 115-124.
- NAPOLITANO, M., RUBIO, M. Á., SANTAMARÍA-GÓMEZ, J., OLMEDO-VERD, E., ROBINSON, N. J. & LUQUE, I. 2012. Characterization of the Response to Zinc Deficiency in the Cyanobacterium *Anabaena* sp. Strain PCC 7120. *Journal of Bacteriology*, 194, 2426-2436.
- NECELA, B. M. & CIDLOWSKI, J. A. 2004. Mechanisms of Glucocorticoid Receptor Action in Noninflammatory and Inflammatory Cells. *Proceedings of the American Thoracic Society*, 1, 239-246.
- NIELSEN, A. L., JØRGENSEN, P., LEROUGE, T., CERVIÑO, M., CHAMBON, P. & LOSSON, R. 2004. Nizp1, a novel multitype zinc finger protein that interacts with the NSD1 histone lysine methyltransferase through a unique C2HR motif. *Molecular and cellular biology*, 24, 5184-5196.
- NOH, H., PAIK, H., KIM, J. & CHUNG, J. 2014. The Alteration of Zinc Transporter Gene Expression Is Associated with Inflammatory Markers in Obese Women. *Biological Trace Element Research*, 158, 1-8.
- OGRUNC, M. & D'ADDA DI FAGAGNA, F. 2011. Never-ageing cellular senescence. *European Journal of Cancer*, 47, 1616-1622.
- OHANA, E., HOCH, E., KEASAR, C., KAMBE, T., YIFRACH, O., HERSHFINKEL, M. & SEKLER, I. 2009. Identification of the Zn<sup>2+</sup> Binding Site and Mode of Operation of a Mammalian Zn<sup>2+</sup> Transporter. *Journal of Biological Chemistry*, 284, 17677-17686.
- OVERBECK, S., UCIECHOWSKI, P., ACKLAND, M. L., FORD, D. & RINK, L. 2008. Intracellular zinc homeostasis in leukocyte subsets is regulated by different expression of zinc exporters ZnT-1 to ZnT-9. *Journal of leukocyte biology*, 83, 368-380.
- PALMITER, R. D., COLE, T. B. & FINDLEY, S. D. 1996a. ZnT-2, a mammalian protein that confers resistance to zinc by facilitating vesicular sequestration. *The EMBO journal*, 15, 1784.

- PALMITER, R. D., COLE, T. B., QUAIFFE, C. J. & FINDLEY, S. D. 1996b. ZnT-3, a putative transporter of zinc into synaptic vesicles. *Proceedings of the National Academy of Sciences*, 93, 14934-14939.
- PALMITER, R. D. & FINDLEY, S. D. 1995. Cloning and functional characterization of a mammalian zinc transporter that confers resistance to zinc. *The EMBO journal*, 14, 639.
- PATRUSHEV, N., SEIDEL-ROGOL, B. & SALAZAR, G. 2012. Angiotensin II requires zinc and downregulation of the zinc transporters ZnT3 and ZnT10 to induce senescence of vascular smooth muscle cells. *PloS one*, 7, e33211.
- PAWLIK, M.-C., HUBERT, K., JOSEPH, B., CLAUS, H., SCHOEN, C. & VOGEL, U. 2012. The zinc-responsive regulon of *Neisseria meningitidis* comprises 17 genes under control of a Zur element. *Journal of bacteriology*, 194, 6594-6603.
- PETERS, J. L., DUFNER-BEATTIE, J., XU, W., GEISER, J., LAHNER, B., SALT, D. E. & ANDREWS, G. K. 2007. Targeting of the mouse *Slc39a2* (*Zip2*) gene reveals highly cell-specific patterns of expression, and unique functions in zinc, iron, and calcium homeostasis. *genesis*, 45, 339-352.
- PINILLA-TENAS, J. J., SPARKMAN, B. K., SHAWKI, A., ILLING, A. C., MITCHELL, C. J., ZHAO, N., LIUZZI, J. P., COUSINS, R. J., KNUTSON, M. D. & MACKENZIE, B. 2011. *Zip14* is a complex broad-scope metal-ion transporter whose functional properties support roles in the cellular uptake of zinc and nontransferrin-bound iron. *American Journal of Physiology-Cell Physiology*, 301, C862-C871.
- POHL, E., HALLER, J. C., MIJOVILOVICH, A., MEYER-KLAUCKE, W., GARMAN, E. & VASIL, M. L. 2003. Architecture of a protein central to iron homeostasis: crystal structure and spectroscopic analysis of the ferric uptake regulator. *Molecular microbiology*, 47, 903-915.
- PRASAD, A. S. 1996. Zinc: The Biology and Therapeutics of an Ion. *Annals of Internal Medicine*, 125, 142-143.
- PRASAD, A. S. 2008. Zinc in human health: effect of zinc on immune cells. *Molecular medicine*, 14, 353.
- PRASAD, A. S. 2012. Discovery of human zinc deficiency: 50 years later. *Journal of Trace Elements in Medicine and Biology*, 26, 66-69.
- RAMIREZ, R. D., MORALES, C. P., HERBERT, B.-S., ROHDE, J. M., PASSONS, C., SHAY, J. W. & WRIGHT, W. E. 2001. Putative telomere-independent mechanisms of replicative aging reflect inadequate growth conditions. *Genes & development*, 15, 398-403.
- RANALDI, G., PEROZZI, G., TRUONG-TRAN, A., ZALEWSKI, P. & MURGIA, C. 2002. Intracellular distribution of labile Zn (II) and zinc transporter expression in kidney and MDCK cells. *American Journal of Physiology-Renal Physiology*, 283, F1365-F1375.
- REDENTI, S. & CHAPPELL, R. L. 2004. Localization of zinc transporter-3 (ZnT-3) in mouse retina. *Vision research*, 44, 3317-3321.

- RINK, L. 2000. Zinc and the immune system. *Proceedings of the Nutrition Society*, 59, 541-552.
- RINK, L. & HAASE, H. 2007. Zinc homeostasis and immunity. *Trends in Immunology*, 28, 1-4.
- RISHI, I., BAIDOURI, H., ABBASI, J. A., BULLARD-DILLARD, R., PESTANER, J. P., SKACEL, M., TUBBS, R. & BAGASRA, O. 2003. Prostate cancer in African American men is associated with downregulation of zinc transporters. *Applied Immunohistochemistry & Molecular Morphology*, 11, 253-260.
- RODEMS, S. M. & FRIESEN, P. D. 1995. Transcriptional enhancer activity of hr5 requires dual-palindrome half sites that mediate binding of a dimeric form of the baculovirus transregulator IE1. *Journal of virology*, 69, 5368-5375.
- RODIER, F. & CAMPISI, J. 2011. Four faces of cellular senescence. *The Journal of cell biology*, 192, 547-556.
- ROH, H. C., COLLIER, S., GUTHRIE, J., ROBERTSON, J. D. & KORNFELD, K. 2012. Lysosome-Related Organelles in Intestinal Cells Are a Zinc Storage Site in *C. elegans*. *Cell metabolism*, 15, 88-99.
- RUTTKAY-NEDECKY, B., NEJDL, L., GUMULEC, J., ZITKA, O., MASARIK, M., ECKSCHLAGER, T., STIBOROVA, M., ADAM, V. & KIZEK, R. 2013. The role of metallothionein in oxidative stress. *International journal of molecular sciences*, 14, 6044-6066.
- RYAN, R. F., SCHULTZ, D. C., AYYANATHAN, K., SINGH, P. B., FRIEDMAN, J. R., FREDER-ICKS, W. J. & RAUSCHER, F. J. 1999. KAP-1 corepressor protein interacts and colocalizes with heterochromatic and euchromatic HP1 proteins: a potential role for Kruppel-associated box-zinc finger proteins in heterochromatin-mediated gene silencing. *Mol Cell Biol*, 19, 4366 - 4378.
- RYU, M.-S., LICHTEN, L. A., LIUZZI, J. P. & COUSINS, R. J. 2008. Zinc Transporters ZnT1 (Slc30a1), Zip8 (Slc39a8), and Zip10 (Slc39a10) in Mouse Red Blood Cells Are Differentially Regulated during Erythroid Development and by Dietary Zinc Deficiency. *The Journal of Nutrition*, 138, 2076-2083.
- SALAZAR, G., FALCON-PEREZ, J. M., HARRISON, R. & FAUNDEZ, V. 2009. SLC30A3 (ZnT3) oligomerization by dityrosine bonds regulates its subcellular localization and metal transport capacity. *PLoS ONE*, 4, e5896.
- SALGUEIRO, M. J., ZUBILLAGA, M., LYSIONEK, A., CREMASCHI, G., GOLDMAN, C. G., CARO, R., DE PAOLI, T., HAGER, A., WEILL, R. & BOCCIO, J. 2000. Zinc status and immune system relationship. *Biological Trace Element Research*, 76, 193-205.
- SAPER, R. B. & RASH, R. 2009. Zinc: an essential micronutrient. *American family physician*, 79, 768.

- SENSI, S. L., TON-THAT, D., SULLIVAN, P. G., JONAS, E. A., GEE, K. R., KACZMAREK, L. K. & WEISS, J. H. 2003. Modulation of mitochondrial function by endogenous Zn<sup>2+</sup> pools. *Proceedings of the National Academy of Sciences*, 100, 6157-6162.
- SERRANO, M., LIN, A. W., MCCURRACH, M. E., BEACH, D. & LOWE, S. W. 1997. Oncogenic ras provokes premature cell senescence associated with accumulation of p53 and p16INK4a. *Cell*, 88, 593-602.
- SEVE, M., CHIMIANTI, F., DEVERGNAS, S. & FAVIER, A. 2004. In silico identification and expression of SLC30 family genes: an expressed sequence tag data mining strategy for the characterization of zinc transporters' tissue expression. *BMC genomics*, 5, 32.
- SHAN, H., ZHANG, S., LI, X., ZHAO, X., CHEN, X., JIN, B. & BAI, X. 2014. Valsartan ameliorates ageing-induced aorta degeneration via angiotensin II type 1 receptor-mediated ERK activity. *Journal of cellular and molecular medicine*.
- SHEN, H., QIN, H. & GUO, J. 2008. Cooperation of metallothionein and zinc transporters for regulating zinc homeostasis in human intestinal Caco-2 cells. *Nutrition Research*, 28, 406-413.
- SHEN, H., QIN, H. & GUO, J. 2009. Concordant correlation of LIV-1 and E-cadherin expression in human breast cancer cell MCF-7. *Molecular biology reports*, 36, 653-659.
- SHIN, J.-H., OH, S.-Y., KIM, S.-J. & ROE, J.-H. 2007. The Zinc-Responsive Regulator Zur Controls a Zinc Uptake System and Some Ribosomal Proteins in *Streptomyces coelicolor* A3(2). *Journal of Bacteriology*, 189, 4070-4077.
- SHIN, L.-J., LO, J.-C. & YEH, K.-C. 2012. Copper chaperone antioxidant protein1 is essential for copper homeostasis. *Plant physiology*, 159, 1099-1110.
- SHUSTERMAN, E., BEHARIER, O., LEVY, S., ZARIVACH, R., ETZION, Y., CAMPBELL, C. R., LEE, I.-H., OKABAYASHI, K., DINUDOM, A. & COOK, D. I. 2014. ZnT-1 extrudes zinc from mammalian cells functioning as a Zn<sup>2+</sup>/H<sup>+</sup> exchanger. *Metallomics*.
- SIM, D. L. C. & CHOW, V. T. K. 1999. The novel human HUEL (C4orf1) gene maps to chromosome 4p12-p13 and encodes a nuclear protein containing the nuclear receptor interaction motif. *Genomics*, 59, 224-233.
- SIM, D. L. C., YEO, W. M. & CHOW, V. T. K. 2002. The novel human HUEL (C4orf1) protein shares homology with the DNA-binding domain of the XPA DNA repair protein and displays nuclear translocation in a cell cycle-dependent manner. *The International Journal of Biochemistry & Cell Biology*, 34, 487-504.
- SLADEK, R., ROCHELEAU, G., RUNG, J., DINA, C., SHEN, L., SERRE, D., BOUTIN, P., VINCENT, D., BELISLE, A. & HADJADJ, S. 2007. A genome-wide association study identifies novel risk loci for type 2 diabetes. *Nature*, 445, 881-885.

- SMIDT, K., PEDERSEN, S. B., BROCK, B., SCHMITZ, O., FISHER, S., BENDIX, J., WOGENSEN, L. & RUNGBY, J. 2007. Zinc-transporter genes in human visceral and subcutaneous adipocytes: lean versus obese. *Molecular and cellular endocrinology*, 264, 68-73.
- SMITH, J. L., XIONG, S., MARKESBERY, W. R. & LOVELL, M. A. 2006. Altered expression of zinc transporters-4 and -6 in mild cognitive impairment, early and late Alzheimer's disease brain. *Neuroscience*, 140, 879-888.
- STEIGER, J. L. & RUSSEK, S. J. 2004. GABAA receptors: building the bridge between subunit mRNAs, their promoters, and cognate transcription factors. *Pharmacology & Therapeutics*, 101, 259-281.
- STOYTICHEVA, Z. R., VLADIMIROV, V., DOUET, V., STOYCHEV, I. & BERRY, M. J. 2010. Metal transcription factor-1 regulation via MREs in the transcribed regions of selenoprotein H and other metal-responsive genes. *Biochimica et Biophysica Acta (BBA) - General Subjects*, 1800, 416-424.
- SUBRAMANIAM, N., TREUTER, E. & OKRET, S. 1999. Receptor Interacting Protein RIP140 Inhibits Both Positive and Negative Gene Regulation by Glucocorticoids. *Journal of Biological Chemistry*, 274, 18121-18127.
- SUN, Q., LI, Q., ZHONG, W., ZHANG, J., SUN, X., TAN, X., YIN, X., SUN, X., ZHANG, X. & ZHOU, Z. 2014. Dysregulation of hepatic zinc transporters in a mouse model of alcoholic liver disease. *American Journal of Physiology-Gastrointestinal and Liver Physiology*, 307, G313-G322.
- SUN, Y., SHAO, H., LI, Z., LIU, J., GAO, L., PENG, X., MENG, Y. & LI, W. 2004. ZNF268, a novel krüppel-like zinc finger protein, is implicated in early human liver development. *International journal of molecular medicine*, 14, 971-975.
- SUZUKI, A. & ENDO, T. 2002. Ermelin, an endoplasmic reticulum transmembrane protein, contains the novel HELP domain conserved in eukaryotes. *Gene*, 284, 31-40.
- SUZUKI, T., ISHIHARA, K., MIGAKI, H., ISHIHARA, K., NAGAO, M., YAMAGUCHI-IWAI, Y. & KAMBE, T. 2005a. Two Different Zinc Transport Complexes of Cation Diffusion Facilitator Proteins Localized in the Secretory Pathway Operate to Activate Alkaline Phosphatases in Vertebrate Cells. *Journal of Biological Chemistry*, 280, 30956-30962.
- SUZUKI, T., ISHIHARA, K., MIGAKI, H., MATSUURA, W., KOHDA, A., OKUMURA, K., NAGAO, M., YAMAGUCHI-IWAI, Y. & KAMBE, T. 2005b. Zinc transporters, ZnT5 and ZnT7, are required for the activation of alkaline phosphatases, zinc-requiring enzymes that are glycosylphosphatidylinositol-anchored to the cytoplasmic membrane. *Journal of Biological Chemistry*, 280, 637-643.
- SUZUKI, Y., YAMASHITA, R., SHIROTA, M., SAKAKIBARA, Y., CHIBA, J., MIZUSHIMA-SUGANO, J., NAKAI, K. & SUGANO, S. 2004. Sequence comparison of human and mouse genes reveals a homologous block structure in the promoter regions. *Genome research*, 14, 1711-1718.

- SWARDFAGER, W., HERRMANN, N., MAZEREEUW, G., GOLDBERGER, K., HARIMOTO, T. & LANCTÔT, K. L. 2013. Zinc in Depression: A Meta-Analysis. *Biological Psychiatry*, 74, 872-878.
- SYDOR, A. M., JOST, M., RYAN, K. S., TURO, K. E., DOUGLAS, C. D., DRENNAN, C. L. & ZAMBLE, D. B. 2013. Metal Binding Properties of Escherichia coli YjiA, a Member of the Metal Homeostasis-Associated COG0523 Family of GTPases. *Biochemistry*, 52, 1788-1801.
- TAI, S.-K., TAN, O. J.-K., CHOW, V. T.-K., JIN, R., JONES, J. L., TAN, P.-H., JAYASURYA, A. & BAY, B.-H. 2003. Differential expression of metallothionein 1 and 2 isoforms in breast cancer lines with different invasive potential: identification of a novel nonsilent metallothionein-1H mutant variant. *The American journal of pathology*, 163, 2009-2019.
- TANIGUCHI, M., FUKUNAKA, A., HAGIHARA, M., WATANABE, K., KAMINO, S., KAMBE, T., ENOMOTO, S. & HIROMURA, M. 2013. Essential role of the zinc transporter ZIP9/SLC39A9 in regulating the activations of Akt and Erk in B-cell receptor signaling pathway in DT40 cells. *PloS one*, 8, e58022.
- TANJI, K., IRIE, Y., UCHIDA, Y., MORI, F., SATOH, K., MIZUSHIMA, Y. & WAKABAYASHI, K. 2003. Expression of metallothionein-III induced by hypoxia attenuates hypoxia-induced cell death in vitro. *Brain research*, 976, 125-129.
- TAYLOR, K., MORGAN, H., JOHNSON, A., HADLEY, L. & NICHOLSON, R. 2003. Structure–function analysis of LIV-1, the breast cancer-associated protein that belongs to a new subfamily of zinc transporters. *Biochem. J*, 375, 51-59.
- TAYLOR, K., MORGAN, H., JOHNSON, A. & NICHOLSON, R. 2004. Structure-function analysis of HKE4, a member of the new LIV-1 subfamily of zinc transporters. *Biochem. J*, 377, 131-139.
- TAYLOR, K. M., HISCOX, S., NICHOLSON, R. I., HOGSTRAND, C. & KILLE, P. 2012. Protein Kinase CK2 Triggers Cytosolic Zinc Signaling Pathways by Phosphorylation of Zinc Channel ZIP7. *Sci. Signal.*, 5, ra11-.
- TAYLOR, K. M., MORGAN, H. E., JOHNSON, A. & NICHOLSON, R. I. 2005. Structure–function analysis of a novel member of the LIV-1 subfamily of zinc transporters, ZIP14. *FEBS Letters*, 579, 427-432.
- TAYLOR, K. M., MORGAN, H. E., SMART, K., ZAHARI, N. M., PUMFORD, S., ELLIS, I. O., ROBERTSON, J. F. R. & NICHOLSON, R. I. 2007. The emerging role of the LIV-1 subfamily of zinc transporters in breast cancer. *Molecular medicine*, 13, 396.
- TAYLOR, K. M. & NICHOLSON, R. I. 2003. The LZT proteins; the LIV-1 subfamily of zinc transporters. *Biochimica et Biophysica Acta (BBA)-Biomembranes*, 1611, 16-30.
- THORNTON, J. K., TAYLOR, K. M., FORD, D. & VALENTINE, R. A. 2011. Differential subcellular localization of the splice variants of the zinc transporter ZnT5 is dictated by the different C-terminal regions. *PloS one*, 6, e23878.

- TIAN, X. & DIAZ, F. J. 2012. Zinc depletion causes multiple defects in ovarian function during the periovulatory period in mice. *Endocrinology* 153, 873-886.
- TOMINAGA, K., KAGATA, T., JOHMURA, Y., HISHIDA, T., NISHIZUKA, M. & IMAGAWA, M. 2005. SLC39A14, a LZT protein, is induced in adipogenesis and transports zinc. *FEBS Journal*, 272, 1590-1599.
- TSAI, R. Y. L. & REED, R. R. 1997. Cloning and functional characterization of Roaz, a zinc finger protein that interacts with O/E-1 to regulate gene expression: implications for olfactory neuronal development. *The Journal of neuroscience*, 17, 4159-4169.
- UNNO, J., SATOH, K., HIROTA, M., KANNO, A., HAMADA, S., ITO, H., MASAMUNE, A., TSUKAMOTO, N., MOTOI, F. & EGAWA, S. 2009. LIV-1 enhances the aggressive phenotype through the induction of epithelial to mesenchymal transition in human pancreatic carcinoma cells. *International journal of oncology*, 35, 813.
- URANI, C., MELCHIORETTO, P. & GRIBALDO, L. 2010. Regulation of metallothioneins and ZnT-1 transporter expression in human hepatoma cells HepG2 exposed to zinc and cadmium. *Toxicology in Vitro*, 24, 370-374.
- URRUTIA, R. 2003. KRAB-containing zinc-finger repressor proteins. *Genome Biology*, 4, 231.
- VALENTINE, R. A., ET AL., 2007. ZnT5 Variant B is a Bidirectional Transporter and Mediates Zinc Uptake in Human Caco-2 Cells. *The Journal of Biological Chemistry* *The Journal of Biological Chemistry*, 282, 14389-14393.
- VALENTINE, R. A., JACKSON, K. A., CHRISTIE, G. R., MATHERS, J. C., TAYLOR, P. M. & FORD, D. 2007. ZnT5 variant B is a bidirectional zinc transporter and mediates zinc uptake in human intestinal Caco-2 cells. *Journal of Biological Chemistry*, 282, 14389-14393.
- VASILE, E., TOMITA, Y., BROWN, L. F., KOCHER, O. & DVORAK, H. F. 2001. Differential expression of thymosin  $\beta$ -10 by early passage and senescent vascular endothelium is modulated by VPF/VEGF: evidence for senescent endothelial cells in vivo at sites of atherosclerosis. *The FASEB Journal*, 15, 458-466.
- VU, T. T., FREDENBURGH, J. C. & WEITZ, J. I. 2009. Zinc: An important cofactor in haemostasis and thrombosis. *Thromb Haemost*, 101, 452-459.
- WALDRON, K. J. & ROBINSON, N. J. 2009. How do bacterial cells ensure that metalloproteins get the correct metal? *Nat Rev Micro*, 7, 25-35.
- WANG, C.-Y., JENKITKASEMWONG, S., DUARTE, S., SPARKMAN, B. K., SHAWKI, A., MACKENZIE, B. & KNUTSON, M. D. 2012. ZIP8 is an iron and zinc transporter whose cell-surface expression is up-regulated by cellular iron loading. *Journal of Biological Chemistry*, 287, 34032-34043.
- WANG, C.-Y., WEN, M.-S., WANG, H.-W., HSIEH, I. C., LI, Y., LIU, P.-Y., LIN, F.-C. & LIAO, J. K. 2008. Increased Vascular Senescence and Impaired Endothelial Progenitor

- Cell Function Mediated by Mutation of Circadian Gene *Per2*. *Circulation*, 118, 2166-2173.
- WANG, F., KIM, B.-E., DUFNER-BEATTIE, J., PETRIS, M. J., ANDREWS, G. & EIDE, D. J. 2004a. Acrodermatitis enteropathica mutations affect transport activity, localization and zinc-responsive trafficking of the mouse ZIP4 zinc transporter. *Human molecular genetics*, 13, 563-571.
- WANG, F., KIM, B.-E., PETRIS, M. J. & EIDE, D. J. 2004b. The Mammalian Zip5 Protein Is a Zinc Transporter That Localizes to the Basolateral Surface of Polarized Cells. *Journal of Biological Chemistry*, 279, 51433-51441.
- WANG, K., ZHOU, B., KUO, Y.-M., ZEMANSKY, J. & GITSCHIER, J. 2002. A novel member of a zinc transporter family is defective in acrodermatitis enteropathica. *The American Journal of Human Genetics*, 71, 66-73.
- WANG, X., VALENZANO, M., MERCADO, J., ZURBACH, E. P. & MULLIN, J. 2013. Zinc Supplementation Modifies Tight Junctions and Alters Barrier Function of CACO-2 Human Intestinal Epithelial Layers. *Digestive Diseases and Sciences*, 58, 77-87.
- WANG, X., WANG, Z.-Y., GAO, H.-L., DANSCHER, G. & HUANG, L. 2006. Localization of ZnT7 and zinc ions in mouse retina—immunohistochemistry and selenium autometallography. *Brain research bulletin*, 71, 91-96.
- WEAVER, B. P., DUFNER-BEATTIE, J., KAMBE, T. & ANDREWS, G. K. 2007. Novel zinc-responsive post-transcriptional mechanisms reciprocally regulate expression of the mouse Slc39a4 and Slc39a5 zinc transporters (Zip4 and Zip5). *Biological chemistry*, 388, 1301-1312.
- WEI, H., DESOUKI, M. M., LIN, S., XIAO, D., FRANKLIN, R. B. & FENG, P. 2008. Differential expression of metallothioneins (MTs) 1, 2, and 3 in response to zinc treatment in human prostate normal and malignant cells and tissues. *Molecular cancer*, 7, 7.
- WILLIS, M. S., MONAGHAN, S. A., MILLER, M. L., MCKENNA, R. W., PERKINS, W. D., LEVINSON, B. S., BHUSHAN, V. & KROFT, S. H. 2005. Zinc-Induced Copper Deficiency: A Report of Three Cases Initially Recognized on Bone Marrow Examination. *American Journal of Clinical Pathology*, 123, 125-131.
- WISTOW, G., BERNSTEIN, S. L., WYATT, M. K., FARISS, R. N., BEHAL, A., TOUCHMAN, J. W., BOUFFARD, G., SMITH, D. & PETERSON, K. 2002. Expressed sequence tag analysis of human RPE/choroid for the NEIBank Project: over 6000 non-redundant transcripts, novel genes and splice variants. *Mol Vis*, 8, 205-220.
- WONG, A., VALLENDER, E. J., HERETIS, K., ILKIN, Y., LAHN, B. T., MARTIN, C. L. & LEDBETTER, D. H. 2004. Diverse fates of paralogs following segmental duplication of telomeric genes. *Genomics*, 84, 239-247.
- WONGDEE, K., TEERAPORNPUKAKIT, J., RIENGROJPITAK, S., KRISHNAMRA, N. & CHAROENPHANDHU, N. 2009. Gene expression profile of duodenal epithelial

- cells in response to chronic metabolic acidosis. *Molecular and cellular biochemistry*, 321, 173-188.
- WORLD HEALTH, O. 2002. *World Health Report 2002: World Health Report: Reducing Risks to Health Noncommunicable Diseases*, World Health Organization.
- WU, W. & WELSH, M. J. 1996. Expression of the 25-kDa Heat-Shock Protein (HSP27) Correlates with Resistance to the Toxicity of Cadmium Chloride, Mercuric Chloride, cis-Platinum(II)-Diammine Dichloride, or Sodium Arsenite in Mouse Embryonic Stem Cells Transfected with Sense or Antisense HSP27 cDNA. *Toxicology and Applied Pharmacology*, 141, 330-339.
- WU, Y. H., FREY, A. G. & EIDE, D. J. 2011. Transcriptional regulation of the Zrg17 zinc transporter of the yeast secretory pathway. *Biochemical Journal*, 435, 259-266.
- YAMASAKI, S., HASEGAWA, A., HOJYO, S., OHASHI, W., FUKADA, T., NISHIDA, K. & HIRANO, T. 2012. A novel role of the L-type calcium channel  $\alpha 1D$  subunit as a gatekeeper for intracellular zinc signaling: zinc wave. *PloS one*, 7, e39654.
- YAMASAKI, S., SAKATA-SOGAWA, K., HASEGAWA, A., SUZUKI, T., KABU, K., SATO, E., KUROSAKI, T., YAMASHITA, S., TOKUNAGA, M., NISHIDA, K. & HIRANO, T. 2007. Zinc is a novel intracellular second messenger. *The Journal of Cell Biology*, 177, 637-645.
- YAN, G., ZHANG, Y., YU, J., YU, Y., ZHANG, F., ZHANG, Z., WU, A., YAN, X., ZHOU, Y. & WANG, F. 2012. Slc39a7/zip7 plays a critical role in development and zinc homeostasis in zebrafish. *PloS one*, 7, e42939.
- YANG, J., ZHANG, Y., CUI, X., YAO, W., YU, X., CEN, P., HODGES, S. E., FISHER, W. E., BRUNICARDI, F. C. & CHEN, C. 2013. Gene profile identifies zinc transporters differentially expressed in normal human organs and human pancreatic cancer. *Current molecular medicine*, 13, 401.
- YU, Y., WU, A., ZHANG, Z., YAN, G., ZHANG, F., ZHANG, L., SHEN, X., HU, R., ZHANG, Y. & ZHANG, K. 2013. Characterization of the GufA subfamily member SLC39A11/Zip11 as a zinc transporter. *The Journal of nutritional biochemistry*, 24, 1697-1708.
- YU, Y. Y., KIRSCHKE, C. P. & HUANG, L. 2007. Immunohistochemical analysis of ZnT1, 4, 5, 6, and 7 in the mouse gastrointestinal tract. *Journal of Histochemistry & Cytochemistry*, 55, 223-234.
- ZAMORA, J., VELASQUEZ, A., TRONCOSO, L., BARRA, P., GUAJARDO, K. & CASTILLO-DURAN, C. 2011. Zinc in the therapy of the attention-deficit/hyperactivity disorder in children. A preliminar randomized controlled trial]. *Archivos latinoamericanos de nutrición*, 61, 242.
- ZHANG, L.-H., WANG, X., ZHENG, Z.-H., REN, H., STOLTENBERG, M., DANSCHER, G., HUANG, L., RONG, M. & WANG, Z.-Y. 2010. Altered expression and distribution

- of zinc transporters in APP/PS1 transgenic mouse brain. *Neurobiology of aging*, 31, 74-87.
- ZHAO, H., BUTLER, E., RODGERS, J., SPIZZO, T., DUESTERHOEFT, S. & EIDE, D. 1998. Regulation of Zinc Homeostasis in Yeast by Binding of the ZAP1 Transcriptional Activator to Zinc-responsive Promoter Elements. *Journal of Biological Chemistry*, 273, 28713-28720.
- ZHAO, L., CHEN, W., TAYLOR, K. M., CAI, B. & LI, X. 2007. LIV-1 suppression inhibits HeLa cell invasion by targeting ERK1/2-Snail/Slug pathway. *Biochemical and biophysical research communications*, 363, 82-88.
- ZHENG, D., FEENEY, G. P., KILLE, P. & HOGSTRAND, C. 2008. Regulation of ZIP and ZnT zinc transporters in zebrafish gill: zinc repression of ZIP10 transcription by an intronic MRE cluster. *Physiological genomics*, 34, 205.
- ZWEIDLER-MCKAY, P. A., GRIMES, H. L., FLUBACHER, M. M. & TSICHLIS, P. N. 1996. Gfi-1 encodes a nuclear zinc finger protein that binds DNA and functions as a transcriptional repressor. *Molecular and Cellular Biology*, 16, 4024-34.

## 7.5 Appendices

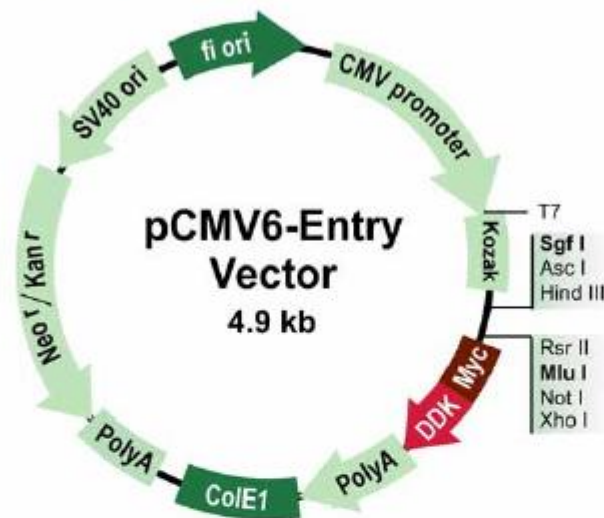
### 1: pCMV6-Entry vector map

#### pCMV6-Entry Vector (Myc-DDK Tagged)

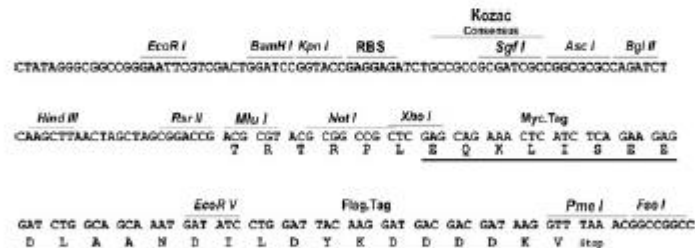
Catalog No.	Description
PS100001	PrecisionShuttle pCMV6-Entry Vector

**Features:**

- ORFs cloned in this vector will be expressed in mammalian cells as a tagged protein with the C-terminal Myc-DDK tags. (DDK is the same as FLAG® which is a registered trademark of Sigma Aldrich).
- Such clones are the best for detection and purification of the transgene using anti-Myc or anti-DDK antibodies.
- Serve as the entry vector in the PrecisionShuttle system to transfer the ORF sequence into any destination vectors for other tagging options or other expression platforms.



**Schematic of the multiple cloning sites:**



Flag® is a registered Trademark of Sigma-Aldrich

PrecisionShuttle Entry Vector Feature Location	
Feature	PrecisionShuttle Entry Vector
CMV promoter	201-925
T7 promoter	953-971
SP6 promoter	n/a
MCS	978-1153
Sgf I 5' cloning site	1020
Mlu I 3' cloning site	1067
Poly-A signal	1206-1291
ColE1	2057-2739
SV40	3998-4300
Kan/Neo	3169-3963

## 2: p3XFLAG-CMV vector map



3060 Spruce Street  
 Saint Louis, Missouri 63103 USA  
 Telephone 800-325-5832 • (314) 771-6765  
 Fax (314) 226-7828  
 email: techserv@sigma.com  
 sigma-usa.com

## Product Information

### p3XFLAG-CMV™-10 EXPRESSION VECTOR

Product No. **E 4401**  
 Store at 0 to -20 °C

#### Product Description

p3XFLAG-CMV™-10 expression vector is a 6.3 kb derivative of pCMV5<sup>1</sup> used to establish transient or stable intracellular expression of N-terminal 3XFLAG fusion proteins in mammalian cells. The vector encodes three adjacent FLAG® epitopes (Asp-Tyr-Lys-Xaa-Xaa-Asp) upstream of the multiple cloning region. This results in increased detection sensitivity using ANTI-FLAG® M2 antibody.<sup>2</sup> The third FLAG epitope includes the enterokinase recognition sequence, allowing cleavage of the 3XFLAG peptide from the purified fusion protein.

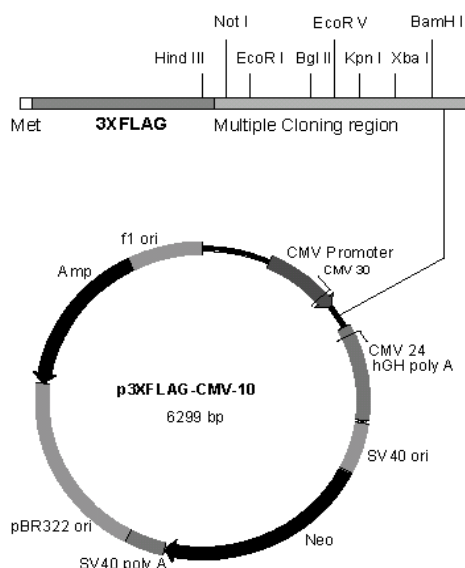
The promoter-regulatory region of the human cytomegalovirus<sup>3</sup> drives transcription of FLAG-fusion constructs. The aminoglycoside phosphotransferase II gene (Neo) confers resistance to aminoglycosides such as G 418,<sup>4</sup> allowing for selection of stable transfectants.

p3XFLAG-CMV-10 expression vector is a shuttle vector for *E. coli* and mammalian cells. Efficiency of replication is optimal when using an SV40 T antigen-expressing host, such as COS cells.

p3XFLAG-CMV-10 expression vector is supplied in 10 mM Tris, 1 mM EDTA, pH 8.0.

#### References

1. Andersson, S., *et al.*, J. Biol. Chem., **264**, 8222-8229 (1989)
2. Hernan, R., *et al.*, Biotechniques, **20**, 789-793 (2000)
3. Thomsen, D.R., *et al.*, Proc. Natl. Acad. Sci. USA, **81**, 659-663 (1984)
4. Jimenez, A. and Davies, J., Nature, **287**, 869-871 (1980)



#### p3XFLAG-CMV-10 Features

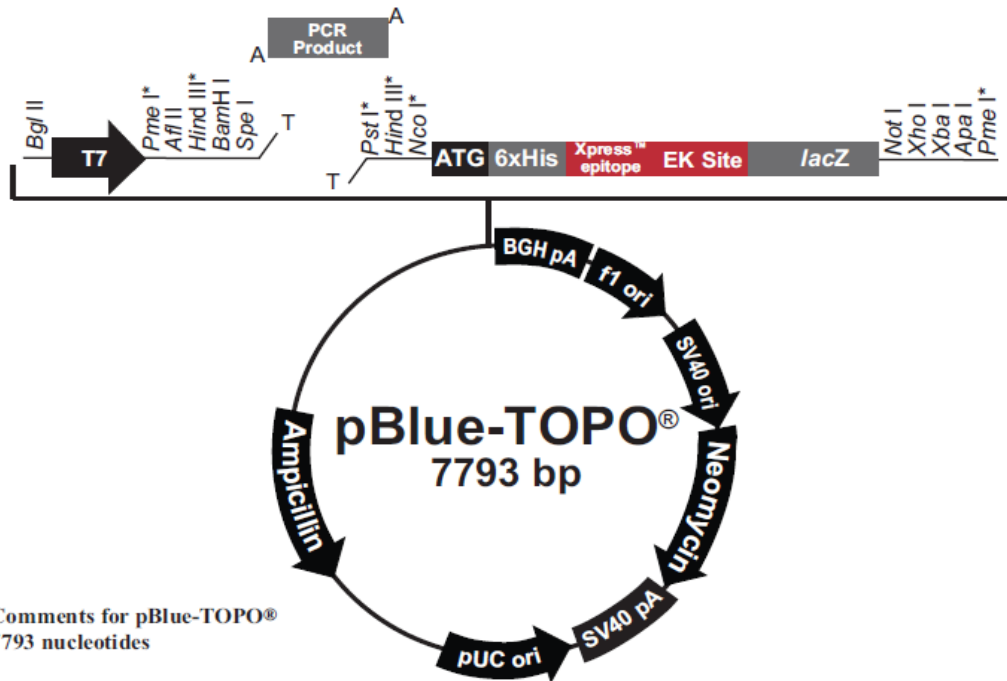
Feature	Map Position
CMV promoter	166-916
CMV 30 sequencing primer	825-854
Translational initiation	928-930
3XFLAG sequence	931-996
Multiple cloning region	994-1056
hGH poly A	1061-1680
CMV 24 sequencing primer	1118-1141
SV40 ori	1699-2037
Neo	2073-2864
SV40 poly A	3511-3609
pBR322 ori	4528-4647
Ampicillin resistance	4824-5684
f1 ori	5847-6299

### 3: pBlue-TOPO vector map

## pBlue-TOPO<sup>®</sup> Map

#### Map

The figure below summarizes the features of the pBlue-TOPO<sup>®</sup> vector. The vector is supplied linearized between base pairs 116 and 117. This is the TOPO<sup>®</sup> Cloning site. The complete nucleotide sequence is available for downloading from our Web site ([www.invitrogen.com](http://www.invitrogen.com)) or from Technical Service (see page 27).

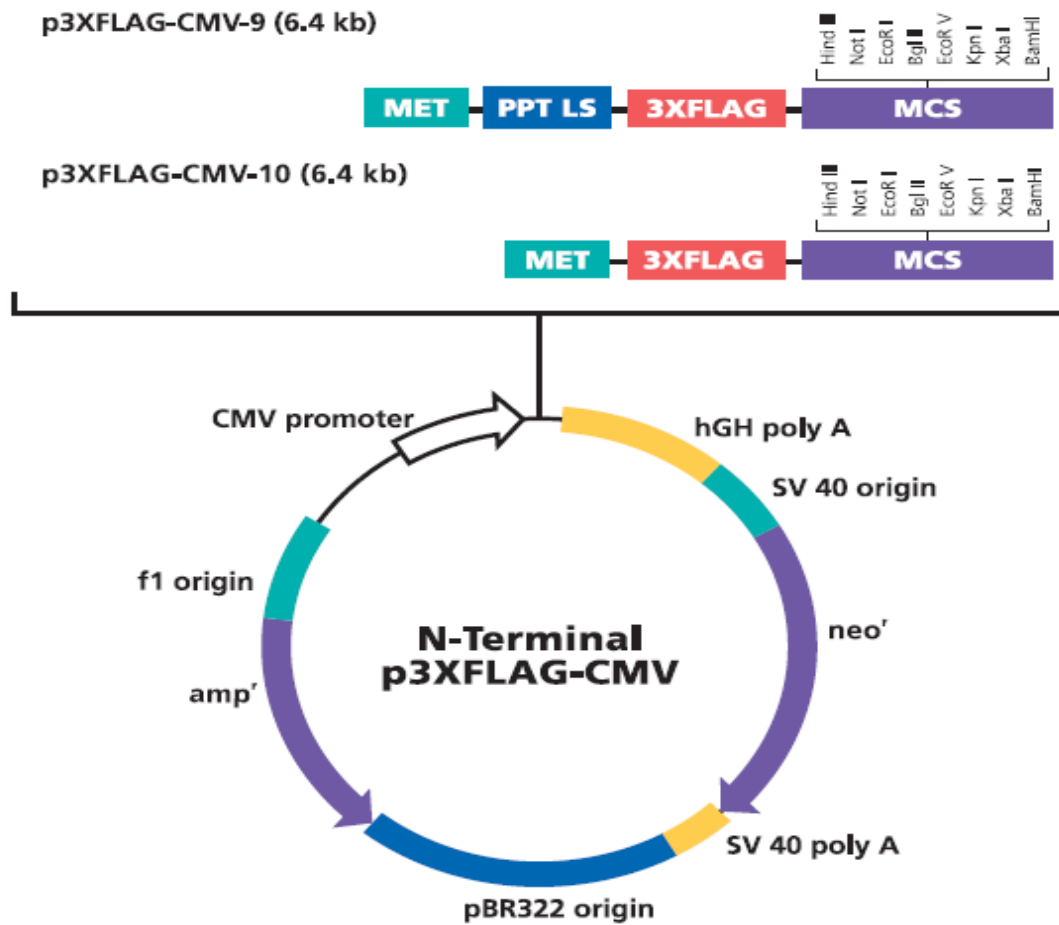


#### Comments for pBlue-TOPO<sup>®</sup> 7793 nucleotides

- T7 promoter/priming site: bases 17-36
- TOPO<sup>®</sup> Cloning site: bases 116-117
- ATG initiation codon: bases 143-145
- Polyhistidine region: bases 155-172
- LacZ Reverse priming site: bases 173-191
- Xpress<sup>™</sup> epitope: bases 212-235
- Enterokinase recognition site: bases 221-235
- LacZ ORF: bases 264-3313
- BGH polyadenylation sequence: bases 3386-3613
- f1 origin: bases 3659-4087
- SV40 promoter and origin: bases 4141-4423
- Neomycin resistance gene: bases 4498-5292
- SV40 polyadenylation sequence: bases 5466-5596
- pUC origin: bases 5979-6652 (complementary strand)
- Ampicillin resistance gene: bases 6797-7657 (complementary strand)

\* These sites are not unique but may be used to excise the PCR product. The *Pme* I sites may be used to excise the reporter cassette, providing there are no *Pme* I sites in the PCR product.

#### 4: p3XFLAG-CMV vector map



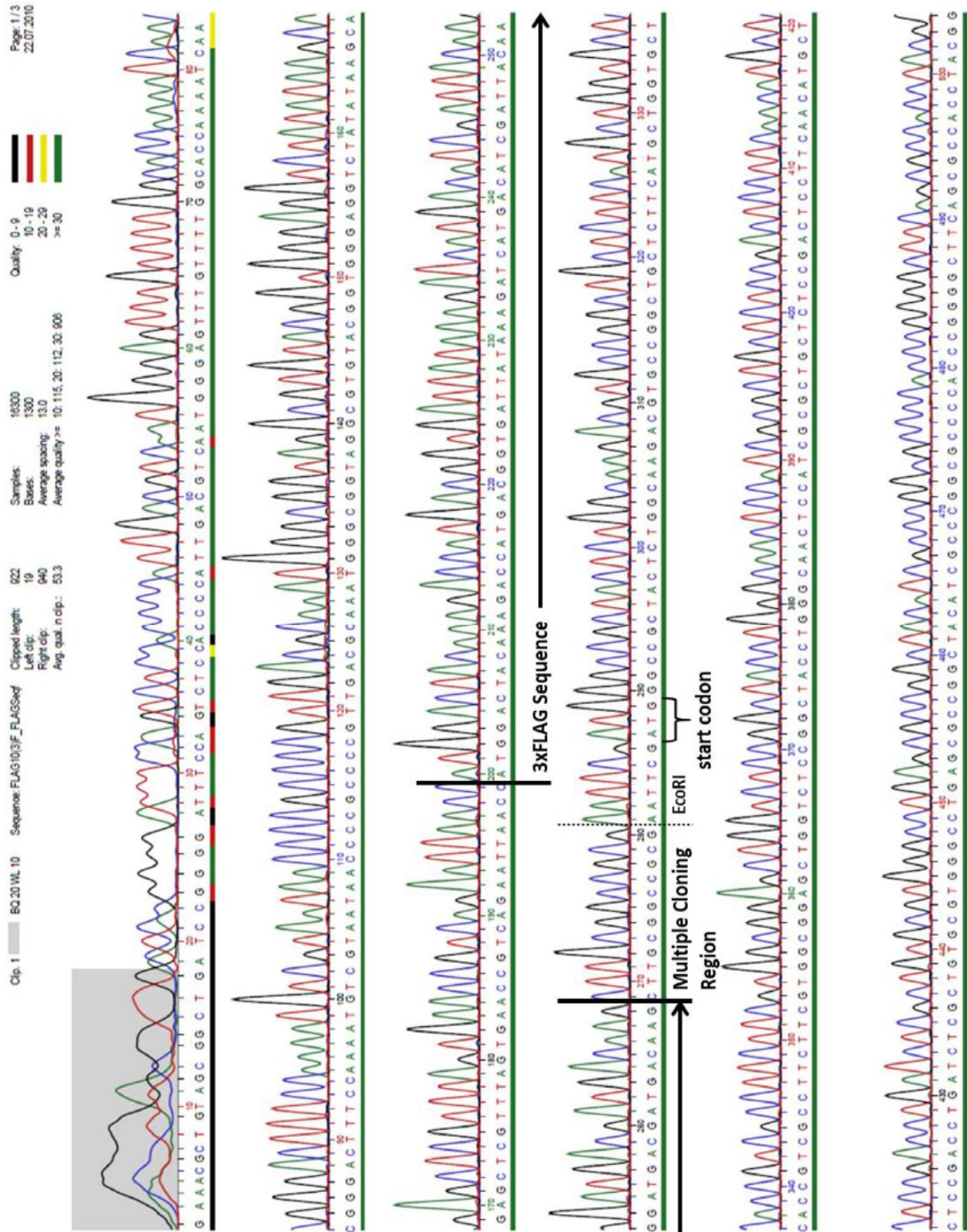
#### Multiple Cloning Site

(p3XFLAG-CMV-9\* and p3XFLAG-CMV-10)

3XFLAG Peptide Sequence															
Met*	Asp	Tyr	Lys	Asp	His	Asp	Gly	Asp	Tyr	Lys	Asp	His	Asp	Ile	
ATG	GAC	TAC	AAA	GAC	CAT	GAC	GGT	GAT	TAT	AAA	GAT	CAT	GAC	ATC	
TAC	CTG	ATG	TTT	CTG	GTA	CTG	CCA	CTA	ATA	TTT	CTA	GTA	CTG	TAG	
3XFLAG Peptide Sequence															
Asp	Tys	Lys	Asp	Asp	Asp	Asp	Lys								
GAT	TAC	AAG	GAT	GAC	GAT	GAC	AAG	CTT	GCG	GCC	GCG	AAT	TCA	TCG	ATA
CTA	ATG	TTC	CTA	CTG	CTA	CTG	TTC	GAA	CGC	CGG	CGC	TTA	AGT	AGC	TAT
								Hind III							
Bgl II	EcoR V		Kpn I		Xba I		Bam HI								
GAT	CTG	ATA	TCG	GTA	CCA	GTC	GAC	TCT	AGA	GGA	TCC	CGG	GTG		
CTA	GAC	TAT	AGC	CAT	GGT	CAG	CTG	AGA	TCT	CCT	AGG	CCC	CAC		

\*For pFLAG-CMV-9, the Met-preprotrypsin leader sequence (PPT LS) precedes the FLAG coding sequence.

## 5: p3XFLAG-CMV vector sequence



## 6: Protein sequences alignment of the human CBWD isoforms using ClusterW2

```

CBWD6_NM_001085457      MLPAVGSVDEEEDPAEEDCPPELVPIETTQSEEEKSGLGAKIPVTIITGYLGAGKTLLN 60
CBWD3_NM_201453        MLPAVGSVDEEEDPAEEDCPPELVPIETTQSEEEKSGLGAKIPVTIITGYLGAGKTLLN 60
CBWD5_NM_001024916    MLPAVGSVDEEEDPAEEDCPPELVPIETTQSEEEKSGLGAKIPVTIITGYLGAGKTLLN 60
CBWD2_NM_172003       MLPAVGSVDEEEDPAEEDCPPELVPIETTQSEEEKSGLGAKIPVTIITGYLGAGKTLLN 60
CBWD1_NM_001145355.1  MLPAVGSVDEEEDPAEEDCPPELVPIETTQSEEEKSGLGAKIPVTIITGYLGAGKTLLN 60
*****_*****.*****.*****

CBWD6_NM_001085457      YILTEQHSKRVAIVILNESGEGSALEKSLAVSQGGELYEEWLELRNGCLCCSVKDNGLRAI 120
CBWD3_NM_201453        YILTEQHSKRVAIVILNESGEGSALEKSLAVSQGGELYEEWLELRNGCLCCSVKDNGLRAI 120
CBWD5_NM_001024916    YILTEQHSKRVAIVILNESGEGSALEKSLAVSQGGELYEEWLELRNGCLCCSVKDNGLRAI 120
CBWD2_NM_172003       YILTEQHSKRVAIVILNEFGEKSALEKSLAVSQGGELYEEWLELRNGCLCCSVKDNGLRAI 120
CBWD1_NM_001145355.1  YILTEQHSKRVAIVILNEFGEKSALEKSLAVSQGGELYEEWLELRNGCLCCSVKDSGLRAI 120
*****_*****.*****

CBWD6_NM_001085457      ENLMQKRGKFDYILLETTGLADPGAVASMFVWDAELGSDIYLDGIIITIVDSKYGLKHLTE 180
CBWD3_NM_201453        ENLMQKRGKFDYILLETTGLADPGAVASMFVWDAELGSDIYLDGIIITIVDSKYGLKHLTE 180
CBWD5_NM_001024916    ENLMQKRGKFDYILLETTGLADPGAVASMFVWDAELGSDIYLDGIIITIVDSKYGLKHLTE 180
CBWD2_NM_172003       ENLMQKRGKFDYILLETTGLADPGAVASMFVWDAELGSDIYLDGIIITIVDSKYGLKHLTE 180
CBWD1_NM_001145355.1  ENLMQKRGKFDYILLETTGLADP-----GIITIVDSKYGLKHLTE 160
*****_*****.*****

CBWD6_NM_001085457      EKPDLGLINEATRQVALADIILINKTDLVPEEDVKKLRRTTIRSINGLGQILETQRSRVVDS 240
CBWD3_NM_201453        EKPDLGLINEATRQVALADIILINKTDLVPEEDVKKLRRTTIRSINGLGQILETQRSRVVDS 240
CBWD5_NM_001024916    EKPDLGLINEATRQVALADIILINKTDLVPEEDVKKLRRTTIRSINGLGQILETQRSRVVDS 240
CBWD2_NM_172003       EKPDLGLINEATRQVALADAILINKTDLVPEEDVKKLRRTTIRSINGLGQILETQRSRVVDS 240
CBWD1_NM_001145355.1  EKPDLGLINEATRQVALADAILINKTDLVPEEDVKKLRRTTIRSINGLGQILETQRSRVVDS 220
*****_*****.*****

CBWD6_NM_001085457      NVLDLHAFDSLGSISLQKQLQHVPGTQPHLDQSIIVTITFEVPGNAKEEHLNMFIQNLLWE 300
CBWD3_NM_201453        NVLDLHAFDSLGSISLQKQLQHVPGTQPHLDQSIIVTITFEVPGNAKEEHLNMFIQNLLWE 300
CBWD5_NM_001024916    NVLDLHAFDSLGSISLQKQLQHVPGTQPHLDQSIIVTITFEVPGNAKEEHLNMFIQNLLWE 300
CBWD2_NM_172003       NVLDLHAFDSLGSISLQKQLQHVPGTQPHLDQSIIVTITFEVPGNAKEEHLNMFIQNLLWE 300
CBWD1_NM_001145355.1  NVLDLHAFDSLGSISLQKQLQHVPGTQPHLDQSIIVTITFEVPGNAKEEHLNMFIQNLLWE 280
*****_*****.*****

CBWD6_NM_001085457      KNVRNKDNHCMEVIRLRLGLVSIKDKSQQVIVQGVHELCDLEETPVSWKDDTERTNRLVLI 360
CBWD3_NM_201453        KNVRNKDNHCMEVIRLRLGLVSIKDKSQQVIVQGVHELCDLEETPVSWKDDTERTNRLVLI 360
CBWD5_NM_001024916    KNVRNKDNHCMEVIRLRLGLVSIKDKSQQVIVQGVHELCDLEETPVSWKDDTERTNRLVLI 360
CBWD2_NM_172003       KNVRNKDNHCMEVIRLRLGLVSIKDKSQQVIVQGVHELCDLEETPVSWKDDTERTNRLVLI 360
CBWD1_NM_001145355.1  KNVRNKDNHCMEVIRLRLGLVSIKDKSQQVIVQGVHELCDLEETPVSWKDDTERTNRLVLI 340
*****_*****.*****

CBWD6_NM_001085457      GRNLDDKILKQLFIATVTETERQWTTTHFKEDQVCT 395
CBWD3_NM_201453        GRNLDDKILKQLFIATVTETERQWTTTHFKEDQVCT 395
CBWD5_NM_001024916    GRNLDDKILKQLFIATVTETERQWTTTHFKEDQVCT 395
CBWD2_NM_172003       GRNLDDKILKQLFIATVTETERQWTTTHFKEDQVCT 395
CBWD1_NM_001145355.1  GRNLDDKILKQLFIATVTETERQWTTTRFQEDQVCT 375
*****_*****.*****

```